THÈSE

En vue de l'obtention du

DOCTORAT DE L'UNIVERSITÉ DE TOULOUSE

Délivré par *l'Université Toulouse III - Paul Sabatier*
Discipline ou spécialité : *Sciences de la Terre et Environnement*

Présentée et soutenue par *Joseline Soledad Tapia Zamora*
Le *19 juillet 2011*

Titre : *Sources, mobility and bioavailability of metals and metalloids in the mining and smelter impacted altiplanean city of Oruro, Bolivia*

JURY
M. Brian TOWNLEY, Professeur, Universidad de Chile, Directeur de thèse
M. Stéphane AUDRY, Directeur de Recherche, CNAP, Directeur de thèse
M. Jacobus LE ROUX, Professeur, Universidad de Chile, Examinateur
M. Martin REICH, Professeur, Universidad de Chile, Examinateur
M. Bernhard DOLD, Professeur, Universidad de Concepción, Rapporteur
M. Jérôme VIERS, Directeur de Recherche, UPS, Examinateur
M. Jörg SCHÄFER, Professeur, CNRS, Rapporteur

Ecole doctorale : *Sciences de l'Univers, de l'Espace et de l'Environnement*
Unité de recherche : *Géosciences Environnement Toulouse*
Directeur(s) de Thèse : *Stéphane Audry et Brian Townley*
Rapporteurs : *Noms des rapporteurs (s'ils ne font pas partie des membre du jury)*

UNIVERSIDAD DE CHILE
Facultad de Ciencias Físicas y Matemáticas
Departamento de Geología

Sources, mobility and bioavailability of trace metals and metalloids in the historically mining and smelter impacted Altiplanean city of Oruro, Bolivia

Tesis para optar al grado de Doctora en Ciencias Mención Geología en Cotutela con la Université Paul Sabatier (Toulouse III)

Joseline Soledad Tapia Zamora

Profesores Guía:

Brian Townley Callejas

Stéphane Audry

Miembros de la Comisión:

Jacobus Le Roux

Martin Reich Morales

Bernhard Dold

Jérôme Viers

Jörg Schäfer

Santiago de Chile

Julio de 2011

RESUMEN DE TESIS
PARA OPTAR AL TÍTULO DE DOCTORA
EN CIENCIAS MENCIÓN GEOLOGÍA
POR: JOSELINE TAPIA ZAMORA
FECHA: 19/07/2011
PROF. GUÍA: BRIAN TOWNLEY
PROF. GUÍA: STÉPHANE AUDRY

Sources, mobility and bioavailability of trace metals and metalloids in the historically mining and smelter impacted Altiplanean city of Oruro, Bolivia

Oruro se localiza en el Altiplano de Bolivia a ∼230 km al sur de La Paz. El principal sistema hidrológico del altiplano es endorreico y está constituido por las subcuencas del lago Titicaca-río Desaguadero-lago Poopó-salar de Coipasa (TDPS). Esta área presenta una estación seca (DS) y una de lluvias (WS). A pesar de la existencia de la WS, las precipitaciones son escasas; sin embargo, interanualmente, la intensidad incrementa asociada a eventos El Niño (ENSO). Geomorfológicamente, esta área esta constituida por el Altiplano y la Cordillera Occidental relacionados a depósitos epitermales y de Cu y la Cordillera Oriental, relacionada a distintas franjas metalogénicas, siendo la de Sn la más conocida. El Departamento de Oruro se localiza en la parte central de esta franja, y a pesar que las actividades mineras se practican desde el siglo XVII, escasamente se conocen las características geoquímicas y los procesos de dispersión que afectan esta zona.

Lo expuesto previamente, motivó el estudio en detalle de testigos sedimentarios lacustres en esta área. Para ello, dos campañas de muestreo (DS y WS) permitieron recuperar un total de 5 testigos sedimentarios, 4 en el lago Uru Uru (2 en la DS y 2 en la WS) y uno en la laguna Cala Cala (18 km al E Oruro), éste último para obtener el background geoquímico local. Los análisis de laboratorio fueron realizados en el *Laboratoire des Mécanismes et Transferts en Géologie* (LMTG, Toulouse), donde un total de 91 muestras de sedimento y 222 muestras de agua intersticial (PW) fueron estudiadas.

El background geoquímico y las fuentes de origen de los metal(oid)es permitieron proponer que As y Sb están enriquecidos de manera importante en comparación con la corteza continental superior (UCC), niveles background mundiales, sitios industrializados y sitios mineros históricos. Estas conclusiones nos permitieron respaldar el uso de factores de enriquecimiento (EF) locales y descartar el uso de la UCC para calcular EFs. Numerosas fuentes potenciales de contaminantes dificultan discriminar aportes naturales de antropogénicos, sin embargo, proponemos que el impacto antropogénico en suelos superficiales se relaciona a la dispersión de elementos traza desde la fundición de Vinto, mientras el contenido de metal(oid)es en el lago Uru Uru está principalmente asociado a actividades mineras.

Estudios de diagénesis temprana, nos permitieron determinar que los metal(oid)es en la laguna Cala Cala son menos disponibles y móviles que en el lago Uru Uru y las concentraciones elevadas de elementos traza en solución se explican por su proximidad a las franjas metalogénicas localizadas a lo largo de la Cordillera Oriental y no por influencia antropogénica. El área norte del lago Uru Uru presenta las menores concentraciones promedio de elementos traza disueltos y su comportamiento está muy asociado a cambios estacionales. De hecho, la disolución reductiva de los oxihidróxidos de Fe y Mn durante la WS es un factor preponderante en la liberación de elementos traza desde el sedimento a la columna de agua. El fraccionamiento en estado sólido (SSP) de los metal(oid)es muestra cambios moderados entre distintas estaciones. Los metal(oid)es en el área sur del lago Uru Uru son los más reactivos, disponibles y móviles. Durante la DS el comportamiento de los elementos traza disueltos está asociado a la evaporación, respuesta no observada durante la WS. Las mayores concentraciones de Sb y Mo disuelto se encuentran en este sector durante las dos temporadas y de Cd sólo en la DS. En esta área el SSP cambia de manera importante el particionamiento durante la WS implicando que los metal(oid)es podrían ser liberados con mayor facilidad al agua intersticial cuando se establecen condiciones reductoras, siendo Mo, U, Sb, Pb y Cd los elementos en estado sólido más inestables. Este sector es el que representa una mayor preocupación ambiental, ya que además de la influencia de la WS, existe influencia antropogénica asociada a la mina de Huanuni, probablemente aportando Sb (y Mo) disuelto, y como ha demostrado otro estudio, la competición de Mo con Cu induce deficiencias en la dieta de animales de granja. Recalcamos que es en esta área donde la mayoría de la flora y fauna vive y habitualmente se practica la pesca.

Con respecto a la influencia de la historia minera y climática en la deposición de sedimentos en el altiplano boliviano, determinamos que durante el último siglo, la explotación y producción de Sn ha influído en la deposición de Sb-Ag-Pb en sedimentos del lago Uru Uru. Adicionalmente, los eventos ENSO podrían jugar un rol importante en la generación de minerales autígenos durante períodos con precipitación intensa. Finalmente, proponemos que en la deposición de metal(oid)es en esta área contribuyen principalmente tres fuentes: geología local, formación de minerales autígenos bajo la influencia de la WS y principalmente durante eventos ENSO fríos (La Niña) y gangas y menas de origen minerogénico.

THESIS ABSTRACT
TO OBTAIN THE DEGREE OF DOCTOR
IN SCIENCES MENTION GEOLOGY
BY: JOSELINE TAPIA ZAMORA
DATE: 19/07/2011
ADVISOR: BRIAN TOWNLEY
ADVISOR: STÉPHANE AUDRY

Sources, mobility and bioavailability of trace metals and metalloids in the historically mining and smelter impacted Altiplanean city of Oruro, Bolivia

Oruro is located on the Bolivian Altiplano at ~230 km south of La Paz. The main hydrological system in the Altiplano is endorheic and is constituted by Lake Titicaca-Desaguadero River-Lake Poopó-Coipasa Salar (TDPS) sub-basins. This area presents a dry (DS) and a wet season (WS). Despite the existence of a WS, precipitation is scarce, nevertheless, intensity increases interannually associated with ENSO events. Geomorphologically, this area is made up of the Altiplano and the Eastern Cordillera related to epithermal and Cu deposits and the Eastern Cordillera related to numerous metallogenic belts, including the well-known Sn belt. Oruro Department is located in the central part of the Sn belt, and despite mining activities having been practiced since the XVIIth century, very little is known about the geochemical characteristics and dispersion processes affecting this area.

The above, motivated the detailed study of lacustrine sedimentary cores in this area. Two coring campaigns (DS and WS) allowed retrieving a total of 5 sedimentary cores, 4 within Lake Uru Uru (2 en the DS y 2 en the WS) and one in Cala Cala Lagoon (18 km E of Oruro), the later to obtain the local geochemical background. Laboratory analysis was performed in the *Laboratoire des Mécanismes et Transferts en Géologie* (LMTG, Toulouse), where a total of 91 sediment samples and 222 pore water samples (PW) were studied.

The geochemical background and metal(loid) sources allowed us to propose that As and Sb are significantly enriched in comparison to the upper continental crust (UCC), world background levels, industrialized areas and historic mining sites. These conclusions allow us to support the use of local enrichment factors (EF) and discard the use of the UCC to calculate EFs. Many potential sources of contaminants make it difficult to discriminate natural from anthropogenic contributions, nevertheless, we propose that anthropogenic impact in superficial soils is related to trace elements dispersion from the Vinto Smelter, while the metal(loid) content within Lake Uru Uru is mainly associated with mining activities.

Early diagenesis processes studies, allowed us to determine that metal(loid)s within Cala Cala Lagoon are less available and mobile than within Lake Uru Uru and high trace element concentrations in pore water are explained by the proximity to the metallogenic belts located along the Eastern Cordillera and not by anthropogenic influence. Northern Lake Uru Uru presents the lower mean dissolved trace element concentration and their behaviour is highly influenced by seasonal changes. Indeed, as the reductive dissolution of Fe- and-Mn oxyhydroxides takes place, metal(loid)s are released mainly from sediments to the water column. In this area solid state partitioning (SSP) of metal(loid)s shows moderate changes between different seasons. Metal(loid)s in southern Lake Uru Uru area are the most reactive, available and mobile. During the DS, dissolved metal(loid) behaviour is associated with evaporation, this was not observed during the WS. The highest dissolved Sb and Mo concentrations are found in this area during both seasons and Cd only in the DS. Solid state partitioning (SSP) changes fractionation greatly during WS so that metal(loid)s can be easily released into the pore water when reducing conditions are achieved, in this area the most unstable elements are Mo, U, Sb, Pb and Cd. This area represents the most important environmental concern, because besides WS, anthropogenic influence associated with the Huanuni Mine exists, probably contributing with dissolved Sb and Mo, and as demonstrated by other study, Mo competition with Cu induces dietary deficiencies in farm animals. We stress that it is in this area where most flora and fauna live and fishing is usually practiced. We recommend to better define metal(loid)s behaviour within the WC, specially during WS and cold ENSO (La Niña) events.

Regarding mining history and climate in relation to sediment deposition within the Bolivian Altiplano, we determined that during the last century, Sn exploitation and production influenced Sb-Ag-Pb deposition in sediments from Lake Uru Uru. Additionally, ENSO events may play an important role in the precipitation of authigenic mineral during early diagenesis processes. Finally, we propose that the contribution of metal(loid)s deposited in this area is mainly related to three sources: local geology, authigenic minerals formation under WS influence and mainly during cold ENSO events (La Niña) and gangues and ores from mining origin.

RÉSUMÉ DU THÈSE
POUR OBTENIR LE GRADE DE DOCTEUR
EN SCIENCES MENTION GÉOLOGIE
PAR: JOSELINE TAPIA ZAMORA
DATE: 19/07/2011
TUTEUR: BRIAN TOWNLEY
TUTEUR: STÉPHANE AUDRY

Sources, mobility and bioavailability of trace metals and metalloids in the historically mining and smelter impacted altiplanean city of Oruro, Bolivia

Oruro est situé dans l'Altiplano Bolivien à ∼230 km au sud de La Paz. Le principal système hydrologique est endoréique et est constitué par les sous-bassins du lac Titicaca-riviére Desaguadero-lac Poopó-salar du Coipasa (TDPS). Cette zone présente une saison sèche (DS) et une saison humide (WS). Malgré l'existence de la WS, les précipitations sont rares, néanmoins, l'intensité augmente interannuellement associé à les événements ENSO. Géomorphologiquement, ce site est composé de: l'Altiplano et la Cordillère Occidentale liés aux dépôts épithermaux et Cu et la Cordillère Orientale liée aux nombreuses ceintures métallogéniques, la plus connue est la ceinture de Sn. Le Département d'Oruro est situé dans la partie centrale de cette ceinture, et malgré le fait que cette ville a été soumis à des activités minières depuis le XVII^{ème} siècle, les caractéristiques géochimiques et les processus de dispersion qui affectent cette zone sont peu connus.

Les faits exposés précédemment, ont motivé une étude géochimique détaillée des carottes sédimentaires lacustres dans ce domaine. Deux campagnes de carottage (DS et WS) ont permit de récupérer 5 carottes sédimentaires, 4 dans le lac Uru Uru (2 en DS et 2 en WS) et une à la lagoon Cala Cala (18 km E d'Oruro), ce dernier pour déterminer le fond géochimique local. Analyses de laboratoire ont été effectuées au L*aboratoire des Mécanismes et Transferts en Géologie* (LMTG, Toulouse), où un total de 91 échantillons de sédiments et 222 échantillons des eaux interstitielles (PW) ont été étudiés.

Le fond géochimique et les sources des éléments traces nous ont permis de proposer que le fond géochimique naturel de As et Sb est significativement plus élevé par rapport de la croûte continentale supérieure (UCC), les niveaux de fond mondial, les centres industriels et les sites miniers historiques. Ces conclusions nous ont permis de soutenir l'utilisation des coefficients d'enrichissement (EF) locaux et jeter l'utilisation de l'UCC pour calculer les EFs. Il existe une multiplicité de sources des contaminants qui ont difficulté la discrimination entre apports naturelles et apports anthropiques dans ce bassin. Cependant, nous proposons que l'impact anthropique dans les sols superficiels est liée à la dispersion des éléments traces par la Fonderie de Vinto, tandis que le lac Uru Uru est plutôt influencé par les activités minières.

Études de diagenèse précoce, nous ont permis de déterminer que les éléments traces au sein du lagoon Cala Cala sont moins disponibles et mobiles que dans le lac Uru Uru et des fortes concentrations des éléments traces en solution sont expliqués par la proximité des ceintures métallogéniques situées le long de la Cordillère Orientale, et non par influence anthropique. Le nord du lac Uru Uru présente des concentrations inférieures moyennes des éléments traces dissous et leur comportement est fortement associée à des changements saisonniers, parce que l'environnement réductrice atteint au cours de la WS entraîne la libération des éléments traces que la dissolution réductrice des oxyhydroxides de Mn a lieu. Dans ce domaine, le comportement des éléments traces dans le état solide montrent des changements modérés entre les différentes saisons. Les éléments traces dans le sud du lac Uru Uru sont les plus réactifs, disponibles et mobiles. Au cours de la DS le comportement des éléments traces dissous est associé à l'évaporation, cette réaction n'a pas été observé au cours de la WS. Les plus fortes concentrations du Sb et Mo dissous se trouvent dans cette région pendant les deux saisons et Cd que pendant la DS. Dans ce domaine, le partitionnement à l'état solide (SSP) montre des changements de fractionnement importants lors de la WS, impliquant que les éléments traces peuvent être facilement libérés dans l'eau interstitielle lorsque les conditions de réduction sont établis, les éléments les plus instables sont Mo, U, Sb, Pb et Cd. Cette zone affiche le souci environnemental plus important, parce que, encore l'influence de la WS, on trouve l'influence anthropique associé à la Mine de Huanuni, probablement en apportant Sb (et Mo) dissous (et comme le montre autre étude, Mo représente une compétition pour le Cu en induisant des carences alimentaires pour animaux de ferme). Nous soulignons que c'est dans ce domaine où la plupart de la flore et faune vive et de la pêche est généralement pratiqué. On recommande de déterminer le comportement des éléments traces dans la WC, spécialement au cours de la WS et La Niña événements.

En ce qui concerne l'influent de l'exploitation minière et le climat sur le dépôt des sédiments dans l'Altiplano, il a été déterminé que au cours du dernier siècle, l'exploitation et la production de Sn a influencé le dépôt de Sb-Ag-Pb dans les sédiments du lac Uru Uru. En outre, événements ENSO pourraient jouer un rôle important dans la production de minéraux authigènes pendant la diagenèse précoce. Enfin, nous proposons que le dépôt des éléments traces est influencé principalement par trois sources: la géologie local, la formation des minéraux authigènes sous l'influence probable des événements froid ENSO (La Niña) et les gangues et minerais d'origine minérogénétiques.

Dedication

... dedicated to my born-family, José, Rosa, Pepe and Carolina ...

... and to my chosen-family, Luis and Antonia

...

Acknowledgements

I thank the financial support from PhD fellowships granted by *CONICYT* (Chile, D-21070053) and the complement granted by *IRD* (France, 625890E).

This study would have not been possible without help provided by the following individuals in the LMTG (OMP, Toulouse): *Frédéric Candaudap* and *Aurélie Lanzanova* for the ICP-MS analyses; *Jonathan Prunier*, *Manuel Henry* and *Carole Boucayrand* for the sediment digestions; *Philippe de Parseval* (microprobe); *Sophie Gouy* and *Thierry Aigouy* (SEM); *Michel Thibaut* (XRD); *Christelle Lagane* (first coring campaign and HPLC standards); *Stéphanie Mounic* (HPLC and S/C Analyser); *Philippe Besson* (ICP-OES); *Fabienne de Parseval* (sediment homogenization). In LA (Laboratoire d'Aerologie, OMP, Toulouse), *Eric Gardrat* and *Corinne Galy-Lacaux* (HPLC-Ammonium). In LEGOS (Laboratoire d'Etude en Géophysique et Océanographie Spatiales) *Pieter Van Beek* (core dating). In the Geology Department of the Universidad de Chile I received valuable help by *Jacobus Le Roux* (English improvement of the paper 1 and manuscript), *Xavier Émery* (French improvement in Conclusions Générales) and *Christian Nievas* (Laser Granulometry). During the Bolivian field campaigns, I received valuable assistance from *Jean-Louis Duprey*, *Jacques Gardon*, *Marcelo Claure*, *Abdul Castillo*, and *Patrick Blanchon*. I also thank the staff of the UMSA (Universidad Mayor de San Andrés): *J. César Calderón*, *Lincy Ugarte*, *Erika Paty*, *Carla Ibáñez*, *Carlos Molina* and *Samantha*, and Mr. *Carlos Wayta*, of Oruro, for their presence in the field campaigns and their valuable help during the coring campaigns.

I thank the *World Bank* for authorising the use of the available data from the Oruro Pilot Project (PPO) for the present study, especially Mr. *Pavel Adamek*, co-director of the PPO who provided valuable information. I thank *Bob Garrett* for the improvement of the paper 1 manuscript by a detailed review and very helpful suggestions. I thank the jury members, *Jacobus*, *Bernhard*, *Jörg*, *Martin* and *Jérôme*, for their constructive and critical comments. I gratefully thank my advisors, *Stéphane* and *Brian* for guiding me and especially for their

patience during these four years.

Finally, I specially thank my friends (*school*, *university*, *doctorate* and *life*), my born-family (*Rosa*, *José*, *Pepe* and *Carolina*) and my chosen-family (*Luis* and *Antonia*), they gave me all the support and emotional help to successfully complete my PhD thesis.

Contents

Contents

List of Figures

LIST OF FIGURES

List of Tables

Chapter 1

Contamination in natural aqueous reservoirs: from general to specific observations

1.1 Geochemistry in environmental sciences and environmental legislation: basic concepts

1.1.1 Introduction

During the 50s, the search for economically exploitable metallic deposits gave rise to the development of new techniques to find cover deposits. Among these techniques, exploration geochemistry was a valuable tool to increase the discovery of these kind of deposits. With time, exploration geochemistry involved the generation of a vast terminology, in which terms such as: geochemical background, threshold, geochemical baseline, anomaly, enrichment factor, among others, are commonly. Nowadays these terms are mainly applied in contamination and/or pollution studies, environmental sciences and environmental legislation, and regarding the last point, most of them are employed to assess the anthropogenic component in different environments of the Earth. Some authors have demonstrated that geochemical backgrounds, baselines, thresholds and anomalies depend on the location (e.g., [1, 2, 3]), scale and analytical techniques used (e.g., [4]).

The following paragraphs will introduce the most important concepts applied in environmental geochemistry surveys and the meaning of geochemical studies to assess the degree of contamination[1] and/or pollution[2] in the environment.

1.1.1.1 Geochemical concepts applied to environmental sciences and environmental legislation

The term ***geochemical background*** comes originally from exploration geochemistry. It was defined by Hawkes & Webb (1962) [5] as: "the normal abundance of an element in barren earth material" and these authors concluded that "it is more realistic to view background as a range rather than an absolute value". The concept of geochemical background was introduced to differentiate between normal element concentrations and ***anomalies***, which might be indicative of an ore occurrence. "By definition, an anomaly is a deviation from the norm. A geochemical anomaly, more specifically, is a departure from the geochemical patterns that are normal for a given area or geochemical landscape" [5]. To be able to differentiate between background and anomaly, the term ***threshold*** was introduced and it was defined as "the upper limit of

[1] Make (something) impure by exposure to or addition of a poisonous or polluting substance.
[2] The presence in or introduction into the environment of a substance or thing that has harmful or poisonous effects. All pollution is contamination, but not all contamination is pollution.

normal background fluctuation". A more general definition is that proposed by Garrett (1991) [6] as "threshold is the outer limit of background variation". Another term frequently used in environmental legislation is ***geochemical baseline***. It was officially introduced in the context of the International Geological Correlation Programme (IGCP, projects 259 and 360; [7]) in order to create a global reference network for national regional geochemical data sets and as an international background database for environmental legislation. This term refers to the prevailing variation in the concentration of an element in the superficial environment [8, 9] and furthermore, indicates the actual content of an element at a given point in time [9]; it includes the ***natural background*** and the diffuse anthropogenic contribution in the soils [1, 10], in which natural background is widely used to infer background levels reflecting natural processes uninfluenced by human activities. This is an important issue (e.g., [7, 11]); however, Reimann & Garrett (2005) [4] believe that "the use of the term baseline gives the impression that there is a single number, line, where in fact there are a range of values characterizing any particular area or region reflecting the heterogeneity of the environment". This was recognized by Darnley *et al.* (1995) [7] who mentioned that "an increasing number of jurisdictions have been engaged in the development of quantitative criteria relating to trace constituents in soil water and sediment" and stated that, "in a number of instances little attention has been paid to variability. . .", finishing with the observation that this was due to the fact that "use of terms such as baseline value has often been assumed to imply that the natural background level for each element is constant".

In environmental geochemistry it is difficult to define background, and this term is settled as "the concentration of a substance in a sample material at a distance to a source where the concentration of the substance can no longer be proven to originate from this source", therefore it is assumed an homogeneous regional (geo)chemistry and that the anthropogenic source is the only cause of variation in relation to the studied element [4].

In the United States of America, background concentrations are often used as soil clean-up criteria following industrial activities, thus definition would be "the elemental concentration(s) before industrialization", which was usually not documented. Reimann & Garrett (2005) [4] stated that "finding equivalent archival material that has not undergone chemical changes, diagenesis, post-formation or deposition is difficult. Environmental materials are part of a living system in an overall biogeochemical cycle, and instances where materials have been frozen-in-time are rare". Regarding the difficulties to find archival materials, ***ambient background*** is used to describe the unmeasurably perturbed and no longer pristine natural background.

Pre-industrial background term is sometimes used when data either come from age-dated materials or are collected from areas believed to represent a survey/study area in its supposed pre-industrialization state [4].

Finally, a concept generally used in environmental sciences is the ***enrichment factor*** (EF). These factors were initially developed to speculate on the origin of the elements in the atmosphere, precipitation or seawater (e.g., [12, 13, 14]). This use was extended to the study of soils, lake sediments, peat, tailings and other environmental materials (e.g., [15, 16]) and have increasingly been used to identify geogenic vs. anthropogenic element sources in environmental studies (e.g., [15, 16, 17, 18, 19]). Several authors have questioned the use and interpretation of the EFs in environmental sciences (e.g., [20, 21]). These questionings are related to the variable composition of the Earth's crust at any given point compared to the global average; the natural fractionation of elements during their transference from the crust to the atmosphere; and the differential solubility of minerals in the weak chemical digestions used in environmental studies [20]. Reimann & de Caritat (2005) [21] recommend the use of local EFs or not to indiscriminately assume that high EFs are related to anthropogenic contamination; this is basically because EFs can be high or low due to a multitude of reasons, of which contamination is but one [21]. Additionally, these authors conclude that "using EFs to detect or *prove* human influence on element cycles in remote areas should be avoided because, in most cases, high EFs cannot conclusively demonstrate, nor even suggest, such influence" [21].

1.1.1.2 Importance of geochemistry in environmental sciences and environmental legislation

Geochemists have been aware of the natural variability of elements in the environment for over 50 years and they know the importance to provide data and maps on, and explain the concept of, background variations of elements to regulators and the general public [4] to improve environmental legislation and the life quality of the population.

To deal with this point, another approach is to set maximum admissible concentration (MAC)[3] values for environmental purposes on the basis of ecotoxicological studies and risk assessments (e.g., [22, 23]). According to Reimann & Garrett (2005) [4], the challenge with this approach is translating the results of ecotoxicological studies into appropriate levels in the solid-phase materials, soils and sediments. Regulatory levels, once set by a state authority, have important financial consequences. For instance, clean-up to levels below the natural occurring

[3] All acronyms are defined in Appendix A.

concentrations can be prohibitively expensive, usually makes no sense, and will likely damage the ecosystem to be protected [4]. There exist cases where natural elevated or too low natural concentrations of elements in drinking water, soils or crops pose a severe health risk to the general population. Two examples correspond to natural high concentrations of As in drinking water wells in India and Bangladesh (i.e., arsenosis, [24, 25]) and on the contrary, selenosis caused by scarce Se concentration (e.g., [26, 27]). In an ideal world, the regulatory levels would preserve the ecosystems they are set to protect. In that context, regulatory levels could even be set in a framework of ecotoxicological considerations, above the upper limits of natural background variation if natural background levels did not cause ecosystem damage [4]. Any definition of a regulatory level should be accompanied by an explanation of how it was derived and the issues taken into consideration. To cover all deleterious situations, it would be necessary to define another set of regulatory lower levels to avoid deficiency-related problems [4].

In the case of South American countries there exists a high necessity to perform studies regarding the natural geochemical characteristics of soils, sediments and water reservoirs. This will improve the environmental legislation and will also allow the development of sustainable industries, specially in the mining, agricultural and silviculture lands, which are the most affected by anthropogenic activities.

1.1.2 Conclusions

In this section, a series of geochemical concepts related to environmental sciences were reviewed. Different works have demonstrated that the idea of being able to define background via a statistical exercise alone is illusive (e.g., [21]) and to estimate the properties of background, the presence of, or complete absence of, anomalous samples (outliers), spatial scale, location, the kind of sample material, and why and for what purpose the background is needed all have to be considered. This implies that no single background range exists for any one element in any sample material except for specific, often spatially local, instances. Background may change both within a project area and between project areas, reflecting the diversity of the physical world. Furthermore, geochemical maps at different scales covering a variety of sample materials and the whole surface area of the planet are needed as basic information for society, just like geological, geophysical and topographical maps.

Table 1.1: Mean concentration of major constituents of riverine water and marine water (from Ryley & Chester 1971 and Martin & Whitfield 1983 [28, 29])

	concentration marine water $[mg \cdot L^{-1}]$	*concentration riverine water* $[mg \cdot L^{-1}]$
Na^{+}	10,733	5.3
K^{+}	399	1.5
Ca^{2+}	412	13.3
Mg^{2+}	1,294	3.1
Cl^{-1}	19,344	6.0
SO_4^{2-}	2,712	8.7
HCO_3^{-}	142	51.7
SiO_2^{3-}	-	10.7

1.2 Trace metals and metalloids in aqueous systems

1.2.1 Introduction

In this section, a brief introduction on the biogeochemical controls interacting in the behaviour of metal(loid)s (MTE) in aquatic systems is given, together with the anthropogenic influence in these media. Main topics discussed are: (1) matter transference between hydrosphere and anthropogenic impact within these transferences, (2) processes affecting MTE speciation, and (3) mechanisms and models of sorption explaining metals behaviour. At the end of this section, a critical discussion on sequential and single extraction procedures is given. This discussion is based on methods used in the literature for the study of solid state MTE partitioning in the aqueous systems. Finally, comments on the chosen extraction procedures are briefly presented.

1.2.2 Matter and hydrosphere transference

Schematically, the Earth may be divided into four compartments or reservoirs, which are: (i) *the atmosphere*, (ii) *the hydrosphere*, (iii) *the lithosphere* and (iv) *the biosphere*. These four different compartments are in continuous interaction by means of matter interchange (i.e., flux). The estimation of these matter fluxes and the parameters governing them will allow documenting and quantifying the biogeochemical cycles involved in the interactions among these compartments. These matter transferences, concerning major and trace elements, are depicted in figure 1.2.1. Each of these four compartments corresponds to an important reservoir of minerals.

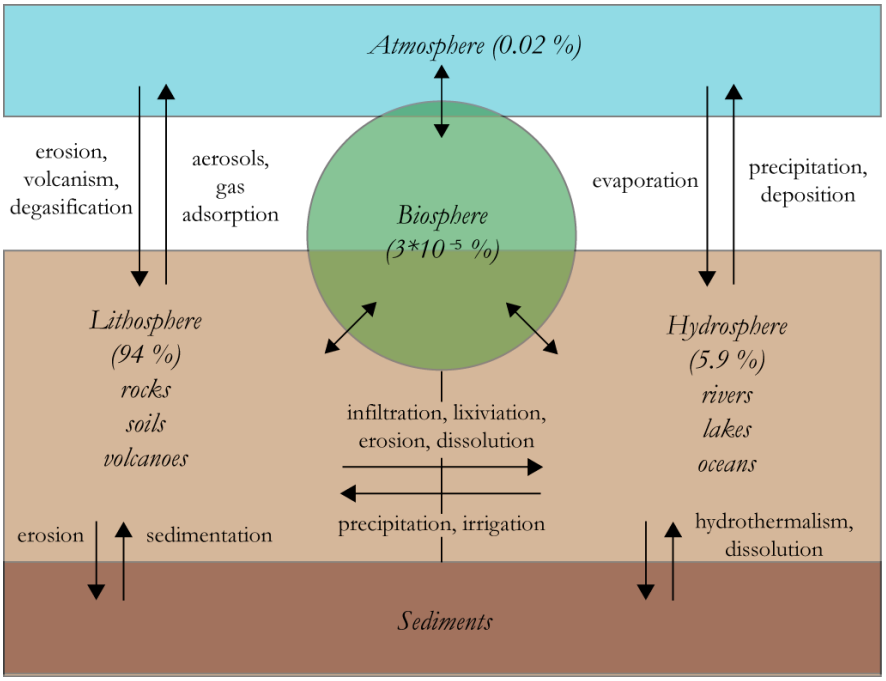

Figure 1.2.1: Matter transference scheme between different Earth reservoirs (from Fergusson 1990 [30])

The hydrosphere, that involves the oceans, superficial (rivers and lakes) and subterranean waters, plays a preponderant role in the transference of matter between these four compartments via the hydrological cycle (Fig. 1.2.2). 80% of water on the Earth is represented by the oceans, 19% by the interstitial waters within rocks, 1% by ice, $2{\cdot}10^{-3}$% by rivers and lakes, and finally $8{\cdot}10^{-4}$% by the atmosphere [31]. Although rivers and lakes only represent a small fraction of the hydrosphere, water flux rate through them is relatively fast in relation to the oceans (3,550 years), with an average residence time of 2 to 6 months for rivers and between 50 to 100 years for lakes [32]. Nevertheless, poorly studied exceptions that may play an important role in the hydrologic system of specific areas, such as Lake Titicaca (Bolivia and Peru) with an average residence time of 1,343 years[4] or Lake Vostok (Antartica) with 13,300 years exist [35].

Numerous studies have documented the chemistry of particulate and dissolved matter (e.g., [31, 36, 37, 38, 39]). The composition of dissolved major (Table 1.1) and trace (Table 1.2) elements in natural waters is the result of the interaction of these with other reservoirs and the contact with gases (O_2, CO_2, among others), solids (diverse reactive geological and biological materials; [40]) and liquids that encounter water streams within the hydrological cycle. Par-

[4]Estimate of volume of water residence time of 70 yr and a conservative non-volatile constituent residence time of 3,440 yr [34].

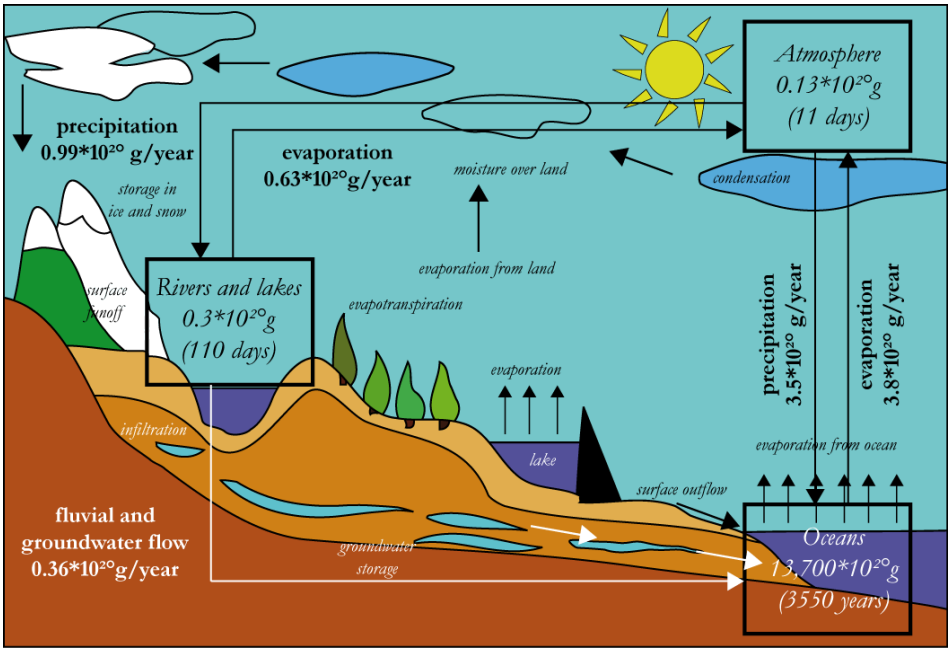

Figure 1.2.2: Hydrological cycle, residence times and matter flux between reservoirs (modified from Drever 1988 [33]); numbers are from Garrels & Mackenzie 1971 [31].

Table 1.2: Mean concentration of trace elements in marine water and particulate and dissolved fluvial phase (from Martin & Whitfield 1983 and Martin & Meybeck 1979 [29, 41]).

	rivers (world mean)		*sea water*
	particulate $[mg \cdot kg^{-1}]$	*dissolved* $[\mu g \cdot L^{-1}]$	$[\mu g \cdot L^{-1}]$
V	170	1.0	2.0
Cr	100	1.0	0.2
Co	201.1	0.2	0.05
Ni	90	0.5	0.5
Cu	100	1.5	0.5
Zn	250	30	2.0
Cd	1	0.05	0.05
Pb	100	0.1	0.03
Mo	3	0.5	10
Th	14	0.1	<0.0005
U	3	0.24	3.3
Fe	48,000	40	2.0
Mn	1,050	8.2	0.2
Al	94,000	50	1.0

ticulate phase composition in rivers (suspended matter) and sediments (particulate matter), depends mostly on primary rock (i.e. the rock that gave rise to these particles) and also on the result of particle evolution in contact and interacting with the dissolved phase. Therefore, a crucial fact is to recognize the main sources of minerals in both, the particulate and dissolved phase. This knowledge is helpful in understanding the metal biogeochemical cycle allowing the assessment of transport, speciation and anthropogenic impact of metals.

1.2.2.1 Geologic contributions

Close to 80% of major and trace elements in sediments and natural waters derive from the physical and chemical weathering of rocks. The transport of these elements by rivers is responsible for most (approximately 90%) of the solutes and particulate matter contributed to the oceans [41]. Main compounds transported by rivers are: (i) nutrients (e.g., P, N, Fe), (ii) oxyhydroxides (Fe and Mn) acting as MTE traps (e.g., [42]) and (iii) dissolved elements (Ca^{2+}, Mg^{2+}, Na^{+}, K^{+}, HCO_3^{-}). Factors controlling physical and chemical weathering, and thus dissolved and particulate composition of riverine and lacustrine waters, are mainly of climatic order, particularly, temperature, precipitation and runoff (e.g., [36, 43, 44]).

Element mobility through rock weathering, depends on: (i) sensitivity of the mineral to chemical weathering and (ii) weathering byproduct's capacity to trap cations in their atomic structure [33, 45, 46]. During weathering, the order of major element mobility is generalized as follows: $Na \geq Ca \geq Mg > K > Si$ [45, 47], mainly transported in silicates. The lower mobility of K is mainly related to its tendency to generate secondary argyles (illite) and its presence in resistive minerals. The lowest mobility of Si is linked to its occurrence in accessory and very resistive minerals such as quartz. During the course of mineral alteration, Al is considered to be the less soluble element in the ionic state (i.e. associated with the particulate phase) [31]. After being discharged from the primary source and transported by rivers in particulate form, Fe and Mn, in alteration profiles, are more mobile than Al and similarly precipitated in the insoluble phases (generally oxides) [41].

1.2.2.2 Atmospheric contributions

Chemical elements from aquatic systems are importantly influenced by atmospheric contributions. These contributions can be by both precipitation (wet deposits) and/or aerosols (dry deposits). The main dissolved major components contributed by the atmosphere are sulphates and nitrates, and less importantly alkaline and alkaline-earth cations [48]. Nevertheless,

aerosols are indicated as the main vectors of MTE contribution to the natural waters from the atmosphere [49]. The main sources of atmospheric aerosols are contributed by eolian particles taken from soils, volcanoes, marine waves and forest fires [50, 51]. Other studies have also demonstrated that particulate organic matter (POC) corresponds to the principal component of rural area aerosols [52] and that this biogenic source can represent between 30 and 50% of MTE in the aerosols [49]. Therefore, the quality of the minerals contributed by the atmosphere will depend on the geographical (urban or isolated areas), climatic and anthropogenic (industrial or rural activities) factors.

1.2.2.3 Biologic component

The biosphere is in close relationship with the other reservoirs (Fig. 1.2.1), and importantly influences the chemical-physical characteristics of the systems [40]. Therefore, biological communities can physically modify aqueous ecosystems by transport and by remobilization of minerals and MTE. This is mostly the case of bioturbating organisms, which remove sediments releasing interstitial water to the bottom waters (often showing lower concentrations of MTE than pore water), because of the frequent presence of anoxic horizons some centimetres underneath the water-sediment interface [53, 54, 55]. On the other hand, as oxygen depth penetration increases in sediments, these bioturbating organisms move the redox fronts and disturb the oxide-reduction reactions that take place during sediment diagenesis [56].

The influence of biological systems in the aquatic environment is therefore of chemical nature, and the main mediators of such interactions are microorganisms [57]. Bacteria actively influence metal partitioning between dissolved and particulate phases, intervening in the reactions of authigenic precipitation and mineral dissolution, and also modifying the chemical conditions of the environment in which bacteria evolve through natural metabolic processes. For instance, the oxidation of Mn(II) to Mn (IV) through bacteria and the subsequent precipitation of Mn oxides has been widely evidenced (e.g., [58]). Numerous studies have demonstrated the dissolution of mineral phases by bacterial reduction during organic matter (OM) decomposition in sediments (e.g., [59, 60]). In this context, bacteria use minerals as the final electron acceptor, linking OM oxidation with reduction of metallic ions (Mn, Fe), thus causing mineral dissolution. In the case of Fe, oxide dissolution in natural environments is dominated by bacteria. This is explained by the slowness of abiotic reaction kinetics, implying that the oxidized form of Fe(III) is dominant in sediments in spite of the anoxic conditions frequently found below the water-sediment interface (WSI) [61, 62]. Evidence demonstrating that bacterial reduction

kinetics depend on the crystallization state of iron oxides exists, amorphous forms [e.g., ferrihidrite ($Fe_5HO_8{\cdot}4H_2O$)] are more rapidly reduced than crystalline iron oxides [e.g., goethite (α-FeOOH)] [63].

The biological component plays an important role in the biogeochemical cycles of C, N, S and in chemical processes that cause Fe, Mn and trace element intervention [64]. In sediments from aquatic environments, this component plays a preponderant role in the oxidation-reduction reactions related to OM degradation during early diagenetic processes.

1.2.2.4 Anthropogenic component

Regardless of the Earth's reservoir, human activities disturb global scale geochemical cycles in relation to major elements and MTE. The hydrosphere is particularly sensitive to anthropogenic contributions, mainly due to important matter fluxes and a relatively short residence time. Therefore, contaminant introduction influences and significantly disturbs major and trace elements composition in waters, suspended particles and sediments in fluvial and lacustrine environments [65]. Human activities release metal(loid)s to the environment, which act under multiple vectors and varying forms (e.g., dissolved and/or particulate).

The input of anthropogenic origin metal(loid)s can be done directly into the aquatic systems, and importantly through domestic and industrial effluents. An indirect MTE release to these systems is related to mining activities. Exploited ores are generally sulphide-bearing minerals (e.g., chalcopyrite-$CuFeS_2$, sphalerite-ZnS, cinnabar-HgS, galena-PbS), that usually contain traces of As, Cd, Sb, among other elements. Mining activities affect reduced areas; however mine waste deposits correspond to one of the most important sources of MTE to be released into the environment. Ore deposits are commonly associated with pyrite and marcasite (FeS_2), the predominant acid mine drainage (AMD) producers [66]. Sulphide-rich rocks in contact with meteoric waters and atmospheric oxygen give rise to fast sulphide alteration, involving MTE release in dissolved form [33]. When these weathering products reach fluvial systems (mainly by runoff transport) an interaction of dispersed metals in both dissolved and particulate forms, occur. Mechanic erosion of mine slag waste can also discharge particulate metals in fluvial streams. As a function of natural recycling efficiency, these metals can be transported far from the source location by rivers [67], thus causing a diffuse contamination in soils, sub-soils and sediments [68].

On the other hand, sources of metals that release particles directly into the atmosphere through mining activities, fossil energies combustion, and industrial manufacture of variable

and multiple products, release metals that are immediately introduced into the superficial waters and soils through precipitation. For instance, estimates of global scale atmospheric inputs determined that 85% of Cd, 41% of Cr, 56% of Cu, 65% of Ni and 66% of Zn in the atmosphere were originated anthropogenically [49]. Similarly, it must be mentioned that indirect MTE sources into the aquatic systems are anticorrosive paints (Cd, Hg, Se, Pb), agricultural fertilizers (Cu, Zn, Se), pesticides (Hg, As), combustibles (Pb), and medical, pharmaceutical and cosmetic products (Ag, Cu, Zn, Sn, Pb, Cd, Hg), among others.

1.2.3 Biogeochemical controls on metallic components in aqueous systems

Aqueous systems are complex and dynamic environments where bioturbating organisms together with microorganisms can change redox fronts as oxygen reaches deeper sediment horizons. Understanding the dynamics of metal behaviour in freshwater environments has been a major focus of environmental geochemists for several decades, and interest in this area continues to grow as regulatory bodies are faced with the myriad complexities of how to regulate, mitigate and remediate contaminated water bodies [57]. Therefore, recognizing the facts and processes controlling the mobility and reactivity of metals in these systems is necessary, and is provided through the study of the transformation of metals in the hydrological system and the assessment of anthropogenic contributions into natural waters.

1.2.3.1 Differences between: dissolved, colloidal and particulate phases

It is well established that trace element concentration in aquatic systems depends on the filter size used to separate dissolved and particulate matter. As an arbitrary sub-division to differentiate both fractions a porosity of 0.45 μm is used. Despite this fact, a continuum of particle sizes exists (e.g., [69]). The existence of this continuum (Fig. 1.2.3) has led to the operationally defined fraction named colloid (0.45 μm - 1 nm) which has a main influence on the speciation of chemical elements. Numerous speciation studies have found non-negligible quantities of MTE associated with the colloidal fraction in different aquatic systems (e.g., [70, 71]). The behaviour of colloidal trace elements is absolutely different from dissolved fraction elements because colloids can suffer relatively fast coagulation and sedimentation processes in contrast to the dissolved phase [69]. Colloids can be of organic or inorganic origin (Fig. 1.2.3). Although colloids cannot be separated by classic filtration, they present similar physical-chemical

properties to solids. Common inorganic colloids correspond to Fe, Mn and Al oxyhydroxides, clays and silicate phases. Generally, this colloid type is amorphous and characterized by large specific surfaces with strong absorption capacity [72]. The organic colloids correspond mainly to humic and fulvic acids. The inorganic and organic colloids generally are in close association and two types of relationships are described for natural waters, (i) *organic colloids and clays* (e.g., [73]) and (ii) *organic colloids and Fe-oxyhydroxides* (e.g., [74]).

1.2.3.2 Contaminants speciation

From a chemical point of view, speciation is defined as the determination of the specific form (monatomic or molecular) or the configuration in which an element or a group of different atoms can be possibly or effectively present in different matrices [75]. From an environmental point of view, speciation is defined as the distribution of the chemical species of a given element in a system [76][5]. Metals are differently reactive, toxic or available for the biota [78]. In fact, total concentration measures contribute only with little information for the prediction of MTE behaviour [77, 79, 80].

1.2.3.3 Superficial reactions

Reactions occurring at solid surfaces play a dominant role in determining metal partitioning between the solid and dissolved phases, and thus, the potential impact of metals in aqueous environments [81].

Reactions occurring at the interface of solid surfaces with their surrounding aqueous medium, stem from the fact that solids carry a surface charge in aquatic environments and thus attract counter-ions from solution to balance that charge. For example, in figure 1.2.4 are shown illustrative reactions that can interfere in the surface of a metal(loid) oxide (from [57]). The potential for reactions involving metal(loid)s to occur at solid surfaces arises from: (i) the existence of unfulfilled charge requirements of molecules or functional groups [e.g., hydroxyl (-OH), carboxyl (-COOH), phosphoryl ($-PO_3^{2-}$)] at the solid surface; (ii) the polar properties of water molecules; (iii) the presence of solution or dissolved elements that also possess non-neutral charges; and (iv) the inherently dynamic nature (strongly driven by biological processes) of aquatic systems that causes constant disequilibrium within the system and the impetus for

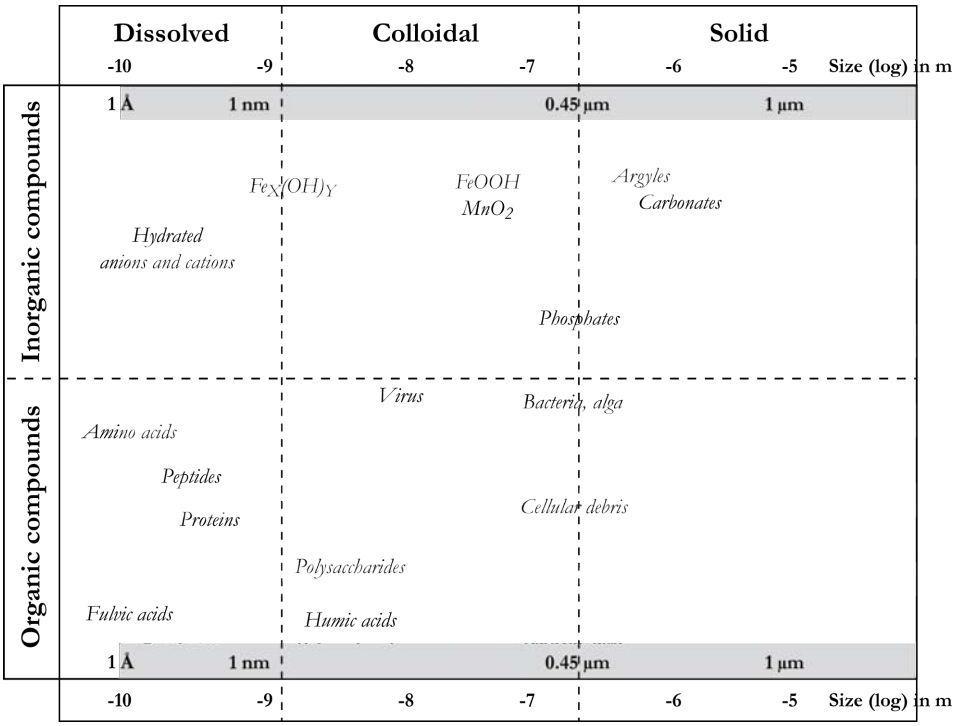

Figure 1.2.3: Organic and inorganic colloids distribution as size function in aqueous systems (from Buffle & Van Leeuwen 1992 [85]).

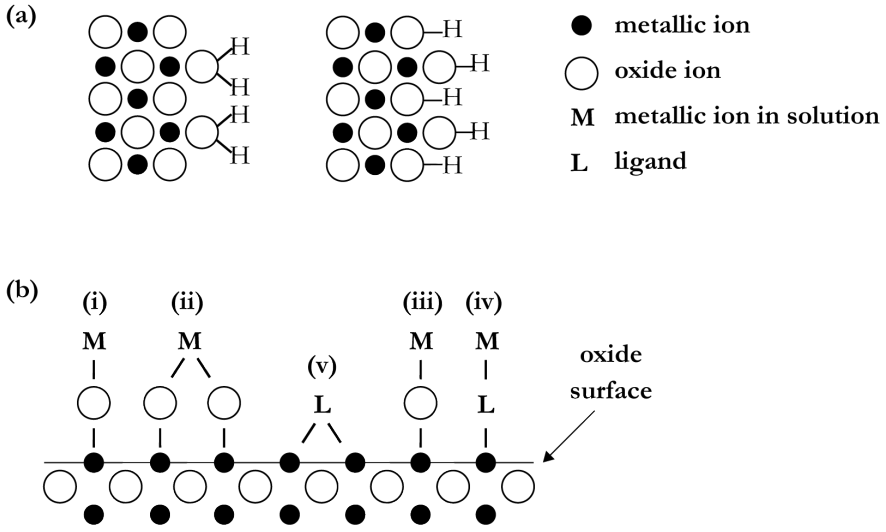

Figure 1.2.4: (a) Metallic oxide transversal surface; (b) possible complexion reactions in the oxide surface (modified from Warren & Zimmerman 1933 [83]).

reactions to occur [57].

Dependent on their respective dissociation constants (i.e. pKa), functional groups at a solid surface can become negatively charged through proton loss (in response to changes in the system chemistry that affect the pH, such as surface functional groups buffering pH by donating protons to solution as solution pH values increase). The deprotonated functional group can then subsequently act as a binding site for positively charged ions such as metal(loid)s [57].

In general, any reaction involving reactions concerning a solution ion with a solid surface functional group that results in a surface association being formed is referred to as a ***sorption reaction*** [82, 84]; sorption includes both covalent bonds and electrostatic complexes, which differ in the strength of their associations with the solid surface. Sorption interactions that include both are called ***adsorption interactions***. Sorption reactions in which a covalent bond is formed between the solute ion and the surface species are termed ***inner sphere complexes*** [57]. In contrast, ***outer-sphere complexes*** are those in which the solute ion and surface species are attracted by electrostatic forces alone. Solutes sorbed as outer-sphere complexes are more weakly associated with the solid surface, and thus, are more easily re-solubilized [57]. Finally, absorption reactions are related to chemical species diffusion within a solid surface [82].

Metal(loid)s are mainly absorbed in the following mineral particle types: non-argillaceous silicates (silica, opal, quartz, feldspar), clays (alumino silicates: illite, smectite, montmorillonite), carbonates [calcite: $CaCO_3$, dolomite: $CaMg(CO_3)_2$], phosphates [apatite: $Ca_{10}(PO_4)_6(OH)_2$], sulphides [pyrite: FeS_2], sulphates [barite: $BaSO_4$], and finally, Fe- and Mn-oxyhydroxides.

1.2.3.4 Parameters controlling superficial reactions and MTE speciation

Generally, the main parameters governing superficial reactions and the speciation of metals are the following:

pH. This parameter dictates the partitioning among dissolved and solid fractions and all the parameters depending on it (e.g., mobility, reactivity, bioavailability, bioaccumulation and toxicity). In aqueous systems pH is considered to be the master variable controlling metal behaviour [57].

Ionic strength. Metal sorption increases with decreasing ionic strength [86]. Particularly,

[5] To this idea other authors include the notion of chemical species transformation [77].

outer-sphere complexes based on electrostatic interactions, are more sensitive to ionic forces than adsorption interactions.

Oxidation/reduction-state. This parameter influences metal(loid) dynamics in different ways. Redox state in metal(loid)s exhibiting more than one possible oxidation state in natural waters exhibit different mobility, solubility, toxicity and reactivity [87, 88, 89]. Highly charged metallic ions [e.g., Cr(VI), As(V), Mn(VI)] tend to exist while oxy-anions in moderate to high pH solution are likely to form covalent interactions. Due to a strong charge, these ions are attracted to the negatively charged sites, thus becoming potential toxins to living organisms [90, 91]. Oxidation-reduction state similarly exerts an influence on the partitioning between dissolved and particulate phase [92, 93].

1.2.3.5 Manganese and iron oxyhydroxides

In the pH range of natural waters, inorganic adsorbents of the type oxyhydroxides of Fe and Mn exhibit a particular affinity to metallic ions because of large specific surface and negative charges in superficial sites [94]. These oxides are frequently found in natural waters in the forms of: (i) suspended fine particles, (ii) films recovered by other mineral types as clays or carbonates (e.g., [95, 96]), or (iii) organic particles [97]. Despite the fact that the mass of Fe- and Mn-oxyhydroxides is negligible in both suspended matter and sediment, these oxides plus OM can be considered as the dominant phases of metal(loid) biogeochemistry in aqueous systems [84, 98].

Metal(loid) sorption in particular mineral phases can be influenced by: (i) crystallinity [99]; (ii) number of available sites, impurities and/or co-precipitated elements [100]; (iii) organic superficial film presence and (iv) particle size [88, 89].

Oxyhydroxides of Fe and Mn are formed by the oxidation of the divalent ions $Fe^{2+}$and Mn^{2+} and subsequent precipitation in the form of oxide, hydroxide or oxyhydroxide[6].

Iron-oxides. These compounds are stable, poorly soluble and with a strong crystallization capacity [101]. Indeed, frequently Fe oxides precipitate as small particles characterized by high surface/volume rates [57] related to highly reactive particles. A great variety of Fe oxides are formed from a common precursor oxide [$Fe(OH)_3 \cdot H_2O$] rapidly transformed

[6] All these compounds are grouped under the generic name of oxides.

in lepidocrocite (γ-FeOOH) and in ferrihidrite ($Fe_5HO_8{\cdot}4H_2O$) [102] in the range of pH of natural waters; both minerals are poorly crystalline [103]. These unstable forms evolve with time to more crystalline species, which are goethite (α-FeOOH) and hematite (α-Fe_2O_3) [104, 105], both forms are simultaneously present in sediments and one of these two forms can dominate depending on pH, temperature and environment composition; under natural water conditions goethite is the principal oxide [99].

Manganese-oxides. Amorphous or poorly crystalline forms are the main oxidation products for Mn oxides [98, 106]: $MnIVO_x$ ($1 \leq x \leq 2$), thermodynamically unstable, forms hausmanite (Mn_3O_4) and feitknechtite (β-MnOOH) [107]. Those forms evolve rapidly into todorokite (γ-MnOOH) a metastable form. Various oxides can be found in the sediments due to ageing of the mentioned forms, the most common are biernessite (γ-MnO_2) and amorphous manganite (δ-MnO_2) [108]. It has been demonstrated that Mn oxides represent effective traps for diverse metals (e.g., [98, 109]) and are potentially more reactive than Fe oxides (e.g., [58, 110]). Although Fe oxidation may be linked to abiotic processes, oxidation of Mn(II) into Mn(IV) is mainly related to microbial interactions [111].

1.2.3.6 Organic matter and trace metal toxicity

The natural organic matter (NOM) includes all the detritic OM in a reservoir or natural ecosystem, excluding living organisms and anthropogenic origin compounds [112]. The NOM corresponds to an important constituent in most of the aquatic systems. Sources of OM are multiple and include alochthonous contributions, sediments as well as autochthonous primary productivity [57]. This last is constituted by aquatic biota excretions and degradation by-products, in this group phytoplanktonic blooms are one of the principal sources [113].

Usually, NOM is divided in three operationally defined categories: (i) dissolved OM (DOM < 0.45 μm); (ii) particulate OM (POM > 0.45 μm); (iii) humic substances (humic and fulvic acids 10^{-2}-10^{-3} μm). Humic acids (soluble in basic water) and fulvic acids (soluble in acid and alkaline solution) both come from terrestrial OM degradation and thus their concentrations in the aqueous environment depends on the nature of the basin draining soils. Estimations indicate that fulvic acids represent between 40 and 80% of the NOM in fresh water environments, while humic acids only represents between 5-10% [113].

The reactivity of OM depends on its: (i) poly-electronic nature and (ii) intrinsic hetero-

geneity [114]. The three dominant categories of functional groups in the NOM are carboxyl (-COOH), hydroxyl (-OH) and amino (-NH_2), each one susceptible to complexing metals by ionic interchange, superficial adsorption or quelation [115].

Superficial characteristics of the NOM involve greater complexation competition than Fe- and Mn-oxyhydroxides. Indeed, Fe- and Mn-oxyhydroxides exhibit just one functional group (i.e. hydroxile), on the contrary, organic compounds are characterized by presenting a diversity of functional groups. Furthermore, a hydroxyl functional group on the surface of NOM shows sorption capacities for low pH (carboxyl pH ~3-5) to high pH (amino: pH ~9; hydroxyl: pH ~10) [57]. Thus in comparison to oxides, NOM shows stronger and more common bonds with organic functional groups [116]. It is thought that the potential release of elements from NOM as a function of physical-chemical changes in the system, is lower than that of mineral phases [57].

1.2.3.7 Composed surfaces

In the paragraphs above, different mineral phases and organic roles in metal(loid)s complexation were discussed. Nevertheless, in aqueous systems the existence of these phases in isolated manner is not common, on the contrary, these associations are found in the form of heterogeneous and singular associations, thus complexation capacities for dissolved metal(loid)s will depend in the type of association. To explain these linkages and metal(loid) reactivity, contradictory theories have been proposed: (i) ***additively theory*** that describes the sorption capacity of a compound surface as the sum of each individual sorption capacity [117, 118]; this means that the presence of a given compound is not affecting the sorption capacity of the other [118, 119]. (ii) On the contrary, the ***non-additively theory*** establishes that the sum of each reactivity phase individually is not equal to the total reactivity of the group [82, 120], meaning that each phase can diminish as well as favour the global absorption of the association as a consequence of non-linear interactions between the different phases.

Oxides/NOM. These are the most common associations. Generally, the adsorption capacity of a metallic ion on the surface of a mineral under OM presence increases with low pH and decreases under high pH [121, 122]. For instance, increases have been shown for Co^{2+}[118], Cd^{2+}[123] and Zn^{2+}[124]. Nonetheless, NOM effects on metal(loid) sorption on the surface of oxides not only depends on the pH, but similarly on: (i) oxide nature, (ii)

humic substance nature, (iii) relative forces of the OM-metal interactions, (iv) superficial extension of oxides recovered by humic substances, and (v) initial concentration of NOM and the organic electrolyte [124]. On the other hand, studies of the absorption effects of NOM on the surface of oxides (hematite) within oxide-metal interactions, demonstrated that: (i) global sorption in compound surfaces of metallic ions with a high affinity to organic functional groups (e.g. Cu), is lower due to the use of certain organic sites for the union with the oxides; (ii) inversely, global sorption of metallic ions that exhibits superior affinity for oxide functional groups (e.g., Cd), is more important due to the negative charge of the compound increased by the association with NOM.

Clays-oxides-OM. These associations are often found. In this kind of configuration, despite the fact that clays posses a high cationic exchange capacity, they are not a dominant phase for adsorption due to competition with OM and oxides coated by clays. In natural waters, the relative complexation capacity of these phases is typically represented by the following sequence: Mn oxides > humic acids > Fe oxides > clay minerals [125].

Oxide-oxide. These associations are characterized by precipitates of amorphous oxides coating older and less reactive oxides.

Mineral-bacteria. Laboratory studies have demonstrated the existence of *mineral - bacteria associations* (e.g., [126, 127, 128]) or even *mineral-OM-bacteria* interactions (e.g., [129, 130]). The principal conclusions of these experimental studies are: (i) in *clays - bacteria* and *Fe oxides-bacteria* associations, the organic fraction is dominant in complexing metals; (ii) bacteria-rich surfaces exhibit an increased quantity of absorbed metals in relation to oxides.

1.2.3.8 Early diagenesis processes

Parameters controlling speciation, reactivity, bioavailability, dissolved/particulate matter partition and transport of MTE in aqueous systems were introduced in the previous paragraphs. The question remaining is: .... Subsequently to carrier phase deposition, what happens to MTE?

Studies performed on marine cores have suggested that changing redox conditions in sediments are responsible for MTE cycle variability as well as the accumulation of several transition

metals [131, 132]. Shaw *et al.* (1990) [133] showed that surface particle modification or metallic speciation intervening in the course of early diagenetic processes of sediments, is capable of remobilizing absorbed MTE on the surface of sedimentary particles. These changes in the chemistry and mineralogy of deposited particles as well as interstitial water chemistry are the direct consequences of POC mineralization during early diagenetic processes. Mineralization is widely governed by biological activity related to microorganisms that live in the first few centimetres of bottom sediments, and is described by a vertical sequence of redox reactions, in which: (i) oxygen is reduced close to the WSI, (ii) Mn nitrates are reduced, (iii) Fe oxides become active, (iv) sulphates are formed and (v) finally methane-genesis (Table 1.3; [134, 135]). Indeed, OM oxidation needs an electron acceptor. The acceptor that produces the highest free energy during OM degradation will govern the order of intervening reactions [134, 136]. This diagenetic sequence is essentially managed by vertical changes in interstitial water and sediment chemistry (Fig. 1.2.5); however, in sediments where the relative position of oxidized and reduced compounds is disturbed y bioturbation, the vertical zoning of reactions might be changed.

During early diagenetic processes, oxidation/reduction, dissolution/precipitation and intervening speciation changes, particularly implying Fe- and Mn-oxyhydroxides and sulphides, play an overwhelming role during the sedimentary cycle of MTE, controlling adsorption/desorption reactions [139, 140]. These processes are well defined and documented for marine and estuarine environments, despite this fact, little is known about diagenesis in continental aqueous systems.

1.2.4 Conclusions

The factors controlling the dynamics, transport, reactivity and bioavailability of MTE in aqueous environments are complex, heterogeneous and associated with a series of physical, chemical and micro-biological processes. The main factors are (i) metal(loid) speciation, (ii) liquid-solid partitioning and (iii) the kind of association in the solid phase (i.e. superficial complexation or precipitation). Interactions between these main factors are schematically summarized in figure 1.2.6.

From this chapter, it is clear that understanding early diagenetic processes within continental basins is necessary. These studies are not well documented, therefore MTE behaviour in continental aqueous basins is yet practically unknown, an important factor taking into account

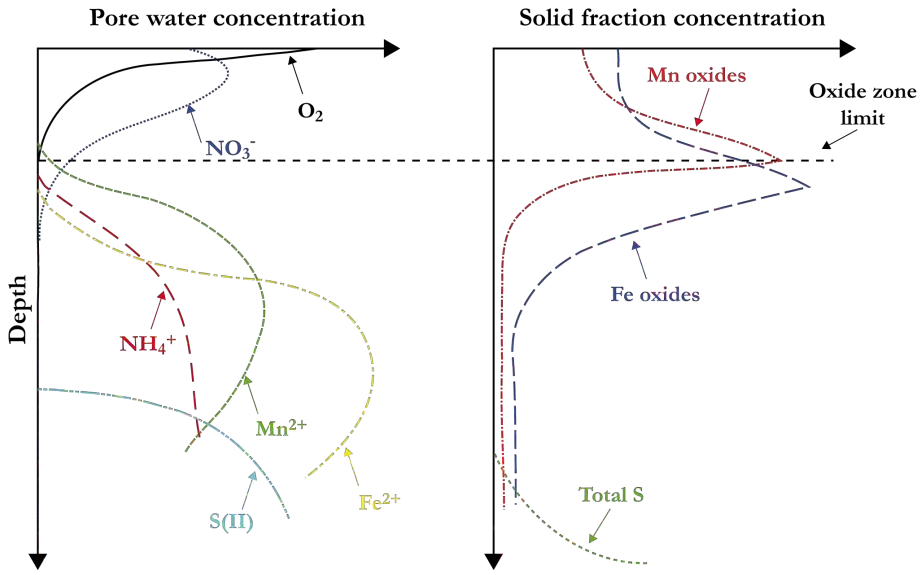

1. O_2 consumption attributed to oxic OM degradation (reaction 1) and to the reoxidation of anaerobic OM degradation [141]

2. Nitrate pick within oxic zone is attributed to the reactions that drive bacterial nitrification from organic N (reaction 1, Table 1.3) and to the diffusion of ammonium with depth (reaction 6, Table 1.3).

3. Nitrate consumption below oxic zone is because of bacterial denitrification (reaction 2, Table 1.3).

4. $NH_4{}^+$ production from anaerobic mineralization of organic N (reactions 4 and 5, Table 1.3).

5. Dissolved Mn^{2+} and Fe^{2+} production within anoxic sediments is attributed to Fe- and Mn-oxyhydroxides assimilative reduction by bacteria (reactions 3 and 4, Table 1.3), involved in particulate Fe- and Mn-oxyhydroxide decrease.

6. Dissolved S(II) increases with depth and total S (S_{tot}) increases because of sulphate reduction (reaction 5, Table 1.3)

Figure 1.2.5: Schematic representation of profiles from compounds intervening during organic matter (OM) degradation in early diagenetic processes (from Froelich *et al.* 1979 [134])

Table 1.3: Organic matter degradation sequence [134, 135] (OM=$C_{106}H_{263}O_{110}N_{16}P$; [137])

Oxygen consummation by aerobic respiration and nitrate production	
$138O_2+OM+18HCO_3^-\rightarrow 124CO_2+16NO_3^-+HPO_4^{2-}+140H_2O$	(1)
Nitrate consummation by denitrification	
$94.4NO_3^-+OM\rightarrow 13.6CO_2+92.4HCO_3^-+55.2N_2+84.8H_2O+HPO_4^{2-}$	(2)
Mn-oxides reduction by anaerobic respiration	
$212MnO_2+OM+332CO_2+120H_2O\rightarrow 212Mn_2^++438HCO_3^-+16NH_4^++HPO_4^{2-}$	(3)
Fe-oxides reduction and ammonium production	
$424Fe(OH)_3+OM+756CO_2\rightarrow 862HCO_3^-+424Fe^{2+}+16NH_4^++HPO_4^{2-}+304H_2O$	(4)
Sulphur and ammonium production by sulphate-reduction	
$53SO_4^{2-}+OM+14CO_2+14H_2O\rightarrow 53H_2S+120HCO_3^-+16NH_4^++HPO_4^{2-}$	(5)
Methanegenesis [138]	
$OM+53H_2O\rightarrow 53CH_4+53HCO_3^-+16NH_4^++HPO_4^{2-}+39H^+$	(6)

that lakes and rivers are important sources of fresh water. Studies dealing with these thematics are deemed necessary to improve the life quality of flora, fauna and human population living within or close to continental aqueous basins.

1.3 Analysis of solid state fractionation: general concepts and state of the art

Speciation techniques can be grouped into two categories: (i) those where the total metal content is determined in operationally defined fractions, and (ii) those that measure total element concentrations [80]. Within the framework of this study, the second type of speciation technique was used. Indeed, detection methods employed (i.e. ICP-MS, ICP-OES) only measure the total element content and must be associated with separation techniques previously performed to extract the desired elemental phase.

1.3.1 Definition

Speciation analysis is defined by the *International Union of Pure and Applied Chemistry* (IUPAC) as follows: "analytical activity for the identification and measuring of the quantity

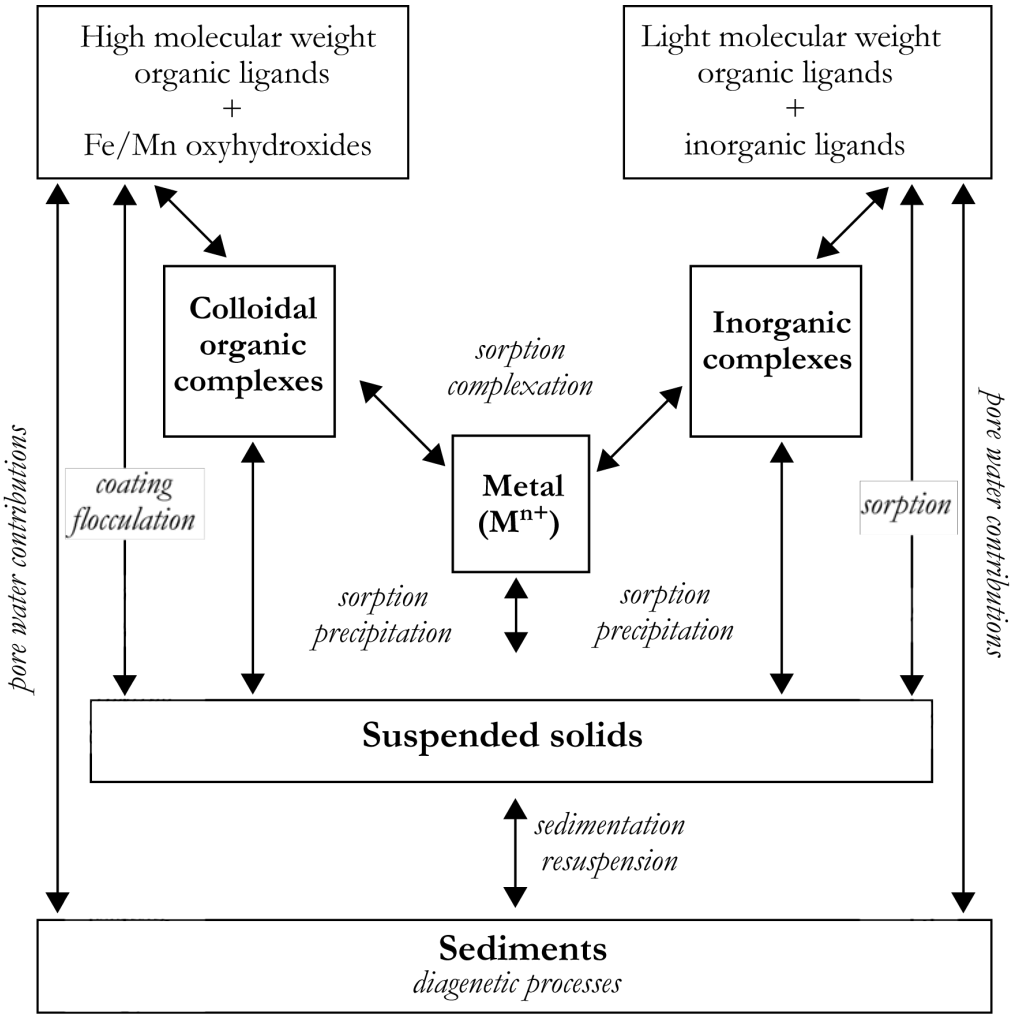

Figure 1.2.6: Principal processes and interactions between dissolved and particulate metallic species in water-sediment interface (from Salomons & Förstner 1984 [79])

of one or more individual chemical species in a determined sample" [76]. Nevertheless, taking into account the procedures and analytical techniques applied, this identification determines the contents of extractable compounds (i.e. fractionation) instead of defined chemical species. Likewise, some authors (e.g., [142, 143]) use the term extractable trace elements instead of speciation in relation to a specific reactive.

1.3.2 Why study speciation of MTE?

The estimation of the potential toxicity of a given element as a function of its chemical form is a primary question in the eco-toxicological assessment of metal(loid) pollution. This toxicity is in strong relationship with the mobility of MTE compounds [79, 144, 145, 146, 147]; therefore, special attention must be paid to the carrier phases of MTE. Indeed, MTEs trapped in the crystalline lattices of minerals are less bioavailable (i.e. less susceptible to go in to solution) than that associated with superficial sites of solids, or those linked to carbonates and/or OM. Furthermore, anthropogenic origin metal(loid)s are released to the environment in association with sensitive phases, which can change under the physical-chemical conditions of the aqueous milieu [79, 148].

Likewise, the estimation of element mobility poses the following query: What are the effects of geochemical perturbations on the bioavailability and propagation of metal(loid)s into the environment? From the environmental point of view, the term mobility acquires a negative aspect because the transference from one milieu to another usually involves increased reactivity and bioavailability of potentially toxic compounds [149].

In systems affected by solid-liquid interactions, metal(loid) speciation is strongly influenced by varying physical (e.g., adsorption, desorption, sedimentation) as well as chemical parameters (e.g., decreasing pH, change in redox conditions, organic or inorganic complexation, species transformation by microbial vectors). Potential metal(loid) release from the solid to dissolved phase is significantly influenced by pH and redox condition changes. For instance, changes from reductive to oxidizing conditions provide sulphur transformations as well as acidification of the milieu, increasing metals mobility, especially those affine to S, such as Hg, Zn, Pb, Cu y Cd [149].

Environmental distortions causing speciation changes, may also influence environmental dynamics in aqueous systems by: (i) mechanical processes involving high energy, such as sediment suspension during floods that can give rise to desorption/disaggregation processes and subse-

quently, the release of contaminants to solution [150, 151, 152]; (ii) the temporary (stationary) variations of biological activity (e.g., phytoplanktonic blooms); (iii) extreme seasonal variations within determined systems [153].

1.3.3 Extraction procedures

1.3.3.1 Principles

As shown, the partition of metal(loid)s (i.e. its chemical form) in sediments determines its behaviour in the environment. The selective chemical extraction procedure is the most complete way to determine this partition. Most of the extraction procedures described in the literature deal with metal distribution through different fractions: exchangeable (F1), carbonates (F2), reducible (F3, Fe- and Mn-oxyhydroxides), oxidizable (F4, NOM & sulphides) and residual metal(loid)s (F5). These selective extractions can be performed following two different procedures: (1) ***sequential extractions*** (based on the use of one aliquot of sample successively subjected to stronger reactives to extract each of the different solid state fractions) and (2) ***single extractions*** (based on the use of aliquots of the same sample for each attack); each one of these procedures has advantages and disadvantages.

1.3.3.2 Diversity of extraction procedures

Most of the processes described in the literature are related to sequential extraction procedures. The procedure proposed by Tessier *et al.* (1979) [154] is the most used (e.g., [155, 156]); however, an important number of extraction schemes have been proposed (e.g., [148, 157, 158, 159, 160, 161, 162]). In general. these schemes are only variations of Tessier *et al.* (1979) [154], and modifications are only changes in: (i) concentration of reactives, (ii) pH, (iii) temperature and (iv) extraction time. The lack of uniformity between the different extraction procedures (sequential or single) have prevented the comparison of results between different laboratories [143, 163, 164, 165]. In fact, various studies have demonstrated that, in the same extraction procedure, experimental variable changes can produce different MTE distributions between the studied fractions [166, 167, 168, 169].

In this context, Ure *et al.* (1993) [142] emphasized the need for a standardized procedure

for studying chemical speciation in soils and sediments. Therefore, the *Bureau Communautaire de Référence* (BCR) of the European community proposed a three-step protocol based on the Tessier *et al.* (1979) [154] extraction procedure [170, 171, 172, 173, 174, 175]. The modifications of Tessier's procedure proposed by the BCR have been tested, yet not showing a significant improvement in relation to accuracy [176]. Likewise, the standardization of speciation analysis is a problem that must be improved; this difficulty is made worse by matrix diversity in natural samples, which makes it impossible to define a unique extraction protocol in any matrix.

1.3.3.3 Selective extraction problems

The main problems related to these procedures are (i) the lack of selectivity of reactives, and (ii) the possible re-adsorption and redistribution of solubilized metals present in other fractions (e.g., [166, 177, 178, 179, 180, 181, 182, 183, 184, 185]).

Lack of selectivity. For instance, the possible dissolution of FeS during carbonate extraction in Tessier's protocol [186] or even the contribution of other sources during the same step [187]. The lack of selectivity can result in overestimation of the extracted metals [184, 185].

Re-adsorption and redistribution. Incomplete dissolution of certain phases and changes of pH can induce re-adsorption and redistribution. For instance, some authors demonstrated Cu, Pb and Zn redistribution during the application of Tessier's procedure [186]; similarly, other authors have reported Pb redistribution in Fe oxides and humic substances [188, 189].

The importance given to these problems has been criticized. Indeed, most of these methodological studies are performed on artificial samples or by contaminants introduced into natural sediments. Tessier & Campbell (1991) [190] queried the validity of experimental procedures using artificial sediments, and concluded that the most important problem is the lack of selectivity of the reactives used to attack the solid phase. Though MTE re-adsorption during subsequent extraction steps exists, the extent does not significantly distort the results [191].

1.3.3.4 Extraction procedure choice

Despite all criticisms and reserves against selective extraction procedures, these techniques continue to be important methods for the study of particulate metal(loid) speciation, allowing the estimation of MTE mobility and bioavailability in the environment [192, 193, 194, 195, 196, 197, 198, 199].

For this study, solid state partitioning was performed through single selective extraction procedures instead of sequential extractions. The single method allows skipping some limitations and problems related to sequential techniques [200]. These problems are: (i) possible speciation changes of an element during the course of successive extraction steps and rinsing of the sample after each step [201]; (ii) multiple risks of sample contamination through the use of successive reactives [165]. Advantages of single extraction procedures include: (i) diminished risk in relation to sample loss during extraction, (ii) a mistake or problem during the extraction procedure does not compromise the integrity of the method [202].

The protocol used during this study is mainly based on the procedures proposed by Tessier *et al.* (1979) [154] employing single selective extractions. Two studies demonstrated that similar results were obtained in extracting MTE (Cr, Ni, Pb, Cu and Zn) when applying the different steps of Tessier's sequential extraction procedure in a single extraction method. For each fraction, the applied protocol and the followed criteria are explained in the following paragraphs; the methodology is explained in Chapter 2.4.3.7.

Fraction 1 (F1) "exchangeable". Metal(loid)s extracted in this operation would include weakly sorbed species, particularly those retained on the soil surface by relatively weak electrostatic interactions and those that can be released by ion exchange processes. Reagents used for this purpose are electrolytes in aqueous solution, such as salts of strong acids and bases or salts of weak acids and bases at pH 7 [203]. The most popular reagent is $MgCl_2$ 1 M which combines the rather strong Mg^{2+}ion-exchange capacity with the weak complexing ability of Cl^-. This reagent does not attack OM, silicates or metal sulphides [145, 154] and corresponds to the chosen reactive for exchangeable fraction extraction.

Fraction 2 (F2) "acid-soluble". This fraction is sensitive to pH changes, and metal release is achieved through dissolution of a fraction of the solid material at pH close to 5. A buffered acetic acid/sodium acetate solution is generally used. The metal fraction recovered in these conditions may be thought to have been present as co-precipitated with carbonate

minerals but also as specifically sorbed to some sites on the surface of clays, OM and Fe- and Mn-oxyhydroxides [145]. This reagent is well adapted to dissolve calcium carbonates [154] but dissolution of dolomite is not total [145, 203]. Furthermore, lowering the pH from 7 (pH of the extracting solution used in F1 extraction) to 5 would release the remaining specifically-adsorbed MTE ions that escaped extraction in the previous step [154].

Fraction 3 (F3) "bound to hydrous oxides of Fe and Mn". Iron and manganese oxides are excellent scavengers of metals [94] and together with OM, can be considered the dominant constituent of MTE distribution in the environment [84, 98]. By controlling the Eh and pH of reagents, dissolution of some or all MTE-oxide phases can be achieved [145]. Hydroxalamine, oxalic acid and dithionite are the most commonly used reagents. Hydroxalamine solution has been used particularly for extracting Mn oxides, nevertheless this solution at pH 4 can also extract carbonates. The extraction with Citrate Dithionite Buffered (CDB; $Na_2S_2O_4/NaHCO_3$) dissolves all ferric phases, amorphous and crystalline [183]. Oxalate/oxalic acid buffered solution appears to be specific for amorphous iron phases with a low degree of cristallinity, yet hydrous Al oxides are simultaneously extracted with iron hydroxides [204], and is not possible to distinguish MTE associated with Al oxides from those associated with Fe oxides. The aim of our study was to extract the most reactive phases linked to Fe- and Mn-oxyhydroxides, therefore we employed an ascorbate leaching, designated to extract the most reactive Fe-oxyhydroxides fraction (amorphous oxides) [184, 205, 206]. This extraction ($C_6H_8O_6/C_6H_5Na_3O_7{\cdot}2H_2O/CHNaO_3$) attacks by reducing amorphous Fe-oxyhydroxides [205] and Mn-oxyhydroxides [56]. This method was successfully used in other surveys dealing with MTE fractionation (e.g., [15, 207]).

Fraction 4 (F4) "oxidizing". Metallic trace elements may be incorporated in many forms of OM (e.g. living organisms, organic coatings on inorganic particles and biotic detritus). In sediments and soils, the organic content comprises mainly complex polymeric material, i.e. humic substances (humic and fulvic acids) and to a lesser extent carbohydrates, proteins, peptides, amino acids, etc. [145]. Polymer complexes have an important role in metal complexation in the environment [71]. Metal(loid)s in this fraction can be solubilized from the sediments by organic phase degradation under oxidant conditions. An oxidant reactive, such as H_2O_2 (e.g., [154, 200]) or NaClO (e.g., [208]) is frequently used. However, the extraction by sodium hypochlorite (NaClO) can also attack the Mn oxides [145] and

dissolve a non-negligible fraction of carbonates [209]. Therefore the H_2O_2 reactive was chosen for the extraction.

Fraction 5 (F5) "residual". Primary and secondary minerals containing metal(loid)s in the crystalline lattice constitute the bulk of this fraction. Its destruction is achieved by digestion with strong acids, such as HF, $HClO_4$, HCl, HNO_3 and H_2O_2. In this study two methods were used, firstly a three-acids attack (HNO_3, HCl and HF) following a method validated by different authors in aqueous environments [207, 210, 211]; secondly, a three-acids protocol (HF, HNO_3 and H_2O_2) validated by the US Environmental Protection Agency (EPA 3052).

1.4 Conclusions

1.4.1 Conclusions of Chapter 1

In Chapter 1 we intended to briefly explain the topics this thesis deals with, introducing the reader to the main subject "Contamination in natural reservoirs". In this chapter special attention was paid to aqueous systems, because our study was developed within a lacustrine environment.

Firstly, Chapter 1 deals with geochemical concepts related to environmental sciences and legislation. Despite the fact that knowledge of geological/geochemical backgrounds and the establishment of baselines are basic to develop environmental legislation, in most South American countries, geochemical backgrounds and baselines are not yet determined, preventing sustainable development in this part of the globe.

The following section of Chapter 1, allowed concluding that the main factors controlling MTEs speciation and their presence in dissolved or solid phase are metal(loid) associations within the solid fraction. Surface complexes or precipitates will determine the transport, reactivity and kind of MTE in the aqueous environment. Indeed, the complexity and heterogeneity of factors controlling MTE dynamic within the aquatic environments prevent the development of simple models of MTE behaviour.

Finally, in Chapter 1 we introduced sequential extraction procedures, concluding that these are useful to study MTE solid state partitioning and the distribution of metal(loid)s in the environment. Nevertheless, it seems that all reagents used in different extraction procedures, have advantages and inconveniences. Besides, standardization of protocols and certified material preparation are still problematic, mainly because of the variable and diverse types of natural matrices. Therefore, the selection of a specific extraction procedure must be related to the objectives of the study and must take into account the type of studied material. The interpretation of selective extraction results must not be done in relation to mineralogical fractions but in relation to the employed reagents associated with the different chemically defined phases when extracting MTE.

Chapter 2

General context, materials and methods

2.1 Introduction: general context of the study area

The study area is located in the Oruro Department of Bolivia which is situated 230 km south of La Paz (Fig. 2.1.1). This area is within the Altiplano, which lies between the western and eastern Andes Cordilleras and contains a deep lake in the north named *Lake Titicaca*, a very shallow lake in the centre called *Lake Poopó*, and dry salt lakes or salars known as *Coipasa* and *Uyuni* further south. Lakes Titicaca and Poopó are linked through the watercourse called *Río Desaguadero*. According to the initials of the sub-basins this system is commonly called *TDPS* (Fig. 2.1.1).

2.1.1 Geomorphologic and geologic setting

The study area is made up of three main geomorphologic features, which are *the Altiplano*, *the western Andes Cordillera* and *the eastern Andes Cordillera* (Fig. 2.1.2). The Altiplano is a 200,000 km^2 intermontane endorheic and tectonic basin which formed during the Pliocene and Early Pleistocene (some 3-2 My), in the central Andes of Peru, Bolivia and Argentina [212]. The Peruvian-Bolivian section is a high plateau above 3,800 m a.s.l. lying between the western and eastern Andes Cordilleras; this basin is filled with predominantly Tertiary continental deposits (Fig. 2.1.3). The western Andes Cordillera consists mostly of andesitic stratovolcanoes and rhyolitic ash-flow tuffs that overlie a basement of Jurassic and Cretaceous sedimentary and volcanic rocks (Fig. 2.1.3). The eastern Andes Cordillera is underlain mainly by a thick sequence of intensely folded, lower Paleozoic, marine clastic sedimentary rocks and overlain locally by similarly deformed Cretaceous–lower Tertiary continental sedimentary rocks, undeformed late Tertiary unconsolidated continental sediments, and late Oligocene to Pliocene volcanic rocks (Fig. 2.1.3) [213, 214, 215, 216].

2.1.2 Metallic ore resources

In the study area, ore mineralization is associated with the tin belt, the gold-antimony belts and the lead zinc belt in the eastern Andes Cordillera; and red-bed copper deposits and epithermal deposits in the Altiplano and western Andes Cordillera [217]. The eastern Andes Cordillera is the host for most of the mineral resources of the Oruro Department and includes the *Lead-Zinc Belt*, the *Gold-Antimony Belts* and the well-known *Bolivian Tin Belt*. The Lead-Zinc Belt corresponds to a series of sedimentary rock-hosted Ag-Pb-Zn veins, with anomalous concentrations of Au and Sb, this belt shows no clear association with magmatic centres that are

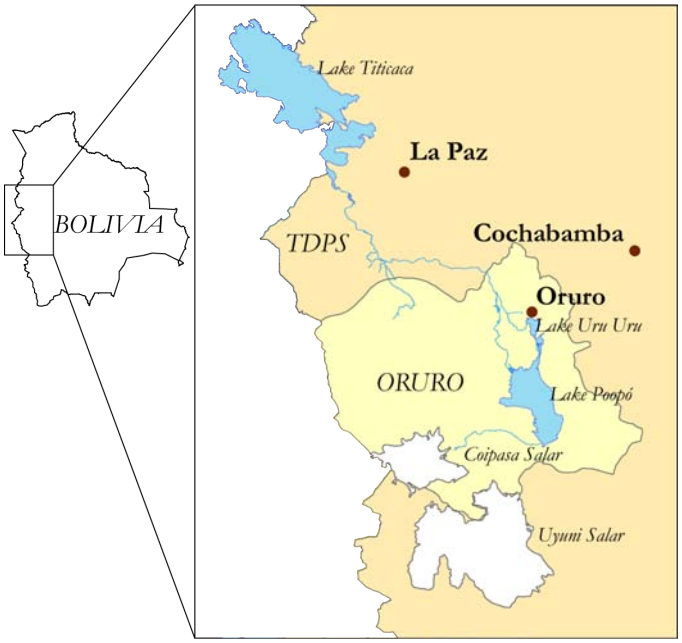

Figure 2.1.1: General map of the study area

located along the length of the central part of the southernmost eastern Andes Cordillera [217]. The Bolivian Gold-Antimony Belts are generally found in the same parts as Sn mineralization related to Mesozoic and Tertiary intrusions and are mainly hosted by Middle Ordovician to Early Silurian sedimentary rocks, in these belts many deposits contain as much as 10 to 20% Sb, consequently, many of these were originally mined for Sb [217]. The Bolivian tin belt is a 900 km long belt extending east-west throughout Bolivia from northernmost Argentina to southernmost Peru and is divided by the prolongation of Arica's elbow to the east into two sections, north and south [218]. The northern part contains Au, W, Sb, Sn, Bi, Zn and Pb mineralization and the southern part is characterized by rich Ag and poor Au polymetallic tin deposits, with a great variety of Sn, Ag and base metal minerals similar to those from the north. Genetically, these deposits are related to small (1-2 km^2) quartz latitic or dacitic porphyry domes or stocks of Neogene-Quaternary age [213, 218, 219, 220]. In the study area, deposits occur within the transition between both sections of this metallogenic belt, where the Huanuni and Bolivar Sn-rich mining districts are well known (Fig. 2.1.3). In the Altiplano and the western Andes Cordillera the Polymetallic Belt is mainly composed of epithermal Ag-Au-Pb-Zn-Cu deposits formed during the middle-late Miocene and early Pliocene [222, 223], while the *Sedimentary-Rock Hosted Copper Deposits* correspond to Miocene to Pliocene stratiform

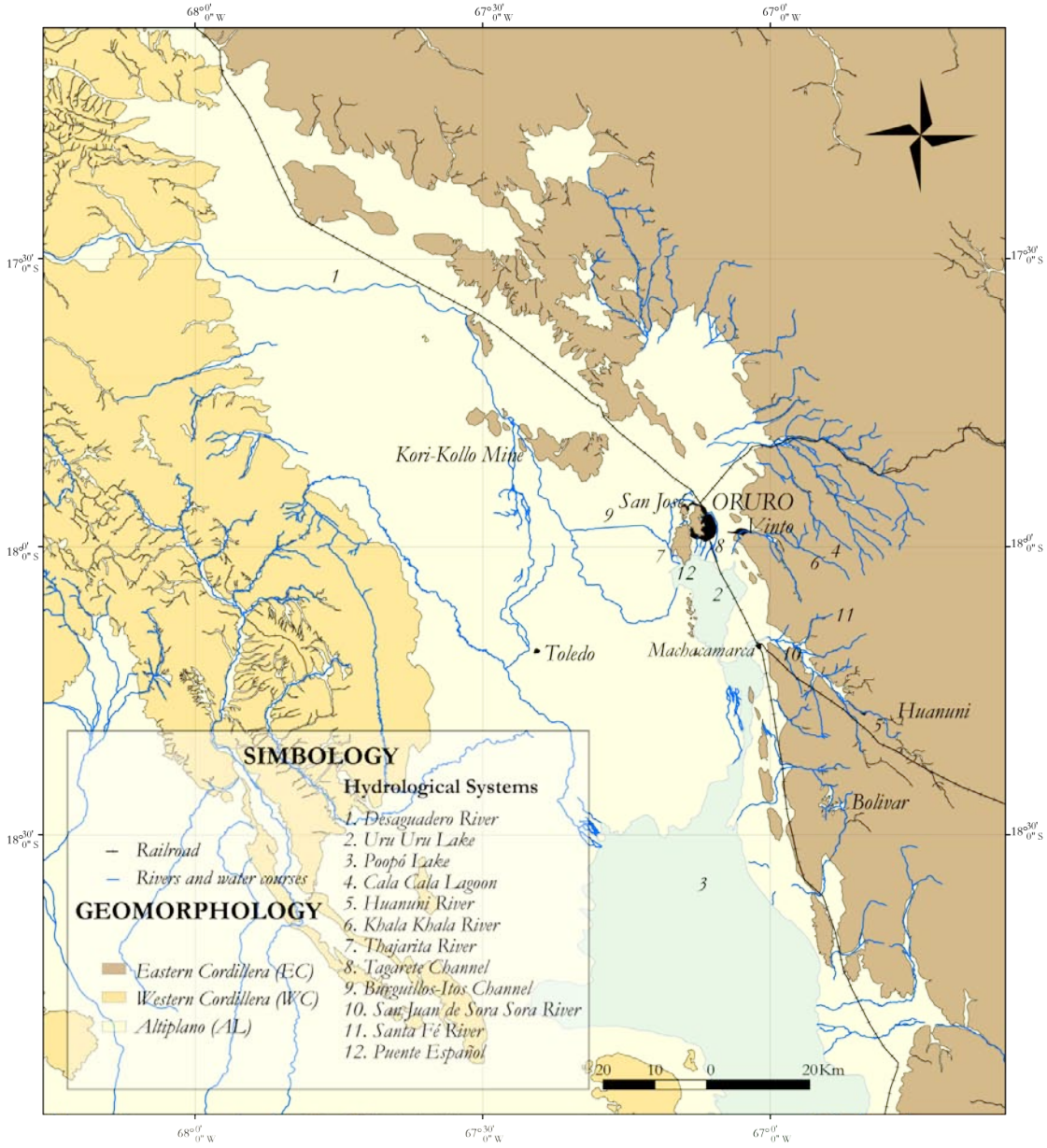

Figure 2.1.2: Geomorphologic setting of the study area, western Andes Cordillera, Altiplano and eastern Andes Cordillera

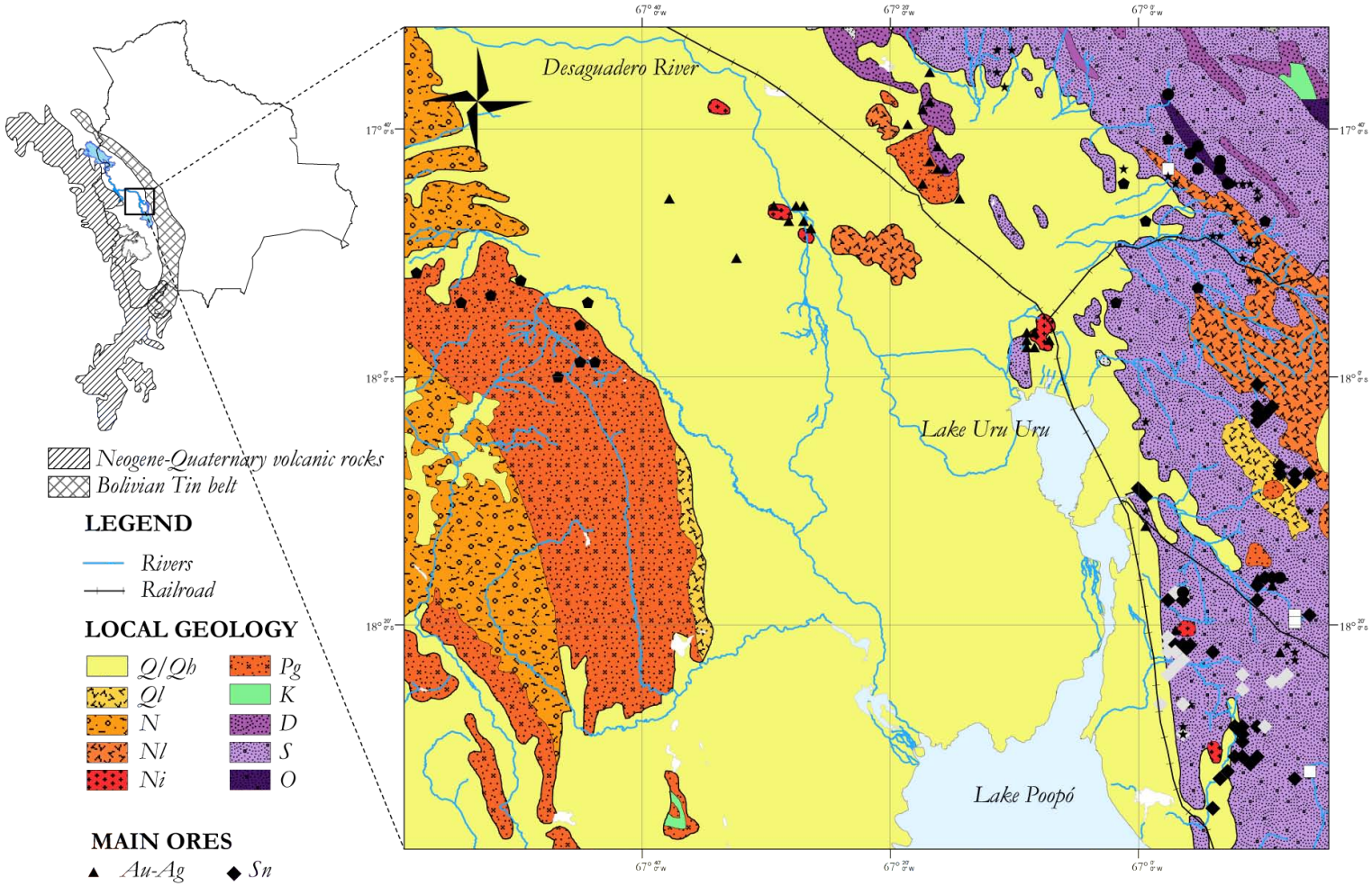

Figure 2.1.3: Geological setting of the study area, location of the main metallogenic belts within eastern and western Andes Cordillera and main ore deposits distribution.

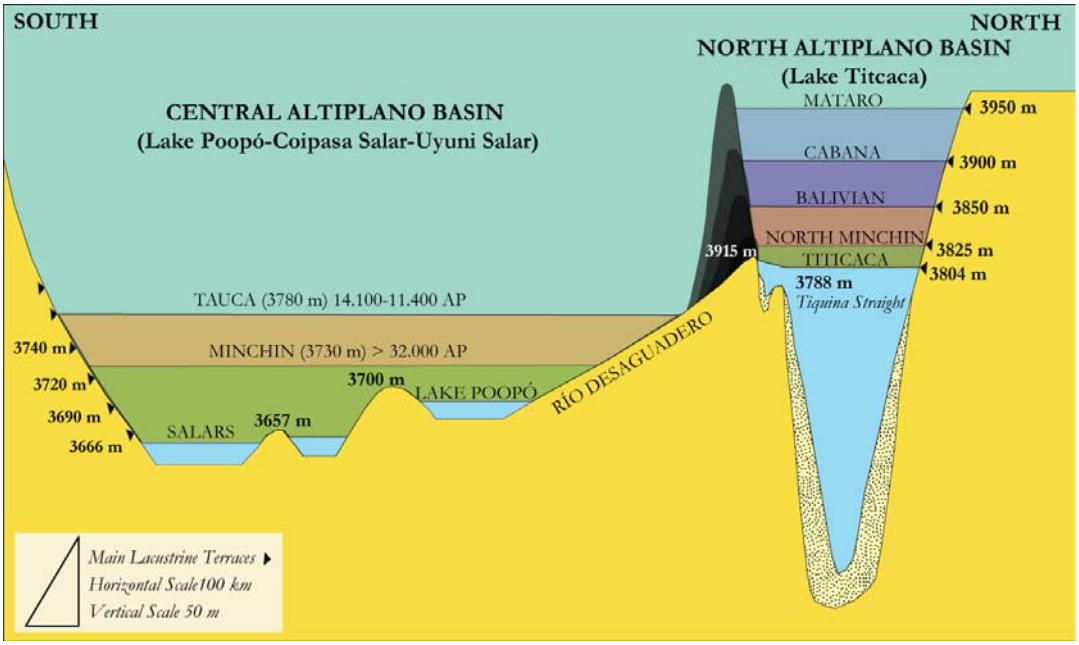

Figure 2.1.4: Main Altiplanic paleolakes modified from Fornary *et al.* 2001 [221].

copper deposits scattered along the length of the Altiplano [217].

2.1.3 TDPS drainage system

After the development of the intermontane Altiplano basin, this area suffered periodic advances and retreats of glaciers, and these resulted in high-amplitude fluctuations of lacustrine phases in the northern and central Altiplano [212, 221, 224, 225, 226, 227]. The various lacustrine basins, from the oldest to the most recent, are known as the paleolakes *Mataro*, *Cabana*, *Ballivian*, *Escara*, *Minchin* and *Tauca* [212, 221, 224, 225, 226, 227, 228, 229, 230, 231] (Fig. 2.1.4); these changes in lake levels are believed to be caused by large-scale climatic changes [232, 233]. A summary of these paleolakes is briefly presented in the following paragraphs together with the present time-*TDPS* status.

2.1.3.1 Paleolake development in northern and central Altiplano

The oldest dated lacustrine event recorded in an ignimbrite from a borehole in the central Altiplano (Salar de Uyuni) was dated as early Pleistocene. This lacustrine episode shows a $^{40}Ar/^{39}Ar$ age of 191,000 ± 5,000 yr B.P. [221] and is called *Escara*; while in the northern Altiplano, lower and middle Pleistocene paleolakes are known only through sedimentary records (which have not been dated yet); the oldest paleolake was named *Mataro* and was assigned to the

early Pleistocene [229], the lake surface level was 140 m above present and was associated with the end of the *Calvario* glaciation [228]. During the middle Pleistocene the paleolake surface was estimated to have been 90 m above present and was called *Cabana* [229]. The retreat of the penultimate glaciation, *Sorata* [228], gave rise to the paleolake known as *Ballivian* [224, 234], estimated at 50 m above the present Lake Titicaca surface. At the end of the Pleistocene, ^{14}C dating yielded an age $<$ 34,400 years B.P. [221] for the paleolake *Minchin* in the central Altiplano; while within the northern Altiplano, ^{14}C dating estimated an age $<$ 31,100 yr B.P. [227] for the *Minchin* paleolake, which was estimated to be 15 m above the present Lake Titicaca surface level [225]. The last lacustrine phase, called *Tauca*, was first ^{14}C-dated in the central Altiplano at ca. 12,000 and 10,000 years B.P. (14,100 and 11,400 cal yr B.P.) [225]; this paleolake was redefined for the northern Altiplano [232, 235], through ^{14}C dating three episodes were determined called *Tauca* (19,100-15,600 cal yr B.P.), *Ticaña* (15,600-13,400 cal yr B.P.) and *Coipasa* (13,400-12,300 cal yr B.P.), temporarily associated with the paleolake *Tauca* on the central Altiplano.

The Holocene was characterized by lower lake levels than those found nowadays [236, 237, 238]. The early Holocene was extremely arid, as evidenced by gypsum deposition [237, 238, 239]. This dry period was followed by an improvement of climatic conditions which allowed the refilling of the basins at c. 8,000 years B.P. Until 3,900 years B.P., basin evolution was related to stable, lower than present, superficial levels. Subsequently, a sudden rise in lake levels occurred, yet lower than present, this lasted until an undetermined recent date ($<$ 1,000 years B.P.). In general, lake levels were relatively stable and lower than 3,809 m a.s.l., yet punctual exceptions such as a dry event registered at c. 2,300 years B.P., characterized by a huge fall in water level, existed [239].

2.1.3.2 Present TDPS basin

Lakes Titicaca, lake Poopó and Salars represent the final evolution of the mentioned paleobasins. Lake Titicaca corresponds to a large (c. 8,000 km^2), warm, monomictic lake [240] that extends between 16°15' S and 17°30' S latitude and 68°30' W and 70° W longitude, at an altitude of c. 3,809 m. It is located in the northern part of the Altiplano of Perú and Bolivia. The lake drains to the south via the Desaguadero River to Lake Poopó and is divided into three main basins (Figs. 2.1.1 & 2.1.4). The northern basin, Lake Chucuito, has a maximum depth of c. 285 m (the maximum depth in the Altiplano) and is separated from the two southern basins, which combine to form Lake Huaiñamarca, by the Tiquina Strait [241] (Fig. 2.1.4).

The only outflow of Lake Titicaca is the Desaguadero River that flows 390 km southward from Lake Titicaca to Lake Poopó. The modern Desaguadero River is a transitional fluvial system. From its headwaters at Lake Titicaca to its terminus at Lake Poopó, the Desaguadero River displays end-member morphologies characteristic of a marsh, a meandering river, and a braided river, as well as non-end-member braided and meandering channel morphologies [242, 243, 244]. Before its outflow into Lake Poopó, the Desaguadero River divides at Chuquiña into two arms, one discharges directly into Lake Poopó and the other into Lake Uru Uru [245] (Fig. 2.1.2).

Lakes Poopó and Uru Uru are located in the central Altiplano. Both are shallow ($<$ 6 m) and exhibit highly variable surface areas [246, 247]. Lake Poopó is situated between 18°21' and 19°10' S latitude and 66°50' and 67°24' W longitude (Figs. 2.1.3 and 2.1.4); its existence is highly correlated with the Desaguadero River discharges, therefore its volume and extension are associated with the Lake Titicaca water level, governed by the *El Niño Southern Oscillation* (ENSO) events [246, 247]. Sediment section studies and historical records showed that Lake Poopó exists periodically, and as a consequence of particularly dry years, disappears completely [246, 247] (Lake Uru Uru is described in detail in Chapter 2.1.5).

Further south, the *Coipasa* and *Uyuni Salars* are located in the topographic low of the southernmost central Altiplano. The Coipasa Salar surface is c. 2,500 km^2 and is located at 3,656 m a.s.l. During rainy years this salar connects Lake Poopó through Río Laca Jahuira, yet most of the time both basins are not permanently linked though they belong to the same endorheic system [239]. In central Coipasa the crust is 2.5 m thick and is underlain by lacustrine sediments. The crust consists of an upper layer of porous halite and of a lower layer composed of crumbly aggregates of mirabilite crystals. Lacustrine sediments are detritals, gypsum, calcite, Artemia faecal pellets, organic matter and clay minerals, which are impermeable and contain interstitial brine [239]. Uyuni Salar is the largest salt flat in the world, its surface covers c. 10,000 km^2 and it is located at 3,656 m a.s.l. [239]. This salar is the latest in a series of at least five lakes covering the southern part of the Altiplano basin during the last 200,000 years [239, 248, 249]. The present time salt crust has a maximum thickness of 11 m and at the southeastern border the crust interfingers with fluviodeltaic sediments. The Uyuni crust is similar to Coipasa and is constituted by layered porous halite with a small amount of fine-grained gypsum and filled with interstitial brine. This crust is underlain by impermeable lacustrine sediments. The salar is completely flooded during the rainy season and dry almost all over its surface during the rest of the year [239].

The TDPS basin is highly vulnerable to anthropogenic influence, because as an endorheic system all the material transported by the water courses (natural weathering material as well as contaminants) are concentrated within the basin; in fact the only known mechanism (with the exception of evaporation and wind transport) to dispose of residual materials is by anthropogenic transport [250].

2.1.4 Climatic conditions

Presently the Altiplano is under the influence of an arid to semi-arid climate, dominated by typical tropical wet (WS) and dry seasons (DS), extending from October to March and May to September, respectively, and implying a wet summer and a dry winter (Fig. 2.1.5) [245]. This climate is also influenced by local orographic effects, related to the seasonal latitudinal movements of the *Inter-Tropical Convergence Zone* (ITCZ). From November to April, the ITCZ occupies the central Andes, and during this period, the warm, moist Amazonian air penetrates the eastern Andes Cordillera from the north-east, bringing stormy rains and causing a steep rainfall gradient from north to south [251]. This is evidenced by annual precipitation of about 700 mm in the north to less than 100 mm in the south [221], while the central Altiplano is characterized by less than 400 mm rainfall per year [245]. In the Altiplanean zone, the air temperature ranges from -20°C at night in winter to 20°C during the day in summer [221]. This zone is periodically affected by ENSO events, which have been associated with historical lacustrine levels since the lower Pleistocene [246, 247]. Regarding wind characteristics and according to data from the Bolivian SENAMHI (Meteorology and Hydrology National Service) prevalent wind directions since 1971 are W-NW during the DS and to the E during the WS (Fig. 2.1.5).

2.1.5 Lake Uru Uru and Cala Cala Lagoon

Lake Uru Uru is located 5 km south of Oruro and is a central part of the TDPS drainage basin. It corresponds to a shallow lake that formed during the last century (1900s) due to the deviation of the Desaguadero River [245] and is divided by a railroad and a highway embankment, allowing a minimum exchange of water between the two separate parts (Fig. 2.1.6) [252]. The eastern branch of the Desaguadero River and the Thajarita River[1] feed the south-western part, the latter discharges into Lake Uru Uru at Puente Español. The Tagarete River, a channelized water course that transports highly contaminated water from the San José Mine and

[1]The Thajarita River receives most of its water from the Desaguadero River via the Burguillos-Itos Channel.

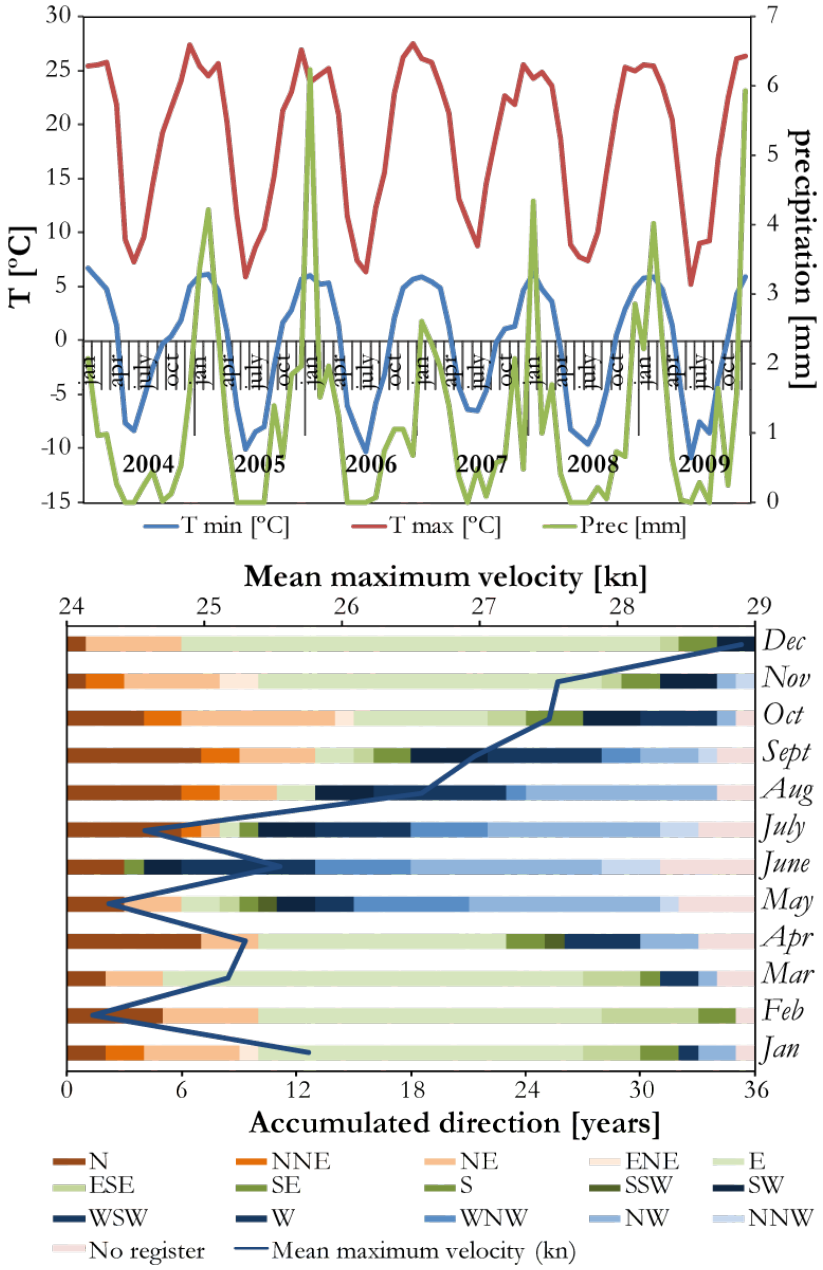

Figure 2.1.5: Temperature [°C], precipitation [mm] since 2004 and Oruro preferential wind directions since 1970 (Bolivian SENAMHI data)

sewage from Oruro feeds the northern part (Fig. 2.1.6) [252, 253]. The Desaguadero River drains the southernmost part of Lake Uru Uru flowing south for approximately 30 km before entering Lake Poopó. The San Juan de Sora Sora River enters into the southernmost limit of Lake Uru Uru from the east (up to 7 km to the south); this river drains the Huanuni and Santa Fé river basins [252]. Lake Uru Uru is very shallow, therefore depth and surface extension vary enormously between the DS and WS and from year to year (depending mainly on the intensity of the WS precipitation and DS evaporation rate). Despite this fact it has not suffered complete desiccation (differencing with respect to Lake Poopó) exposing its maximum continuous lake water surface in 1986 (150 km^2) [252].

2.1.6 Anthropogenic influence in the ecosystem

The existence of important metallogenic belts has historically established Bolivia as one of the major Sn and Sb producers in the world, having led to the construction of the Vinto Smelter in 1971 to process Bolivian Sn-Sb mineral concentrates locally. The complexity of ores and the related smelting procedures have caused emissions of approximately 14,000 tons of SO_2 per year and between 400 and 1,000 tons of metallic particles per year, representing an important anthropogenic contaminant source of airborne particulates [254].

Several surveys performed in this area [245, 246, 247, 250, 252, 253, 254, 255, 256, 257, 258, 259] showed that this zone is strongly affected by anthropogenic activities, especially mining, and that Lake Uru Uru operates as a natural MTE receptacle [252, 257].

The Cala Cala Lagoon, in contrast to Lake Uru Uru, is located 18 km east of Oruro within the eastern Andes Cordillera sedimentary rocks[2]. This lagoon is artificial in origin and channels water from the Khala Khala River through mineralized rocks of the eastern Andes Cordillera. One interesting feature of the Cala Cala Lagoon is that its watershed is characterized by the absence of mining activities (details in Chapter 3).

[2]Cala Cala Lagoon is within the Uncia and Catavi Formations, that correspond to sedimentary sequences.

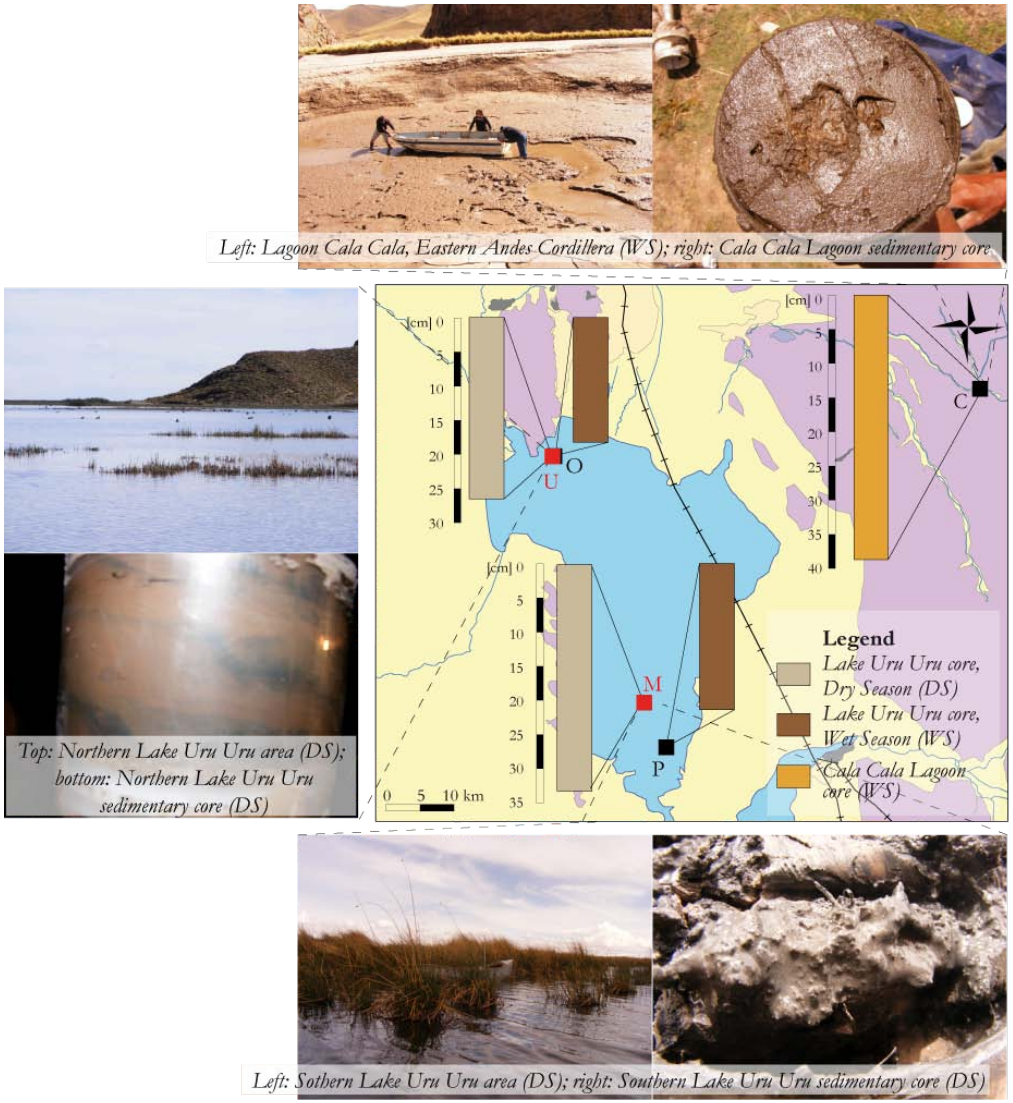

Figure 2.1.6: Lake Uru Uru and Cala Cala Lagoon sampling sites during the WS (U, M) and DS (O, P and C).

2.2 Hypothesis and objectives

2.2.1 Hypothesis

The lack of documented studies dealing with (i) geochemical backgrounds in highly mineralized areas and (ii) early diagenesis in contaminated continental areas, enhances the relevance to assess the processes governing the dispersion of MTE in these regions and the processes intervening in MTE behaviour within aqueous environments such as lakes in continental contaminated areas. The Altiplano of Bolivia presents both natural ore deposits and dispersion associated with anthropogenic activities. In addition, climatic conditions interfering in both MTE dispersion and MTE behaviour are not easily found in literature. This motivated the following working hypothesis:

"Within the endorheic hydrological system of Lake Uru Uru polymetallic contamination is associated with the natural existence of ore deposits linked to the Bolivian Tin Belt, the Gold-Antimony Belts and the Lead-Zinc Belt in the eastern Andes Cordillera and Sedimentary Copper Deposits and Polymetallics in the western Andes Cordillera. Anthropogenic contamination associated with the exploitation of these ores also exists. The dispersion and degree of contamination are controlled by bottom water-sediment interactions within drainage areas, such as within lacustrine sediment accumulation areas. Natural processes of contaminant accumulation in lacustrine systems allow the dispersal of contamination to large distances from the source, yet this represents a delicate biologic equilibrium where human activity can easily enhance contaminant dispersion in a dissolved phase and cause pollution to the biologic system, which can strongly affect flora, fauna and humans in this lacustrine system. Finally, historic mining and seasonal plus interannual climatic variations in the Altiplano have influenced the composition of sediments in Lake Uru Uru".

Our work hypothesis can be broken down into the following sub-hypothesis:

1. The study area is contaminated.
2. The study area is naturally rich in ore deposits.
3. The main sources of contamination are ore deposits and mining waste, the Vinto Smelter and sewage from Oruro.
4. In Lake Uru Uru, it is possible to observe contaminants generated by mining activities.
5. Some of the metal(loid)s within the lake can cause damage to the different biotic inhabitants of this system and to population health.

6. This lacustrine environment has been influenced by historic mining activities and by seasonal (DS and WS) plus interannual climatic variations (ENSO events).

2.2.2 Objectives

To answer the proposed hypothesis, two lacustrine environments in the Altiplano of Bolivia were studied in detail. The study firstly focused on understanding the geochemical spatial distribution and sources of metal(loid)s in sediments from the Altiplano of Oruro, one of the most naturally ore-rich regions in the world. After determining the first objective, the second issue was deciphering early diagenesis processes under extreme and particular conditions, such as those found in the Altiplano region (a continental aqueous system surrounded by unique geologic features and characterized by seasonal and interannual climate fluctuations). The following objective was to determine solid state partitioning of MTE to establish the most mobile contaminants of this system. Finally, the last objective was to determine possible mechanisms to understand how these elements may or may not intervene in the biota of this lacustrine environment.

Our objectives can be broken down into the following main elements:

1. Determining the geochemical background and baseline of Altiplanic lacustrine sediments.
2. Determining main redox reactions controlling MTE behaviour.
3. Determining solid state fractionation of MTE to stress which contaminants are most mobile in this environment.
4. Determining possible mechanisms affecting MTE behaviour within Lake Uru Uru.
5. Determining the relationship between historic mining industry and sediment contamination in the Oruro Department.

To accomplish our principal objectives, the following actions were carried out:

1. Collecting sedimentary cores during DS and WS.
2. Creating a geochemical baseline based on bibliographic data plus sediment data from this work.
3. Determining metal(loid) distribution and possible sources through a Geographical Information System (GIS).
4. Determining major, trace and nutrient content in pore water.

5. Determining the main mineralogy and minerals associated with the metal(loid)s.
6. Determining solid state partitioning through single selective extractions.
7. Dating sedimentary cores to estimate mining history and/or climatic influence in the sediment composition of Lake Uru Uru.

2.3 Sampling sites

2.3.1 Selection of the sites

For both seasons the northern and southern areas of Lake Uru Uru were sampled. These sites were chosen due to the contrasted sources of water input in both areas: the northern source is linked to the Thajarita River and the Tagarete Channel, which transport waste from the San José (Ag-Pb-Zn-Au) Mine and sewage from Oruro, and the southern part is related to the San Juan de Sora Sora River, which transports waste material from the Huanuni (Sn) Mine. Due to the constant desiccation of the eastern side, all cores from Lake Uru Uru were retrieved from the western area, where the depth ranged between 0.8 and 2.0 m at the sampling sites.

Cala Cala Lagoon sediment (Fig. 2.1.6) was sampled in order to compare the composition of lacustrine sediments of the eastern Andes Cordillera with that of the Altiplano and to determine the geochemical background of lacustrine sediments probably not impacted by mining and/or smelting activities in the eastern Andes Cordillera.

2.3.2 Coring campaigns

Sampling procedures were performed following the experimental protocols of Audry (2003) [207] and Audry *et al.* (2004) [15]. A total of five sedimentary cores were retrieved in the field: four from Lake Uru Uru and one from Cala Cala Lagoon. Cores from Lake Uru Uru were sampled at the beginning of the DS (21-25 April 2008) and during the WS (2-6 February 2009). Cores were collected using a Large Bore Interface Corer (Aquatic Research Instruments®) equipped with a polycarbonate core tube (60 cm length, 10 cm inner diameter). This corer enables sampling the uppermost decimetres of the sediments without any disturbance of the water–sediment interface (WSI). Immediately after recovery, bottom water (BW) was sampled from the undisturbed WSI of the core through a 20 mL syringe, then filtered through cellulose acetate syringe filters (0.2 µm porosity; Nalgene®) and kept in three different 10 mL acid cleaned vials (for nutrients, sulphate and chloride, and MTE). Then, the sediment core was extruded and sliced with an acid-cleansed plastic cutter. A decreasing vertical resolution of slicing was applied: (i) 5-mm resolution for the first 5 cm below the WSI, (ii) 10-mm resolution for the following 5 cm of sediment, and (iii) 25-mm resolution down to the bottom of the core. The length of the cores ranged from 18 to 40 cm. All samples were immediately collected in acid-cleaned 200 mL propylene centrifuge vials and centrifuged at 4,000 r.p.m. for 20 minutes

Table 2.1: Summary of total samples, ME: major elements; TE: trace elements; NT: nutrients; PS: porosity; SD: sediment; DS: dry season; WS: wet season

		SAMPLES				
Season	Location	dissolved fraction			particulate fraction	
		ME	TE	NT	PS	SD
DS	North Lake Uru Uru	14	12	15	20	20
	South Lake Uru Uru	20	13	18	22	23
WS	North Lake Uru Uru	9	8	9	12	12
	South Lake Uru Uru	11	13	11	12	14
	Cala Cala Lagoon	23	23	23	22	22
TOTAL OF SAMPLES		77	69	76	88	91

to separate solid from dissolved fractions. For each centrifuged sample, the supernatant was filtered through cellulose acetate syringe filters (0.2 µm porosity; Nalgene®) and then divided into three aliquots for nutrient, sulphate and chloride, and MTE analyses. Aliquots for nutrient analysis were stored in 5 mL polycarbonate tubes and immediately frozen at -5°C until analysis; aliquots for sulphate and chloride analysis were stored in 5 mL polypropylene tubes and kept at 4°C; aliquots for MTE measurements were stored in acid-cleansed tubes, acidified (pH ~1; HNO_3 ultra-pure 1%) and stored at 4°C. The same protocol was applied to BW samples. The sediment samples were kept in sealed bags until analysis under inert atmosphere by the addition of N_2 gas. In addition, at each sampled interval and immediately after slicing, a sub-sample for porosity was taken from the rim of the core and kept in previously weighted vials. A schematic sampling recovery scheme during the coring campaigns is presented in figure 2.3.1; a summary of the samples taken in the field is shown in Table 2.1[3].

All vials used during the coring campaigns were previously acid-cleansed in the *Laboratoire des Mécanismes et Transferts en Géologie* (LMTG) as follows: 2/3 of vial capacity was filled with commercial HCl for 24 hours, then the vials were turned upside down and were left for 24 more hours, subsequently the vials were rinsed with Milli-Q® water five times, finally they were dried under laminar air flow until completely dry. Dry vials were kept in plastic sealed bags until use.

2.4 Analytical methods

In this section a brief explanation of the methods used to generate a geochemical baseline and background of the study area is presented. This is followed by the methodological procedures

[3]Detailed information of coring campaign samples is found in Appendix B.

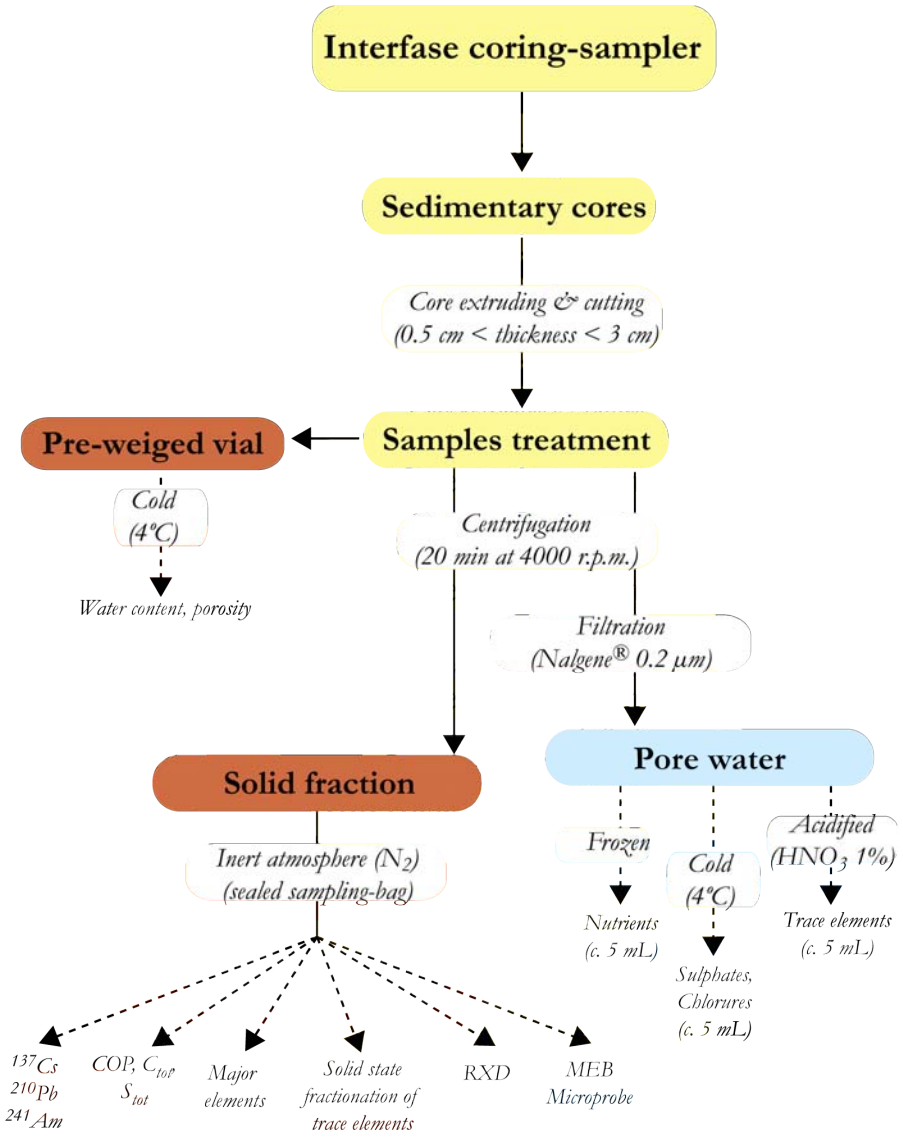

Figure 2.3.1: Schematic sample procedure followed during this study.

employed in the laboratory.

2.4.1 Data base generation

In addition to the total metal content (TMC) of the sediments obtained from the 2008 and 2009 coring campaigns at Lake Uru Uru and Cala Cala Lagoon, a complementary database previously acquired within the framework of the *Oruro Pilot Project* (PPO) [260] was used[4] (all details in Chapter 3).

2.4.1.1 Statistics

A statistical evaluation of sediment and soil data was done to ascertain threshold values separating anomalies from background data, including the determination of significant descriptive parameters of centring, dispersion and shape such as: mean, median, 95^{th} percentile, minimum, maximum, median absolute deviation (MAD), standard mean error, kurtosis, asymmetry coefficient, second (Q_2) and third (Q_3) quartile. Local and cortical enrichment factors (EFs) based on Ti[5] were calculated for the Cala Cala Lagoon samples to characterize the influence of geological factors on element concentration in a non-mining and smelter-impacted site. In addition, EFs for Lake Uru Uru sediments were calculated in order to determine the extent of a possible metal and metalloid contamination in the Bolivian highlands and also to query the use of the Upper Continental Crust (UCC) [261] average concentration to evaluate the degree of contamination in an area surrounded by numerous different metallogenic belts (details in Chapter 3).

2.4.1.2 GIS and MTE spatial distribution

In order to compare the general composition of sediments and soils from different environments in the Bolivian highlands, and to identify outliers and extreme values that lie outside the expected distribution range in the sediments and soils of the area: (i) box and whisker plots, (ii) probability plots, (iii) contour and distribution maps and (iv) concentration versus distance plots were constructed for the most important mining districts [Kori Kollo (Au-Ag), Itos (Ag-Zn-Pb-Au), Huanuni (Sn), Bolivar (Sn) and San José (Ag-Zn-Pb-Au)] and the Vinto Smelter (details in Chapter 3).

[4] Detail of PPO database used is found in Appendix C.
[5] Ti is a conservative element present in rocks from the eastern Andes Cordillera.

2.4.2 Analytic environment in the laboratory

Over the last years, considerable progress related to analytical techniques has been made: lower detection limits (DL) and reproducibility of equipment, multi-element analysis, etc. These improvements provide more and more reliable analytical results, yet requiring increasing care and rigour in the different sampling steps, both in the analytical environment and sample manipulation in the laboratory. Indeed, the amount of MTE with concentrations of the order of $ng{\cdot}L^{-1}$ involve particular precautions to preserve samples from external contamination. Furthermore, containers are important in the preparation of chemical reactives, and the application of tests (e.g., analytical blanks, sampling blanks, certified sediments and solutions standards) allow the quality and accuracy of the different measurements to be verified. Laboratory procedures and measurements are performed in highly pressurized rooms that are equipped with an air filtration system that assures an appropriate ultra-clean environment that minimizes the risk of sample contamination. All manipulations required the employment of propylene gloves and aprons. All vials used during the course of reactive preparations, digestions and measurements of MTE (diverse type of vials, cones, pipettes, digestion bombs, etc.) are of propylene or Teflon®, materials that are resistant to acids and that minimize all MTE adsorption and/or desorption reactions within the inner surface of these containers. Before employment, all vials were decontaminated following the protocol explained in Chapter 2.3.2. Ultrapure or suprapure reactives were preferentially used. Solid weighing was performed in the Clean Room of the LMTG under the appropriate conditions.

2.4.3 Solid fraction[6]

In the laboratory, sediment samples were oven-dried (50°C) until completely dry. Subsequently samples were homogenized with a manual agate mortar.

2.4.3.1 Water content and porosity

Sediments for porosity calculations were preserved in pre-weighed vials; the samples were weighed before being oven-dried (50ºC) and again when completely dry. The difference between humid weight and dry weight provided the water content (%). Porosity (ϕ, %) was inferred

[6]Solid fraction results in Appendix D.

using quartz density (2.65 g·cm^{-3}) within equation 2.4.1.

$$Porosity\,(\phi) = \frac{[W_{\text{sed}} - D_{\text{sed}}]}{[W_{\text{sed}} - D_{\text{sed}}] + \frac{D_{\text{sed}}}{2.65}} \cdot 100 \tag{2.4.1}$$

where W_{sed} corresponds to wet sediment and D_{sed} to dry sediment.

2.4.3.2 Granulometry

The granulometry was determined only for WS sediments from northern Lake Uru Uru and Cala Cala Lagoon. This analysis was performed at the *Sedimentology Laboratory* (Universidad de Chile) in a Mastersizer 2000 laser granulometer. This instrument allows a broad range of materials from 0.02 μm to 2,000 μm, to be analysed with an accuracy of $\pm$ 1% on the Dv50 and instrument-to-instrument reproducibility better than 1% RSD on the Dv50 using the Malvern Quality Audit Standard.

2.4.3.3 Total carbon (C_{tot}), particulate organic carbon (POC), particulate inorganic carbon (PIC) and total sulphur (S_{tot})

The principle of measuring C_{tot} and S_{tot} in solid samples is by oxidation of organic and sulphured compounds contained within the sample through combustion under oxygen flux; thereafter, CO_2 and SO_2 measurements are performed. The employed instrument was a Horiba Jobin Yvon Emia-320V C/S Analyser (at LMTG), which measures carbon and sulphur extracted during combustion through a furnace without conversion. Sample combustion is obtained within a high-frequency induction furnace method under oxygen flow. Oxidized carbon and sulphur are detected and measured by a non-dispersive infrared (NDIR) gas analyser (λCO_2=4.3 μm, λSO_2=7.4 μm). A catalysing oven (mixture Cu/Pt) allows to transform CO and SO produced by combustion into CO_2 and SO_2.

Measurements of POC, C_{tot} and S_{tot} were performed in the *Chemistry Laboratory* at LMTG in lacustrine sediments from the sampled cores in c. 100 mg sediment. These samples were placed in ceramic crucibles and just before the analyses, samples, standards and blanks (empty crucibles) were covered with c. 1.5 g tungsten and c. 0.3 g tin as accelerators.

Before POC measuring, samples were decarbonated (to destroy non-organic carbonaceous compounds) by means of HCl 2N addition; subsequently samples were oven dried for 24 hours to remove excess acid. Particulate total carbon (C_{tot}) measurements proceeded similarly, yet excluding decarbonation. Particulate inorganic carbon (PIC) was calculated subtracting C_{tot} –

Table 2.2: C_{tot} and S_{tot} standards results.

			measured concentration		*certified concentration*
standard	*element*	*n*	*concentration [%]*	*error [%]*	*concentration [%]*
HOR-007	C_{tot}	*3*	*3.255*	*0.001*	*3.750*
JSS242	S_{tot}	*3*	*0.023*	*0.000*	*0.032*
HC16024	C_{tot}	*24*	*3.603*	*0.010*	*3.590*
HC16024	S_{tot}	*24*	*0.036*	*0.000*	*0.033*

POC (%)[7].

Each series of measurements was calibrated to correct the gross concentration of C_{tot}, COP and S_{tot}. Calibration of the instrument was through the measurement of three blanks and by fixing the mean measured concentration as zero. The method accuracy was determined by certified C and S standards HOR-007 (C_{tot} 3.75%), JSS242-11 (S_{tot} 0.032%) and HC16024 (C_{tot} 3.59% & S_{tot} 0.033%) (Table 2.2). Measurement precision depends on the exact weight of the sample. In the case of the HC16024 standard, C accuracy was better than 3% and precision better that 10%, whereas S accuracy was better than 6% and precision better than 10%. Results are given in %.

2.4.3.4 X-Ray diffraction (XRD)

This technique applies equation 2.4.2, known as Bragg's law: In this equation, θ corresponds to the diffraction angle, λ is the wave length emitted by an anticathode, d is the atomic distance between two crystalline lattices of the same crystal, and n is an integer number.

$$2dsin\theta = n\lambda \tag{2.4.2}$$

The anticathodic source is known and diffraction angles are measured; the atomic distance is measured through equation 2.4.2. Atomic or inter-atomic distance is characteristic for each mineral, allowing its identification.

Homogenized sediment samples from DS were analysed by XRD within total sediment in the *XRD laboratory* of LMTG, this was performed using an anticathode (Co Ka; wave length 1.789Å). Acquisition time was c. 1,800 s and the applied electric charge was c. 40 kV. Mineral identification was performed through comparison with a data base of mineral cards PCPDFWIN [262] and X-RAY Spacing [263]. The results provided a general idea of the mineral composition of these sediments. Weakly crystallized minerals or small-size granulometry minerals (< 2 µm)

[7] Results from C_{tot}, S_{tot}, POC and PIC are detailed in Appendix D.1.

cannot be determined by this means, therefore MEB-EDS was applied for small-size mineral determination.

2.4.3.5 Microprobe and scanning electron microscopy (SEM)

These analyses were performed only on a reduced number of samples (a total of 6, 3 northern and 3 southern Lake Uru Uru samples) that were prepared in the *Rocks Laboratory* at LMTG (by de Parseval). Selected sediments were placed on the surface of cylindrical (c. $\pi \cdot 2^3$ cm^3 volume) epoxy plugs that were covered (by evaporation) with a 20 to 50 nm carbon film before analytical observation. Microprobe and SEM analyses were performed in the *Laboratory of Microanalyses and Electronic Microscopy* at LMTG.

Scanning microscopy was done through a 6360 LV (Low Vacuum) SEM JEOL brand, this SEM is associated with an Energy Dispersion Spectrometer (EDS) SDD (Sahara Silicon Drift Detector) PTG brand. Obtained images were in the modalities: (i) Backscattered Electron Composition (BEC); (ii) Secondary Electron Image (SEI); (3) Backscattered Electron Shadow (BES). Analyses were performed under accelerations in the range of 15 to 20 kV. During the observations, the SEI mode images allowed the morphologies of the minerals in the sample to be examined, while BEC mode allowed samples to be characterized as a function of their chemical composition. These images are constituted by light areas associated with minerals formed by high atomic number elements[8] and dark areas linked to minerals composed of lighter weight elements [264]; this modality facilitated the research of MTE. Advantages of both BEC (composition contrast) and SEI (topographic contrast) modalities are found in the BES mode. Energy spectra obtained through EDS allowed characterizing the chemistry of the studied minerals qualitatively.

Quantitative analyses of interesting mineral chemistry was performed through the Cameca SX50 microprobe. These quantifications required two analytical programs, one for sulphides and one for oxides. These programs were applied just after calibration by specific standards (pure metals, metalloids and natural or synthetic minerals). For each element the counting time was 10 s, except for Cd which was measured for 20 s in the sulphides program. The acceleration tension was c. 15 kV for oxides and c. 25 kV for sulphides. For both programs the beam size was 2·2 µm with a current of 20 nA. Detection limits in the described conditions for sulphides are given in table 2.3. During oxide measurements, blanks were not determined, therefore oxide

Table 2.3: Microprobe detection limits for sulphides.

element	*S*	*Fe*	*Co*	*Ni*	*Cu*	*Zn*	*As*	*Sn*	*Sb*	*Pb*
error %	*0.41*	*0.29*	*2.22*	*2.87*	*0.53*	*1.24*	*1.44*	*3.23*	*3.10*	*4.63*

DL was not calculated.

2.4.3.6 Sedimentary core dating

Lead 210 (^{210}Pb) is a radioactive form of lead. It is one of the last elements created by the radioactive decay of the isotope ^{238}U. ^{210}Pb forms naturally in sediments and rocks that contain ^{238}U, as well as in the atmosphere, a by-product of radon gas. Within 10 days of its creation from radon, ^{210}Pb falls out of the atmosphere. It accumulates on Earth's surface where it is stored in soils, lake and ocean sediments, and glacial ice. The ^{210}Pb finally decays into a non-radioactive form of lead. ^{210}Pb has a half-life of 22.3 years. If the sediment layers are uninterrupted, then as the sediment ages it slowly loses its radioactivity. Therefore it can be determined how old a sediment layer is by its ^{210}Pb content. It takes about 150 years for the ^{210}Pb in a sample to reach near-zero radioactivity (USGS). Generally, ^{210}Pb dates are confirmed using ^{137}Cs profiles, when the latter are sufficiently intact [265]. The radionuclide ^{241}Am can be used to corroborate ^{137}Cs dates when the profile has been disturbed; moreover, there is growing evidence that ^{241}Am is less mobile in lake sediments than ^{137}Cs [266] and it is more strongly particle-associated than caesium, especially under low pH conditions [267].

Selected sediment samples undertaken during DS in Lake Uru Uru and WS in Cala Cala Lagoon were isotope-counted in the *Ariège Underground Laboratory*; which is managed by LEGOS (Laboratoire d'Etude en Géophysique et Océanographie Spatiales), LMTG and ECOLAB (Laboratoire d'Écologie Fonctionnelle) research teams from the OMP (Observatoire Midy-Pyrinees) Laboratory. Ariège laboratory uses a gamma spectrometer with a 280 cm^3 pure type Ge crystal, constructed with ultra low background materials and placed within an underground gallery below 80 m of solid rock, assuring an effective protection against cosmic rays; background generated by cosmic particles ($>$ 5 MeV) is also attenuated. Before isotope counting at the Arriège Laboratory, samples were weighed at LEGOS within cylindrical vials following two different geometries (3 or 1 cm high) dependent on sample abundance. In the Arriège Laboratory, each sample was counted during 24 hours for ^{210}Pb, ^{226}Ra, ^{137}Cs, ^{228}Ra, ^{40}K, ^{228}Th and ^{241}Am.

[8] MTE are probably found in light areas obtained by BEC mode.

Concentrations of the counted isotopes are given in unities of $Bq \cdot kg^{-1}$.

2.4.3.7 Partial and total digestion procedures and protocols

For each single extraction, reactive blanks were analysed; these blanks were subtracted from the metal(loid) concentrations. Selective digestions were conducted in 50 mL polypropylene centrifugation vials (Greiner bio-one®) previously decontaminated (following Section 2.3.2). Samples were manually and mechanically agitated. Reactive pH was measured with a pH-meter, and pH standardization was performed for each digestion through three standard solutions (pH 3, 5, 7). After each single extraction, samples were centrifuged for 10 min at 4,000 r.p.m.; immediately thereafter the supernatant was collected and filtered through a 0.2 μm porosity polycarbonate syringe-filter (SFCA Nalgene®), and stored cold (4°C) until analysis (See Fig. 2.4.1 for details).

- ***Fraction 1 $MgCl_2$ (exchangeable metals and metalloids).*** 200 mg of the sample is digested in a solution $MgCl_2$ 1 M at pH 7. Immediately thereafter, the samples are continuously agitated for 1h[9].

- ***Fraction 2 acetate (metals and metalloids associated with carbonates).*** 500 mg of the sample is weighed and then added to 10 mL of acetate solution (NaOAc 1 M) buffered at pH 5 with acetic-acid (HOAc). Samples are agitated during 5 hours. After 1h, 1h30 and 2h30 of agitation, the pH is adjusted with 500 µL of HOAc (5M)[10].

- ***Fraction 3 ascorbate (metals and metalloids associated with reactive Fe- and Mn-oxyhydroxides).*** 200 mg of the sample is weighed. Then, ascorbate solution is prepared mixing 50 g sodium-hydrogen-carbonate (buffered solution, keeping pH at 8) and 50 g of sodium citrate di-hydrated (metal complexing in solution) within 1 L of Milli-Q® water; immediately after mixing, 20 g of ascorbic acid (oxide reducer) is added to the solution. Subsequently, 12.5 mL of ascorbate solution is added to the previously weighed samples. Samples are continuously agitated during 24h[11].

- ***Fraction 4 H_2O_2 (metals associated with OM and sulphides).*** 200 mg of the sample is weighed and 1.6 mL of H_2O_2 30% pH 5 (NaOH) is added to the sample. Samples are heated at 85°C on a hot-plate during 2h. While heating, the samples are

[9] Results from F1 are found in Appendix D.2.
[10] Results from F2 are found in Appendix D.3.
[11] Results from F3 are found in Appendix D.4.

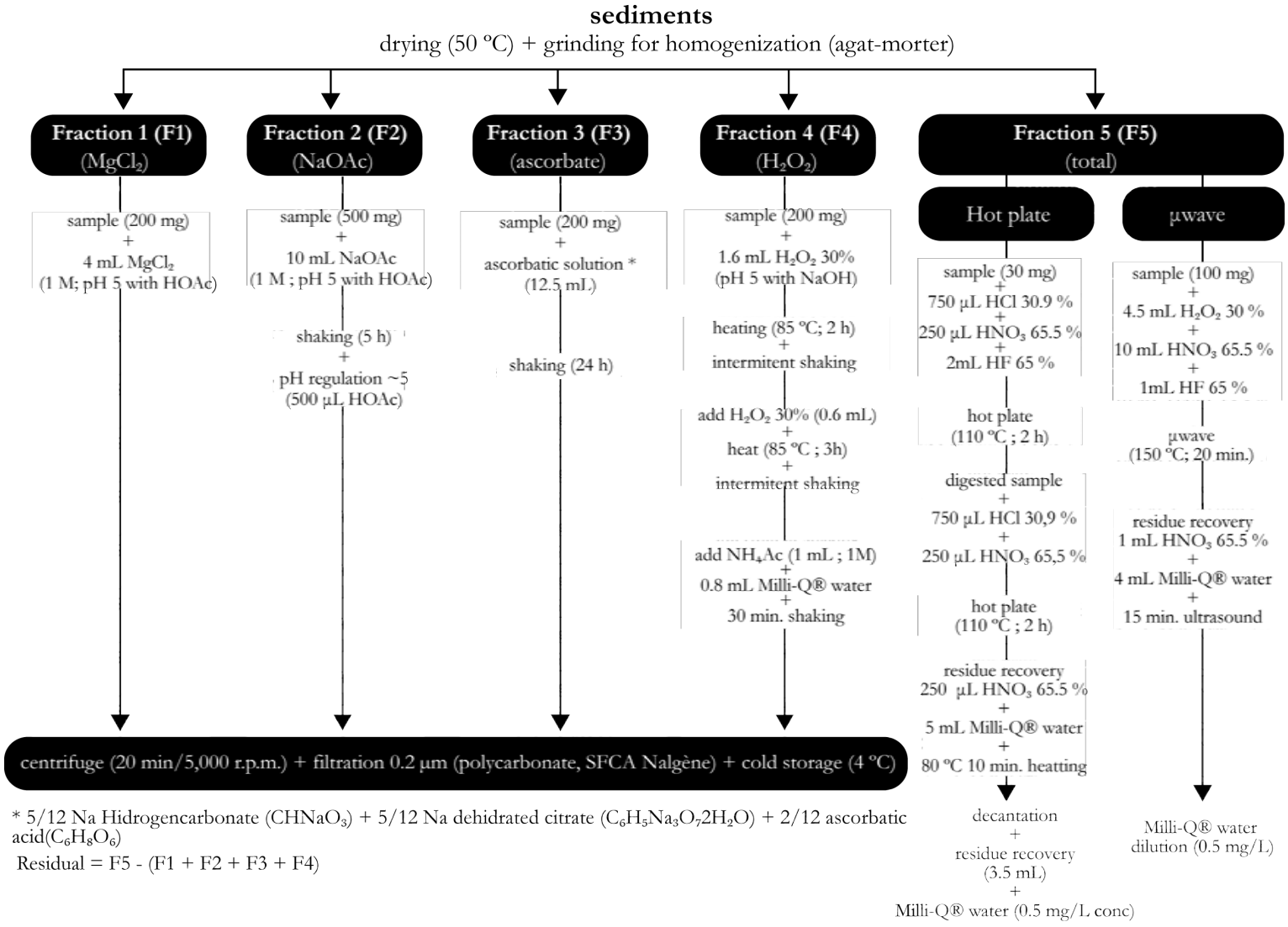

Figure 2.4.1: Scheme of single selective digestion extraction followed in this study.

intermittently agitated. Then 0.6 mL H_2O_2 30% pH 5 is added and samples are heated at 85°C and intermittently agitated for 3h. After cooling, 1 mL of ammonium-acetate solution (NH_4OAc) 1M (dissolved metals complexing) is added and samples are diluted adding 0.5 mL Milli-Q® water. Finally, the samples are agitated for 30 min[12].

- ***Fraction 5 (total digestion).*** Total digestion protocols were different between samples from DS and WS. 30 mg DS samples was weighed in acid-cleansed Teflon® bombs (Savilex®), then digested with 750 µL HCl (30.9%) + 250 µL HNO_3 (65.5%) (*aqua regia*) + 2 mL HF (65%) on a hot plate at 110°C for 2h within hermetically closed Teflon® bombs. After cooling, condensed droplets on bomb-caps were recovered with a rinse of Milli-Q® water using a wash bottle. Evaporation of the bomb contents was effected by 12h heating at 100°C. Due to the precipitation of solid phases during the evaporation step, samples were re-digested in *aqua regia* for 2h. The samples were evaporated on a hot plate and the digestion residue recovery was done with a mixture of 250 µL HNO_3 (65.5%) + 5 mL Milli-Q® water heated for 10 min at 80°C on a hot plate. Supernatant samples were recovered (3.5 mL) and then diluted with Milli-Q® water until 0.5 mg·L^{-1} concentration. To avoid two consecutive digestions, WS samples were digested in a high pressure microwave-accelerated reaction system (MARS model of CEM Corporation®) equipped with an XP-1500 plus Liner system. Digestion was performed through the addition of 1 mL HF (65%) + 10 mL HNO_3 (65.5%) + 4.5 mL H_2O_2 (30%) for 20 min at 150°C following a reviewer digestion protocol from the US Environmental Protection Agency (EPA 3052). Supernatant samples were recovered through 1 mL HNO_3 (65.5%) + 4 mL Milli-Q® water + 15 min ultrasound. Finally, samples were diluted with Milli-Q® water until 0.5 mg·L^{-1} concentration[13].

2.4.4 Dissolved fraction[14]

2.4.4.1 Chlorine (Cl^-), sulphate (SO_4^{2-}) and nutrients (nitrate and ammonium)

High performance liquid chromatography (HPLC) works under an ionic exchange principle. Ionic separation is performed through a positively charged column in the case of anion separation or negatively charged, in the case of cations.

[12] Results from F4 are found in Appendix D.5.
[13] Results from F5 are found in Appendix D.6.
[14] Dissolved fraction results in Appendix E.

Major elements, Cl^- and SO_4^{2-}, and nutrients such as nitrate (NO_3^-) were determined through HPLC in the *Chemistry Laboratory* at LMTG. The instrument used was a Dionex ICS 2000 Chromatographer. In this analysis an anionic column that separates the anions was used. Column eluent was a solution of KOH. After being separated, sample constituents entered into a chemical suppressor, which eliminated the eluent cation (K^+)[15]. Sample anions transformed in acid form, were then detected and measured by conductivity. The accuracy of HPLC measurements was obtained through 4 standard samples (from Christelle Lagane) and ion-915. After measuring 10 samples, analytical drift was controlled and calibrated by standard 3[16]. Detection limits for SO_4^{2-}, Cl^- and NO_3^- were 0.02, 0.04 and 0.002 mg·L^{-1}, while accuracy and precision were better than 3%.

Ammonium is part of pore water positively charged nutrients. The analysis of ammonium was determined through HPLC measurements at the *Laboratory of Chemistry* of AEROLOGIE OBSERVATORY (OMP, Toulouse), where a cationic column for measuring cations (NH_4^+) was available. The used instrument corresponds to a Dionex ICS 1000 Chromatographer. Anionic column eluent was CH_3SO_3H. Since 1996, this laboratory has the WMO (*World Meteorological Organization*) quality label; analytical accuracy has been estimated c. 5% or better for chromatography[17].

2.4.5 Metal and metalloid concentration: inductively coupled plasma-optical emission spectrometry (ICP-OES) and inductively coupled plasma-mass spectrometry (ICP-MS)

To perform this study, accurate measurement of MTE contained within dissolved and particulate fraction of collected samples was needed. This was completed through the establishment and strict enforcement of rigorous analytical protocols. Results validation was achieved by controlling the accuracy of assays using international standards of water and sediment.

2.4.5.1 ICP-OES and major cations

The measurement principle is based on the nebulization and ionization of the liquid sample under an argon plasma (6,000-8,000°C). The atoms in the sample are excited to a higher energy level. The return to a stable state is accompanied by the emission of a series of electromagnetic

[15] Which has a high conductivity and provides a proton (H^+).
[16] Cl^-=15.014; SO_4^{2-}=0.973; NO_3^-=2.42; F^-=0.985; PO_4^{3-}=0.274 all values in mg·L^{-1}.
[17] Major dissolved elements results are detailed in Appendix E.1.

Table 2.4: ICP-OES calibration; RSD: relative standard deviation from standards 1 to 5.

	RSD [%]	
element	*F1*	*F3*
Ca	*1.340*	*9.930*
Mn	*3.903*	*1.764*
Co	-	*5.902*

waves in the range of the visible/UV spectrum characteristic of each element; then the different wavelengths are separated by a spectrometer. The intensity of this emission is indicative of the concentration of the element within the sample.

The optic spectrometer allowed measuring Ca, Co and Mn within the samples subjected to F1 (exchangeable) and F3 (Fe- and Mn-oxyhydroxides) extractions. Element concentration was calculated in the *Laboratory of Chemistry* at LMTG. For these measurements an "Ultima 2" brand Horiba Jobin Yvon ICP-OES was used. Calibration of ICP-OES was performed through 5 internal standards[18]; Co was under DL. After measuring 10 samples, analytical drift was controlled and calibrated by standard 3. Relative standard deviation from internal standards 1 to 5 is shown in table 2.4.

2.4.5.2 ICP-MS

This spectrometer allowed to measure a multi-elementary matrix of elements considered dangerous for the environment and the ecosystem. These elements were: V, Mn, Fe, Co, Cu, Zn, As, Mo, Cd, Sb, Pb and U. ICP-MS was used for calculating the element concentration in pore water and sediments subjected to selective and total digestions. These measurements were performed in the *ICP-MS Laboratory* at LMTG that counts with a quadrupole ICP-MS 7500 ce. Agilent Technologies, characterized by eliminating multiple polyatomic interferences of critical elements (such as As, V and Fe) and dynamic concentration range analyses[19]. Before analysis, samples were diluted to c. 0.5 $mg{\cdot}L^{-1}$ concentration.

For analytical drift control during analysis, an internal calibration was carried out. Two internal standards were used, ^{115}In for the correction of signal variation, and ^{187}Re served to validate the correction [268], both standards were added in known concentration before the analyses. For all analytical series, blanks (MilliQ® water + HNO_3) were measured and the mean blank concentration value was subtracted from measured values in pore water samples.

[18] Containing c. 1, 5, 10, 30 and 50 $mg{\cdot}L^{-1}$ for standards 1 to 5 respectively for F3 measurements and c. 20/0.5, 50/1.0, 100/3.0, 200/5.0 and 350/10 $mg{\cdot}L^{-1}$ Ca/Mn in F1 measurements.

[19] From low-ppt to 1000's of ppm in the same analytical run.

For selective and total digestions of particulate matter, blanks were also subtracted.

2.4.5.3 Results: accuracy and detection limits of ICP-MS

For results validation, international standards for river water and lacustrine sediments were used. Validation of pore water analyses was determined through the SLRS-4 [269] international standard. The accuracy of total digestion procedures was validated through LKSD-1 and LKSD-3 reference standards for lacustrine sediments. Detection limits were calculated from analytical blanks. The mean blank concentration was subtracted from the measured concentrations. Detection limits were calculated as 3 times the blank standard deviation (3 σ) and corresponded to a confident interval larger than 95% (Tables 2.5 and 2.6).

Pore water accuracy was calculated by SLRS-4 analysis. Despite the fact that these concentrations are close to the calculated detection limits, most elements show accuracy and reproducibility better than 5%, yet Mn and As were underestimated (∼16 and ∼10% respectively) and Pb was overestimated (∼40%; Table 2.6)[20].

The total digestion validation of the solid fraction calculated through standard analysis was satisfactory with values lower than 10%, excepting Fe and Mn (∼12 & ∼13%, respectively; Table 2.6).

[20] Dissolved trace elements results are detailed in Appendix E.2.

Table 2.5: Measured and certified concentrations of LSRS-4 standard. All concentrations in µg·L^{-1}, DL (detection limit) for elements measured within blank samples.

	LSRS-4						*DL*
element	*measured value*			*certified value*			
V	*0.287*	±	*0.018*	*0.317*	±	*0.033*	-
Cr	*0.196*	±	*0.011*	*0.208*	±	*0.023*	*0.057*
Mn	*3.31*	±	*0.16*	*4.33*	±	*0.18*	*1.655*
Fe	*85.1*	±	*3.8*	*91.2*	±	*5.8*	*35.731*
Co	*0.02*	±	*0.004*	*0.05*	±	-	-
Ni	*0.539*	±	*0.035*	*0.476*	±	*0.064*	-
Cu	*16.9*	±	*0.5*	*17.4*	±	*1.3*	-
Zn	*1.032*	±	*0.022*	*0.845*	±	*0.095*	*4.605*
As	*0.325*	±	*0.020*	*0.413*	±	*0.039*	-
Mo	*0.2*	±	*0.006*	*0.5*	±	-	*2.032*
Cd	*0.008*	±	*0.0003*	*0.006*	±	*0.0014*	-
Sb	*0.316*	±	*0.005*	*0.300*	±	-	-
Pb	*0.135*	±	*0.011*	*0.081*	±	*0.006*	-
U	*0.1*	±	*0.01*	*0.1*	±	-	*0.003*

Table 2.6: Measured and certified concentrations of LKSD-1 and LKSD-3 certified lacustrine sediment reference standards. All concentrations in $mg \cdot kg^{-1}$, except DL in $\mu g \cdot kg^{-1}$ (certified values errors from Lynch 1999 [270]).

	LKSD-1						*LKSD-3*						*DL*
element	*measured value*			*certified value*			*measured value*			*certified value*			*blank·3σ*
Ti	*3,114*	±	*18*	*3,010*	±	*260*	*3,244*	±	*36*	*3,330*	±	*330*	*0.0578*
V	*54*	±	*0.4*	*50*	±	*5*	*87*	±	*1*	*82*	±	*8*	*0.0043*
Cr	*25*	±	*0.2*	*31*	±	*3*	*83*	±	*1*	*87*	±	*8*	*0.0251*
Mn	*673*	±	*4*	*700*	±	*30*	*1,212*	±	*11*	*1,440*	±	*80*	*0.0121*
Fe	*22,794*	±	*134*	*29,000*	±	*1000*	*36,559*	±	*537*	*40,000*	±	*2,000*	*0.5748*
Co	*10*	±	*0.1*	*11*	±	*1*	*32*	±	*0.17*	*30*	±	*2*	*0.0043*
Ni	*17*	±	*0.1*	*16*	±	*3*	*55*	±	*0.34*	*47*	±	*5*	*0.0078*
Cu	*47*	±	*0.4*	*44*	±	*5*	*37*	±	*0.36*	*35*	±	*3*	*0.0091*
Zn	*345*	±	*2*	*331*	±	*22*	*146*	±	*0.96*	*152*	±	*14*	*0.0638*
As	*37*	±	*0.3*	*40*	±	*2*	*28*	±	*0.29*	*27*	±	*6*	*0.0019*
Mo	*10*	±	*0.1*	*10*	±	*2*	*1.2*	±	*0.03*	*<5*	±	-	*0.0105*
Ag	*0.7*	±	*0.01*	*0.6*	±	*0.05*	*2.9*	±	*0.02*	*2.7*	±	*0.11*	*0.0018*
Cd	*1.5*	±	*0.03*	*1.4*	±	*0.3*	*0.7*	±	*0.02*	*1.2*	±	*0.6*	*0.0037*
Sb	*1.2*	±	*0.02*	*1.2*	±	*0.1*	*1.3*	±	*0.01*	*1.3*	±	*0.1*	*0.0242*
Pb	*95*	±	*0.34*	*82*	±	*5*	*33*	±	*0.38*	*29*	±	*3*	*0.0049*
U	*10.4*	±	*0.1*	*9.7*	±	-	*4.3*	±	*0.04*	*4.6*	±	-	*0.0003*

Chapter 3

Geochemical background and baseline of sediments in Oruro Department, anthropogenic and natural sources of MTE

Introduction

The objectives of this chapter were to determine (1) the geochemical background and baseline of sediments in the Altiplano of Bolivia and (2) the probable anthropogenic and natural sources of contaminants in this environment. We reached these objectives through 91 samples from lacustrine sediments taken in Lake Uru Uru (Altiplano) and Cala Cala Lagoon (eastern Andes Cordillera). We completed the data of this study with Oruro Pilot Project (PPO) base data.

We determined the total metal(loid) content (TMC) of sediments through total digestions and compared our results to the PPO base data. Statistics and geographical information system (GIS) analyses allowed us to determine that in this area the natural geochemical background of As and Sb is significantly enhanced in comparison to the Upper Continental Crust (UCC) concentration, world background levels, industrial sites and historical mining sites. The use of a local enrichment factor (EF) normalized by the mean concentrations of Cala Cala Lagoon (CCLAC), demonstrated that using the UCC concentrations to calculate EFs (EF_{UCC}) is inadequate for this highly mineralized environment and therefore is not supported. Regarding metal(loid)s, the strong multiplicity of sources in this environment makes it difficult to discriminate between natural and anthropogenic input into this endorheic drainage basin, although it is suggested that superficial soils are probably impacted by airborne particulates dispersed from the Vinto (Sb-Sn) Smelter, while Lake Uru Uru is influenced by mining activities, particularly drainage waste of the San José and Huanuni Mines. As a final contribution to Chapter 3, a geochemical background and a present-time baseline for Bolivian highlands sediments are provided, which will be helpful for the improvement of environmental legislation and for the future interpretation of geochemistry data in contamination and/or pollution studies in the Altiplanic area.

This study represents one of the first attempts to understand metal(loid) distribution and sources in the Altiplano of Bolivia, an importantly mineralized high plateau. We stress that geochemical backgrounds and baselines are poorly developed in developing countries and represent an important issue for environmental legislation and sciences. Chapter 3 was accepted for publication in *Geochemistry: exploration, environment, analysis* (GEEA) of *The Geological Society of London* in January 2011 and will be published in the August 2011 edition[1].

[1] http://geea.allentrack.net/cgi-bin/main.plex?el=A2Dc3CN3B2Kb3F2A9oUIlpV4l2r1Vz7XBEu1ivwZ

Paper 1. Geochemical background, baseline and origin of trace metals and metalloids from lacustrine sediments in the mining-impacted Altiplano and Eastern Cordillera of Oruro, Bolivia

J. Tapia[1,2]; S. Audry[1]; B. Townley[2]; J.L. Duprey[3]

[1]Université de Toulouse, OMP/LMTG, 14 Av. Edouard Belin, 31400 Toulouse, France

[2]Departamento de Geología, Universidad de Chile, Plaza Ercilla 803, casilla 13518, correo 21, Santiago, Chile

[3]Institut de Recherche pour le Développement, US IMAGO 191, CP 9214 La Paz, Bolivia

Abstract

Oruro, located on the Bolivian Altiplano, has been subjected to intense mining and smelting activities since Colonial times (XVIIth century), yet the current geochemical composition of sediments and trace element behaviour is practically unknown. A collection of 91 sediment samples retrieved from five sedimentary cores from Lake Uru Uru (Altiplano) and Cala Cala Lagoon (Eastern Cordillera) subjected to a total digestion technique, plus a compilation of pre-existent data base of trace element concentration in soil and lacustrine sediment obtained from the Oruro Pilot Project (PPO) allowed to propose a geochemical background and a present-time baseline for As, Cd, Cu, Pb, Sb and Zn in sediments from this area.

Results obtained by statistics and geographical information system (GIS) analyses showed that the natural geochemical background of As and Sb is significantly enhanced in comparison to the Upper Continental Crust (UCC) concentration, world background levels, industrial sites and historical mining sites. The use of a local enrichment factor (EF) normalized by the mean concentrations of Cala Cala Lagoon (CCLAC), demonstrated that using UCC concentrations to calculate EFs (EF_{UCC}) is inadequate for this highly mineralized environment and therefore is not supported. Regarding metals and metalloids, the strong multiplicity of sources in this environment makes it difficult to discriminate between natural and anthropogenic input into this endorheic drainage basin, although it is suggested that superficial soils are probably impacted

by airborne particulates dispersed from the Vinto (Sb-Sn) Smelter, while Lake Uru Uru is influenced by mining activities, particularly drainage waste of the San José and Huanuni Mines. As a final contribution, a geochemical background and a present-time baseline for Bolivian highlands sediments is provided, which will be helpful for the improvement of environmental legislation and for the future interpretation of geochemistry data in contamination and/or pollution studies in the Altiplanic area.

Resumen

Oruro, localizada en el Altiplano de Bolivia, ha sido sujeta a actividades mineras intensas desde los tiempos coloniales (siglo XVII), sin embargo la composición actual de sedimentos y el comportamiento de los elementos traza son prácticamente desconocidos. Un total de 91 muestras de sedimento obtenidas a partir de cinco testigos sedimentarios del Lago Uru Uru (Altiplano) y la Laguna Cala Cala (Cordillera de los Andes Oriental) sujetos a técnicas de digestión total, más una compilación de datos pre-existentes de concentración de elementos traza en suelos y sedimentos obtenidos del Proyecto Piloto Oruro (PPO) permitieron proponer un background geoquímico, y una línea de base actual para As, Cd, Cu, Pb, Sb y Zn en sedimentos de esta área.

Los resultados obtenidos a través del análisis estadístico y de sistemas de información geográfica (SIG) mostraron que el background geoquímico natural de As y Sb está enriquecido significativamente en comparación con la corteza continental superior (UCC), niveles background mundiales, sitios industrializados y sitios mineros históricos. El uso de un factor de enriquecimiento (EF) local normalizado por la concentración promedio de la Laguna Cala Cala (CCLAC), demostró que el uso de las concentraciones de la UCC para calcular EFs (EF_{UCC}) es inadecuado para este ambiente altamente mineralizado y por lo tanto no se sugiere su uso. Con respecto a los metales y metaloides, la gran multiplicidad de fuentes en este ambiente hace difícil discriminar entre aportes de fuentes naturales y antropogénicos a este sistema endorreico, sin embargo se sugiere que los suelos superficiales están probablemente impactados por partículas atmosféricas diseminadas desde la Fundición de Vinto (Sb-Sn), mientras el Lago Uru Uru está influenciado por actividades mineras, particularmente drenaje de las Minas San José y Huanuni. Como contribución final de este estudio, se generó un background geoquímico y una línea de base actual para sedimentos altiplánicos de Bolivia, las que serán útiles para mejorar la legislación ambiental y la interpretación en el futuro de datos geoquímicos en estudios de

contaminación y/o polución en el Altiplano.

Résumé

Oruro, située dans les hauts plateaux de Bolivie, a fait l'objet d'intenses activités minières depuis l'époque coloniale (XVII^{eme} siècle), mais la composition actuelle des sédiments et le comportement des éléments traces sont pratiquement inconnus. Un total de 91 échantillons de sédiments obtenus à partir de cinq carottes de sédiments du lac Uru Uru (Altiplano) et lagune Cala Cala (Cordillère des Andes Orientale) soumis à des techniques de digestion total, ainsi que une base des données pré-existantes des concentrations d'éléments traces dans les sols et les sédiments provenant du Projet Pilote Oruro (PPO), a permis de proposer un bruit du fond géochimique et une ligne de fond géochimique actuelle pour As, Cd, Cu, Pb, Sb et Zn dans les sédiments de cette zone.

Les résultats menés par analyses de statistique et des systèmes d'information géographique (SIG) ont montré que le fond géochimique naturel de As et Sb est significativement plus élevé par rapport à la composition de la croûte continentale supérieure (UCC), niveaux de fond mondial, les centres industriels et sites miniers historiques. L'utilisation d'un facteur d'enrichissement (EF) local normalisé par la concentration moyenne de la Lagune Cala Cala (CCLAC) a montré que l'utilisation de la concentration moyenne de l'UCC par calculer les EFs (EF_{UCC}) est insuffisante pour cet environnement fortement minéralisé et donc son utilisation n'est pas appropriée. En ce qui concerne les métaux et les métalloïdes, la multiplicité de sources dans cet environnement fait difficile de distinguer les apports naturels et anthropiques des MTE dans ce basin endoréique. Cependant, malgré la multiplicité des sources des MTE, l'impact humain sur la surface du sol est lié principalement à la diffusion des polluants provenant de la Fonderie de Vinto (Sb, Sn), tandis que le lac Uru Uru est affecté par les activités minières, notamment les résidus du passé et actuels des Mines San Jose et Huanuni. Finalement, nous avons généré un un bruit du fond géochimique et un ligne de fond géochimique pour les sédiments de l'Altiplano bolivien, qui sera utile pour améliorer la législation environnementale et l'interprétation future des données géochimiques des études du contamination et/ou du pollution sur l'Altiplano.

3.1 Introduction

At present two terms are commonly used to establish the geochemical composition of soils, sediments, rocks or water for any defined area, viz. the geochemical background and geochemical baseline. The term *geochemical background* derives originally from exploration geochemistry, and was defined by Hawkes & Webb (1962) [5] as "the normal abundance of an element in barren earth material". These authors concluded that "it is more realistic to view background as a range rather than an absolute value". The term *geochemical baseline* was officially introduced in the context of the International Geological Correlation Programme (IGCP, projects 259 and 360; [7]) in order to create a global reference network for national regional geochemical data sets and as an international background database for environmental legislation. This term refers to the prevailing variation in the concentration of an element in the superficial environment [8, 9] and furthermore, indicates the actual content of an element at a given point in time [9]; it includes the geogenic natural concentrations (natural background) and the diffuse anthropogenic contribution in the soils [1, 10].

As pointed out by many authors [4, 8, 9], background concentrations depend on numerous factors, which are: (1) the kind of sample material investigated; (2) grain size; (3) extraction method; (4) spatial scale; (5) location; and (6) why and for what purpose the background is needed. The importance of the latter point lies mainly in environmental legislation, which prescribes limits for contaminants in soils and other superficial materials, and also allows political decision-making in the assessment of contaminated areas [8, 9]. In terms of environmental legislation, it is important that regulators recognize that backgrounds (and therefore baselines) depend on location and scale, implying that they change from area to area and with the scale of the area investigated [4].

The idea of being able to define a geochemical background concentration via a statistical exercise alone is illusive [4, 271]. Therefore, the analysis of data via multiple data-treatments is a tool to assess the degree of contamination in determined areas, allowing specific environmental legislation that depends on the characteristics of each site.

Based on pre-existent data from lacustrine superficial sediments and soils [260], and sampling and analysis of lacustrine sedimentary cores for this study, a geochemical background and a present time baseline of the Bolivian highlands via statistics and Geographical Information System (GIS) analysis is proposed. This was motivated by the fact this region has been subjected since the XVII$^{\text{th}}$ century to intense mining activities and, despite that, very little is

known about the geochemical characteristics and dispersion processes affecting this area. The background and present time baseline as determined in this study will allow a better understanding of the current geochemical composition of sediments. Furthermore, it will provide data for future interpretation of geochemistry in this region together with an improvement of environmental data for coverage and quality legislation in this particular environment.

3.2 Study area

Throughout the 20^{th} century, mining was Bolivia's top industry, producing much of the world's Sb, Bi, Pb, Ag, Sn, W and Zn. Presently, Bolivia is ranked as the third largest producer of Sb in the world, as well as ranking fourth in Sn and Zn, and sixth in W [217]. A significant proportion of these commodities is located in the Oruro Department, where the capital city of Oruro was founded in 1606, the same year as the opening of the San José Mine [254]. Since then, intense mining activities across the whole region have taken place. The development of Oruro Department has depended mainly on the exploitation and refining of mineral resources and, according to Bolivian INE (National Statistics Institute; INE), in the past 10 years, 95% of exports from Oruro were related to mining and metal processing and these activities have accounted for nearly 97% of the income in the region. The absolute economic dependence on non-renewable resources has generated poverty and environmental degradation in the area [253, 254] and at present there is no other recognized economic activity to replace the exploitation and refining of metals. Hence, the only current solution to economic and social instability is by the improvement and revitalization of the mining sector, which also implies an improvement of environmental management and legislation.

3.2.1 Regional description: Hydrology, climate, geomorphology and geologic setting

The study area is located 230 km south-east of the city of La Paz, within the Bolivian highlands between 3,700 and 4,200 m a.s.l. and extends for approximately 6,200 km^2. The main drainage basin corresponds to the Lake Titicaca-Desaguadero River-Lake Poopó-Coipasa Salar (TDPS, Fig. 3.2.1) endorheic hydrologic system. This basin is highly vulnerable to anthropogenic influence, because as an endorheic system all the material transported by the water courses (natural weathering material as well as contaminants) are concentrated within the system. The only mechanism (with the exception of evaporation and wind transport) to

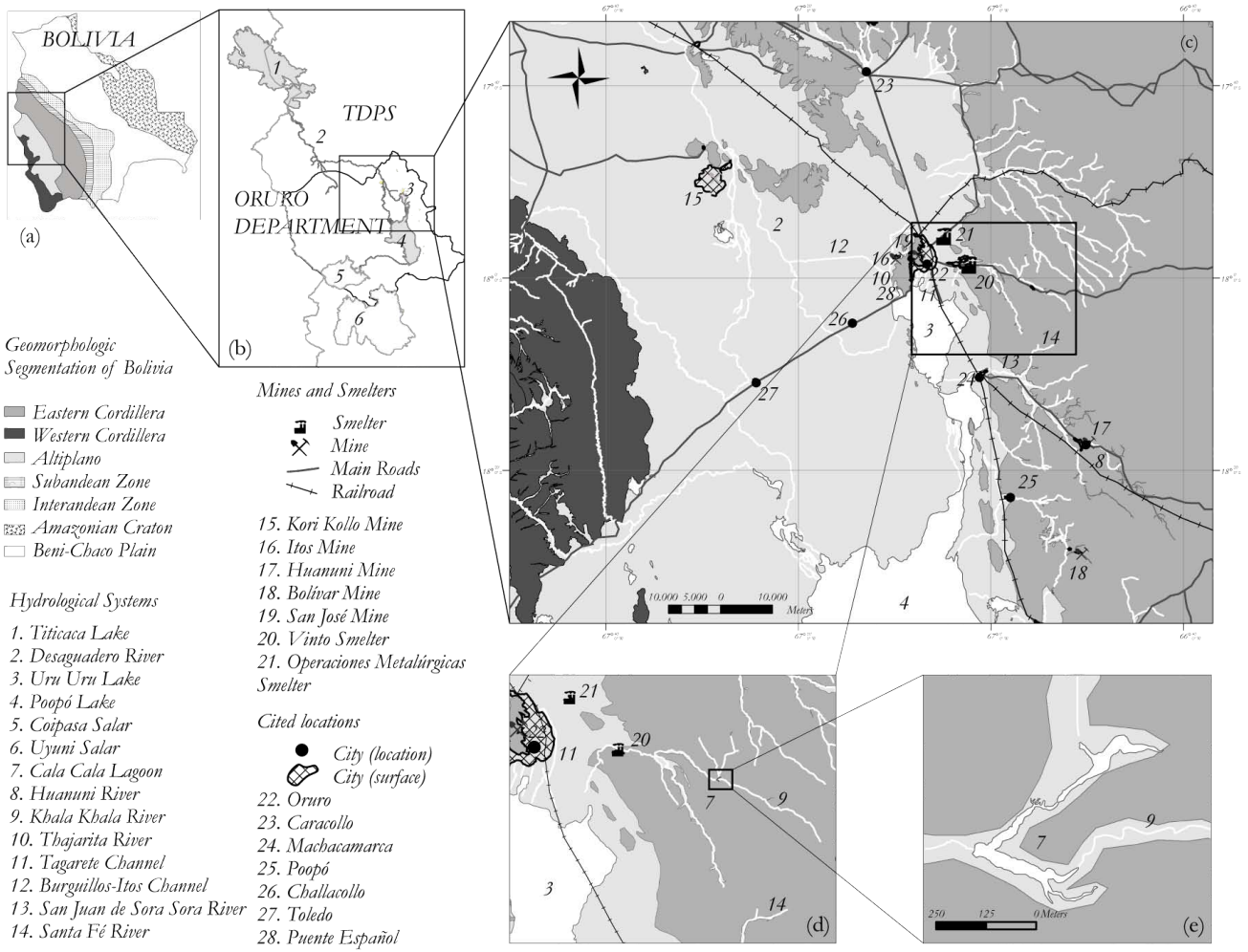

Figure 3.2.1: (a) Geomorphologic segmentation of Bolivia (modified from Redwood & Rice 1997 [272]); (b) Lake Titicaca-Desaguadero River-Lake Poopó-Coipasa Salar (TDPS) endorheic hydrologic system; (c) Oruro Department detail; (d) Khala Khala River basin; (e) Detail of Cala Cala Lagoon.

dispose of residual materials is by anthropogenic transport [250].

In the Bolivian highlands two distinct climatic seasons are observed, a dry season (DS) and a wet season (WS), extending from May to September and October to March, respectively, and implying a wet summer and a dry winter. Scarcity of precipitation is characteristic of this region (less than 400 mm per year; [245]). According to data from Bolivian SENAMHI (Meteorology and Hydrology National Service) prevalent wind directions since 1971 are W-NW during the DS and to the E during the WS.

Geomorphologically, this zone is made up of: (i) the Altiplano, (ii) the Western Cordillera, and (iii) the Eastern Cordillera (Figs. 3.2.1 and 3.2.2). The Altiplano (AL) is a broad longitudinal tectonic basin filled with predominantly Tertiary continental deposits and is flanked on the east by the Eastern Cordillera and on the west by the Western Cordillera (Figs. 3.2.1 and 3.2.2). The Western Cordillera (WC) consists mostly of andesitic stratovolcanoes and rhyolitic ash-flow tuffs that overlie a basement of Jurassic and Cretaceous sedimentary and volcanic rocks (Fig. 3.2.2). The Eastern Cordillera (EC) is underlain mainly by a thick sequence of intensely folded, lower Palaeozoic, marine clastic sedimentary rocks and overlain locally by similarly deformed Cretaceous-lower Tertiary continental sedimentary rocks, undeformed late Tertiary unconsolidated continental sediments, and late Oligocene to Pliocene volcanic rocks (Fig. 3.2.2; [213, 214, 215, 216]). In this area, ore mineralization is associated with red-bed copper deposits and epithermal deposits in the AL and WC; and the tin belt, the gold-antimony belts, and the lead zinc belt in the EC [217]. In the AL and WC Sedimentary-Rock Hosted Copper Deposits correspond to Miocene to Pliocene stratiform copper deposits scattered along the length of the AL [217], while the Polymetallic Belt is mainly composed of epithermal Ag-Au-Pb-Zn-Cu deposits formed during the Middle-Late Miocene and Early Pliocene [222, 223]. The EC is the host for most of the mineral resources of Oruro Department and includes the well-known Bolivian Tin Belt, the Gold-Antimony Belts and the Lead-Zinc Belt. The Bolivian tin belt is a 900 km long belt extending east-west throughout Bolivia from northernmost Argentina to southernmost Peru. This belt is divided by the prolongation of Arica's elbow to the east into two sections, north and south [218], where the northern part contains Au, W, Sb, Sn, Bi, Zn and Pb mineralization and the southern part is characterized by rich Ag and poor Au polymetallic tin deposits, with a great variety of Sn, Ag and base metal minerals similar to those from the north. These deposits are genetically related to small (1-2 km^2) quartz latitic or dacitic porphyry domes or stocks of Neogene-Quaternary age [213, 218, 219, 220] and in the study area, occur within the transition between both sections of this metallogenic belt, the Huanuni

and Bolivar Sn-rich mining districts being well known (Figs. 3.2.1 and 3.2.2). The Bolivian Gold-Antimony Belts are generally found in the same parts that tin mineralization related to Mesozoic and Tertiary intrusions and are mainly hosted by Middle Ordovician to Early Silurian sedimentary rocks, and many deposits contain as much as 10 to 20% Sb, consequently, many of these were originally mined for Sb [217]. The Lead-Zinc Belt is a series of sedimentary rock-hosted Ag-Pb-Zn veins, with anomalous concentrations of Au and Sb, and no clear association with magmatic centres that are located along the length of the central part of the southernmost EC [217]. The existence of these metallogenic belts has historically established Bolivia as one of the major Sn and Sb producers in the world, having led to the construction of the Vinto Smelter in 1971 to process Bolivian Sn-Sb mineral concentrates locally. The complexity of ores and the related smelting procedures have caused emissions of approximately 14,000 tons of SO_2 - per year and between 400 and 1,000 tons of metallic particles per year, representing an important anthropogenic contaminant source of airborne particulates [254].

3.2.2 Sampling sites

Lake Uru Uru is located 5 km south of Oruro and is in the central part of the TDPS drainage basin. It is a shallow lake that formed during the last century (1900s) due to the deviation of the Desaguadero River [245] and is divided by a railroad and a highway embankment, allowing a minimum exchange of water between the two separate parts (Fig. 3.2.1; [252]). The western part is fed by the eastern branch of the Desaguadero River and by the Thajarita River (that receives most of its water from the Desaguadero River via the Burguillos-Itos Channel), which discharges into Lake Uru Uru at Puente Español (Fig. 3.2.1). The northern part is fed by the Tagarete River, a channelized water course (Fig. 3.2.1; [252]). The southernmost part is drained through the Desaguadero River, flowing south for approximately 30 km before entering Lake Poopó. The San Juan de Sora Sora River enters the main channel from the east transporting its waters into the southern outflow of Lake Uru Uru (up to 7 km to the south); this river drains the Huanuni and Santa Fé river basins [252]. Lake Uru Uru is very shallow, therefore depth and surface extension vary enormously between the DS and WS and from year to year (depending mainly on the intensity of the WS precipitation and DS evaporation rate). Despite this fact it has not suffered complete desiccation (main difference with respect to Lake Poopó) attaining its maximum continuous lake water surface in 1986 (150 km^2; [252]).

Preliminary studies undertaken in this area [245, 247, 252, 253, 255, 256, 258, 259, 273, 274, 275] demonstrated that surrounding areas and Lake Uru Uru are strongly affected by

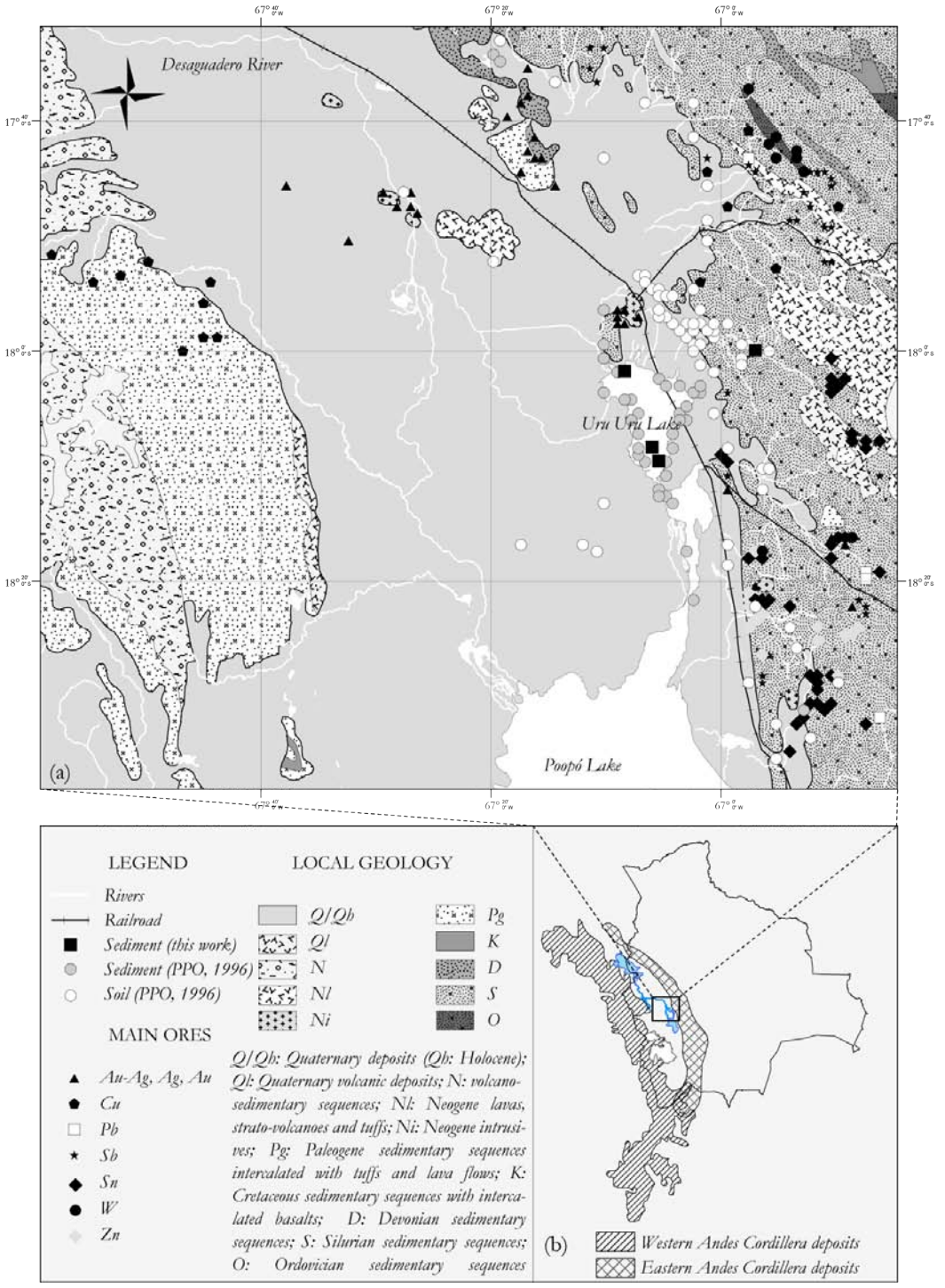

Figure 3.2.2: (a) Regional geology, sampling sites, pre-existent data location and principal ores of the study region. (b) Bolivian Tin Belt and Neogene-Quaternary volcanic rocks spatial distribution (modified from Wallianos *et al.* 1999 [219]).

anthropogenic activities, especially mining, and that this lake operates as a natural receptacle for trace metals and metalloids [252, 257]. In contrast to Lake Uru Uru, Cala Cala Lagoon, located 18 km east of Oruro within EC sedimentary rocks (Uncia and Catavi Formations), corresponds to an artificial lagoon that channels water from the Khala Khala River (Figs. 3.2.1 and 3.2.2) through EC mineralized rocks. One interesting feature of the Cala Cala Lagoon is that its watershed is characterized by the absence of mining activities. Normalization of trace element concentrations to a conservative (i.e. insoluble) element are widely used to differentiate between the lithogenic and anthropogenic origins of trace metals and metalloids (e.g., [15, 276]). Ti-normalized depth-profiles of trace metals and metalloids from the Cala Cala Lagoon (not shown) exhibit rather flat shapes (e.g. mean Sb/Ti: 2.2E–03 ± 2.2 E–04; mean Zn/Ti: 2.2E–02 ± 2.2E–03). This indicates a minimal influence of anthropogenic inputs and particularly that the Cala Cala Lagoon sediments are likely not the recipient of airborne particulates from the Sb-Sn Vinto smelter, either directly or via soil/sediment transfer from its watershed. Accordingly, the Cala Cala Lagoon was selected as the most suitable candidate for the determination of a geochemical background in lacustrine sediments from this densely mineralized region.

3.3 Materials and methods

3.3.1 Sampling and analytical procedures

In the field, a total of five sedimentary cores were retrieved: four from Lake Uru Uru and one from Cala Cala Lagoon. Cores from Lake Uru Uru were collected at the beginning of the DS (21-25 April 2008) and during the WS (2-6 February 2009). For both seasons the northern and southern parts of the lake were sampled. These sites were chosen due to the contrasting sources of water input in both areas: the northern source is linked to the Thajarita River and the Tagarete Channel, which transports waste from the San José (Ag-Pb-Zn-Au) Mine and sewage from Oruro, and the southern part is related to the San Juan de Sora Sora River, which transports waste material from the Huanuni (Sn) Mine. Due to the constant desiccation of the eastern side, all cores from Lake Uru Uru were retrieved from the western part where the depth ranged between 0.8 and 2.0 m at the sampling sites. The Cala Cala Lagoon core (Figs. 3.2.1 and 3.2.2) was collected in order to compare the composition of lacustrine sediments of the EC with that of the AL and to determine the geochemical background of sediments probably not impacted by mining and/or smelting from the EC. Cores were collected using a Large Bore

Interface Corer (Aquatic Research Instruments®) equipped with a polycarbonate core tube (60 cm length, 10 cm inner diameter). This corer enables sampling the uppermost decimetres of the sediments without any disturbance of the water-sediment interface. Immediately after recovery, the sediment core was extruded and sliced with an acid-cleansed plastic cutter. A decreasing vertical resolution of slicing was applied: (i) 5-mm resolution for the first 5 cm below the water-sediment interface, (ii) 10-mm resolution for the following 5 cm of sediment, and (iii) 25-mm resolution down to the bottom of the core. The length of the cores ranged from 18 to 40 cm. Immediately after slicing, the sediment samples were centrifuged in the field at 4000 r.p.m. to remove pore water and the resultant sediment samples were kept in sealed bags until analysis (for sampling details see [15, 207]). In the laboratory, sediments were dried at 50°C to constant weight and then powdered and homogenized with an agate mortar. The sediment samples from the DS were digested in acid-cleansed, closed Teflon bombs (Savilex®) with aqua regia plus HF on a hot plate at 110°C for 2 hours, then re-digested in aqua regia for two hours due to the precipitation of solid phases during the evaporation step. To avoid two consecutive digestions, the WS sediment samples were digested with HF + HNO_3 + H_2O_2 using a high pressure microwave accelerated reaction system (MARS model of CEM Corporation®) equipped with an XP-1500 plus Liner system for 20 minutes at 150°C following a reviewer digestion protocol from the US Environmental Protection Agency. Each batch of samples included method blanks and digestion of certified international reference material (LKSD01 & LKSD03). Element concentrations were measured using a quadrupole ICP-MS 7500 ce. (Agilent Technologies). Analytical drift was controlled and calibrated by an internal Re-In standard. Regardless of the digestion technique, accuracy was within 5% of the certified values and the analytical error (relative standard deviation) was generally better than 5% for concentrations 10 times higher than the detection limits for most of the elements (excepting Pb, the digestion recovery was within 15% of the certified values; see Table 3.1 for details).

3.3.2 Complementary data source

In addition to the data obtained from the 2008 and 2009 field campaigns at Lake Uru Uru (see above) a complementary database previously acquired within the framework of the Oruro Pilot Project [260] was used. This project was funded by The World Bank and SIDA (Swedish International Development Authority), and was undertaken by the Swedish Geological AB (SGAB) and the Servicio Geológico Minero de Bolivia (SERTECGEOMIN) between 1993 and 1996. This study provided data for: (i) 30 Lake Uru Uru surface sediment (up to 5 cm

Table 3.1: Total digestion geochemistry of the standardized sediments LKSD-1 and LKSD-3. Concentrations in mg/kg. HP: hot plate digestion; µwave: high pressure microwave digestion; CV: certified values [270]; ±: confidentiality range.

	LKSD-1						*LKSD-3*			
	HP	±	*µwave*	±	*CV*	±	*µwave*	±	*CV*	±
As	*33*	*0.11*	*39*	*0.51*	*40*	*2*	*28*	*0.37*	*27*	*2*
Cd	*1.5*	*0.04*	*1.4*	*0.04*	*1.4*	*0.3*	*0.66*	*0.01*	*0.8*	*0.6*
Cu	*50*	*0.85*	*46*	*0.63*	*44*	*5*	*37*	*0.44*	*35*	*3*
Pb	*90*	*0.12*	*97*	*0.90*	*82*	*5*	*33*	*0.49*	*29*	*3*
Sb	*1.0*	*0.01*	*1.2*	*0.04*	*1.2*	*0.1*	*1.26*	*0.01*	*1.3*	*0.1*
Zn	*345*	*0.19*	*345*	*3.49*	*331*	*22*	*146*	*1.39*	*152*	*14*
Ti	*2,923*	*12*	*3,210*	*32*	*3,010*	*230*	*3244*	*44*	*3,330*	*330*

depth) samples retrieved in 1995 at a 2-km spacing, these samples were digested with aqua regia and measured using an ICP-MS at the Svensk Grundänesanalys AB Laboratory in Sweden and (ii) 75 surface soil samples, 52 soil samples from depths up to 5 cm, and 49 soil samples from depths between 20 to 25 cm. Element concentrations were determined from 3-kg soil samples in the Spectrolab Laboratory, Oruro, Bolivia. This soil geochemical data base was used only for comparison purposes, because the analytical procedures and QA/QC (quality assurance/quality control) were not available (for more analytical details see PPO reports [260]).

3.3.3 Statistics, enrichment factors and Geographical Information System (GIS)

A statistical evaluation of sediment and soil data was undertaken to estimate threshold values separating anomalies from background data, including the determination of significant descriptive parameters of centring, dispersion and shape such as: mean, median, 95th percentile, minimum, maximum, standard deviation, median absolute deviation (MAD), kurtosis, skewness, second (Q_2) and third (Q_3) quartile (Table 3.2 and Fig. 3.3.1). The mean provides a better estimate of location, even for skewed populations if the extreme values truly belong to this population, though their presence may require a data transformation to meet normality assumptions. Nevertheless in many cases, the regional distribution of elements is influenced by more than one process/source, resulting in multi-modal, and often skewed, distributions. In these cases, the median is far superior to the mean as a robust estimator of location [277], and the MAD is an appropriate measure of data spread instead of the standard deviation [271].

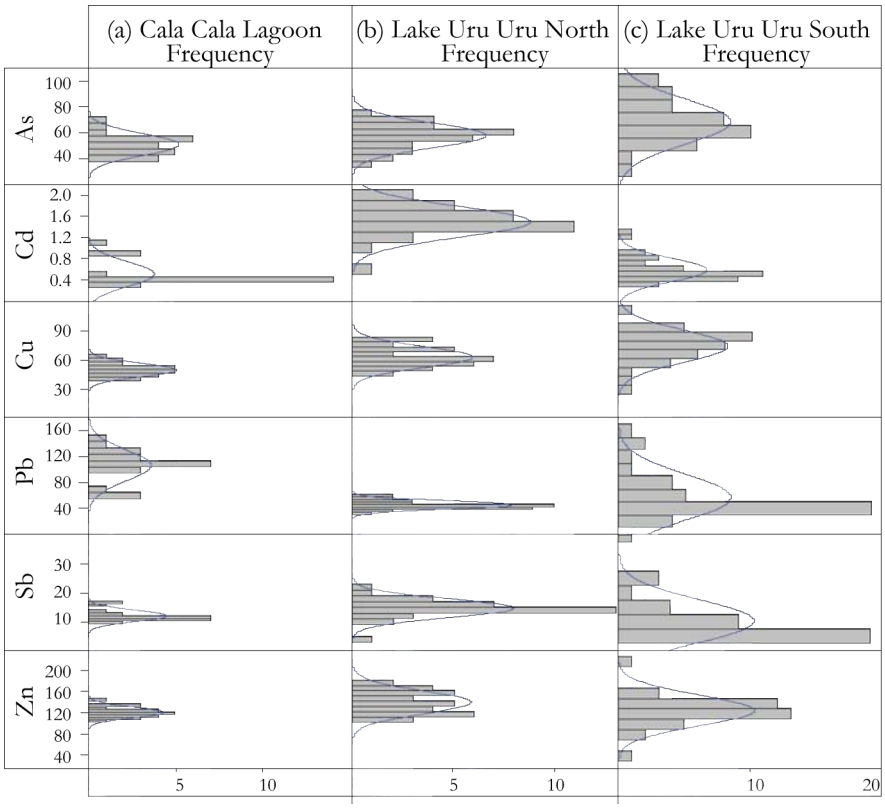

Figure 3.3.1: Distribution histograms for (a) Cala Cala Lagoon sediments; (b) North Lake Uru Uru sediments; (c) South Lake Uru Uru sediments.

Table 3.2: Summary of statistical descriptive parameters of centering, dispersion and shape. Concentration in mg/kg. N: north; S: south; 1: this work; 2: Oruro Pilot Project (PPO); MAD: median absolute deviation; Q2: second quartile; Q3: third quartile.

element (mg/kg)	n	mean	median	95^{th} percentile	min	max	standard deviation	MAD*	skew	asymmetry coefficient	Q_2	Q_3
Arsenic	sed	C^1	22	51	51	64	38	72	8	5	1	0.6
		N^1	32	57	59	70	37	76	10	8	-1	-0.2
		S^1	37	67	65	99	30	104	17	13	0	0.4
		NS^1	69	63	60	89	30	104	15	9	1	0.7
		LUU^2	34	78	53	276	15	431	94	20	9	2.9
	soil	Sup^2	74	257	240	404	133	463	81	53	0	0.7
		5 cm^2	52	33	32	50	14	63	9	4	1	0.8
		25 cm^2	49	20	19	24	12	26	3	2	0	-0.1
		5-25 cm^2	101	27	24	48	12	63	10	6	1	1.2
Cadmium	sed	C^1	22	0.5	0.4	0.9	0.3	1.1	0.2	0.0	1	1.7
		N^1	32	1.5	1.5	1.9	0.6	2.0	0.3	0.2	2	-0.7
		S^1	37	0.6	0.5	1.0	0.3	1.3	0.2	0.1	2	1.5
		NS^1	69	1.0	0.9	1.8	0.3	2.0	0.5	0.5	-1	0.3
		LUU^2	34	0.7	0.4	2.3	0.0	3.3	0.7	0.1	8	2.7
	soil	Sup^2	74	6	4	17	1	22	5.4	2.0	1	1.5
		5 cm^2	52	3	3	4	0	6	0.8	0.2	5	-1.2
		25 cm^2	49	3	3	4	2	5	0.6	0.3	2	0.7
		5-25 cm^2	101	3	3	4	0	6	0.7	0.3	5	-0.8
Copper	sed	C^1	22	49	49	60	39	66	7	5	0	0.5
		N^1	32	62	59	80	43	81	11	9	-1	0.3
		S^1	37	79	80	103	28	115	18	9	1	-0.7
		NS^1	69	71	71	101	28	115	17	13	0	0.1
		LUU^2	34	63	56	134	10	167	42	31	0	0.8
	soil	Sup^2	74	57	47	98	8	535	62	13	48	6.4
		5 cm^2	52	34	26	65	10	339	45	7	42	6.2
		25 cm^2	49	37	27	54	10	524	72	7	46	6.7
		5-25 cm^2	101	36	26	65	10	524	59	7	53	7.0

Table 3.2: Summary of statistical descriptive parameters of centering, dispersion and shape. Concentration in mg/kg. N: north; S: south; 1: this work; 2: Oruro Pilot Project (PPO); MAD: median absolute deviation; Q2: second quartile; Q3: third quartile.

element (mg/kg)	n	mean	median	95th percentile	min	max	standard deviation	MAD*	skew	asymmetry coefficient	Q_2	Q_3
Lead	sed	C^1	22	107	109	140	61	149	24	10	0	-0.7
		N^1	32	45	44	58	33	60	6	4	0	0.8
		S^1	37	57	43	140	13	163	35	9	2	1.7
		NS^1	69	51	43	117	13	163	27	5	7	2.6
		LUU^2	34	80	43	268	9	527	100	17	12	3.3
	soil	Sup^2	74	235	104	782	22	3307	432	67	35	5.4
		5 cm^2	52	118	51	277	16	1930	268	18	43	6.3
		25 cm^2	49	130	49	254	19	2793	395	17	46	6.7
		5-25 cm^2	101	124	49	259	16	2793	334	17	50	6.8
Antimony	sed	C^1	22	12	12	17	10	17	2	1	1	1.4
		N^1	32	15	14	20	4	22	3	1	3	-0.6
		S^1	37	10	7	24	3	38	7	2	5	2.2
		NS^1	69	12	13	22	3	38	6	4	3	1.2
		LUU^2	34	3	0	11	0	34	6	0	20	4.2
	soil	Sup^2	74	346	71	1002	9	1173	398	46	-1	0.7
		5 cm^2	52	74	59	194	10	495	78	29	17	3.7
		25 cm^2	49	71	53	125	9	694	99	26	34	5.4
		5-25 cm^2	101	73	57	151	9	694	88	27	29	4.9
Zinc	sed	C^1	22	121	119	137	104	147	10	5	1	0.8
		N^1	32	143	140	175	107	183	22	17	-1	0.2
		S^1	37	127	127	166	43	222	29	12	4	0.3
		NS^1	69	134	134	174	43	222	27	13	2	0.0
		LUU^2	34	139	119	308	38	605	113	20	12	3.4
	soil	Sup^2	74	158	130	296	25	1214	148	36	35	5.3
		5 cm^2	52	125	78	353	53	717	138	17	13	3.6
		25 cm^2	49	101	78	221	46	625	88	16	27	4.8
		5-25 cm^2	101	113	78	273	46	717	116	17	17	4.1

Enrichment factors (EFs) were initially developed to speculate on the origin of the elements in the atmosphere, precipitation or seawater (e.g., [12, 13, 14]). This use was extended to the study of soils, lake sediments, peat, tailings and other environmental materials (e.g., [15, 16]) and have increasingly been used to identify geogenic vs. anthropogenic element sources in environmental studies (e.g. [15, 16, 17, 18, 19]). Several authors have questioned the use and interpretation of the EFs in environmental studies (e.g., [20, 21]). These questionings are related to the variable composition of the Earth's crust at any given point compared to the global average; the natural fractionation of elements during their transference from the crust to the atmosphere; and the differential solubility of minerals in the weak chemical digestions used in environmental studies [20]. To avoid erroneous interpretations regarding the use of these factors, a local EF from the average composition of Cala Cala Lagoon normalized by Ti (a conservative element present in rocks from the EC) was calculated to determine the geologic

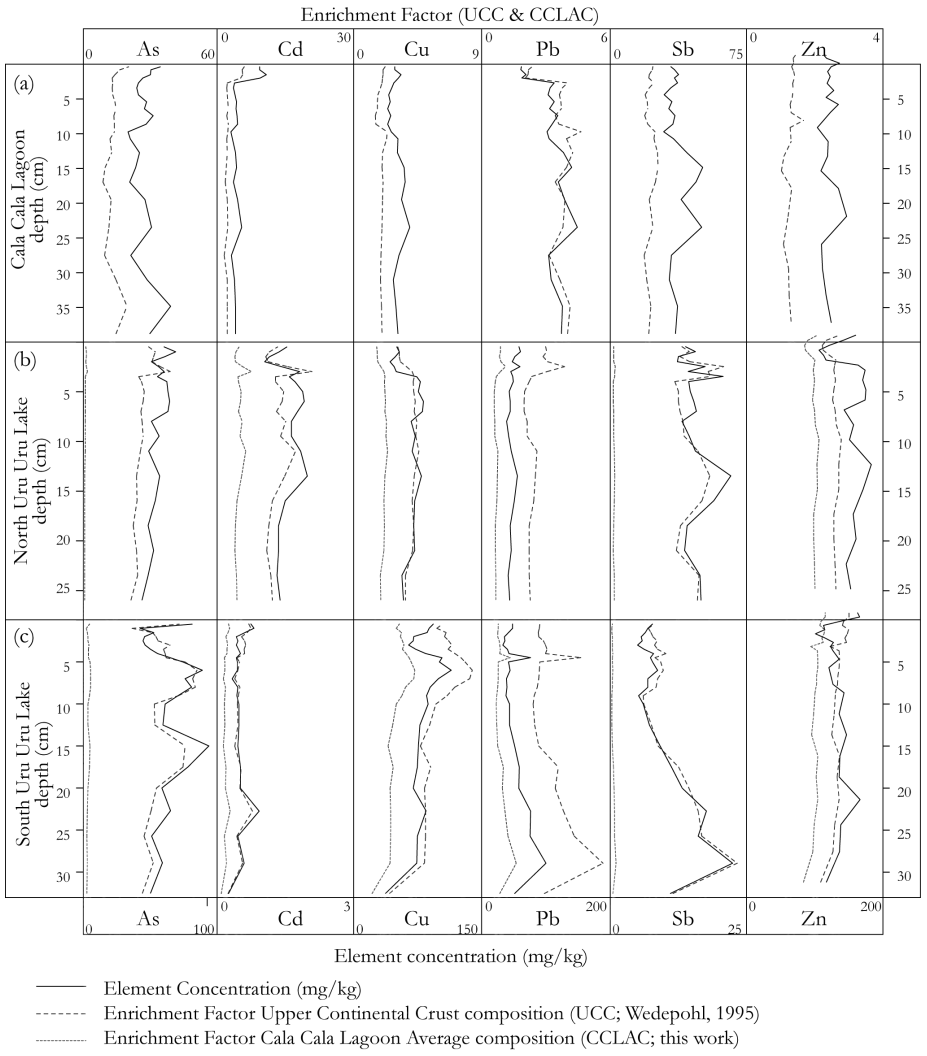

Figure 3.3.2: Concentration- and enrichment factor- depth profiles for: (a) Cala Cala Lagoon; (b) North Lake Uru Uru; (c) South Lake Uru Uru.

influence of metallogenic belts in sediments from a non-mining impacted site following equation 3.3.1 below. In addition, EFs for Lake Uru Uru sediments were calculated following equations 3.3.1 and 3.3.2 in order to determine the extent of a possible metal and metalloids contamination in the Bolivian highlands (Fig. 3.3.2 and Table 3.3) and also to query the use of the UCC average concentration to evaluate the degree of contamination in an area surrounded by many different metallogenic belts.

$$EF_{UCC=}\left[\frac{M_s}{M_{Ti}}\right]/\left[\frac{M_{UCC}}{Ti_{UCC}}\right] \tag{3.3.1}$$

$$EF_{CCLAC=}\left[\frac{M_s}{M_{Ti}}\right]/\left[\frac{M_{CCLAC}}{Ti_{CCLAC}}\right] \tag{3.3.2}$$

In these equations M corresponds to the metal(loid) of interest, Ti to Titanium, subscript s

Table 3.3: Summary of Enrichment Factors (EFs) obtained for Cala Cala Lagoon and Lake Uru Uru sediments. For the Cala Cala Lagoon, EFs were calculated in relation to the Upper Continental Crust (UCC, [261]), and for Lake Uru Uru in relation to the UCC and also to the Cala Cala Lagoon Average Composition (CCLAC).

	Upper Continental Crust Composition, Wedepohl (1995)									*Cala Cala Lagoon Average Composition*					
	Cala Cala Lagoon			*North Uru Uru Lake*			*South Uru Uru Lake*			*North Uru Uru Lake*			*South Uru Uru Lake*		
	med	*max*	*min*	*med*	*max*	*min*	*med*	*max*	*min*	*med*	*max*	*min*	*med*	*max*	*min*
As	*14*	*21*	*10*	*25*	*39*	*18*	*37*	*61*	*21*	*2*	*3*	*1*	*3*	*4*	*1*
Cd	*2*	*6*	*2*	*13*	*21*	*6*	*6*	*13*	*2*	*5*	*8*	*2*	*2*	*5*	*1*
Cu	*2*	*2*	*1*	*4*	*5*	*3*	*7*	*9*	*3*	*2*	*2*	*2*	*3*	*5*	*1*
Pb	*4*	*5*	*2*	*2*	*4*	*2*	*3*	*10*	*2*	*1*	*1*	*1*	*1*	*3*	*1*
Sb	*22*	*26*	*19*	*42*	*62*	*13*	*29*	*107*	*18*	*2*	*3*	*1*	*1*	*5*	*1*
Zn	*1*	*2*	*1*	*2*	*3*	*2*	*3*	*4*	*2*	*2*	*2*	*2*	*2*	*3*	*2*

indicates sediment concentration (mg/kg), subscript UCC is for the Upper Continental Crust concentration [261] and CCLAC subscript is the Cala Cala Lagoon Average Composition. Equations applied to Lake Uru Uru sediments are intended to determine whether these are enriched in relation to the UCC (EF_{UCC}, 3.3.1) and/or the EC (EF_{CCLAC}, 3.3.2).

In order to compare the general composition of sediments and soils from different environments in the Bolivian highlands, and to identify outliers and extreme values that lie outside the expected distribution range in the sediments and soils of the area, probability plots were constructed with all sediments and soil data (Fig. 3.3.3).

Given the log-normal or positively skewed distribution of elements in geological materials (e.g., [8, 271]), the median (value at the 50^{th} percentile of the data) was assumed as the sediments and soils geochemical baseline for each element in contour and distribution maps generated with GIS (ArcGis 9.3.1). Contour maps (Fig. 3.4.1) show only sediment data of Lake Uru Uru and were generated for As, Cd, Cu, Pb, Sb and Zn; concentrations were divided into values lower than the 25^{th} percentile, between the 25^{th} percentile and the median, between the median and the 75^{th} percentile, between the 75^{th} and 90^{th} percentile, between the 90^{th} and 95^{th} percentile and larger than the 95^{th} percentile. Contour maps were made with Inverse Distance to a Power and Natural Neighbour interpolations (due to the lack of a continuous sampling grid and the distance between samples). The latter interpolation method was also used to generate a wireframe map to show the 3D metal(loid) distribution in superficial sediments of Lake Uru Uru (Fig. 3.4.1).

Box and whisker plots were constructed using soil data to investigate metal(loid) potential provenance (Fig. 3.5.1).

Distribution maps were generated in the entire region for superficial soil (asterisk) and sediment (cross) for the same elements as for the contour maps (As, Cd, Cu, Pb, Sb and Zn) and using the same contour intervals (less the 25^{th} percentile; Fig. 3.5.2). Regarding the cores, the plotted concentration for both contour and distribution maps corresponds to the average composition for the first 5 cm (according to PPO sediments).

To discriminate between element background concentrations with respect to the expected mining-related metal dispersion and pollution from the Kori Kollo (Au-Ag), Itos (Ag-Zn-Pb-Au), Huanuni (Sn), Bolivar (Sn) and San José (Ag-Zn-Pb-Au) Mines and the Vinto Smelter (Sn-Sb), concentration versus distance plots were constructed (Fig. 3.5.3).

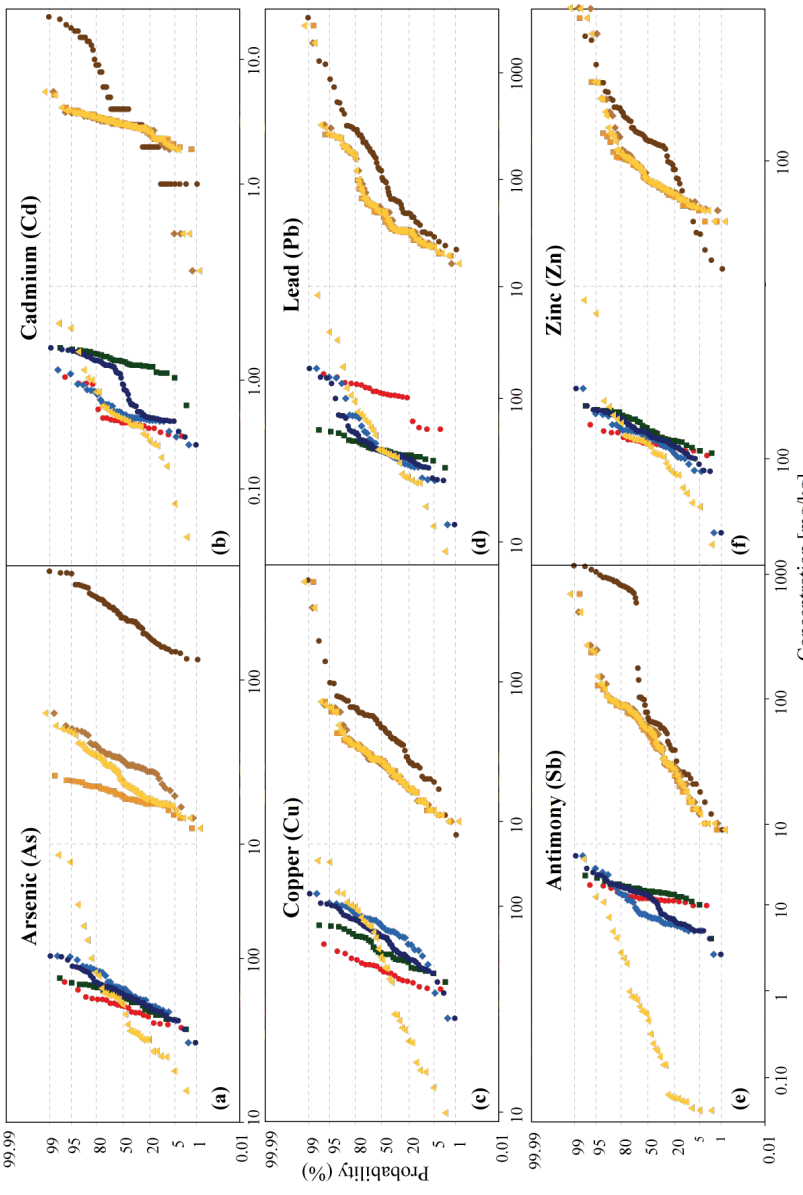

Figure 3.3.3: Probability plots for Lake Uru Uru and Cala Cala Lagoon sediments and Oruro Department soils.

3.4 Results

Results from descriptive statistic parameters and EFs are shown in the following paragraphs. If not specified, all values in brackets correspond to the median concentration in mg/kg and EFs in dimensionless units.

3.4.1 Cala Cala Lagoon

3.4.1.1 Cala Cala Lagoon vs Lake Uru Uru sediments

Based on the descriptive statistics (Table 3.2 and Fig. 3.3.1), concentration-EF profiles (Fig. 3.3.2) and probability plots (Fig. 3.3.3) from Cala Cala Lagoon and the overall composition of Lake Uru Uru sediments, it was observed that Cala Cala Lagoon exhibits the highest median Pb concentration (109 vs. 43), and the lowest Cu (49 vs. 71) and Cd (0.4 vs. 0.9) median concentrations. Arsenic (51), Zn (119) and Sb (12) exhibit similar median concentrations to those from Lake Uru Uru (60, 134 and 13, respectively), although PPO Sb concentrations are markedly lower (0.5) (Fig. 3.3.3e). Most of the elements in Cala Cala Lagoon sediments follow relatively normal distributions, excepting Cd, Pb and Sb, that suggest the presence of two data populations (Table 2 and Fig. 3.3.1a). Concentration-depth profiles for the Cala Cala Lagoon (Fig. 3.3.2a) exhibit slight variations with depth, with the exception of Cd, that shows the highest concentration in the topmost section of the profile (1 mg/kg mean in the topmost section vs. 0.4 mg/kg mean in the bottom section), whereas EF-depth profiles (Fig. 3.3.2a) indicate the maximum values for As (21) and for Sb (26). Cadmium, Cu, Pb and Zn show EF_{UCC} equal or lower than 6 (Table 3.3 and Fig. 3.3.2a). The Cala Cala Lagoon has only a few outliers, for instance Cd upper and Pb lower outliers are related to the topmost section of the core, Sb and Zn upper outliers are located in the central section of the core, and As and Cu exhibit no outliers (Fig. 3.3.2).

3.4.1.2 Cala Cala Lagoon sediments vs Oruro Department soils

In comparison to soils from the Oruro Department, the Cala Cala Lagoon sediments exhibit lower median concentrations than surface soil for As, Cd and Sb (240, 4 and 71 vs. 51, 0.4 and 12, respectively), and similar median concentrations for Cu, Pb and Zn (47, 104 and 130 vs. 49, 109 and 119, respectively). In deeper soil horizons (5-25 cm depth; Table 3.2) As, Cu, Pb and Zn (24, 26, 49 and 78, respectively) concentrations are slightly lower than that determined

for the Cala Cala Lagoon sediments (51, 49, 109 and 119, respectively). In all soil horizons, Cd and Sb exhibit higher concentrations than that determined for Cala Cala Lagoon sediments (Table 3.2 and Fig. 3.3.3).

3.4.2 Uru Uru Lake

3.4.2.1 Sediment profiles: Uru Uru Lake concentration and enrichment factors

Descriptive statistics parameters (Table 3.2 and Fig. 3.3.1), concentration-EFs depth profiles (Fig. 3.3.2) and probability plots (Fig. 3.3.3) show that the general composition of Lake Uru Uru sediments is similar to that of Cala Cala Lagoon, with the exception of Pb, Cu and Cd (as mentioned above).

In Lake Uru Uru, the northern part exhibits the highest median concentrations of Cd (1.5), Sb (14) and Zn (140) and all elements follow relatively normal distributions (Table 3.2 and Fig. 3.3.1). In this part of the lake the highest median Sb (42), As (25) and Cd (13) EF_{UCC} and the highest median Cd (5) EF_{CCLAC} are observed (Fig. 3.3.2b and Table 3.3). The southern part presents the highest concentrations of As (65) and Cu (80), and in this part As, Cu and Zn follow relatively normal distributions, whereas Cd, Pb and Sb follow positively skewed, possibly log-normal, distributions (Table 3.2 and Fig. 3.3.1c). Likewise, the highest median As (37), Sb (29) and Cu (7) EF_{UCC} and the highest median Cu (3) and As (3) EF_{CCLAC} are observed (Fig. 3.3.2c and Table 3.3). Lead median concentration is similar in the northern (44) and southern areas (43) and no important EF_{UCC} and/or EF_{CCLAC} were determined (Table 3.3). Dry season concentration-depth profiles of Lake Uru Uru (Figs. 3.3.2b and 3.3.2c) show that despite the fact that concentration ranges are not extremely different from those of Cala Cala Lagoon sediments, these profiles present much more variance than those determined in Cala Cala Lagoon (Fig. 3.3.2a); for instance Cu and Zn present the highest concentrations in the topmost section of the cores, whereas Sb dominates in the bottom (Table 3.2 and Fig. 3.3.2). The Lake Uru Uru data exhibit some outliers: in the southern sedimentary cores upper outliers are observed, for instance As in the central, Pb in isolated levels and Zn in the topmost section of these cores (Fig. 3.3.2). Upper outliers for As, Cd, Pb and Zn in superficial sediments are also observed in the southernmost outflow of Lake Uru Uru (Fig. 3.4.1).

3.4.2.2 Uru Uru Lake sediments vs. soils of the area

Lake Uru Uru sediments as compared to soils from the Bolivian highlands exhibit the highest

concentrations of Cu (71; Fig. 3.3.3c), nevertheless Cd (0.9) and Sb (13) concentrations tend to be low in comparison to all soil horizons (Table 3.2; Figs. 3.3.3b and 3.3.3e). Arsenic exhibits a lower median concentration than superficial soils (240) and higher than the deeper soil horizons (25; Fig. 3.3.3a), while the median Zn concentration (134) is similar to that of superficial soils (130), yet higher than the deeper soil horizons (78; Fig. 3.3.3f). Median Pb concentrations, on the other hand, are lower than that observed in superficial soils, though similar to the deeper soil horizons (43 vs. 104 and 49, respectively; Fig. 3.3.3d).

3.4.2.3 Spatial distribution of Lake Uru Uru superficial sediments

For most elements, superficial sediments from Lake Uru Uru show the highest concentrations of elements in the southern and northern areas, as depicted by contour and 3D wireframe maps (Fig. 3.4.1). However, the distribution of Cu exhibits higher concentrations along the western border of the lake (Fig. 3.4.1c), Sb is significantly concentrated at the eastern border next to the railroad (Fig. 3.4.1e) and Pb exhibits elevated concentrations in the southern part of the lake (Fig. 3.4.1d).

3.4.3 Oruro Department soils geomorphologic source area

The vertical distribution of soil horizon compositions from the AL and EC (Fig. 3.5.1) shows qualitatively that As exhibits the highest concentration in superficial soil regardless of provenance (Fig. 3.5.1a). A similar vertical and geomorphologic distribution is observed, yet not so obviously, for Cu and Zn (Figs. 3.5.1c and 3.5.1f, respectively). Lead and Sb levels are higher in AL superficial soil (Figs. 3.5.1d and 3.5.1e, respectively), contrarily, Cd levels are higher in EC superficial soils (Fig. 3.5.1b).

3.4.4 Oruro Department soil and sediment spatial distribution

Concentration maps for superficial sediments and soils (Fig. 3.5.2) exhibit spatial element distributions that evidence the following: (i) As and Zn are scatterly distributed in superficial sediments and soils (Figs. 3.5.2a and 3.5.2f, respectively), (ii) the highest values for Cd are mainly distributed in the EC (Fig. 3.5.2b), (iii) high Cu concentrations are mainly located along the western border of Lake Uru Uru (Fig. 3.5.2c) and (iv) Pb and Sb are spatially related to the Vinto Smelter area (Figs. 3.5.2d and 3.5.2e, respectively).

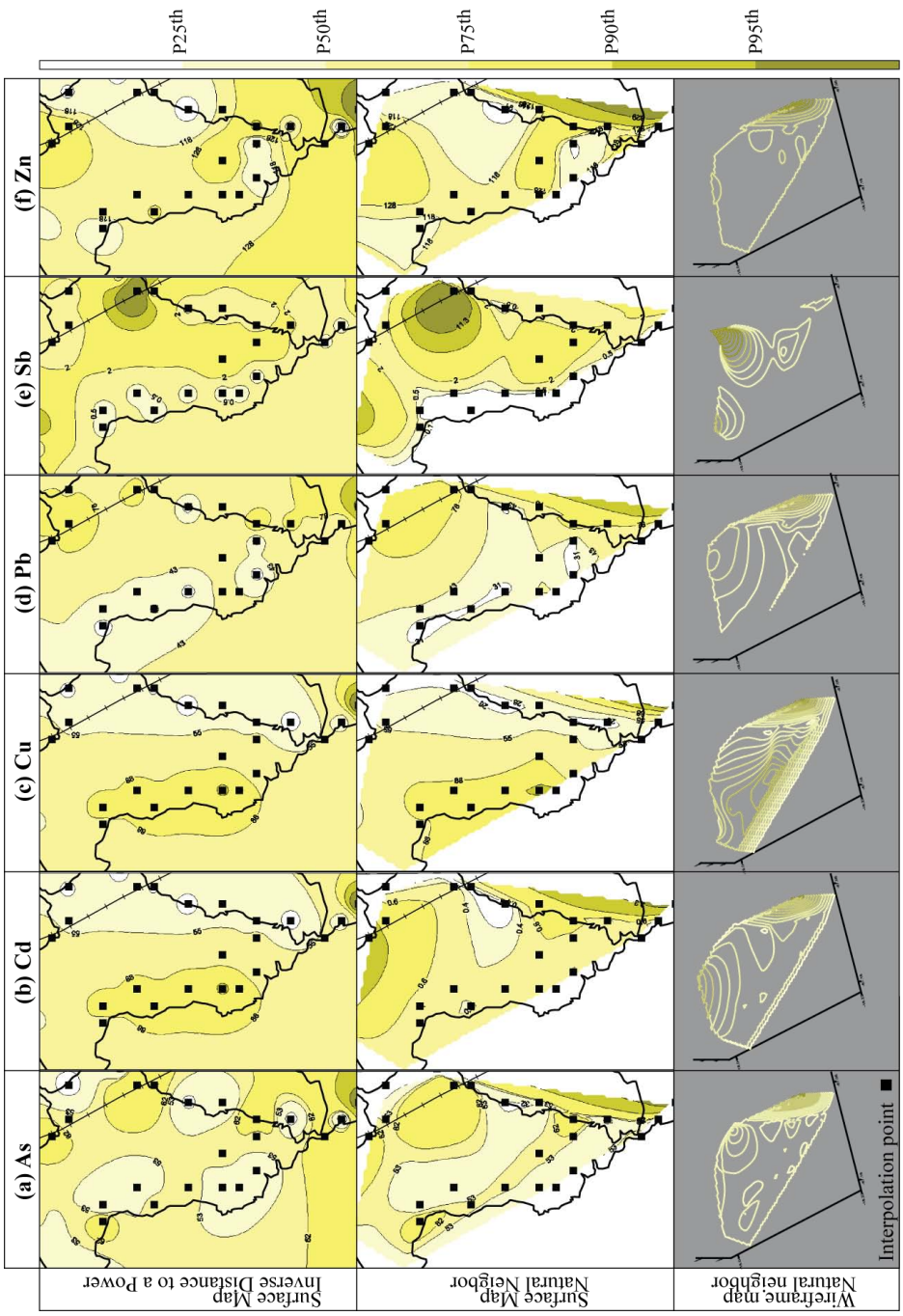

Figure 3.4.1: Surface and wire-frame maps for Lake Uru Uru superficial lake sediment composition. Black line delineates Lake Uru Uru area.

3.5 Discussion and conclusions

Undoubtedly, the studied region corresponds to a very particular environment in the world, characterized by an endorheic drainage basin, high altitude (3,700-4,200 m a.s.l.), extreme aridity (< 400 mm of precipitation per year) and a singular geomorphology: a Quaternary sediment-filled basin bounded by both branches of the Andes Range, constituted to the east by mineralized (Bolivian Tin, Gold-Antimony and Lead-Zinc Metallogenic Belts) Palaeozoic sedimentary rocks and Tertiary volcanics (EC), and to the west by mineralized (Bolivian Sedimentary-Rock Hosted Copper Deposits and Polymetallic Belt) Jurassic-Cretaceous sedimentary rocks and Mio-Pliocene volcanics (WC). The elements selected to establish this Bolivian highlands geochemical background and present-time baseline generally exhibit higher concentrations in the superficial soils (PPO study) than that determined for the lacustrine sediments (this study and PPO studies), which is most likely related to the different nature of the sampled materials and the respective dispersion processes and mobility of elements among these media.

3.5.1 Bolivian highlands vs. other industrial mining/smelting-impacted sites

For comparison purposes data from the literature were selected from three well characterized sites: (i) stream sediments from the industrialized Campania Region (Italy); (ii) soils from the metal mining district of Linares (province of Jaén, Southern Spain); and (iii) background concentrations of mining-impacted sediments from Lake Coeur d'Alene (CDA, Idaho, USA).

The Campania region is the second most populated in Italy; morphologically it is made up of the Apennine Mountains to the east and by two coastal plains to the west (Campania and Sele, traversed by the Volturno and Sele Rivers). The Apennines lithology consists mostly of sedimentary and volcanic rocks, spanning from the Triassic to Recent times [278]. Agriculture is an important activity in the region, being also the foremost consumer of fertilizers in southern Italy. Industries present a scattered spatial distribution, most of them developed close to the main cities and around agricultural areas. No economic mineral deposits occur in this region [1]. Oruro presents two similarities with Campania, which are the proximity to industries (in the case of Oruro bricks and cement, without considering mining-related industries) and that both sites present similar lithologies (sedimentary and volcanic rocks), yet not mineralized in Campania. In comparison to sediments from Lake Uru Uru and Cala Cala Lagoon, Campania exhibits lower concentrations for all elements (Table 3.4).

The Linares metal mining district was exploited for veins of galena (PbS) associated with zinc-blende (ZnS), chalcopyrite ($CuFeS_2$) and barite ($BaSO_4$) [279], hosted within Palaeozoic granites, Triassic shales and Miocene marls. The abundance of ores enabled the development of a large-scale extracting mining industry, minerallurgic industry and smelting industry over hundreds of years [2]. The Oruro and Linares mining districts share an historic association with mining activities; ores similar to those of Linares are found in Oruro (among others); yet both sites do not present similar bedrock types. As compared to soils from Oruro, Linares district soils exhibit lower As (17), Sb (3) and Cd (0.2), slightly lower Cu (54) and Zn (72) and higher Pb (1279) median concentrations (Table 3.4 and Fig. 3.5.1). This is explained by the geological features of the Linares district, where mineralization is mainly related to galena (PbS; [2]).

The Coeur d'Alene (CDA) River basin is the location of the most productive mining district in Idaho (primarily Ag and Pb, and secondly Au and Cu), where ore minerals are mainly Ag-Pb bearing sulphides (acanthite, boulangerite, bournonite, galena, silver, stephanite). This basin has been the subject of numerous geochemical studies intended to assess the impact of mining and mining-related activities which have been ongoing since the 1880s (e.g., [183, 280, 281, 282]). Until 1968, mining and ore-processing wastes were discharged directly into the basin [283, 284], causing elevated trace element concentrations (Ag, As, Cd, Cu, Hg, Pb, Sb and Zn) in association with suspended, surface and subsurface sediments [280, 281]. Oruro and Coeur d'Alene are mine-related districts that share similar ore minerals and both Lake Coeur d'Alene and Lake Uru Uru have received direct waste from mining activities. When comparing sediments from the study region with that of CDA background levels, CDA exhibits lower concentrations for As (5), Cu (25), Pb (24), and Sb (0.7), similar to Zn (110) and higher for Cd (2.8). The latter is probably related to sphalerite presence in this metal mining district.

Comparisons with other industrial and metal mining-impacted sites show that Oruro exhibits a higher median concentration (for all elements) than an industrialized area with similar, yet not mineralized, lithologies, while As and Sb exhibit the highest median values in comparison to industrial and mining-impacted areas. Copper and Zn exhibit higher or similar median values in relation to mining-impacted sites, whereas lower concentrations were found for Pb in comparison to soils from a galena-rich district, and Cd in comparison to background levels of lacustrine sediments from the CDA river basin impacted by historical Ag-Pb mining activities. These results indicate, as in other studies (e.g., [2, 3]), that regional geology is an important

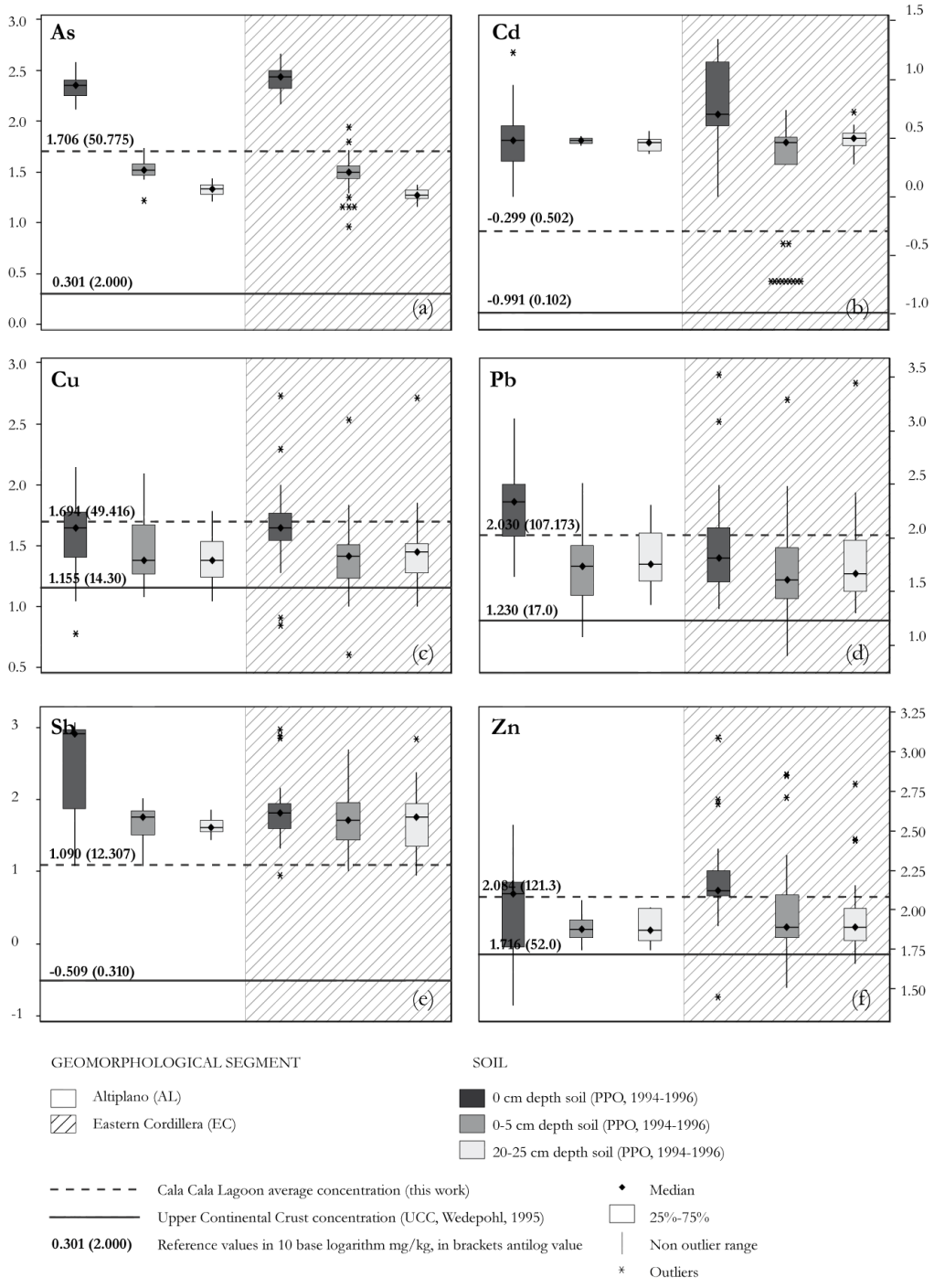

Figure 3.5.1: Box and whisker plots of soils from the Bolivian Highlands (PPO data). Also shown Upper Continental Crust composition [261], mean composition of Cala Cala Lagoon Sediments (this work) and Linares metal mining district median concentration [2].

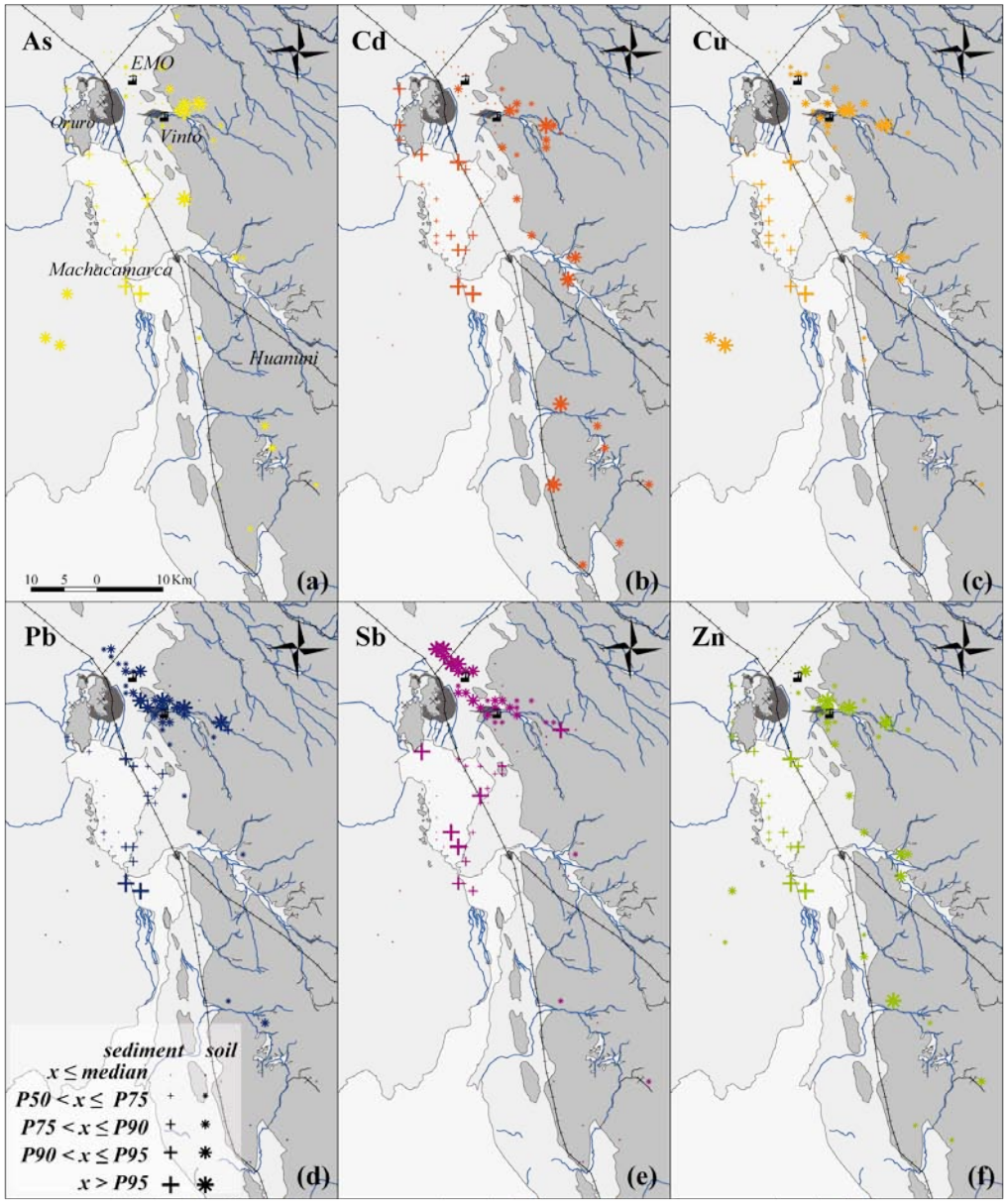

Figure 3.5.2: Concentration distribution maps of superficial soils and sediments of the study area.

determinant of trace element concentration.

3.5.2 Sediment enrichment factors, comparison with international backgrounds and proposed geochemical background and present time baseline for the Altiplano sediments

In sediments from the study area, it is noteworthy that all the studied medians, and most values, of the elements exhibit higher concentrations than the UCC (Table 3.4) and that in the general composition of sediments from Lake Uru Uru and Cala Cala Lagoon, Sb and As are the most enriched elements in comparison to the UCC, reaching up to 107 and 61, respectively (Table 3.3). EF_{CCLAC} are lower than EF_{UCC} with the highest EFs exhibited by Cd and Cu (up to 8 and 5, respectively; Table 3). Despite the fact that EF_{UCC} are one order higher than EF_{CCLAC}, through this study it is stressed that the use of the UCC as the normalizing factor appears to be useless in an isolated and highly mineralized area like the Altiplano of Bolivia. The interpretability issues related to the UCC as the normalizing concentration is in accordance to Reimann & de Caritat [20, 21], who suggested that the concept of normalizing element concentrations to an average total crust value is of doubtful merit, which is clearly demonstrated by this study. This is basically because EFs can be high or low due to a multitude of reasons, of which contamination is but one [21]. Furthermore, these authors have concluded that "using EFs to detect or "prove" human influence on element cycles in remote areas (as the Altiplano) should be avoided because, in most cases, high EFs cannot conclusively demonstrate, nor even suggest, such influence" [21].

The Cala Cala Lagoon concentration profiles exhibit relatively constant concentrations with depth, which may be explained mainly by weathering of regional outcrops. Nonetheless, in the sediment of Lake Uru Uru, element concentrations are highly variable according to depth, which may be explained by mining activities in this area that have been extremely dependent on fluctuating international metal(loid) prices. These have controlled Sn exploitation in Bolivia since the beginning of the 20^{th} century [253], yet more studies are necessary to confirm this hypothesis. The Cala Cala Lagoon sediment profiles show less-variable elemental concentrations than those of Lake Uru Uru, nevertheless exhibit exceptionally high concentrations of As and Sb. These are well above the background levels from Canada and the US and well-known highly impacted industrial and metal mining districts around the world (Table 3.4). This suggests that in this zone a natural positive contrast with respect to world backgrounds

Table 3.4: Lake Uru Uru and Cala Cala Lagoon sediments median concentration, general soil composition and 5 to 25 cm depth soil composition (PPO), bedrock concentration in Milluni Valley (20 km north from La Paz), the composition of the Upper Continental Crust (UCC, [261]); the median concentration of soils in Linares (South Spain) metal mining site [2]; the median concentration for stream sediments in Campania region (Italy; [1]) and Coeur d'Alene Lake (CDA) sediments background concentration [281]. All data in mg/kg.

	Bolivian Altiplano						*World References*						*Comparisons*			
	Lake Uru	*Cala Cala*	*all soil*	*5-25cm*	*Milluni*(3)		*UCC*	*Linares*	*Campania*	*CDA*	*Background levels*		(10)		(11)	
	Uru(1)	*Lagoon*(1)	(2)	*soil*(2)	*UF*	*CF*	(4)	(5)	(6)	(7)	*US*(8)	*Canada*(9)	*US*	*Canada*	*US*	*Canada*
As	60	51	34	25	17	269	2	17	6	5	7	4.2	9	14	7	12
Cd	0.9	0.4	3	3	0.3	6.3	0.1	0.2	0.2	2.8	(-)	1.1	(-)	1	(-)	0
Cu	71	49	30	26	19	60	14	54	30	25	20	25	4	3	2	2
Pb	43	109	58	49	14	174	17	1279	22	24	23	23	2	2	5	5
Sb	13	12	63	53	(-)	(-)	3	3	0.3	0.7	0.6	(-)	22	(-)	20	(-)
Zn	134	119	96	77	134	1950	52	72	71	110	88	65	2	2	1	2

(1) Median Sediment concentration in Lacustrine environments of Oruro Department, Bolivia (this work)

(2) Median Soil concentration from Oruro Department, Bolivia (PPO 1993-1996)

(3) Average bedrock concentration in Milluni Valley, [16]

(4) Upper Continental Crust composition by [261] (mg/kg)

(5) Soils in Linares (South Spain) metal mining site District, [2]

(6) Stream sediments in Campania region (Italy), [1]

(7) Coeur d'Alene sediments

(8) US background levels [285]

(9) Canadian background levels [286]

(10) Lake Uru Uru sediments vs background levels

(11) Cala Cala Lagoon sediments vs background levels

UF: Uncia Formation

CF: Catavi Formation

(-) no available estimate

from anthropogenically impacted and non-impacted sites for both Sb and As exists. Since the Bolivian highlands of Oruro Department evidence naturally abundant concentrations for these elements, a background and a present-time baseline for Altiplanic sediments are proposed in Table 3.5. The background for EC sediments is based on the concentration of elements in the bottom-most section of Cala Cala Lagoon core, whereas the Altiplanic sediments baseline is based on the median concentration presented by all sediment samples from the PPO, plus the top 5 cm of cores from this study. Both background and baseline are essential for the distinction of geochemical sediment concentration derived from either natural or anthropogenic processes, Bolivian legislation and/or the interpretation of geochemical data of this area.

3.5.3 Origins of elements in Lake Uru Uru sediments: anthropogenic and natural sources

3.5.3.1 Vinto Smelter, San Juan de Sora Sora River Basin and Tagarete Channel

Background, baseline and distribution analysis of geochemistry in lacustrine sediments and soils in the Oruro Department region, while not directly indicating the sources of elements, does provide insight regarding dispersion patterns and processes that may be linked to either natural and/or anthropogenic sources and processes.

No clear relationships could be recognized between metal(loid) spatial dispersion and the location of the principal mining sites of the district (Bolivar, Huanuni, Kori Kollo and San José), making it difficult to decipher the influence of each mining site over the whole region. Nevertheless, when comparing metal(loid) concentration in soils to the distance from the Vinto Smelter, an inverse relationship was observed for Pb and Sb, whereas no obvious relationships were determined for As, Cd, Cu and Zn (Fig. 3.5.3). As expected, no spatial relations for lacustrine sediments were obtained (Fig. 3.5.3). A probable hypothesis to explain soil and sediment metal dispersion in relation to the Vinto Smelter is that soils are fed with airborne particles enriched with metals and metalloids, mostly originating from this smelter (400-1,000 tons/year metallic particles; [275]). The influence of emissions from Vinto in superficial soils was also reported in Mercado *et al.* (2009) [259] and Goix *et al.* (2009) [287]. Indeed, Goix *et al.* [287] observed that airborne particles (<2.5 µm) collected in the Vinto Smelter area are highly enriched in Sb, Cd and As. Lacustrine sediments from Lake Uru Uru are mainly fed by suspended particulate matter originating from mining waste drainage, principally, the San José Mine in the northern part and the Huanuni Mine in the southern part. In fact, the San José

Table 3.5: Proposed geochemical background and present time geochemical baseline. Background corresponds to the median composition Cala Cala Lagoon bottom sediments. N: northern sediments; S: southern sediments. Bold printed values correspond to the best candidate for the geochemical present time baseline concentration. Values in mg/kg.

Preliminary geochemical background Cala Cala Lagoon (mg/kg)

Element	*As*	*Cd*	*Cu*	*Pb*	*Sb*	*Zn*
med	*52*	*0.4*	*52*	*119*	*12*	*119*
max	*72*	*0.5*	*66*	*149*	*17*	*147*
min	*38*	*0.3*	*40*	*102*	*10*	*104*

Present time geochemical baseline (mg/kg)

Element		*As*		*Cd*		*Cu*		*Pb*		*Sb*		*Zn*	
Compartment		*med*	*mean*	*med*	*mean*	*med*	*med*	*med*	*mean*	*med*	*mean*	*med*	*mean*
	general	*56*	*68*	*0.5*	*0.8*	*57*	*63*	*44*	*66*	*6*	*6*	*120*	*131*
	LUU (total)	*58*	*70*	*0.5*	*0.8*	*61*	*66*	*42*	*63*	*4*	*6*	*120*	*132*
sediment	*LUU (N)*	*61*	*58*	*1.4*	*1.4*	*55*	*57*	*44*	*46*	*14*	*13*	*124*	*134*
	LUU (S)	*59*	*62*	*0.5*	*0.5*	*79*	*78*	*36*	*38*	*6*	*6*	*114*	*113*
	CCL	*51*	*52*	*0.7*	*0.7*	*47*	*47*	*86*	*86*	*12*	*11*	*121*	*123*

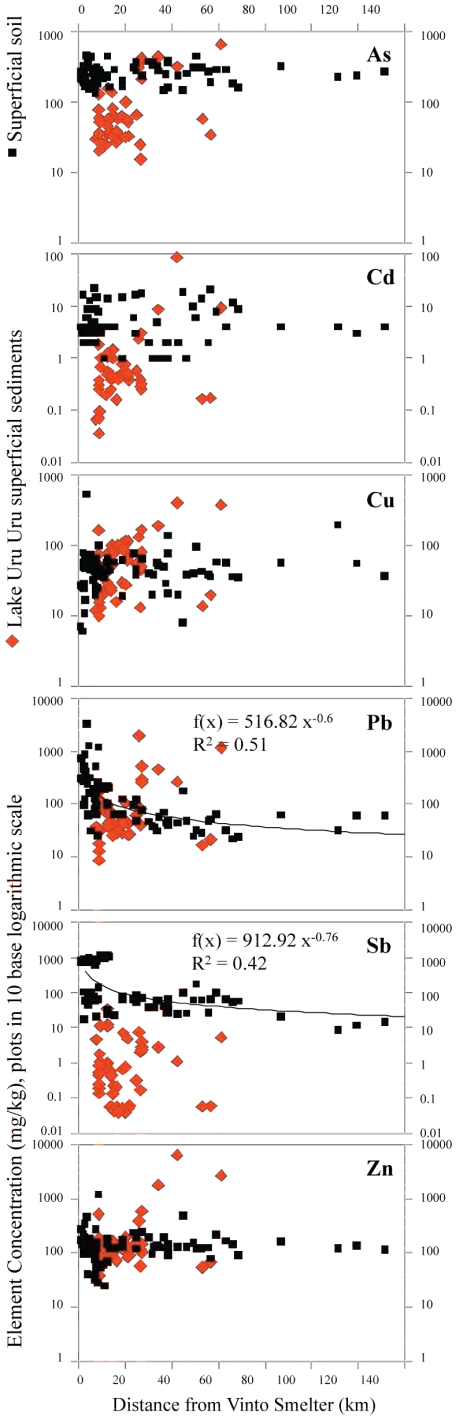

Figure 3.5.3: Arsenic, Cd, Cu, Pb, Sb and Zn distribution of soils and sediments respect to the distance from the Vinto Smelter. Regression models are for soils where fits exceeded 40% (R^2>0.4).

Mine discharges waste into the Tagarete Channel with an extremely acid pH (1.2 - 2.5). At the channel's entrance to Lake Uru Uru, in spite of dilution and mixing with other effluents, the pH continues to be acid (3.4 - 4.4) and importantly charged with metals, mainly Fe, Cu, Pb and Sb [252]. The Huanuni Mine, on the other hand, discharges acidic mine water (1.9 - 4.5) with a significant concentration of metals and water from refining processes directly into the Huanuni River, which flows into the San Juan de Sora Sora River. The outflow of this river basin impacts the southern limit of Lake Uru Uru (where elevated metal concentrations have been measured in solution close to Machacamarca (Fig. 3.2.1): 0.6 mg/L Cd, 1.3 mg/L Cu, 0.1 mg/L Pb and 42 mg/L Zn; [252]) and the northern part of Lake Poopó, probably causing environmental threats to the limnic environment when Lake Poopó is not completely desiccated [252].

3.5.3.2 Arsenic (As) and Cadmium (Cd)

These elements are mainly concentrated in superficial soils. The sediments from Lake Uru Uru exhibit slightly higher As and Cd concentrations compared to sediments from the Cala Cala Lagoon, and EF_{UCC} plus EF_{CCLAC} indicate that As is naturally abundant in the entire studied region (EC and AL) and Cd is moderately enriched in the northern part of Lake Uru Uru. In soils, both elements exhibit no-clear relationship with distance from the Vinto Smelter (Figs. 3.5.2 and 3.5.3) and spatial distribution of Cd is mainly related to the EC, whereas As is highly heterogeneous (Fig. 3.5.2). An explanation for the As heterogeneity could be related to both branches of the Andes Range. For instance: bedrocks in the Milluni Valley [16], hosted in the same geologic formations as that of the Cala Cala Lagoon (Catavi and Uncia Formations) present markedly different concentrations (Table 3.4). Dacitic and especially rhyolitic volcanics occurring in these areas have generally enhanced contents of As (dacites 11-69 mg/kg and rhyolites 7-810 mg/kg), with brecciated and alteration zones within the volcanics containing up to 1405 mg/kg of this element [288]. Therefore, the variability and mixed sources (WC and EC) could explain the heterogeneity and difficulties in resolving the As distribution, this conclusion being in accordance with PPO [250, 275].

3.5.3.3 Copper (Cu)

This element is more concentrated in Lake Uru Uru sediments than in the entire area, these enhanced concentrations have been linked to Huanuni and San José mining waste [252]. Nevertheless, EF_{CCLAC} exhibits slight to moderate enrichments in Cu, which is probably related

to a non-EC source region and/or anthropogenic and/or a WC source region, in which Cu mineralization is linked to the Sedimentary-Rock Hosted Copper Deposits and the Bolivian Polymetallic Belt. The latter observation is in accordance with contour maps of Lake Uru Uru (Fig. 3.4.1c), which exhibit the highest concentrations of Cu along its western border. It can be concluded that besides the anthropogenic source previously determined, a probable WC source region must be related to Cu enrichments in Lake Uru Uru sediments.

3.5.3.4 Lead (Pb)

The highest Pb concentrations are observed in sediments from the EC and superficial soils from the AL, where particularly high values are exhibited near the Vinto Smelter (in agreement with [275, 259, 287]; Figs. 3.5.2 and 3.5.3), implying that this anthropogenic source influences soil metal(loid) contents considerably. While soils are significantly influenced by the Vinto Smelter, in lacustrine sediments no relationships were determined. The median EF_{UCC} value for Pb is higher in sediments from the EC, implying a natural and/or mining-related EC source. Lake Uru Uru sediments show the most important concentrations at the southernmost limit, where the San Juan de Sora Sora River discharges mining waste from Huanuni containing median values of 0.1 mg/L of Pb in solution ([252]; WHO guideline for drinking water 0.01 mg/L); thus an anthropogenic source of Pb is proposed for the southernmost Lake Uru Uru area.

3.5.3.5 Antimony (Sb)

Antimony shows a similar distribution to Pb, the difference lying in the fact that this element, besides evidencing an important degree of anthropogenic influence in superficial soils from the Vinto Smelter emissions (Figs. 3.5.2 and 3.5.3; [275]), also exhibits a strong natural geochemical signature related to geological abundance as determined from sediments located in both the EC and AL sub-regions. Although the Sb concentration in sediments is lower than in soils, it is higher than that reported for the mean Earth's crust, worldwide background levels, industrial sites and mining-impacted sites (Table 3.4) suggesting that an Sb background in the study zone (and therefore in Bolivian environmental legislation) must be established in accordance to natural concentrations of this specific environment. Lake Uru Uru distribution patterns (Fig. 3.4.1e) show the highest concentrations at the eastern border of the lake next to the railroad embankment; this positive contrast anomaly derives from mine waste used for the construction of the railroad that crosses the lake [252].

3.5.3.6 Zinc (Zn)

The Zn median concentration in superficial soils and sediments from the EC and AL are quite similar, and higher than that of the deeper soil horizons. EF_{CCLAC} and EF_{UCC} in sediments are lower than 4. The regional scale distribution pattern is scattered and concentration maps of superficial sediments tend to associate this element with the northern and southern limit of Lake Uru Uru and to a lesser extent with its western border. The natural presence of this element in both EC (Lead-Zinc Belt) and WC (Polymetallic Belt), the fact that Bolivia is the fourth larger Zn producer in the world [217], the scattered spatial distribution, the EFs and the median concentrations of Zn do not provide enough evidence to determine the Zn source region, indicating that for Zn, a highly ubiquitous element in the global environment, it is very difficult to discriminate between anthropogenic and natural sources.

3.6 Concluding remarks

Important conclusions drawn from this study are: Firstly, in the Bolivian highlands of the Oruro Department the natural geochemical background of As and Sb is significantly enhanced in comparison to the UCC composition, world background levels, industrial sites and historical mining sites, therefore, environmental legislation should be generated according to the characteristic geochemical signature of Bolivian highlands, especially for these elements. Secondly, the use of EFs based on the UCC average concentration cannot exhibit the natural geochemical characteristics of this area, as demonstrated by the use of a local EF_{CCLAC} based on the average composition of EC lacustrine sediments, therefore the use of the UCC for normalizing and calculating EFs, is not supported for determining contaminant enrichment. Thirdly, a strong multiplicity of metal(loid) sources makes it difficult to discriminate between natural and anthropogenic input into this endorheic drainage basin. Fourthly, despite the multiplicity of metal(loid) sources it is proposed that the anthropogenic impact on superficial soils is mainly related to the spreading of contaminants from the Vinto Smelter, while Lake Uru Uru is influenced by mining activities, particularly past and present drainage waste of San José and Huanuni Mines. Finally, the generation of a geochemical background and a present-time baseline for Bolivian Altiplanic sediments is provided. These results and conclusions will be most helpful for: (i) environmental legislation in the Altiplanic zone; and (ii) the future interpretation of data from contaminant studies in this region. As a recommendation, more studies are deemed necessary, especially for the determination of: (a) the geochemical composition of sediments from Lake Poopó; (b) the WC geochemical signature; (c) the geochemical signature of AL sediments in non-contaminated areas; and (d) the speciation of metals in lacustrine sediments from this region.

Chapter 4

Early diagenetic processes in Altiplanean lacustrine sediments

Introduction

The objectives of this chapter were: (1) to document the main diagenetic processes occurring within lacustrine sediments in the Bolivian Altiplano and (2) to determine the impact of such processes on the post-depositional redistribution of metal(loid)s and their effect on metal(loid) mobilization, particularly into the overlying water column (OLW). These objectives were achieved through single selective extractions mainly based on Tessier *et al.* (1979) protocols and high resolution concentration-depth pore water profiles in contrasted dry (DS) and wet (WS) seasons.

We stress that this is the first detailed study ever performed on dissolved and solid fractions from lacustrine sediments of the Altiplano comparing the effects of seasonal changes in metal(loid)s behaviour. This survey is innovative in the fact that studies on early diagenetic processes in continental saline lakes are not common, especially in a very unique environment such as the Altiplano of Bolivia, where climatic, geomorphologic and geologic conditions are particular and extremely hard to find in any other region of the world. The unique characteristics of the Altiplano allow us to better constrain the influence of precipitation/evaporation rates and geological features in this endorheic hydrologic basin.

Conclusions reached by this survey include that during the WS metal(loid)s are easily released, and this effect is greatest within the southern Lake Uru Uru area, where most biota coexist and fishing is usually practiced. Care must be taken in future studies, in which the determination of trace metal(loid) behaviour within the water column of Lake Uru Uru would be useful to assess WS effects on biota and therefore on the inhabitants of this very particular environment. This chapter is in preparation to be submitted to Applied Geochemistry.

Paper 2. Early diagenesis and availability of trace metals (Cu, Zn, Mo, Cd, Pb and U) and metalloids (As, Sb) in mining and smelting-impacted and non-impacted lacustrine environments of the Bolivian Altiplano

J. Tapia[1,2,3]; S. Audry[1]; B. Townley[2]

[1]Université de Toulouse, OMP-GET, 14 Avenue Edouard Belin, 31400 Toulouse, France

[2]Departamento de Geología, Universidad de Chile, Plaza Ercilla 803, casilla 13518, correo 21, Santiago, Chile

Abstract

Lake Uru Uru (Altiplano) and Cala Cala Lagoon (Eastern Andes Cordillera) are two lacustrine environments located on the Altiplano of Bolivia. These environments were sampled during two different seasons between 2008 and 2009 to determine metal(loid) behaviour and mobility during early diagenesis processes. During both coring campaigns a total of 5 cores were retrieved.

Major redox species, dissolved metal(loid) behaviour, diffusive fluxes, single selective extractions and mineralogical features allow us to propose that in the studied lacustrine environments, metal(loid)s within Cala Cala Lagoon are less available and mobile than within Lake Uru Uru and that high concentrations of dissolved elements are explained by the proximity to different metallogenic belts located along the Eastern Andes Cordillera and not by anthropogenic influence. Northern Lake Uru Uru exhibits the lowest mean concentration of dissolved metal(loid)s (except Cu) and their behaviour is highly influenced by evaporation/precipitation rates. The reducing environment reached during the wet season (WS) entails the release of metal(loid)s as reductive dissolution of Fe- and Mn-oxyhydroxides takes place. In this area particulate metal(loid) behaviour shows moderate changes between different seasons and despite the fact that anthropogenic influence exists in this area, the most important influence on metal(loid) behaviour is renewed water input in the water column and WS. Metal(loid)s within southern

Lake Uru Uru area are the most reactive, available and mobile. During the dry season (DS) dissolved metal(loid) behaviour is probably influenced by evaporation, whereas no influence is present during the WS. Dissolved concentrations of pore water are nearly the same in both seasons, and the highest concentrations of dissolved Sb and Mo are found in this area during both seasons, with Cd dominating in the DS. Solid state partitioning (SSP) significantly changes fractionation during the WS and metal(loid)s can be easily released to the pore water when reducing conditions are established. We discovered that the most unstable metal(loid)s in the solid phase are Mo, U, Sb and Pb, which increase while Cd diminishes their availability during the WS. This area presents the highest environmental concern. This is because, beside the influence of WS, anthropogenic influence (mainly linked to the Huanuni Mine) might be causing the highest concentrations of dissolved Sb and Mo (Mo competition with Cu may induce dietary deficiencies in farm animals). We stress that it is in this area where most flora and fauna live and fishing is usually practiced. We recommend that metal(loid) behaviour in the OLW should be studied in more detail, especially during the WS and La Niña events.

Resumen

El lago Uru Uru (Altiplano) y la laguna Cala Cala (Cordillera de los Andes Oriental) son dos ambientes lacustres ubicados en el Altiplano de Bolivia. En estos ambientes se tomaron muestras durante dos temporadas diferentes entre 2008 y 2009 para determinar el comportamiento y la movilidad de los metal(oid)es durante los procesos de diagénesis temprana. En las dos campañas de muestreo un total de 5 testigos de sedimento fueron extraídos. Las especies redox principales, el comportamiento de los metal(oid)es disueltos, los flujos difusivos, las extracciones paralelas y la mineralogía, llevaron a proponer que, en los ambientes lacustres estudiados, los metal(oid)es en la laguna Cala Cala son menos disponibles y móviles que en el lago Uru Uru y que las altas concentraciones de elementos disueltos se explican por la proximidad de varios cinturones metalogénicos situados en la Cordillera de los Andes Oriental y no por la influencia humana. El sector norte del lago Uru Uru tiene la menor concentración media de metal(oid)es disueltos (excepto Cu) y su comportamiento está fuertemente influenciado por las tasas de precipitación/evaporación. El ambiente reductor alcanzado durante la estación húmeda (WS) provoca la liberación de los metal(loid)es a medida que la disolución reductiva de oxihidróxidos de Fe y Mn tiene lugar. En este sector, el comportamiento de los metal(loid)es en estado particulado muestra cambios moderados entre las diferentes estaciones y pese a que el influjo

antropogénico en esta zona existe, la influencia más importante en el comportamiento de los metal(oid)es es el ingreso de agua renovada en la columna de agua y la WS. Los metal(oid)es en la zona sur del lago Uru Uru son los más reactivos, disponibles y móviles. Durante la estación seca (DS) el comportamiento de los metal(oid)es disueltos es probablemente influenciada por la evaporación, mientras que ninguna influencia se determinó en WS. Las concentraciones de agua intersticial son casi las mismas en ambas temporadas y las mayores concentraciones de Sb y Mo disuelto se encuentran en esta área durante las dos temporadas, mientras Cd se concentra en la DS. El particionamiento en estado sólido (SSP) muestra cambios significativos de fraccionamiento durante WS, donde los metales pueden ser fácilmente liberados en el agua intersticial cuando las condiciones reducctivas se establecen. Se encontró que los metales más inestables en la fase sólida son Mo, U, Sb y Pb aumentando la disponibilidad y Cd disminuyendo la disponibilidad en WS. Esta área representa la mayor preocupación ambiental. Esto se debe a que además de la influencia de la WS, la influencia humana asociada principalmente a la Mina de Huanuni podría provocar altas concentraciones de Sb y Mo disuelto (la competición de Mo con Cu puede inducir carencias en la dieta de animales de granja). Hacemos hincapié en que ésta es el área donde la mayoría de la flora y la fauna habitan y la pesca se practica generalmente. Recomendamos que el comportamiento de los metal(oid)es en la OLW debe estudiarse, sobre todo durante la WS y los episodios de La Niña.

Résumé

Le lac Uru Uru (Altiplano) et la lagune Cala Cala (Cordillère des Andes Orientale) sont deux milieux lacustres situés dans l'Altiplano bolivien. Ces environnements ont été échantillonnés pendant deux saisons différentes entre 2008 et 2009 afin de déterminer le comportement des métaux et la mobilité au cours des processus de diagenèse précoce. Dans les deux campagnes de carottage un total de 5 carottes ont été extraites. Les principales espèces redox, le comportement des métaux dissous, les flux diffusifs, les extractions sélectives et la minéralogie ont permis de proposer que, dans les environements lacustres étudiés, les métaux dans la lagune Cala Cala sont moins disponibles et mobiles que dans le lac Uru Uru et que des concentrations élevées des éléments dissous est expliqué par la proximité des différentes ceintures métallogéniques situés le long de la Cordillère des Andes Orientale et non par l'influence anthropique. Le nord du lac Uru Uru présente la concentration moyenne plus faible pour des métaux dissous (sauf Cu) et leur comportement est fortement influencé par des taux de précipitation/évaporation.

L'environnement réductrice atteint pendant la saison humide (WS) entraîne la libération de métaux par la dissolution réductrice des oxyhydroxides de Fe et Mn. Dans ce domaine, les comportements des métaux dans la fraction solide montrent des changements modérés entre les différentes saisons. En dépit que l'influence anthropique dans ce domaine est présente, les influences plus importants au cours de la liberation des métaux sont les apports d'eau dans la colonne d'eau et la WS. Les métaux dans la zone sud du lac Uru Uru sont les plus réactifs, disponibles et mobiles. Pendant la saison sèche (DS) le comportement des métaux dissous est probablement influencé par l'évaporation, alors que pas d'influence est présent lors de la WS, las concentrations de l'eau interstitielle dissous sont presque les mêmes dans les deux saisons, et les plus fortes concentrations de Sb et Mo dissous se trouvent dans cette zone pendant les deux saisons et Cd dans la DS. Le partitionnement à l'état solide (SSP) montre des changements significatifs de fractionnement pendant la WS, où les métaux peuvent être facilement libéré dans l'eau interstitielle lorsque les conditions de réduction sont établis. Nous avons découvert que les métaux les plus instables dans la phase solide sont Mo, U, Sb et Pb en croissante disponibilité et Cd en decroissante disponibilité au cours de la WS. Cette zone présente la plus forte préoccupation environnementale. C'est parce que, en plus de l'influence de la WS, l'influence anthropique, principalement liée à la Mine de Huanuni, pourrait être à l'origine des fortes concentrations de Sb (et Mo) dissous (la compétition de Mo avec Cu peut induire une alimentation carencée en animaux de ferme). Nous soulignons que c'est dans ce domaine où la plupart de flore et faune vivent et de la pêche est généralement pratiqué. Nous recommandons que le comportement des métaux dans l'OLW doit être étudié, spécialement au cours de la WS et les événements La Niña.

4.1 Introduction

In the idealized steady-state view of early diagenesis, a sediment deposit consists of defined zones within which only certain redox reactions can take place [134]. Yet, redox boundaries between zones are generally blurred, since the pore water composition can be affected by temporal variations in organic carbon input, sedimentation rate, temperature and chemical composition of the overlying bottom water (BW). This causes fluctuation in the depth of the oxic-anoxic boundary, creating zones where metals are alternately oxidized and reduced and where sulphides are alternately precipitated and dissolved [289]. During early diagenesis, part of the organic matter (OM) deposited in sediments is mineralized close to the water-sediment interface (WSI), with O_2, NO_3^- , Fe- and Mn-oxyhydroxides or SO_4^{2-} acting as electron acceptors [134, 135]. When surface sediments are enriched in Mn- and/or Fe-oxyhydroxides and are characterized by high physical or biological mixing rates, Fe and Mn reduction coupled to OM oxidation can become important [290, 291]. This coupling is either direct, with Mn- and Fe-oxyhydroxides acting as electron acceptors in the mineralization of organic material [290], or indirect, with Mn- and Fe-oxyhydroxides acting as intermediates between, for instance, sulphide and O_2 produced during SO_4^{2-} reduction [291].

Early diagenetic processes have been widely and intensively studied and documented in marine environments (e.g., [55, 292, 293, 294, 295, 296, 297, 298, 299, 300, 301, 302, 303]) through either field studies (e.g., [304, 305, 306]) or multi-component reactive-transport diagenetic modelling (e.g., [307, 308]). However, while studies are increasingly published (e.g., [302, 309, 310, 311, 312]), our knowledge about early diagenesis in freshwater environments is fragmentary. Post-depositional redistribution of metallic (metalloids included) trace elements (MTE) in continental aqueous systems, such as lakes, and the relationships between this and temperature, pore water chemistry, overlying water (OLW) depth, among other factors, are poorly studied [313, 314], making it difficult to understand the controlling factors of MTE mobility and impact on these environments.

Evidence that pore water properties can fluctuate significantly is mostly limited to environments subject to seasonal temperature variations (e.g., [291]). Extreme interannual fluctuations are characteristic of the Bolivian highlands, this area experiencing periodical droughts (due to both rain scarcity and high evaporation rates) and floods [245, 253] and depleted atmospheric oxygen at high altitude (3,600 to 4,200 m a.s.l.). No studies have reported a comprehensive assessment of the processes and controlling factors of post-depositional redistribution of MTE

in high altitude environments, such as the Bolivian Altiplano, which is additionally subjected to heavy anthropogenic activities such as mining and smelting [315]. Therefore, this region represents an ideal site to study MTE particulate partitioning and early diagenesis-related fluxes of dissolved trace metals through the WSI, with their possible impact on biota.

To understand MTE behaviour during early diagenesis, a total of five sediment cores were studied to document post-depositional redistribution between particulate and dissolved (pore water) fractions. The cores were retrieved from (i) an Altiplanic lacustrine environment heavily impacted by mining and smelting activities during different seasons and, for comparison, (ii) from a non-anthropogenically impacted mountainous lake [315]. Based on high-resolution (mm) vertical profiles of dissolved and total particulate MTE, redox-sensitive elements (N-species, sulphate, Fe and Mn), authigenic minerals and diffusive fluxes, we propose a conceptual model of MTE behaviour during early diagenesis within a contaminated and a non-impacted lake of the Bolivian Altiplano, stressing the importance of seasonal changes, especially the increase of precipitation and its probable impact on biota.

4.2 Background and methods

4.2.1 The Altiplano of Oruro, TDPS and Altiplanic lakes

Oruro Department is located on the Altiplano of Bolivia, a 200,000 km^2 intermontane endorheic and tectonic basin which formed during the Pliocene and early Pleistocene (some 3-2 Ma), in the central Andes of Peru, Bolivia and Argentina [229]. This basin is bounded to the west by the Western Andes Cordillera and to the east by the Eastern Andes Cordillera, both characterized by being highly mineralized geomorphological features ([217, 315, 316] and references therein).

The main hydrological system of the Altiplano corresponds to the endorheic Lake Titicaca-Desaguadero River-Lake Poopó-Coipasa Salar (TDPS; Fig. 4.2.1). Climatically, this area has a dry (DS) and a wet season (WS) extending from May to September and October to March, respectively. Despite the scarcity of precipitation ($<$ 400 mm, [245]), intermittent flood periods have affected the Altiplano, great floods having been observed during 1921, 1930-1935, 1964, 1985, 1987 [253]. These were associated with cold ENSO events (La Niña), which have been associated with historically high lacustrine levels since the early Pleistocene [247, 260]. On the contrary, extended droughts have also affected this area, these associated with the warm ENSO

(El Niño) phenomenon; important events observed during modern times were 1937, 1944, 1947, 1956, 1967-1968, 1983, 1988 [253].

4.2.2 Sample collection and handling

Lake Uru Uru is located north of Lake Poopó. It is drained by the Desaguadero River, and thus belongs to the TDPS system (Fig. 4.2.1). In contrast, the Cala Cala Lagoon is located within the Eastern Andes Cordillera and is drained by the Khala Khala River (Fig. 4.2.1) [315]. Sampling of sedimentary cores from Lake Uru Uru and Cala Cala Lagoon was conducted in April 2008 and February 2009. During these coring campaigns, northern and southern areas of Lake Uru Uru were sampled during DS (21^{st}-25^{th} of April 2008) and WS (2^{nd}-6^{th} of February 2009). Both areas are affected by the mining industry [315]. Additionally, the Cala Cala Lagoon, a non-mining impacted area [315], was sampled during WS (2^{nd}-6^{th} of February 2009) for comparison purposes (Fig. 4.2.1). Coring campaigns resulted in a total of five sediment cores. Sampling was done using a Large Bore Interface Corer (Aquatic Research Instruments®) equipped with a polycarbonate core tube (60 cm length, 10 cm inner diameter). This corer enables sampling the uppermost decimetres of the sediments without any disturbance of the WSI. Immediately after recovery, bottom water (BW) was sampled from the undisturbed WSI of the core through a 20 mL syringe, then filtered through cellulose acetate syringe filters (0.2 µm porosity; Nalgene®) and kept in three different 10 mL acid-cleansed vials (for nutrients, sulphate and chloride, and MTE). Cores were extruded and sliced with an acid-cleansed plastic cutter (details in [315]) with a vertical resolution of up to 0.5 cm. All samples were immediately collected in acid-cleansed 200 mL propylene centrifuge vials and centrifuged at 4000 r.p.m. for 20 min. For each sample, the supernatant was filtered through cellulose acetate syringe filters (0.2 µm porosity; Nalgene®) and then divided into three aliquots for nutrient, sulphate and chloride, and MTE analysis. Aliquots for nutrient analysis were stored in 5 mL polycarbonate tubes and immediately frozen at -5°C until analysis; aliquots for sulphate and chloride analysis were stored in 5 mL polypropylene tubes and kept at 4°C; aliquots for MTE measurements were stored in acid-cleansed tubes, acidified (pH ~1; HNO_3 ultra-pure 1%) and stored at 4°C. The same protocol was applied to BW samples.

4.2.3 Pore water analysis

Sulphate, chloride and nitrate concentrations were analysed by ion chromatography with a

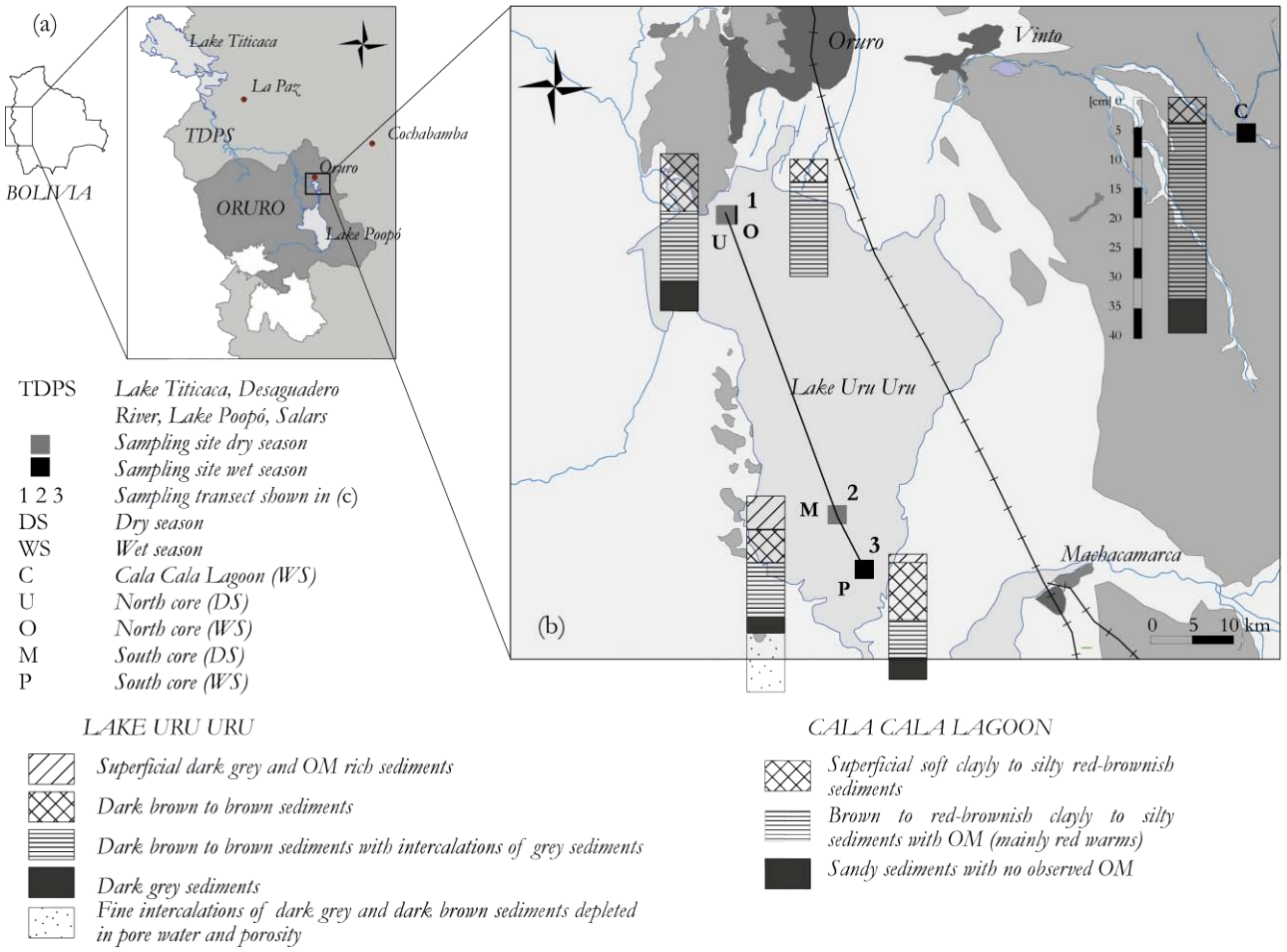

Figure 4.2.1: (a) TDPS endorheic hydrological system. (b) Sampling sites.

Dionex ICS 2000 Chromatographer. The detection limits (DL) for sulphate, chloride and nitrate were 0.02, 0.04 and 0.002 mgL^{-1} respectively. Accuracy was better than 5% and reproducibility better than 3%. Ammonium was analysed by ion chromatography with a Dionex ICS 1000 Chromatographer, with an accuracy better than 5%.

4.2.4 Solid analysis

The granulometry was determined using a laser granulometer (2.0 Mastersizer 2000). Particulate organic carbon (POC), total carbon (C_{tot}) and total sulphur (S_{tot}) were measured from the dry, powdered and homogenized material using a carbon/sulphur analyser (Horiba Jobin Yvon Emia-320V C/S Analyser). Inorganic carbon was eliminated by HCl addition prior to analysis of POC. Particulate inorganic carbon (PIC) was determined subtracting C_{tot} to POC.

Single chemical extractions (i.e., using a separate aliquot of the same sample for each reagent) were applied on all sediment samples. The single extraction procedures used in this study were principally based on the sequential extraction scheme according to Tessier *et al.* (1979) [154]. Previous studies (e.g., [202, 317]) showed that similar results for trace metal partitioning (Cu, Cr, Ni, Pb, and Zn) were obtained from the conventional sequential extraction method [154] and from single extractions using identical operating conditions applied in each individual extraction. Single extractions were chosen over sequential extractions in order to avoid (1) possible changes in elemental speciation during the successive extraction steps, (2) changes or losses of elemental species during the residue washing step [201] and (3) multiple risks of sample contamination from the successive reagents used [165]. Similar single selective extractions were successfully applied in studies dealing with mining- and smelting-impacted aquatic systems (e.g., [302, 314]). The single extraction protocols and the five operationally-defined target fractions are presented in Table 4.1.

Mineralogical determinations were performed by XRD, SEM and microprobe. XRD was used to determine the main mineralogical phases. Detailed observations were performed to selected sediments placed on the surface of cylindrical epoxy plugs covered with a 20 to 50 nm carbon film before analytical observation; analyses were performed under accelerations comprised in the range 15 to 20 kV. During the observations, the SEI mode images allowed studying of the morphologies of the minerals in the sample, while the BEC mode allowed to characterize samples as a function of their chemical composition. Selected minerals observed through SEM were analysed by microprobe (Cameca SX50) to determine the chemical composition of sulphides and oxides. Acceleration tension was c. 15 kV for oxides and c. 25 kV for sulphides. For

Table 4.1: Operating conditions employed during single extraction procedures

Fraction	*sample weight [mg]*	*reagent*	*shaking time temperature [°C]*	*reference*
F1: exchangeable	*200*	*$MgCl_2$ 1M pH 7*	*1h at 25°*	*[154]*
F2: carbonate	*500*	*10 mL NaOAc 1 M + HOAc (pH 5)*		*[154]*
		pH adjustments with HOAc 5 M		
		during the extraction		
F3: Fe- and Mn-oxyhydroxides (reducible)	*200*	*12.5 mL ascorbate solution (pH 8)*	*24 h at 25°*	*[206, 302]*
F4: Organic matter/sulphides (oxidizable)	*200*	*1.6 mL H_2O_2 30% + NaOH (pH 5)*	*2 h at 85°*	
		0.6 mL H_2O_2 30% + NaOH	*hotplate*	
		then 1 mL NH_4OAc 1 M + 0.8 mL H_2O Milli-Q®	*30 min at 25°*	*[318]*
F5: TMC	*30 (DS)*	*HCl 12 N + HNO_3 14N + HF 26 N*	*2 h at 110°*	*[211] (modified)*
		then HCl 12 N + HNO_3 14N	*2 h at 110°*	
	100 (WS)	*HF 26 N + HNO_3 14N + H_2O_2 30%*	*20 min at 150°*	*EPA 3052*
			microwave	

sulphides and oxides the beam size was 2·2 µm with a current of 20 nA.

4.2.5 Diffusive fluxes

Diffusive fluxes were determined from BW to the first interstitial water sample following Fick's first law $J_{sed} = -\phi \cdot D_{sed} \cdot \frac{\partial C}{\partial \chi}$, where J_{sed} is the diffusive flux in the sediment [M m^{-2} year^{-1}]; ϕ is the porosity; D_{sed} is the sediment diffusion coefficient [cm^2 s^{-1}] and $\frac{\partial C}{\partial \chi}$ is the concentration gradient [M m^{-3} m^{-1}]. Values for D_{sed} were calculated on the basis of a dimensionless tortuosity (θ^2) and the diffusion coefficient in free solutions (D_0) following $D_{sed} = D_0/\theta^2$ [cm^2 s^{-1}], dimensionless tortuosity was determined by $\theta^2 = 1 - \ln(\phi^2)$ [319]. D_{sed} was not corrected for any random transport mechanism such as biodiffusion, gas ebullition or wave-induced mixing. Regarding As, Sb, Mo and U, D_{sed} was estimated using the molecular self diffusion coefficient (D_0) for the arsenate [320], antimonate, molybdate and uranium dioxide species. Positive J_{xi} indicates an upward-directed flux (efflux from the sediment into the overlying water column) and negative J_{xi} indicates a downward-directed flux (influx from the water column into the sediment). Values of D_0 were based on experimental data from Li & Gregory (1974) [321] obtained at 18°C and 25°C. We employed both temperatures because 18°C resembles the lake temperature, and 25°C to estimate diffusive fluxes of As, Sb, Mo and U, because these authors only obtained D_0 for these molecules at 25°C. Fluxes were not integrated over a year and are reported as semestrial fluxes to stress J_{sed} differences between the DS and WS.

4.2.6 MTE measurements

Total dissolved and particulate contaminant concentrations were measured using a quadrupole ICP-MS 7500 ce (Agilent Technologies). The analytical methods employed were quality-checked by analysis of certified international reference water (SLRS-4; Table 4.2). Total sediment digestion included method blanks and digestion of certified international reference material (LKSD-1 & LKSD-3; Table 4.2). Accuracy was within 5% of the certified values and the analytical error (rsd) generally better than 5% for concentrations 10 times higher than the detection limits. Exceptions were dissolved Pb (~40% overestimated) and solid Pb (~15% overestimated) in LKSD-1; dissolved Mn and As (~16% and ~10% underestimated respectively) and particulate Fe (~20% underestimated in LKSD-1). The concentrations of Mn subjected to exchangeable (Mn_{MgCl_2}) and ascorbate (Mn_{asc}) digestions were measured through ICP-OES ("Ultima 2"

Table 4.2: Measured and certified concentrations of LSRS-4 water standard and LKSD-1, LKSD-3 sediment standard. Water concentrations in $\mu g \cdot L^{-1}$ and sediment in $\mu g \cdot g^{-1}$. [a][270].

	LSRS-4			*LKSD-1*			*LKSD-3*					
	measured	*value*	*certified*	*value*	*measured*	*value*	*certified*	*value*	*measured*	*value*	*certified*	*value*
Mn	*3.31*	*0.16*	*4.33*	*0.18*	*673*	*40*	*700*	*30*[a]	*1,212*	*110*	*1,440*	*80*[a]
Fe	*85.1*	*3.8*	*91.2*	*5.8*	*22,794*	*1,340*	*29,000*	*1,000*[a]	*36,559*	*5,370*	*40,000*	*2,000*[a]
Cu	*16.9*	*0.5*	*17.4*	*1.3*	*47*	*4*	*44*	*5*[a]	*37*	*4*	*35*	*3*[a]
Zn	*1.032*	*0.022*	*0.845*	*0.095*	*345*	*20*	*331*	*22*[a]	*146*	*10*	*152*	*14*[a]
As	*0.325*	*0.020*	*0.413*	*0.039*	*37*	*3*	*40*	*2*[a]	*28*	*3*	*27*	*2*[a]
Mo	*0.2*	*0.006*	*0.5*	-	*10*	*1*	*10*	*2*[a]	*1.2*	*0.3*	<5	-
Cd	*0.008*	*0.0003*	*0.006*	*0.0014*	*1.5*	*0.3*	*1.4*	*0.3*[a]	*0.7*	*0.2*	*0.8*	*0.6*[a]
Sb	*0.316*	*0.005*	*0.300*	-	*1.2*	*0.2*	*1.2*	*0.1*[a]	*1.3*	*0.1*	*1.3*	*0.1*[a]
Pb	*0.135*	*0.011*	*0.081*	*0.006*	*95*	*3.4*	*82*	*5*[a]	*33*	*4*	*29*	*3*[a]
U	*0.1*	*0.01*	*0.1*	-	*10.4*	*1*	*9.7*	-	*4.3*	*0.4*	*4.6*	-

Horiba Jobin Yvon); the analytical error (rsd) was less than 3.9% for Mn_{MgCl_2} and less than 1.8% for Mn_{asc}.

4.3 Results

4.3.1 Solid phase

4.3.1.1 Water content, porosity and granulometry

The pore waters from Lake Uru Uru are characterized by decreasing water content and porosity with depth due to sediment compaction. The northern area exhibits high variability in the top section of the profile during DS. In contrast, the Cala Cala Lagoon sediments show porosity and water content variability with depth (Table 4.3 and Fig. 4.3.1).

Granulometry was determined only for WS sediments in the Cala Cala Lagoon and northern Lake Uru Uru (Table 4.3.1). The Cala Cala Lagoon shows sand as the dominant particle size (79%), while silt and clay are less representative (14 and 7% respectively). The dominant sizes in northern Lake Uru Uru are silt (41%), sand (35%) and clay (24%). Silt contents are constant within the profile, while sand occurs mostly in the upper parts of the sedimentary core and clay tends to increase with depth (from 17% in the top to 30% in the bottom of the core).

4.3.1.2 Particulate organic carbon (POC), particulate inorganic carbon (PIC) and total sulphur (S_{tot})

The sediments of the Cala Cala Lagoon exhibit variable POC contents with depth, with concentrations ranging from 1.5% to 2.3% (Fig. 4.3.1a & Table 4.3). POC contributes to 98% of the C_{tot} on average. Accordingly, PIC concentrations remain very low (<0.15%) along the vertical profile. S_{tot} shows relatively low concentrations decreasing to 0.03% down to 17 cm below the WSI and then increasing downward up to 0.08%. The northern and southern parts of Lake Uru Uru show contrasted particulated carbon and sulphur contents and profiles (Fig. 4.3.1b,c respectively & Table 4.3), with the highest POC, PIC and S_{tot} average concentrations observed in the southern part. In the northern core, POC contributes to 60% (DS) and 74% (WS) of C_{tot} on average and during DS shows first increasing concentrations below the WSI and then decreasing concentrations toward the bottom of the core. Constant POC profiles are observed during WS. S_{tot} is characterized by similar profiles in DS and WS and with profile

Table 4.3: Water content, porosity, particulate organic carbon (POC), particulate inorganic carbon (PIC), total sulphur (S_{tot}) and granulometry. C: Cala Cala Lagoon, WS; U: northern Lake Uru Uru, DS; O: northern Lake Uru Uru, WS; M: southern Lake Uru Uru, DS; P: southern Lake Uru Uru, WS.

		water content [%]	*porosity* ϕ [%]	*POC* [%]	*PIC* [%]	S_{tot} [%]	*granulometry [%]* *clay* $\leq 2\,\mu m$	*silt* $2-63\,\mu m$	*sand* $0.063-1\,mm$
C	*mean*	*42*	*65*	*1.81*	*0.04*	*0.05*	*7*	*14*	*79*
	median	*42*	*65*	*1.72*	*0.05*	*0.05*	*7*	*13*	*80*
	range	*31-54*	*55-76*	*1.45-2.30*	*0.00-0.13*	*0.03-0.08*	*1-35*	*1-25*	*65-98*
U	*mean*	*42*	*66*	*1.14*	*0.72*	*0.21*	-	-	-
	median	*43*	*66*	*0.98*	*0.71*	*0.18*	-	-	-
	range	*34-48*	*58-71*	*0.74-1.57*	*0.14-1.42*	*0.07-0.38*	-	-	-
O	*mean*	*38*	*62*	*0.82*	*0.28*	*0.11*	*24*	*41*	*35*
	median	*43*	*66*	*0.83*	*0.28*	*0.10*	*26*	*43*	*31*
	range	*33-64*	*56-83*	*0.72-0.91*	*0.08-0.43*	*0.07-0.19*	*16-30*	*31-47*	*26-53*
M	*mean*	*53*	*74*	*2.12*	*0.75*	*1.10*	-	-	-
	median	*48*	*71*	*1.05*	*0.59*	*1.30*	-	-	-
	range	*37-86*	*61-94*	*0.49-6.04*	*0.00-2.36*	*0.08-1.62*	-	-	-
P	*mean*	*45*	*67*	*2.68*	*1.10*	*1.08*	-	-	-
	median	*41*	*65*	*1.40*	*0.87*	*1.38*	-	-	-
	range	*31-81*	*54-92*	*0.90-6.51*	*0.14-2.54*	*0.14-1.58*	-	-	-

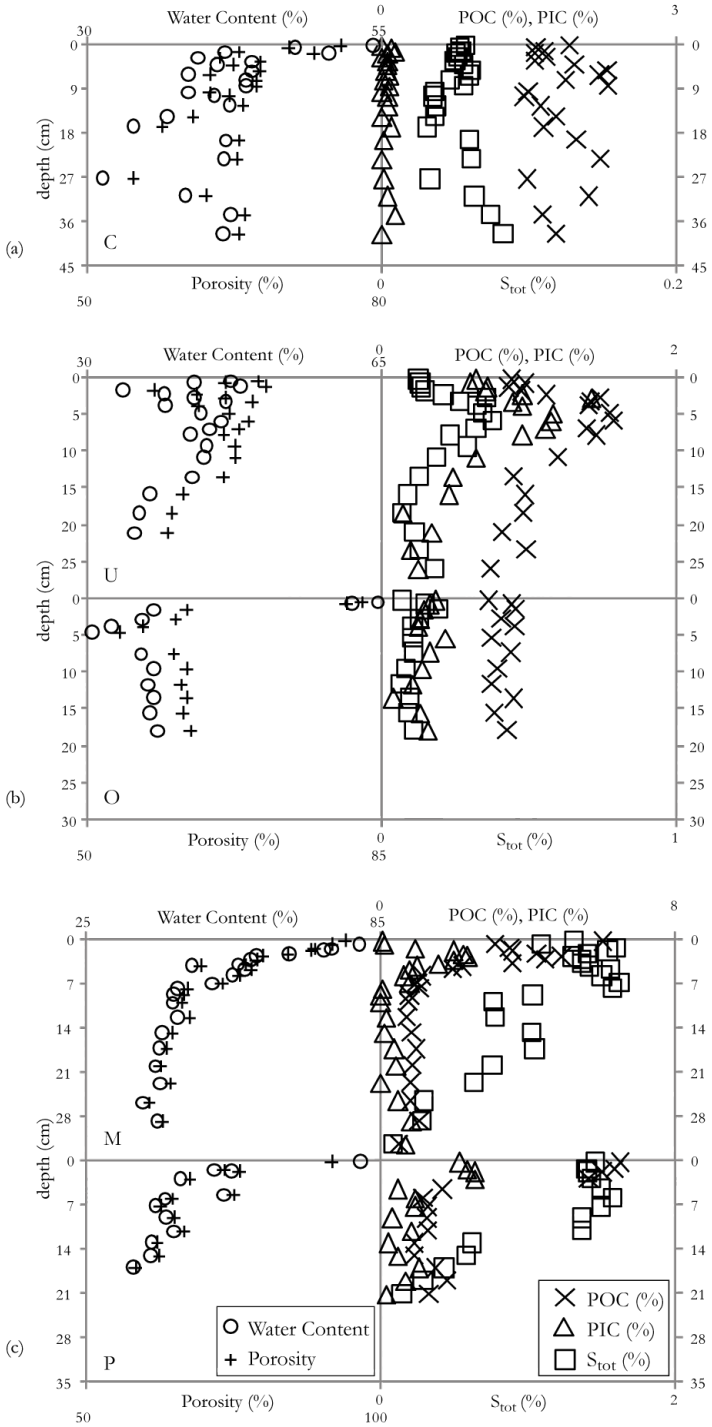

Figure 4.3.1: Porosity (%), water content (%), particulate organic carbon (POC, %), particulate inorganic carbon (PIC, %) and total sulphur (S_{tot}, %). (a) Cala Cala Lagoon; (b) Northern Lake Uru Uru; (c) Southern Lake Uru Uru. C: Cala Cala Lagoon WS; U: northern Lake Uru Uru, DS; O: northern Lake Uru Uru, WS; M: southern Lake Uru Uru, DS; P: southern Lake Uru Uru, WS.

patterns similar to those of POC (DS) and PIC (DS and WS). In the southern core, POC, PIC and S_{tot} show similar trends, with decreasing concentrations with depth for both seasons. POC average contributions to C_{tot} (i.e. 71% for WS and 74% for DS) are comparable to that of the northern core.

4.3.1.3 Total particulate metals and metalloids

Total particulate Fe and Mn show more or less constant values in the Cala Cala Lagoon and Lake Uru Uru. The mean Fe concentration is 38,700±3,300 $\mu g\,g^{-1}$ for the Cala Cala Lagoon, 31,000±3,700 $\mu g\,g^{-1}$ (28,700±2552 $\mu g\,g^{-1}$ in DS and 34,843±1,697 $\mu g\,g^{-1}$ in WS) and 28,500±4,900 $\mu g\,g^{-1}$ (28,532±2,771 $\mu g\,g^{-1}$ in DS and 28,422±7,291 $\mu g\,g^{-1}$ in WS) for northern and southern Lake Uru Uru (Figs. 4.3.2, 4.3.3, 4.3.4). The mean Mn concentration is 657±68 $\mu g\,g^{-1}$, 614±80 $\mu g\,g^{-1}$ (654±73 $\mu g\,g^{-1}$ in DS and 547±31 $\mu g\,g^{-1}$ in WS) and 486±114 $\mu g\,g^{-1}$ (531±17 in DS and 411±126) for the Cala Cala Lagoon, northern and southern Lake Uru Uru, respectively. The upper parts of all cores exhibit more variability (Figs. 4.3.2, 4.3.3, 4.3.4), but less variable contents are shown by the Cala Cala Lagoon followed by northern Lake Uru Uru sediments. The southern Lake Uru Uru sediments are the most variable showing the highest values for solid Mn and the lowest for the solid Fe fraction in the top sections of DS and WS profiles (Fig. 4.3.3c).

Previously calculated enrichment factors (EFs) for the whole area demonstrated that in comparison to the upper continental crust (UCC), elements such as As and Sb are significantly enriched. Compared to calculations based on the average composition of Cala Cala Lagoon sediments, our reference site, shows one order of magnitude lower EFs for both elements (Table 4.4). These observations were largely discussed by [315]. Therefore, we can infer higher background levels than those found in the UCC and that the Altiplano sediments show unique characteristics (Table 4.4). In addition, solid MTE profiles are highly variable, especially within southern Lake Uru Uru sediments (Fig. 4.3.2 and Table 4.4), where several standard deviations represent more than 40% and 70% of the mean during DS (Mo 47% and Sb 49%) and WS (Mo 74%, Pb 77% and Sb 84%), respectively.

4.3.2 Dissolved phase

4.3.2.1 Sulphate, chloride and nutrients

Cala Cala Lagoon. This lagoon exhibits SO_4^{2-} concentrations that range from DL to 0.3

Table 4.4: Total particulate trace metal(loid) concentration–depth profiles. C: Cala Cala Lagoon, WS; U: northern Lake Uru Uru, DS; O: northern Lake Uru Uru, WS; M: southern Lake Uru Uru, DS; P: southern Lake Uru Uru, WS.

		Mn	*Fe*	*Cu*	*Zn*	*As*	*Mo*	*Cd*	*Sb*	*Pb*	*U*
						$[\mu g\, g^{-1}]$					
C	*mean*	*657*	*38,707*	*49*	*121*	*51*	*1.2*	*0.5*	*12*	*107*	*4.3*
	med	*636*	*38,083*	*49*	*119*	*51*	*1.2*	*0.4*	*12*	*109*	*4.1*
	min-max	*572-833*	*34,434-47,840*	*39-66*	*104-147*	*38-72*	*0.9-1.7*	*0.3-1.1*	*10-17*	*61-149*	*3.1-5.7*
	stdv	*68*	*3,299*	*7*	*10*	*8*	*0.2*	*0.2*	*2*	*24*	*0.8*
	EF_{UCC}	*1*	*1*	*2*	*1*	*14*	*0*	*3*	*22*	*4*	*1*
U	*mean*	*654*	*28,700*	*65*	*152*	*62*	*1.3*	*1.6*	*16*	*48*	*2.9*
	med	*656*	*28,135*	*69*	*157*	*62*	*1.2*	*1.6*	*15*	*45*	*2.9*
	min-max	*508-743*	*23,853-34,769*	*43-81*	*107-183*	*49-76*	*0.9-3.0*	*1.1-2.0*	*12-22*	*38-60*	*2.5-3.5*
	stdv	*73*	*2,552*	*13*	*22*	*7*	*0.4*	*0.3*	*3*	*6*	*0.3*
	EF_{UCC}	*1*	*1*	*4*	*3*	*28*	*1*	*14*	*45*	*3*	*1*
	EF_{CCLAC}	*2*	*1*	*2*	*2*	*2*	*2*	*5*	*2*	*1*	*1*
O	*mean*	*547*	*34,843*	*57*	*127*	*49*	*1.1*	*1.3*	*13*	*41*	*2.3*
	med	*543*	*34,527*	*58*	*127*	*47*	*1.1*	*1.4*	*14*	*40*	*2.4*
	min-max	*481-591*	*32,378-38,440*	*49-63*	*109-138*	*37-60*	*0.9-1.3*	*0.6-1.7*	*4-17*	*33-50*	*1.8-2.8*
	stdv	*31*	*1,697*	*4*	*8*	*7*	*0.1*	*0.3*	*4*	*4*	*0.3*
	EF_{UCC}	*1*	*1*	*4*	*2*	*23*	*1*	*12*	*39*	*2*	*1*
	EF_{CCLAC}	*1*	*1*	*2*	*2*	*2*	*1*	*4*	*2*	*1*	*1*
M	*mean*	*531*	*28,532*	*82*	*133*	*70*	*2.5*	*0.5*	*9*	*51*	*3.7*
	med	*519*	*28,067*	*85*	*136*	*66*	*2.2*	*0.5*	*7*	*43*	*3.3*
	min-max	*381-650*	*22,778-35,767*	*38-115*	*101-167*	*47-103*	*0.6-5.4*	*0.3-0.9*	*5-23*	*33-100*	*2.1-5.3*
	stdv	*77*	*2,771*	*16*	*17*	*16*	*1.2*	*0.1*	*4*	*17*	*1.0*
	EF_{UCC}	*1*	*1*	*6*	*3*	*37*	*2*	*5*	*31*	*3*	*2*
	EF_{CCLAC}	*2*	*1*	*3*	*2*	*3*	*4*	*2*	*1*	*1*	*2*
P	*mean*	*411*	*28,422*	*73*	*116*	*63*	*2.9*	*0.7*	*12*	*67*	*2.9*
	med	*375*	*30,864*	*78*	*108*	*61*	*2.3*	*0.6*	*7*	*36*	*2.6*
	min-max	*298-647*	*10,176-36,702*	*28-103*	*43-222*	*30-104*	*0.8-8.6*	*0.3-1.3*	*3-38*	*13-163*	*1.9-5.4*
	stdv	*126*	*7,291*	*20*	*40*	*19*	*2.2*	*0.3*	*10*	*52*	*1.0*
	EF_{UCC}	*1*	*1*	*7*	*3*	*43*	*3*	*9*	*46*	*5*	*2*
	EF_{CCLAC}	*2*	*2*	*4*	*2*	*3*	*7*	*3*	*2*	*1*	*2*

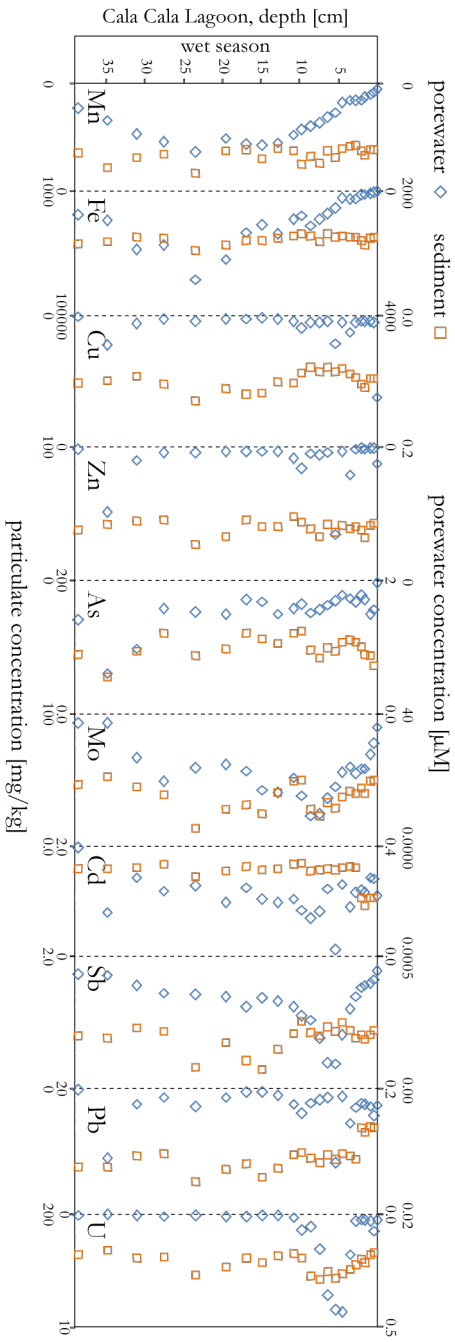

Figure 4.3.2: Total metal(loid)s concentration of pore water and sediment in Cala Cala Lagoon.

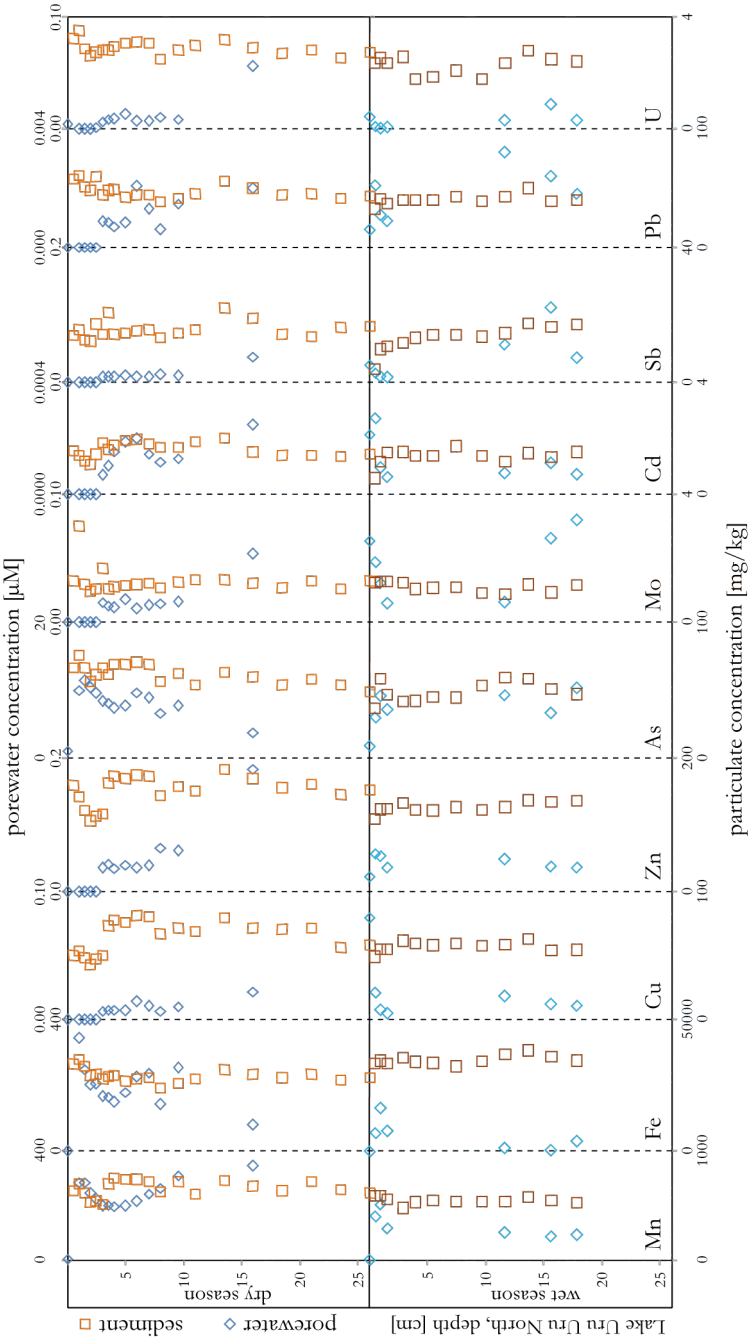

Figure 4.3.3: Total metal(loid)s concentration of pore water and sediment in northern Lake Uru Uru area.

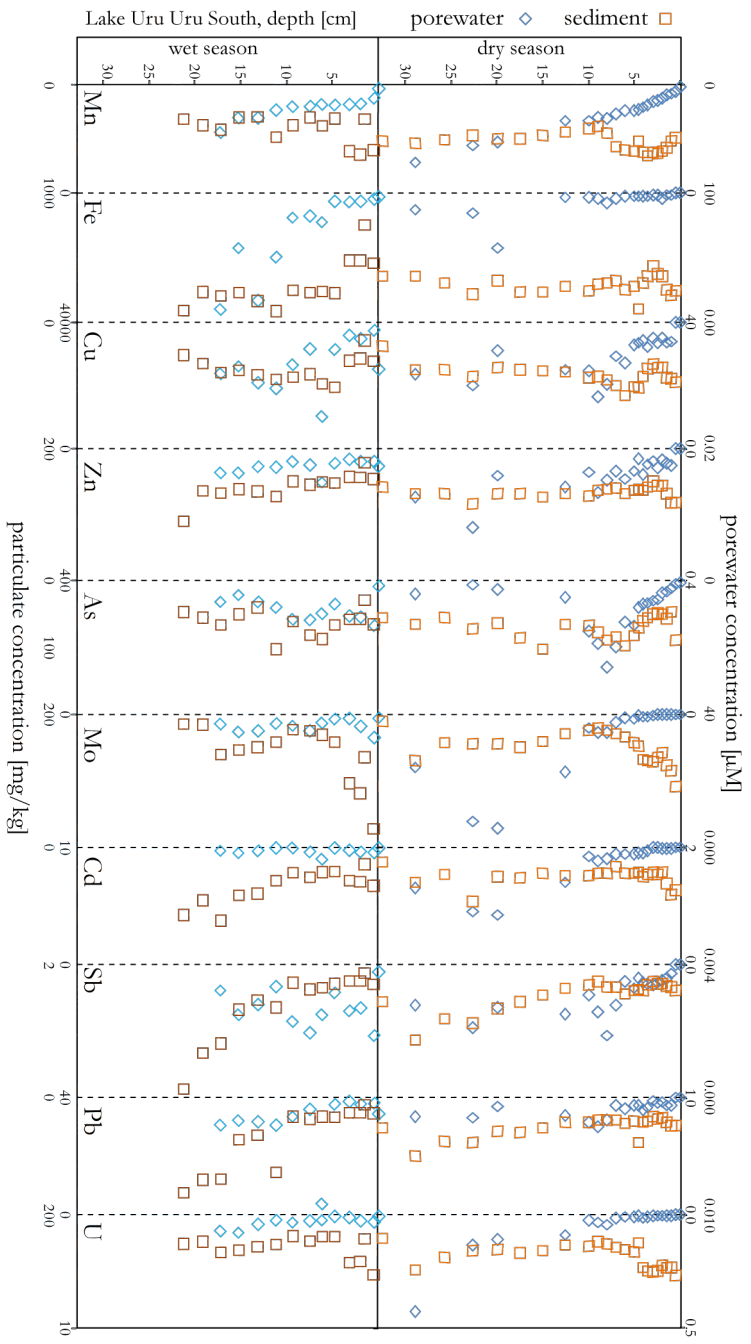

Figure 4.3.4: Total metal(loid)s concentration of pore water and sediment in southern Lake Uru Uru area.

mM, showing the highest values in the top of the profile, which decrease sharply to 5 cm depth reaching the lowest concentration (Fig. 4.3.5a). The chloride profile exhibits a steep decrease to 5 cm depth, then concentrations are relatively constant to 20 cm depth and increase in the bottom pore water (C-like shape, Fig. 4.3.5a). Nitrate concentrations range from 1.0 to 5.6 µM and show a very scattered pattern with depth (Fig. 4.3.5a). Ammonium increases with depth ranging from 0.2 to 1.5 mM (Fig. 4.3.5a and Table 4.5).

Northern Lake Uru Uru. Dissolved SO_4^{2-} shows a constant increase with depth during DS (2.5-10.9 mM) and relatively constant values during WS (2.9±0.3 mM; Fig. 4.3.5b and Table 4.5). Chloride profiles show an increase with depth (Fig. 4.3.5b) during DS (8-48 mM), while during WS, Cl^- values tend to stay relatively constant (14.9±2.3 mM). In the DS, NO_3^- concentrations range between 0.2-2.2 µM showing a relative increase with depth (Fig. 4.3.5b and Table 4.5). During the WS, NO_3^- concentrations range between 0.8-7.6 µM, showing a relative increase in concentration with depth, yet the highest values are located 3 cm below the WSI (Fig. 4.3.5b and Table 4.5). NH_4^+ concentrations are below the DL during both seasons (Table 4.5)

Southern Lake Uru Uru. This area shows an important decrease of SO_4^{2-} during the DS and WS from BW until 1 cm depth (2.2 to 1.2 mM and 8.4 to 4.9 mM in DS and WS respectively), then concentrations increase as in the northern area (1.3-22.7 and 6.5-9.1 mM in DS and WS respectively; Fig. 4.3.5c). Chloride profiles show an increase with depth (Fig. 4.3.5c) during the DS (10-79 mM), while during the WS, Cl^- values tend to stay relatively constant (48.8±10.6 mM). During the DS, NO_3^- concentrations range between 0.1-8.3 µM, showing a relative increase with depth (Fig. 4.3.5c and Table 4.5). During the WS, NO_3^- concentrations range between 0.2-5.2 µM, showing a relative increase of concentration with depth, yet the highest values are located 3 cm below the WSI (Fig. 4.3.5c and Table 4.5). This area exhibits increasing concentrations of NH_4^+ with depth ranging from DL to 0.78 mM during the DS. During WS only 3 samples are above DL with concentrations ranging from 0.43 to 0.45 mM (Fig. 4.3.5c and Table 4.5).

4.3.2.2 Dissolved Fe and Mn

Cala Cala Lagoon. Maximum dissolved values for these elements are observed at this site. Both patterns are quite similar, Mn increasing from BW to 15 cm depth (89 to 1,145 µM). The concentration is nearly constant from 15 to 24 cm depth (1,135±107 µM) and decreases substantially to the bottom of the profile (up to 453 µM). Dissolved Fe increases from BW to

Table 4.5: Dissolved phase major elements, nutrients and metal(loid) concentration. DL: detection limit. C: Cala Cala Lagoon, WS; U: northern Lake Uru Uru, DS; O: northern Lake Uru Uru, WS; M: southern Lake Uru Uru, DS; P: southern Lake Uru Uru, WS.

		SO_4^{2-}	Cl^-	NO_3^-	NH_4^+	*Mn*	*Fe*	*Cu*	*Zn*	*As*	*Mo*	*Cd*	*Sb*	*Pb*	*U*
		mM	*mM*	*µM*	*mM*	*µM*	*µM*	*nM*	*nM*	*µM*	*nM*	*nM*	*nM*	*nM*	*nM*
C	*mean*	0.037	0.38	2.81	0.59	660	876	17	204	9	172	0.22	71	3	85
	med	0.004	0.31	2.47	0.38	671	781	9	84	8	172	0.21	61	2	26
	min	0.00	0.2	1.02	0.16	89	9	1	21	1-28	27	0.00	23	0	2
	max	0.33	0.84	5.61	1.45	1267	2822	125	1309	28	306	0.47	162	12	432
U	*mean*	4.75	20.29	0.54	DL	228	186	6	38	8	12	0.10	8	0.8	9
	med	4.04	19.20	0.29	DL	231	190	6	37	8	12	0.11	9	0.8	7
	min	2.46	8.12	0.20	DL	2	DL	DL	DL	1	DL	DL	DL	DL	DL
	max	10.85	48.14	2.19	DL	346	346	21	183	12	54	0.25	37	2.1	56
O	*mean*	2.94	14.92	2.63	DL	109	44	22	41	7	45	0.13	37	1.7	8
	med	3.02	15.88	1.62	DL	103	33	13	37	7	47	0.10	25	1.8	8
	min	2.43	10.46	0.82	DL	4	1	5	22	2	15	0.06	8	0.6	1
	max	3.27	17.06	7.60	DL	201	134	79	56	10	81	0.27	112	3.2	22
M	*mean*	7.41	35.28	1.98	0.51	25	3	5	84	8	340	0.54	232	1.1	48
	med	5.18	29.53	1.30	0.48	23	1	4	71	6	63	0.24	165	0.8	11
	min	1.24	10.48	0.10	DL	2	DL	DL	DL	1	DL	DL	DL	DL	0
	max	22.72	78.94	8.28	0.78	71	17	12	240	26	1706	2.28	530	2.5	427
P	*mean*	6.71	48.05	1.88	0.44	21	12	7	57	9	180	0.14	321	2.0	35
	med	6.43	46.68	1.55	0.43	19	8	7	53	9	164	0.12	337	1.5	32
	min	4.95	27.98	0.20	DL	4	2	1	36	2	49	0.05	59	0.4	10
	max	9.05	67.92	5.16	0.45	45	36	15	102	13	366	0.44	532	9.1	78

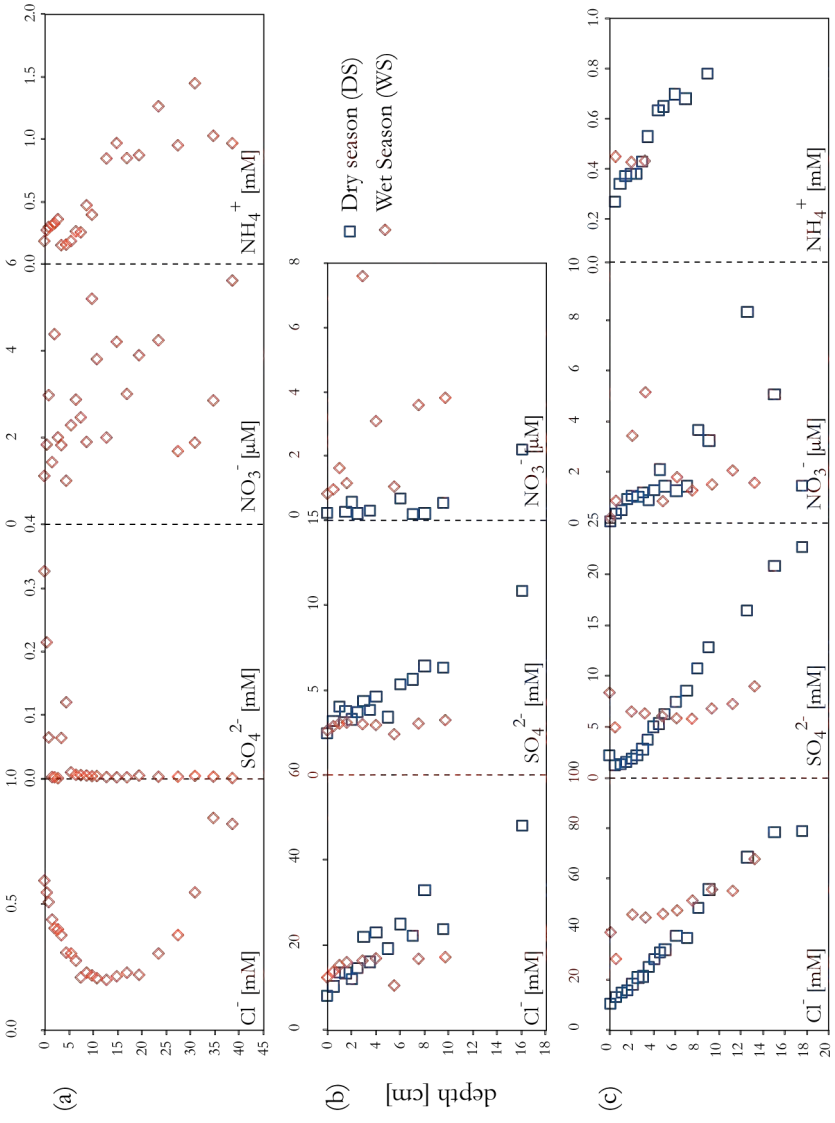

Figure 4.3.5: Dissolved SO_4^{2-}, Cl^- and nutrients pore water profiles. (a) Cala Cala Lagoon; (b) Northern Lake Uru Uru; (c) Southern Lake Uru Uru

24 cm (9 to 2,822 µM) and decreases from 24 cm to the bottom of the core (up to 753 µM; Fig. 4.3.2).

Northern Lake Uru Uru. During the DS and WS these elements exhibit the lowest concentration in BW (Mn 2 & 4 µM and Fe DL & 1 µM). At 1 cm below the WSI, values increase (Mn 281 & 201 µM and Fe 346 & 134 µM). During the DS, below 1 cm depth concentrations decrease to 4 cm (Mn 195 & Fe 152 µM) and Mn then increases to the bottom (up to 346 µM), whereas Fe exhibits a noisy pattern, yet the general trend tends to decrease (up to 81 µM; Fig. 4.3.3). During the WS, in the bottom part of the pore water profile, Mn exhibits constant concentrations (94±9 µM) and Fe tends to increase (up to 33 µM; Fig. 4.3.3).

Southern Lake Uru Uru. In southern Lake Uru Uru, the lowest dissolved mean Mn and Fe values are observed. During the DS and WS, dissolved Mn tends to increase with depth (to 71 and 45 µM respectively). During the DS, dissolved Fe shows constant concentrations to 12 cm depth (1.3±0.7 µM) and the highest concentration at 20 cm (17 µM). During the WS, dissolved Fe shows an increase to 11 cm depth (20 µM), then concentrations are variable and range from 17 to 36 µM (Fig. 4.3.4).

4.3.2.3 Dissolved trace metals and metalloids

Cala Cala Lagoon. Maximum mean values for dissolved Cu, Zn, Pb and U are observed in this lagoon (Table 4.5). Based on pore water profiles, we separated the data into three groups.

Copper & Zinc: These elements decrease in concentration from BW (125 nM Cu & 251 nM Zn) to 0.5 (11 nM Cu & 22 nM Zn) cm below the WSI, subsequently concentrations are nearly constant to 3 cm depth (9.4±1.3 nM Cu & 28±6 nM Zn), from 11 up to 31 cm concentrations are lower and nearly constant (7±3 nM Cu & 95±48 nM Zn), at 3.5, 5.5, 10 and 35 cm depth Cu (25, 42, 20 and 45 nM) and Zn (421, 1309, 329 and 981 nM) show the highest values (Fig. 4.3.2).

Cadmium & Lead: These elements share a similar pattern below 2 cm depth, where the highest concentrations for both are reached at 3.5 (Cd 0.28 & Pb 5.4 nM), 5.5 (Cd 0.47 & Pb 11.8 nM) and 35 (Cd 0.30 & Pb 11 nM) cm depth. In the topmost section Cd decreases from BW to 1 cm depth (0.22 to 0.14 nM), and Pb increases between BW and 0.5 cm depth (2.6 to 4.3 nM; Fig. 4.3.2).

Arsenic, Molybdenum, Antimony & Uranium: The main characteristic for all these elements is that they exhibit a highly different behaviour among them and with the previously defined groups. For instance, As shows an increase from BW (1 µM) to 1 cm depth (10 µM), then

concentrations are nearly constant to 27 cm depth (7.3±1.9 µM) where a pronounced increase is observed (up to 28 µM); Mo increases below the WSI to 9 cm depth (40 to 306 nM), below this depth dissolved Mo decreases in concentration down to 10 cm (191 nM), values are nearly constant to 28 cm (193±35 nM) and decrease markedly in the bottom of the core (133 to 28 nM); a steady increase of dissolved Sb is observed from BW (23 nM) to ~6 cm (162 nM) below the WSI. Below this depth, decreasing dissolved Sb concentration from 124 to 27 nM indicates Sb removal down to the bottom of the core; dissolved U increases below the WSI to 4.5 cm (26 to 432 nM), then is almost totally consumed to 10 cm (432 to 70 nM); from that depth on concentrations are relatively constant (7±4 nM; Fig. 4.3.2).

Northern Lake Uru Uru. This area exhibits the lowest mean values for dissolved Zn, Mo, Sb and U and during WS the highest dissolved Cu mean concentration is observed within this zone. Pore water profiles allowed us to separate metal(loid) behaviour into different behavioural groups during the DS and WS.

Dry season

Arsenic: This element exhibits a similar behaviour to dissolved Fe and Mn, showing the lowest concentration in BW (1 µM) and increasing at 1 cm below the WSI (12 µM). Below this depth, the general trend tends to decrease (up to 4 µM; Fig. 4.3.3)

Copper, Zinc, Molybdenum, Cadmium, Antimony, Lead & Uranium: Al these elements exhibit concentrations below the DL until 2.5 cm depth, at 3 cm concentrations appear (Cu 6, Zn 36, Mo 15, Cd 0.07, Sb 9, Pb 0.9 & U 6 nM). Below this depth all elements exhibit a general increasing trend, yet the central parts of the profiles are very different, in the most bottom section all these elements show the highest concentration (Cu 21, Zn 183, Mo 54, Cd 0.25, Sb 37 & U 56 nM) excepting Pb (Fig. 4.3.3).

Wet season

Arsenic: This element, as dissolved Mn and Fe, exhibits the lowest concentrations in BW (2 µM) and increases to 1 cm depth (9 µM). In the bottom part of the pore water profile As increases (up to 10 µM respectively; Fig. 4.3.3).

Copper & Molybdenum: These elements exhibit an important decrease from BW (79 & 63 nM) to 2 cm depth (5 & 15 nM). In the bottom both show different trends, for instance, Cu is nearly constant (14±4 nM) and Mo increases (up to 81 nM; Fig. 4.3.3).

Zinc, Cadmium & Lead: These elements exhibit low concentrations in BW (Zn 22, Cd 0.21 & Pb 0.6 nM) and increase to 0.5 cm depth (Zn 56, Cd 0.27 & Pb 2.1 nM). At the bottom these elements show variable patterns; Zn is nearly constant, Cd slightly variable and Pb shows

the highest value at 12 cm depth (3.2 nM), then decreases (Fig. 4.3.3).

Antimony and Uranium: Both elements decrease slightly from BW (Sb 25 & U 11 nM) to 1 cm depth (Sb 8 & U 1 nM) and at 16 cm exhibit the highest values (Sb 112 & U 22 nM; Fig. 4.3.3).

Southern Lake Uru Uru. This area exhibits the highest concentration of dissolved Mo and Sb during both seasons and Cd during DS. Based on pore water profile characteristics, metal(loid)s were classified into different groups during each season.

Dry season

Copper, Zinc & Lead: These elements are characterized by exhibiting concentrations below DL to 0.5 cm depth, at 1 cm all appear (Cu 3, Zn 53 & Pb 0.7 nM). Down to 8 cm depth the pattern is very noisy and from 9 cm to the bottom all elements exhibit a similar behaviour, with maximum concentrations at 9 (Cu 12, Zn 135 & Pb 2.5 nM) and 23 cm depth (Cu 10, Zn 240 & Pb 1.7 nM; Fig. 4.3.4).

Arsenic & Antimony: The main characteristic of dissolved As and Sb is that concentrations exhibit the highest value at 8 cm depth (As 26 µM & Sb 530 nM; Fig. 4.3.4).

Molybdenum & Cadmium: Both elements share the same pattern of pore water profile, showing concentrations below DL until 0.5 cm and then increasing slightly to 9 cm depth (Mo 282 & Cd 0.48 nM). From here they increase sharply, showing an inverted "C" shape with maximum values at 20 cm depth (Mo 1706 & Cd 2.3 nM; Fig. 4.3.4).

Uranium: Dissolved U increases slightly to 10 cm below the WSI (12±12 nM); below this depth concentrations increase markedly reaching 427 nM at the bottom of the pore water profile (Fig. 4.3.4).

Wet season

Copper, Zinc & Lead: These elements exhibit a similar trend in pore water profiles, concentrations decrease from BW (Cu 8, Zn 54 & Pb 1.5 nM) to 0.5 cm (Cu 1, Zn 41 & Pb 0.5 nM), at 6 cm depth all show maximum concentrations (Cu 15, Zn 102 & Pb 9.1 nM) and from that depth on Zn and Pb exhibit a slight increase and Cu is variable (Fig. 4.3.4).

Arsenic, Molybdenum, Antimony & Uranium: During this season Mo and U present lower concentrations than during the DS. All these elements follow a similar trend increasing in dissolved concentration from BW (As 2 µM, Mo 49, Sb 59 & U 3 nM) to 0.5 cm depth (As 13 µM, Mo 366, Sb 532 & U 36 nM). Thereafter they exhibit a nearly zigzagging trend, showing

low values at 5 (As 7 µM, Mo 65, Sb 208 & 11 nM) and high values at 7.5 cm depth (As 12 µM, Mo 264, Sb 518 & U 32 nM); from that depth to the bottom of the pore water profile As shows a C-like shape, Mo and Sb an inverted C-like shape and U increases in concentration (Fig. 4.3.4).

Cadmium: Dissolved Cd values are lower than during the DS (Table 4.5), Cd increases from BW to 0.5 cm (0.06 to 0.21 nM), at 6 cm below the WSI the highest concentration is observed, viz. 0.44 nM (5 times lower than the DS maximum); below this depth concentrations are nearly constant (0.11±0.05 nM; Fig. 4.3.4).

4.3.3 Diffusive fluxes

Within Cala Cala Lagoon, effluxes from the sediment into the OLW are observed for nitrate, Mn, Fe, As, Mo, Sb, Pb and U, and influxes from the OLW into the sediment for sulphate, chlorine, Cu, Zn and Cd (Table 4.6).

Within northern Lake Uru Uru, effluxes from the sediment into the OLW are observed for sulphate, chlorine, Mn, Fe and As during the DS and for sulphate, chlorine, nitrate, Mn, Fe, Zn, As, Cd and Pb during the WS, whereas influxes from the OLW into the sediment are observed for nitrate and U during the DS and for Cu, Mo, Sb and U during the WS (Table 4.6).

Within southern Lake Uru Uru, effluxes from the sediment into the OLW are observed for chlorine, nitrate, Mn, Fe, As and U in the DS, and for nitrate, Mn, Fe, As, Mo, Cd, Sb and U during the WS, whereas influxes from the water column into the sediment are observed for sulphate during the DS and for sulphate, chlorine, Cu, Zn and Pb during the WS. During the DS diffusive fluxes were not calculated for elements with dissolved concentrations below DL (Table 4.6).

4.3.4 Solid State Partitioning (SSP)

Cala Cala Lagoon. Within major redox species, Fe shows low reactivity (11±3%), while Mn is potentially highly mobile (154±31%). In the Cala Cala Lagoon the most mobile trace metal(loid)s are Cd (74%), As (53%) and U (43%), while the less mobile elements are Cu (8%), Zn (13%), Pb (15%), Sb (24%) and Mo (35%), the latter element shows the most different partitioning in comparison to Lake Uru Uru sediments (35±14%; Table 4.7).

Lake Uru Uru. These sediments show important changes of SSP between the DS and WS. The northern and southern areas exhibit different SSPs and behave distinctively.

Table 4.6: Diffusive flux (J) of metal(loid)s within Lake Uru Uru and Cala Cala Lagoon pore-water-sediments system. C: Cala Cala Lagoon, WS; U: northern Lake Uru Uru, DS; O: northern Lake Uru Uru, WS; M: southern Lake Uru Uru, DS; P: southern Lake Uru Uru, WS; nc: no coefficient available; dl: detection limit.

	$t°$	SO_4^{2-}	Cl^-	NO_3^-	Mn	Fe	Cu	Zn	As^a	Mo^b	Cd	Sb^c	Pb	U^d
	[°C]													
	18	-1.4	-1.1	0.016	0.49	0.31	-0.95	-1.98	nc	nc	-0.0007	nc	0.019	nc
C	24	-1.7	-1.4	0.019	0.59	0.38	-1.18	-2.31	54	0.41	-0.0008	0.18	0.023	0.25
	18	4	22	-0.002	1.0	1.2	dl	dl	nc	dl	dl	dl	dl	nc
U	24	5	26	-0.003	1.2	1.5	dl	dl	26	dl	dl	dl	dl	-0.018
	18	4	44	0.004	1.7	0.6	-0.63	0.39	nc	nc	0.0007	nc	0.022	nc
O	24	5	52	0.005	2.0	0.7	-0.78	0.46	38	-0.17	0.0008	-0.12	0.026	-0.07
	18	-23	113	0.012	0.06	dl	dl	dl	dl	dl	dl	dl	dl	nc
M	24	-27	135	0.014	0.07	dl	dl	dl	3	dl	dl	dl	dl	0.002
	18	-59	-348	0.021	0.09	0.006	-0.07	-0.15	nc	nc	0.0018	nc	-0.015	nc
P	24	-71	-413	0.024	0.11	0.008	-0.09	-0.17	108	0.72	0.0021	9.66	-0.018	0.19

[a] $H_2AsO_4^-$
[b] MoO_4^{2-}
[c] $H_2SbO_4^-$
[d] UO_2^{2+}

Table 4.7: Solid state partitioning of Cala Cala Lagoon sediments. F1: exchangeable; F2: carbonates; F3: Fe- and Mn-oxyhydroxides; F4: sulphides and/or OM; F5=TMC-(F1+F2+F3+F4), negative values of F5 were obtained when single digestions addition exceeds TMC because of selectivity problems of the reagents used. *m:* mean; σ: standard deviation.

	Mn		*Fe*		*Cu*		*Zn*		*As*		*Mo*		*Cd*		*Sb*		*Pb*		*U*		*Global*	
	m	σ	*m*	σ	*m*	σ	*m*	σ	*m*	σ	*m*	σ	*m*	σ	*m*	σ	*m*	σ	*m*	σ	*m*	σ
F1	*13*	*10*	*0*	*0*	*0*	*0*	*3*	*1*	*0*	*0*	*7*	*8*	*41*	*15*	*2*	*2*	*0*	*0*	*0*	*0*	*7*	*4*
F2	*21*	*6*	*3*	*1*	*4*	*1*	*3*	*1*	*10*	*2*	*0*	*0*	*6*	*6*	*4*	*2*	*9*	*4*	*19*	*5*	*8*	*3*
F3	*48*	*16*	*8*	*2*	*2*	*2*	*6*	*2*	*43*	*10*	*15*	*6*	*12*	*9*	*16*	*4*	*6*	*3*	*21*	*7*	*18*	*6*
F4	*72*	*12*	*0*	*0*	*2*	*1*	*1*	*0*	*0*	*0*	*13*	*3*	*15*	*6*	*2*	*0*	*0*	*0*	*3*	*1*	*11*	*2*
F5	*-54*	*31*	*89*	*3*	*91*	*2*	*88*	*3*	*47*	*12*	*65*	*14*	*26*	*24*	*76*	*5*	*85*	*6*	*57*	*13*	*57*	*11*

Northern Lake Uru Uru. These sediments are potentially more reactive than those of the Cala Cala Cala Lagoon (Table 4.8). During the DS, sediments are less reactive than during the WS and particulate fractions were extracted as follows: Fe (6%) < Zn (17%) < Cu (26%) < U (34%) < Pb (38%) < Sb (44%) < Mo (70%) < As (81%) < Cd (94%) < Mn (95%). This potential metal(loid) availability within the solid phase shows, for major redox species, similar characteristics to those from the Cala Cala Lagoon. Among the trace metal(loid)s, Cd, As and Mo are the most reactive during the DS. During the WS, the sediments are in general, more reactive than during the DS, and the particulate fraction was extracted as follows: Fe (9%) < Zn (22%) < Cu < (30%) < U (31%) < Pb (47%) < Sb (60%) < Mo (80%) < Cd (88%) < As (98%) < Mn (112%). As usual in the northern area, major redox species show the lowest (Fe) and highest (Mn) potential availability. Metal(loid)s such as Sb, Mo and As increase their potential availability and Cd diminishes.

Southern Lake Uru Uru. During the DS and WS, major redox species present low reactivity for Fe (18 and 22% respectively) and high reactivity for Mn (89 and 112% respectively). During the DS the mean potential availability from the particulate fraction is: Fe (18%) < Pb (26%) < Cu (28%) < Zn (38%) < Sb (49%) < U (67%) < As (75%) < Mn (89%) < Cd (90%) < Mo (123%), and during the WS: Fe (22%) < Zn (23%) < Cu (36%) < Pb (63%) < Sb, Cd (65%) < As (83%) < Mn (112%) < U (113%) < Mo (159%). During WS most metal(loid)s increase their potential dangerousness (U, Pb, Mo, Mn and Sb) increasing the contribution of the different chemically defined fractions, and as in northern area, Cd diminishes its potential availability (Table 4.9).

4.4 Discussion

4.4.1 Sediment redox conditions and early diagenesis processes

The depth distribution of major dissolved redox species (Mn, Fe, SO_4^{2-}, NO_3^-) is characterized by concentration gradients just below the WSI driven by the bacterially mediated oxidation of OM [134, 304]. Within the studied Altiplanic lakes, the major dissolved redox species distribution exhibits different patterns during both the DS and WS, within northern and southern Lake Uru Uru and within Cala Cala Lagoon sediments (Figs. 4.3.3, 4.3.4, 4.3.2). In these sediments, OM mineralization proceeds mainly through anaerobic reactions. OM mineralization is supported by the fact that the POC overall decreases with depth in Lake Uru Uru

Table 4.8: Solid state partitioning of northern Lake Uru Uru sediments. F1: exchangeable; F2: carbonates; F3: Fe- and Mn-oxyhydroxides; F4: sulphides and/or OM; F5=TMC-(F1+F2+F3+F4), negative values of F5 were obtained when single digestions addition exceeds TMC because of selectivity problems of the reagents used. *m:* mean; σ: standard deviation. *m:* mean; σ: standard deviation.

	Mn		*Fe*		*Cu*		*Zn*		*As*		*Mo*		*Cd*		*Sb*		*Pb*		*U*		*Global*	
	m	σ	*m*	σ	*m*	σ	*m*	σ	*m*	σ	*m*	σ	*m*	σ	*m*	σ	*m*	σ	*m*	σ	*m*	σ
												Dry Season										
F1	*4*	*1*	*0*	*0*	*1*	*0*	*2*	*1*	*2*	*1*	*14*	*8*	*54*	*15*	*2*	*1*	*0*	*0*	*3*	*2*	*8*	*3*
F2	*32*	*7*	*1*	*0*	*18*	*3*	*5*	*2*	*20*	*3*	*0*	*0*	*23*	*5*	*9*	*3*	*26*	*4*	*14*	*5*	*15*	*3*
F3	*48*	*8*	*5*	*1*	*1*	*1*	*10*	*2*	*56*	*11*	*27*	*13*	*7*	*13*	*27*	*6*	*12*	*3*	*15*	*6*	*21*	*6*
F4	*11*	*3*	*0*	*0*	*6*	*1*	*0*	*0*	*3*	*1*	*29*	*13*	*10*	*4*	*6*	*1*	*0*	*0*	*2*	*1*	*7*	*2*
F5	*4*	*13*	*94*	*2*	*74*	*4*	*83*	*4*	*20*	*14*	*29*	*31*	*7*	*23*	*56*	*10*	*62*	*6*	*66*	*13*	*50*	*12*
												Wet Season										
F1	*4*	*1*	*0*	*0*	*1*	*0*	*2*	*0*	*1*	*0*	*17*	*7*	*43*	*7*	*6*	*3*	*0*	*0*	*5*	*1*	*8*	*2*
F2	*40*	*8*	*3*	*1*	*24*	*3*	*9*	*3*	*24*	*3*	*0*	*0*	*27*	*6*	*11*	*4*	*33*	*6*	*12*	*3*	*18*	*4*
F3	*53*	*18*	*6*	*1*	*0*	*1*	*11*	*3*	*71*	*8*	*23*	*10*	*6*	*11*	*36*	*5*	*14*	*3*	*12*	*4*	*23*	*6*
F4	*15*	*5*	*0*	*0*	*5*	*1*	*0*	*0*	*2*	*1*	*40*	*14*	*12*	*3*	*7*	*1*	*0*	*0*	*2*	*1*	*8*	*2*
F5	*-12*	*19*	*91*	*2*	*70*	*3*	*78*	*5*	*2*	*7*	*19*	*26*	*12*	*15*	*40*	*7*	*53*	*9*	*69*	*9*	*42*	*10*

Table 4.9: Solid state partitioning of southern Lake Uru Uru sediments. F1: exchangeable; F2: carbonates; F3: Fe- and Mn-oxyhydroxides; F4: sulphides and/or OM; F5=TMC-(F1+F2+F3+F4), negative values of F5 were obtained when the addition of single digestions contribution exceeds TMC (due to selectivity problems of the reagents used). *m*: mean; σ: standard deviation.

	Mn		*Fe*		*Cu*		*Zn*		*As*		*Mo*		*Cd*		*Sb*		*Pb*		*U*		*Global*	
	m	σ	*m*	σ	*m*	σ	*m*	σ	*m*	σ	*m*	σ	*m*	σ	*m*	σ	*m*	σ	*m*	σ	*m*	σ
Dry Season																						
F1	11	4	0	0	2	0	3	1	1	1	20	6	46	13	3	2	0	0	5	3	9	3
F2	34	17	2	1	19	6	19	6	11	5	0	0	22	10	6	3	19	9	26	10	16	6
F3	28	7	16	7	1	0	15	4	62	7	66	17	1	2	38	8	7	5	31	13	26	7
F4	16	19	0	0	6	4	1	2	1	1	37	18	21	26	2	1	0	0	5	3	9	8
F5	11	22	82	8	73	5	63	6	26	10	-23	31	11	29	51	9	75	10	33	27	40	16
Wet Season																						
F1	13	6	0	0	0	2	1	0	0	27	13	22	9	6	3	0	0	14	7	9	4	
F2	61	37	5	3	24	8	13	9	18	6	0	0	33	13	10	2	46	14	41	28	25	12
F3	27	13	17	15	1	1	12	8	64	26	74	36	0	0	44	18	17	12	50	36	31	17
F4	11	18	0	0	11	14	0	1	1	1	58	23	10	21	5	4	0	0	8	6	10	9
F5	-13	54	78	17	64	17	73	17	16	30	-59	61	35	28	35	25	36	23	-13	75	25	35

and Cala Cala Lagoon (Fig. 4.3.1).

4.4.1.1 Major redox species

Cala Cala Lagoon

Sulphate reduction is evidenced by decreasing dissolved sulphate concentrations just below the WSI (Fig. 4.3.5). In addition, reductive dissolution of Fe- and Mn-oxyhydroxides is suggested by the increase of dissolved Fe and Mn concentrations with increasing depth. The shape of the profile of both metals suggests that the active layer for reductive dissolution is situated around 25 cm, where dissolved Mn and Fe reach their maximum (Fig. 4.3.2). The occurrence of sulphate reduction and reductive dissolution of Fe and Mn is supported by the overall increasing ammonium concentration with depth. Because of the scattering and roughly increasing nitrates with depth, denitrification is not evidenced in the Cala Cala Lagoon sediments (Fig. 4.3.5a). On the contrary, nitrate is produced (anoxic nitrification), likely through the reduction of Mn-oxyhydroxides by ammonium [305, 322]. It is therefore possible that little denitrification actually occurs in these sediments while being masked by higher rates of anoxic nitrification; therefore, if occurring at all, denitrification is accessory in comparison with other freshwater lakes (e.g., Lake Haringvliet, [323]). Rapid consumption of sulphate (within the first 5 cm below the WSI) might explain the prevailing OM mineralization pathway, yet low sulphate concentrations in the OLW might explain its rapid consumption.

Denitrification and sulphate reduction are not conclusive OM mineralization pathways. Therefore, we suggest that reductive dissolution of Fe- and Mn-oxyhydroxides is the prevalent pathway in the anoxic sediments of Cala Cala Lagoon, as demonstrated for amorphous ferric oxyhydroxides in anaerobic freshwater and brackish water sediments of the Potomac River Estuary [324].

Below the active layer of reductive dissolution, the decrease of dissolved Fe and Mn indicates removal from pore water and consequent sequestration in the solid phase, which might be attributed to authigenic phases as indicated by Fe and Mn SSP profiles (Fig. 4.4.1), where in the bottom section Mn increases for carbonates and sulphides, while Fe increases for carbonates, suggesting that below the Fe and Mn active layer, Fe might be sequestered by carbonates and Mn by carbonates and/or sulphides (Fig. 4.4.1).

Northern Lake Uru Uru

One important characteristic of this area, and the main difference with southern Lake Uru Uru, is that when the scarcity of precipitation and/or high evaporation rate is extreme, i.e. DS, this area loses its OLW. This is supported by the porosity and water content scattered profiles during this season (Fig. 4.3.1b). The POC and S_{tot} are highly related during the DS (R=0.90) and lesser during the WS (R=0.65), relationship often found in other sediments (e.g., [325]).

The Altiplano area is also characterized by the presence of sulphates, mainly in the form of gypsum ($CaSO_4 \cdot 2H_2O$) and anhydrite ($CaSO_4$), which are important constituents of the Altiplano salars (e.g., Salar de Coipasa and Salar de Uyuni; [239]), and alunite-$KAl_3(SO_4)_2(OH)_6$, which is one of the major constituents of the alteration zones surrounding the Sb mineralization in the Tertiary volcanic rocks of the Bolivian Andes [326]. The increase with depth of dissolved SO_4^{2-} in northern Lake Uru Uru during the DS area can be related to extremely high input of dissolved sulphate originating from the Altiplano salars and alteration zones, which is supported by diffusive fluxes (Table 4.6) showing that sediments are a source for sulphates. In addition, this area is affected by high evaporation rates [245]. These two processes preclude detecting sulphate reduction from the pore water profile, while it is likely that the later OM mineralization pathway actually takes place in these sediments. The control of evaporation-related processes on pore water profiles is further supported by the linear increase of dissolved Cl^- with depth (Fig. 4.3.5b). During the WS an increase in sulphate and chlorine is not observed, probably because of pore water dilution related to increased freshwater input in this season and the consequent percolation of diluted water below the WSI.

The sharp increase of dissolved Fe and Mn just below the WSI during both seasons indicates reductive dissolution of Fe- and Mn-oxyhydroxides. It also suggests the rapid onset of reductive dissolution processes after dry periods. The total (WS) and nearly total (DS) removal of dissolved Fe at depth indicates authigenic precipitation of a phase incorporating Fe, which is not elucidated through SSP (Fig. 4.4.1). No removal of dissolved Mn is observed within the sampling depth, therefore Mn is kept in solution because it probably reaches equilibrium with the particulate phase and/or competes with other cations for sorption on mineral surfaces.

The vertical distribution of Fe and to a lesser extent Mn in the ascorbate fraction (Fig. 4.4.1) suggests that reoxidation of reduced dissolved Fe and lesser Mn in the sediment can be a significant process during periods when this part of the lake is dry, as indicated by Fe (and lesser Mn) oxide precipitation above 20 cm depth, dissolution below 20 cm and precipitation

in the bottom of the profile. This behaviour is not observed in Fe_{asc} profiles during the WS, suggesting that Fe (and lesser Mn) oxides are reoxidized during the DS (Fig. 4.4.1).

Southern Lake Uru Uru

This area has not suffered complete desiccation of the OLW in recent years. Additionally, no relationships are found between the POC and S_{tot} , distinguishing this area from northern Lake Uru Uru. Similarly to the northern part of the lake, this area is influenced, in a lesser extent though, by evaporation/concentration processes, as evidenced by increasing pore water sulphate and chlorine concentrations with depth (Fig. 4.3.5c). However, sulphate reduction just below the WSI for both seasons is suggested by decreasing pore water sulphate concentration in the first centimetre of the sediment.

As shown by the nearly linear and relatively weak concentration gradient of dissolved Mn (more evident in the DS; Fig. 4.3.4), we suggest that the reactive layer for the Mn reductive dissolution proceeds deeper than the bottom of the core. Dissolved Mn production with depth is probably evidence for reductive dissolution of Mn-oxyhydroxides as shown by the overall decrease of the Mn_{asc} profile (Fig. 4.4.1). Additionally, dissolved Mn production might be related to carbonate dilution, as suggested by the decreasing shape of the Mn_{NaOAc} profile (Fig. 4.4.1) and as proposed for the hypersaline Dead Sea, where carbonates were found to be the main source of dissolved Mn [327].

Despite the very low Fe^{2+} concentration and flat profiles in at least the first 5 cm of the sediment, in which Fe-oxyhydroxides account for 22±5% and 31±18% of the total Fe during the DS and WS respectively (Fe_{asc} digestion; Fig. 4.4.1), the production of dissolved Fe at depth observed in both seasons may suggests that reductive dissolution of Fe-oxyhydroxides is occurring in these sediments. This is supported by the peak of Fe in pore water (at around 20-cm depth) during the DS, increasing pore water Fe for the WS and decreasing concentration of Fe_{asc} with depth. The flat profiles of pore water Fe observed below the WSI could be explained by biological uptake of dissolved Fe due to the density of aquatic plants (e.g., totora, ruppia, chara) that characterize the southern part of the lake. Indeed, it has been experimentally demonstrated that totora successfully removes this metal [328, 329]. In addition to reductive dissolution, the observed decrease of Fe_{asc} contribution with depth for both seasons can be explained by the ageing of these minerals (then less and less extracted by the ascorbate solution with increasing depth; Fig. 4.4.1).

The observed differences in redox species behaviour between the northern and the southern

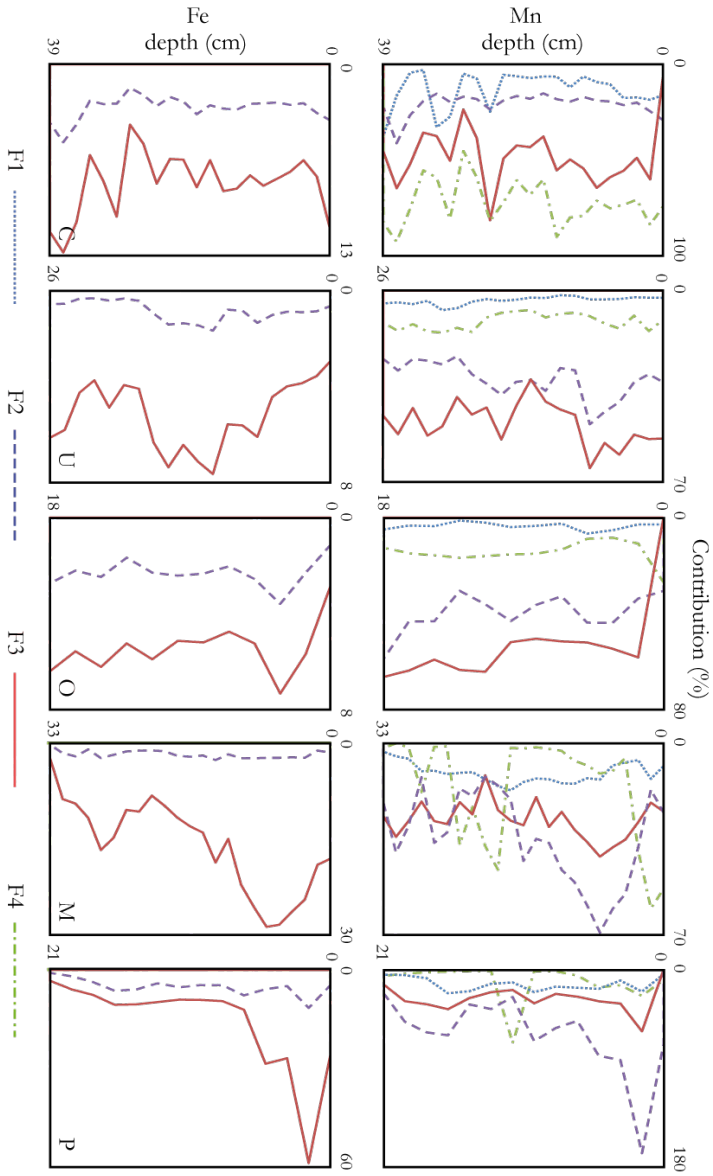

Figure 4.4.1: Single extractions results for Mn (top) and Fe (bottom). Depth (cm) X axis and concentration ($\mu g\, g^{-1}$) Y axis.

part of Lake Uru Uru might be explained by the fact that the northern area has been subjected to intermittent sediment drying (i.e., disappearance of the OLW) while the southern part of the lake has not suffered complete desiccation in recent years. In southern Lake Uru Uru, nitrate and ammonium pore water profiles are difficult to interpret in terms of redox processes as it seems that concentration/evaporation mask the denitrification and ammonium production that are likely to occur jointly with sulphate reduction and reductive dissolution of Fe- and Mn-oxyhydroxides.

4.4.2 Trace metal(loid) behaviour during early diagenesis

Overall, trace metals and metalloids in lacustrine sediments from the Eastern Andes Cordillera and Altiplano of Bolivia are affected by multiple and complex early diagenetic processes. For all situations, dissolved trace metal(loid) concentrations are variable, with global values of about DL-125 nM (Cu), DL-1,309 nM (Zn), 1-28 µM (As), DL-306 nM (Mo), DL-2.3 nM (Cd), DL-0.5 µM (Sb), DL-9.1 nM (Pb) and DL-432 nM (U) (Table 4.5).

Dissolved element pore water profiles (Figs. 4.3.2, 4.3.3 and 4.3.4), major redox species (Fig. 4.3.5), diffusive fluxes (Table 4.6), solid state partitioning (Figs. 4.4.1 and 4.4.2) and mineralogical observations (Fig. 4.4.3), allowed us to interpret metal(loid) behaviour within different environments in the Bolivian Altiplano. These behaviours evidence changes between Cala Cala Lagoon and Lake Uru Uru. Lake Uru Uru shows important differences between its southern and northern parts and between the DS and WS.

4.4.2.1 Cala Cala Lagoon

It seems that evaporation/precipitation rates play a preponderant role in metal(loid) behaviour from the Altiplano, therefore, determination coefficients for dissolved metal(loid)s and dissolved Cl^- and SO_4^{2-} were calculated (Table 4.10). Low determination coefficients show that evaporation/precipitation rates do not exert an important role in dissolved metal(loid) behaviour from this lagoon, therefore Cala Cala is not significantly influenced by evaporation/precipitation rates.

Some dissolved metal(loid)s (Mo, Cd, Sb, Pb & U) are produced close to the WSI, i.e. within the sulphate reduction zone and well above the active layers of reductive dissolution of Fe- and Mn-oxyhydroxides, suggesting that these trace elements are not released from these oxides.

Dissolved Zn, Cd, Sb, Pb and U peaks occur at 5.5 cm depth, implying that these are

released from the same carrier phase at this depth. One suggestion might be related to changes in mineralogy, yet we have no mineralogical data available from this depth. The SSP does not provide enough evidence to determine the particular phase source and we cannot assume destruction of carbonates with depth, because below the WSI, the PIC plot shows values closer to the DL (Fig. 4.3.1a). According to figure 4.3.1a, high OM contents are observed between 5 and 9 cm depth, the same depth as the dissolved Zn, Cd, Sb, Pb and U peak. As suggested by Tessier (1993) [84] and Tessier *et al.* (1996) [98], OM (together with Fe- and Mn-oxyhydroxides) can be considered to be the dominant phases of metal(loid) biogeochemistry in aqueous systems, suggesting that the carrier phase of metal(loids) is likely OM, from which MTEs are released upon mineralization.

At the bottom of the core (35 cm depth), a peak of dissolved Cu, Zn, As, Cd & Pb is observed. Nevertheless, at this depth the OM content (1.64%) is closer to the minimum values for the Cala Cala Lagoon sediments (1.45%), therefore OM is not the carrier phase for these elements. At this depth, a decrease in grain size is observed; the average grain size within the Cala Cala Lagoon corresponds to 8% clay, 15% silt and 77% sand, and from 28 to 35 cm depth the grain size decreases (11% clay, 21% silt & 69% sand), in addition at 28 cm the water content is least (31%) increasing again at 35 cm depth (42%). To explain metal(loid) release at the bottom of the core we assume that clays and silt contain more metal(loid)s than sand and an abrupt increase of water content in the sediment might involve metal(loid) release. Therefore, at this depth trace element release is mostly related to the source of metal(loid)s and is not a consequence of early diagenetic processes.

With the exception of As, most metal(loid)s are removed from the pore water, suggesting that these are precipitating within the Cala Cala Lagoon sediments. Dissolved Cu (and less obviously Zn) is removed in the first centimetre below the WSI, which might indicate that Cu is sequestrated through the authigenic precipitation of its distinct sulphides as reported for other freshwater sediments (e.g., [312]). In addition, Cu affinity to biogenic material is very well known [57], release of Cu from OM likely takes place, however at a lower rate than removal, therefore, we observe a decreasing gradient. Zinc, in a lesser extent though, shows a similar behaviour, this element also being characterized by high affinity to OM.

Uranium is known to be associated with OM and carbonates, yet within the Cala Cala Lagoon, relationships between dissolved U and particulate C_{tot}, POC and PIC are not statistically significant; nevertheless U_{NaOAc} and dissolved U are moderately correlated (R^2=0.57). This might support the hypothesis that production of dissolved U just below the WSI (likely

under the form of $[UO_2(CO_3)_3^{4-}]$) could be explained by U release into pore water from OM during mineralization and/or release from dissolving carbonates. Association of U with OM was previously reported in other freshwater sediments (e.g., [207]). Nearly complete removal of U from pore water around 15 cm depth is in agreement with the insoluble nature and very strong affinity of this element to binding sites present on the surface of particles [330]. The removal of U from the dissolved phase, which means the reduction of U(VI) into U(IV), is observed at the depth where sulphate reduction is occurring (Fig. 4.3.2). Therefore, as suggested by [331], U(VI) is likely reduced by HS^- released in the pore water during sulphate reduction. Additionally, U(VI) could also be reduced to U(IV) through bacterial enzymatic reduction [332] coupled to OM oxidation, with U acting as an electron acceptor. Indeed, some authors [333] have shown that sulphate reduction microorganisms can effectively reduce U(VI). Therefore, the concentration-profile of dissolved U suggests that sulphate reduction microorganisms control U release into pore water and subsequent adsorption onto particulates.

Solid phase profiles show little variability with depth (Cu 49±7; Zn 121±10; As 51±8; Mo 1.2±0.2; Cd 0.5±0.2; Sb 12±2; Pb 107±24; U 4.3±0.8) and these seem not to be related with the dissolved phase (Fig. 4.3.2). Nevertheless, SSP profiles show that some metal(loid)s are sequestered by easily extractable phases (mainly carbonates and Fe- and Mn-oxyhydroxides). For instance, 74% Cd, 52% As, 43% U, 35% Mo, 24% Sb, 15% Pb, 12% Zn & 9% of Cu are characterized by high potential mobility. Most of these metal(loid)s are associated with Fe- and Mn-oxyhydroxides and carbonates (Fig. 4.4.2). As previously determined, metal(loid)s are not released from Fe- and Mn-oxyhydroxides, which might be explained by the fact that Fe- and Mn-oxyhydroxides, carrying significant amounts of metal(loid)s, are of detritical origin and do not undergo reductive dissolution in the sediment (while nevertheless being extracted by ascorbate leaching). Fe- and Mn-oxyhydroxides undergoing reductive dissolution do not contain significant amounts of metals and could originate from precipitation in the OLW and therefore be more reactive than the detritical ones. Discarding Fe- and Mn-oxyhydroxides, the main sources of dissolved metal(loid)s might be carbonates, OM/sulphides, and exchangeable fractions. Despite the fact that Devonian to Ordovician sedimentary bedrocks, with intercalations rich in Ca-carbonates, constitute the most abundant outcrops in the Eastern Andes Cordillera within the study area [315], no relationships are found between dissolved metal(loid)s and particulate Ca and C_{tot}, COP and PIC, thus evidencing that within the Cala Cala Lagoon, Ca-carbonates do not exert an important role in metal(loid) release into the dissolved phase. Metal(loid)s can be mainly released by OM mineralization/sulphides and/or exchangeable phases, these repre-

senting the lower percentages in SSP (11±2% & 7±4% respectively; Fig. 4.4.2). Despite the fact that these fractions represent the lowest contributions, we suggest that OM mineralization, sulphides and exchangeable phases control early diagenesis processes within this lagoon. This does not discard contributions from carbonates and/or Fe- and Mn-oxyhydroxides, but only suggests that the most abundant fractions do not contribute significantly to the dissolved elements of this environment.

4.4.2.2 Lake Uru Uru

Sediments from this Altiplanic lake are mainly constituted by calcite ($CaCO_3$), quartz (SiO_2) and clays, as demonstrated by XRD (not shown). Lake Uru Uru shows important differences compared to the Cala Cala Lagoon, and moreover, between its northern and southern areas. The fact that the northern area has been subjected to intermittent disappearance of the OLW, has enormously influenced dissolved metal(loid) behaviour within pore water, which is not evidenced in southern Lake Uru Uru. The main differences between Cala Cala Lagoon and Lake Uru Uru, and between northern and southern Lake Uru Uru areas during the DS and WS are discussed below.

Northern Lake Uru Uru

During the DS only Mn, Fe and As show positive concentration gradients just below the WSI (Table 4.6), while the other metal(loid)s show concentrations below the DL. These very low concentrations most likely picture the effect of sediment drying during the DS. To support the idea that dissolved metal(loid) behaviour is strongly influenced by evaporation rates, especially in this area and during the DS, we calculated determination coefficients (R^2) between dissolved Cl^- and SO_4^{2-} and dissolved metal(loid)s (Table 4.10) and as suggested, during the DS Cu, Zn, Mo, Sb and U show a high affinity with dissolved Cl^- and SO_4^{2-}, Cd and Pb show moderate relationships, whereas Mn, Fe and As exhibit very low associations with these dissolved phases. During the WS, the dissolved concentration of metal(loid)s in the BW and first centimetres of pore water are higher than in the DS, probably the result of ongoing redox processes that release previously particulate-associated trace metal(loid)s into the dissolved phase. Determination coefficients show that Cu, As, Mo, Sb and U are strongly related to dissolved Cl^- and SO_4^{2-}, Mn, Fe and Cd moderately and Zn and Pb exhibit very low relationships.

Studied metal(loid)s with more than 1 oxidation state (Cu, Mo, Sb and U) are strongly associated with dissolved Cl^- and SO_4^{2-} during both the DS and WS, whereas $Zn^{(2+)}$, $Cd^{(2+)}$

Table 4.10: Determination coefficients between dissolved Cl^-, SO_4^{2-} and dissolved metal(loid)s. C: Cala Cala Lagoon WS; U: northern Lake Uru Uru DS; O: northern Lake Uru Uru WS; M: southern Lake Uru Uru DS; P: southern Lake Uru Uru WS.

Site	R^2	*Mn*	*Fe*	*Cu*	*Zn*	*As*	*Mo*	*Cd*	*Sb*	*Pb*	*U*
C	Cl^-	*0.24*	*0.07*	*0.11*	*0.04*	*0.25*	*0.75*	*0.19*	*0.38*	*0.10*	*0.05*
	SO_4^{2-}	*0.33*	*0.21*	*0.50*	*0.00*	*0.11*	*0.21*	*0.02*	*0.07*	*0.00*	*0.01*
U	Cl^-	*0.32*	*0.42*	*0.73*	*0.89*	*0.10*	*0.83*	*0.62*	*0.89*	*0.56*	*0.74*
	SO_4^{2-}	*0.42*	*0.23*	*0.71*	*0.88*	*0.08*	*0.78*	*0.48*	*0.83*	*0.53*	*0.74*
O	Cl^-	*0.43*	*0.55*	*0.85*	*0.16*	*0.77*	*0.98*	*0.65*	*0.87*	*0.01*	*0.68*
	SO_4^{2-}	*0.58*	*0.63*	*0.94*	*0.30*	*0.86*	*0.93*	*0.51*	*0.96*	*0.03*	*0.82*
M	Cl^-	*0.86*	*0.40*	*0.75*	*0.78*	*0.39*	*0.75*	*0.84*	*0.72*	*0.71*	*0.79*
	SO_4^{2-}	*0.80*	*0.37*	*0.71*	*0.72*	*0.40*	*0.76*	*0.85*	*0.70*	*0.67*	*0.79*
P	Cl^-	*0.72*	*0.67*	*0.24*	*0.02*	*0.03*	*0.00*	*0.04*	*0.01*	*0.03*	*0.17*
	SO_4^{2-}	*0.06*	*0.39*	*0.15*	*0.01*	*0.59*	*0.08*	*0.19*	*0.42*	*0.01*	*0.01*

and $Pb^{(2+,\ 4+)}$ diminish or remain constant and As increases between both seasons. This means that Cu, Mo, Sb and U behaviour is mostly associated with evaporation/precipitation rates and during the WS, decreasing dissolved concentration just below the WSI (Cu, Mo, Cd) might not be solely reflecting sorption and/or co-precipitation with authigenic minerals, but also mirror the effect of temporal variability in environmental conditions.

Regarding early diagenetic processes, pore water profiles help to elucidate that when conditions become less dry, the sediments are submitted to the onset of redox processes (and anoxia) with Fe- and Mn-oxyhydroxides (and associated As) very responsive to new redox conditions. Indeed, as conditions get more reducing, As is reduced from As(V) to As(III) and is released into its dissolved form as arsenite (more toxic and soluble than arsenate and stable at reducing conditions [334]) close to the WSI during both seasons; moreover, in the WS the release of Zn, As, Cd and Pb concomitantly with that of Mn and Fe indicates that these trace elements are released as a consequence of the destruction of their carrier phases, Fe- and Mn-oxyhydroxides and OM.

While OLW evaporates, the pore water becomes more and more concentrated in elements, and these elements likely sorbe and/or co-precipitate with mineral phases, leaving the pore water exhausted in metal(loid)s. Higher dissolved concentrations in the bottom part of the core during the DS might reflect the fact that deeper redox conditions (partial or total anoxia) are preserved, keeping reactions going and keeping (part) of trace metal(loid)s in the dissolved phase. The removal of Cu from pore water in the first cm of sediment in the WS, just after the DS, is explained by the fact that pore water is so Cu-depleted, that when input of dissolved Cu into the OLW and therefore to the WSI increases (due to increased water fluxes originating

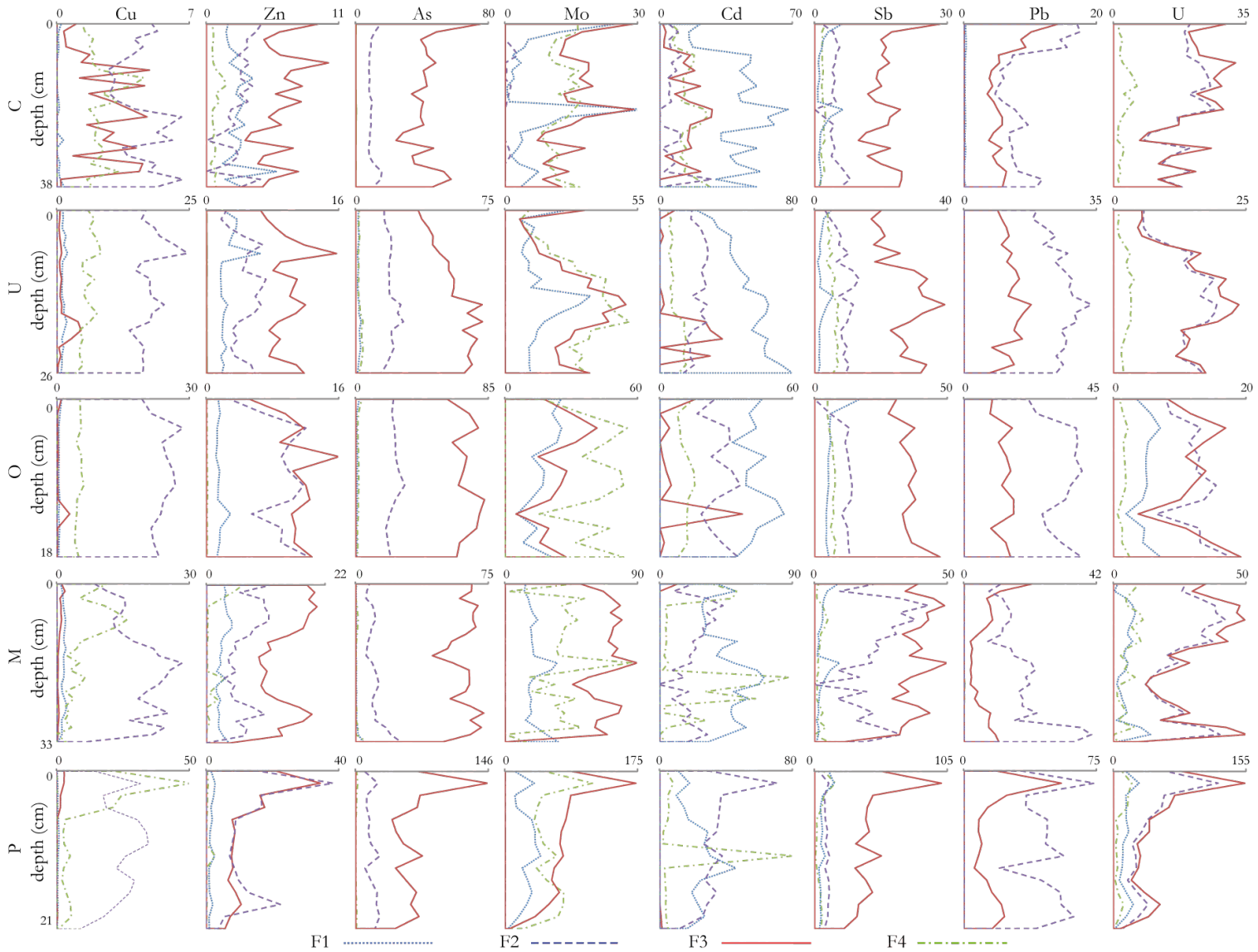

Figure 4.4.2: Solid state partitioning of Cala Cala Lagoon and Lake Uru Uru. Depth X axis, contribution (%) Y axis. C: Cala Cala Lagoon (O-39 cm depth); U: northern Lake Uru Uru, DS (0-26 cm depth); O: northern Lake Uru Uru, WS (0-18 cm depth); M: southern Lake Uru Uru, DS (33 cm depth); P: southern Lake Uru Uru, WS (21 cm depth).

from increased rainfall), the sediments become a sink for dissolved Cu. Probably, the same process occurs for Mo and to a lesser extent Sb and U.

Southern Lake Uru Uru

The main difference with respect to the northern area is that southern Lake Uru Uru has not been affected by intermittent OLW disappearance, and therefore the dissolved metal(loid) concentration in the BW and the first centimetres of sediment are comparable between the DS and WS. This might be attributed to a lesser control of evaporation on redox processes. In addition, in comparison to the northern area, sulphate reduction is not hidden by evaporation and occurs just below the WSI. In table 4.10, determination coefficients between dissolved metal(loid)s and dissolved Cl^- and SO_4^{2-} suggest that southern Lake Uru Uru is influenced by evaporation only during the DS. Therefore, evaporation probably affects metal(loid) behaviour, yet this influence is minor in the southern area and is only evidenced during the DS, in which most dissolved metal(loid)s (excepting Mn, Fe and As) are influenced by evaporation (Table 4.10).

In previous sections (see section 4.3.2.2) we established that the active layer of reductive dissolution of Mn oxides is probably located below the bottom of the core and the active Fe reductive dissolution layer is situated around 20 cm depth. Dissolved As is released into the pore water at shallower depth, and therefore this release cannot be attributed to the direct destruction of Fe-oxyhydroxides. However, Fe- and Mn-oxyhydroxides and OM obviously play an important role in the post-depositional redistribution of metalloids such as As. Particulate As is probably provided to the WSI associated with Fe- and Mn-oxyhydroxides [335, 336] and phytoplankton debris [337]. Some authors [338, 339] have reported from laboratory experiments that under reducing conditions part of the As bound to Fe-oxyhydroxides is released before Fe implying reductive desorption from Fe-oxyhydroxides rather than reductive dissolution. Accordingly, the shallow release of As in the southern part of Lake Uru Uru sediments is attributed to both reductive desorption from Fe-oxyhydroxides and mobilization from OM upon oxidation. Below 8 cm depth, dissolved As starts to precipitate. At this depth, As_{NaOAc} contribution starts to increase (from 8±2% to 14±5%; Fig. 4.4.2), in addition framboidal sulphides with traces of As were determined through SEM-EDS and microprobe analysis (63.8% S, 35.9% Fe and 0.2% As average; Fig. 4.4.3). The association of As with authigenic sulphides suggests that As solubility is controlled by sulphide minerals as previously reported for other systems [340, 341] and additionally, As_{NaOAc} profiles indicate precipitation into calcareous phases below 8 cm depth.

The peak of Sb at depth (same depth as Fe) indicates a contribution from reductive dissolution of Fe-oxyhydroxides, as previously observed in other freshwater lakes [342]. At depth, and similarly to As, Fe-sulphides are likely controlling Sb removal from pore water and subsequent sequestration into the sediments. As reported for other freshwater lakes [342] removal of Sb is less efficient as pore water Sb concentrations remain relatively high, this may be explained by the fact that under the anoxic conditions prevailing in the studied sediments, thioantimonite complexes (HSb_2S_5 and $Sb_2S_6^{2-}$) are produced [343]. These anionic S-coordinated complexes tend to condense to form large polymeric molecules [344] stabilizing Sb in the pore water and preventing part of its removal with the sulphide phase.

Metals partly controlled by evaporation, also show behaviour driven by diagenesis. Dissolved Cu release is strongly related to OM degradation, this is evidenced by the strong relationship between POC and $Cu_{H_2O_2}$ throughout the core (R^2=0.82; confirming a high affinity of Cu to OM as previously observed [57]). In addition, nearly constant concentrations of dissolved Cu below 10 cm depth occur together with a marked decrease of $Cu_{H_2O_2}$ (8.2±4.3% to 2.6±1.5%; Fig. 4.4.2), implying that Cu is released from OM material but not sequestrated within the particulate sulphide phase. Cu forms only weak chloride or sulphate complexes, yet inorganic species of Cu in natural waters are dominated by carbonate complexes [296], suggesting that dissolved Cu below 10 cm depth might be associated with dissolved carbonates. Dissolved Zn and Pb behave similarly to dissolved Cu, yet Pb is removed completely below 20 cm depth. Statistical relationships between POC and $Zn/Pb_{H_2O_2}$ are not significant (R^2_{Zn} =0.16; R^2_{Pb} =0.05), additionally, particulated Zn and Pb are mostly associated with the residual fraction (Zn: 74±8%; Pb: 75±10%), and less with Fe- and Mn-oxyhydroxides (Zn: 15±4%; Pb: 7±5%) and carbonates (Zn: 7±3%; Pb: 19±9%). In the Eastern Andes Cordillera, Zn and Pb deposits are related to the Pb-Zn belt, being hosted mainly by carbonaceous sedimentary rocks [217]. As shown by the SSP, Zn and Pb are not highly mobile elements within the solid phase during the DS, suggesting that both are mostly from detrital origin. The observed increase of dissolved Cu (and Zn) at depth very close to the layer where Fe- and Mn-oxyhydroxides are reductively dissolved, points to the possible release of Cu (and Zn) from these mineral phases, which is not observed for dissolved Pb.

Dissolved Mo and Cd exhibit similar pore water profiles in the DS. The main characteristic of these elements is that they are highly reactive according to their particulate partitioning. For instance, Cd is significantly present in all fractions except in Fe- and Mn-oxyhydroxides (F1: 46±13%; F2: 22±10%; F3: 1±2%; F4: 21±26%; F5: 11±29%) and some samples exhibit more

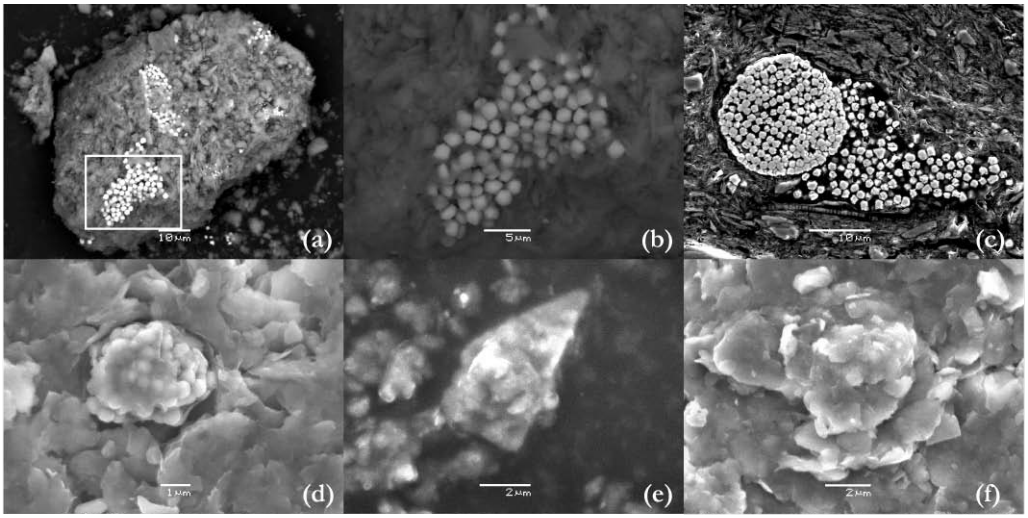

Northern Lake Uru Uru sulphides (%)

	S	Fe	Co	Ni	Cu	Zn	As	Sn	Sb	Pb
mean	64.9	34.8	0.0	0.0	0.0	0.0	0.2	0.0	0.0	0.0
median	65.4	34.2	0.0	0.0	0.0	0.0	0.2	0.0	0.0	0.0
max	66.5	42.7	0.0	0.0	0.1	0.0	0.3	0.0	0.0	0.0
min	57.0	33.3	0.0	0.0	0.0	0.0	0.0	0.0	0.0	0.0

Southern Lake Uru Uru sulphides (%)

	S	Fe	Co	Ni	Cu	Zn	As	Sn	Sb	Pb
mean	63.8	35.9	0.0	0.0	0.0	0.0	0.2	0.0	0.0	0.0
median	64.0	35.6	0.0	0.0	0.0	0.0	0.2	0.0	0.0	0.0
max	67.2	39.9	0.0	0.0	0.1	0.0	0.5	0.0	0.0	0.0
min	59.7	32.7	0.0	0.0	0.0	0.0	0.1	0.0	0.0	0.0

Figure 4.4.3: Authigenic sulphides and silicate to clayey particles associated with metal(loid)s in northern and southern Lake Uru Uru areas during DS. (a), (b) and (c) framboidal sulphides from northern Lake Uru Uru area, (a) particle appearance; (b) zoom from (a), framboidal sulphide; (c) framboidal sulphide with As traces (microprobe determination); (d), (e), (f) southern Lake Uru Uru area, (d) framboidal sulphide in silicate matrix; (e) chalcopyrite particle within silicate matrix; (f) silicate to clay particle with trace metal(loid)s.

than 100% extractability. Extraction of Mo was on average higher than 100% (123±31%) and predominately associated with Fe- and Mn-oxyhydroxides (F3: 66±17%). These results clearly suggest insufficient selectivity of the reagents used to extract Mo and Cd from the four targeted fractions, and additionally that Mo (and to a lesser extent Cd) is very reactive and potentially highly mobile in sediments, as suggested by Audry *et al.* (2006b) [302] when more than 100% of the solid phase is extracted by chemical reagents. Within this context, numerous studies have determined that the exchangeable fraction (F1) is overestimated by $MgCl_2$, particularly in the case of Cd (e.g., [185, 209, 345]). Mo might also be overestimated by this reagent, shown by the fact that $MgCl_2$ values were higher than NaOAc (carbonate) extraction.

Dissolved U behaves distinctively to the other metal(loid)s from this environment, increasing in concentration with depth. Additionally, dissolved U is clearly associated with dissolved Mn (R^2=0.72), suggesting that precipitation is probably occurring below the bottom of the core, associated with the Mn reactive layer. Indeed, U release into solution has been related to the reduction of Mn-oxides [346, 347].

During the WS, evaporation exerts less influence on dissolved metal(loid) behaviour and does not mask the diagenetic redistribution of trace elements (Table 4.10).

With the exception of Cu, Cd and Pb, and as suggested for other freshwater environments [309], the decreasing profile of Fe_{asc} (and lesser Mn_{asc}; Fig. 4.4.1) together with decreasing MTE_{asc} contribution profiles with increasing depth (Fig. 4.4.2), implies that metal(loid)s are significantly associated with reductive dissolution of Fe^{3+} (and to a lesser degree Mn^{4+}) in the sediment. Additionally, the incomplete Fe_{asc} (and Mn_{asc}) consumption with depth indicates slow dissolution kinetics despite the reducing conditions [309]. Therefore, we suggest that generally in southern Lake Uru Uru during the WS, MTEs are released by slow dissolution kinetics of Fe- and/or Mn-oxyhydroxide reductive dissolution.

Dissolved As and Sb show positive gradients just below the WSI (Table 4.6 and Fig. 4.3.4) and both are strongly related within the dissolved phase (R^2=0.80). Particulated As and Sb do not show the same profile (Fig. 4.3.4), suggesting that these metalloids are probably carried and released by the same phase. Yet at depth, Sb is mainly associated with the residual fraction, as suggested by the SSP, where F5 increases dramatically with depth (from 3±2 to 15±6 $\mu g \cdot g^{-1}$, however in terms of contribution the increase is not so dramatic from 31±27% to 49±9%, not shown). During the DS we suggest that As and Sb are probably released by both reductive desorption from Fe-oxyhydroxides and mobilization from OM upon oxidation, which might also occur during the WS, because the maximum concentration for these trace

elements occurs much shallower (7.5 and 12 cm depth) than the depth of Fe and Mn reductive dissolution, located below the bottom of the core (21 cm). Despite this fact and based on the suggestion of Canavan *et al.* (2007) [309] (see above), we also propose that the decreasing As_{asc} and Sb_{asc} contribution with depth (Fig. 4.4.2) must be linked to the reductive dissolution of Fe- and Mn-oxyhydroxides. We suggest that the same process takes place for dissolved Mo and U, which also show a positive gradient just below the WSI. In the solid fraction, particulated Mo_{asc} and U_{asc} are strongly related (R^2=0.93). Additionally, both metals change significantly SSP during the WS, meaning that they are potentially more mobile than during the DS. Like As and Sb, both metals show decreasing Mo_{asc} and U_{asc} profiles with increasing depth (Fig. 4.4.2), therefore the oxidized solid fraction of Mo and U might be released by reductive dissolution of Fe- and Mn-oxyhydroxides (see explanation above).

Dissolved Zn and Pb are strongly related within the dissolved phase (R^2=0.77) and also show decreasing MTE_{asc} profiles with increasing depth, implying that both are released from the same Fe- and/or Mn-oxyhydroxide during reductive dissolution. Additionally, both metals are clearly associated with carbonates (Fig. 4.4.2). Low reactivity was established for these elements during the DS and this characteristic was attributed to a probable detrital origin (associated with the Bolivian Pb-Zn belt). During this season, particulate Zn shows a similar SSP than during the DS (F5: 73±17% > F2: 13±9% > F3: 12±8%), while Pb changes its SSP significantly (F2: 46±14% > F5: 36±23% > F3: 17±12%) being mostly related to carbonates. We suggest that both elements are released by Fe- and/or Mn-oxyhydroxides reductive dissolution, yet Pb would potentially be more mobile than Zn under reductive and acidic conditions.

Dissolved Cu behaves differently from the other dissolved metal(loid)s, showing a negative gradient just below the WSI (Table 4.6; probably explained by the same reasons suggested for the northern area, without being totally removed from pore water after the DS) and is not associated with Fe- and Mn-oxyhydroxides (values close to DL). As observed during the DS, in WS $Cu_{H_2O_2}$ and POC are related (R^2=0.74). Three cm below the WSI the $Cu_{H_2O_2}$ contribution decreases markedly (from 29±14% to 3±2%; Fig. 4.4.2) and simultaneously the dissolved Cu concentration increases (Fig. 4.3.4). If we assume a strong relationship between Cu and OM (as during the DS and as proposed by some authors [57]), we might suggest that during the WS, dissolved Cu is mainly controlled by OM mineralization in the top of the profile, yet dissolution of Cu below 3 cm depth is controlled by carbonates, as suggested by the indirect relationship between Cu_{NaOAc} and dissolved Cu profiles (Figs. 4.3.4 and 4.4.2).

Dissolved Cd shows a positive gradient just below the WSI (Table 4.6). It is not related to Fe- and Mn-oxyhydroxides and the dissolved and particulate fractions behave differently from the other studied metal(loid)s (Figs. 4.3.4 and 4.4.2). This is probably related to the high potential mobility of Cd (F1 22±9%; F2 33±13; F4 10±21%) in this environment and to the fact that Cd is not controlled by Fe- and/or Mn-oxyhydroxides, thus differing from the general behaviour of metal(loid)s within this system. As the main contribution of Cd is not associated with the crystalline structure of minerals (but also weakly sorbed onto exchangeable, carbonates and/or OM/sulphides), we suggest that any environmental change might involve variations in Cd behaviour, for instance release in the top of the profile might be related to OM mineralization as observed in estuarine sediments [302] and freshwater environments [309], or dissolved Cd release might be associated with carbonate dissolution, as observed in the Dead Sea [327].

4.4.2.3 Conceptual model of dissolved metal(loid) behaviour

Based on all data from the Cala Cala Lagoon and Lake Uru Uru and the effects of seasonal changes in dissolved and solid phases, we propose a conceptual model to explain early diagenetic processes in the lakes of the Eastern Andes Cordillera and Altiplano of Bolivia (Fig.4.4.4).

In these models we stress the influence of the WS in metalloid behaviour and changes in their availability when reducing conditions are caused by precipitation during the WS.

4.4.3 Metal sequestration and mobility of sediments from the Cala Cala Lagoon and Lake Uru Uru

In general, lacustrine sediments from the Altiplano of Oruro show that they are affected by multiple and complex early diagenetic processes (Figs. 4.4.4). Reactivity and mobility of metal(loid)s were inferred from (1) the most important sources of dissolved metal(loid)s and (2) the contribution of reactive fractions (F1-F2-F3-F4-F5) into the TMC.

Our work allowed us to determine the solid state mean mobility (Table 4.11) through single selective chemical digestions. Considering that within this region Fe is not highly reactive (13±10%), this is explained by the fact that the ascorbate leaching was designed to extract the most reactive Fe-oxyhydroxide fraction (amorphous oxides) [205, 206, 302], and within the Cala Cala Lagoon sediments Fe_{asc} represents 8±2%, in northern Lake Uru Uru 5±1% in the DS and 6±1% in the WS, whereas in southern Lake Uru Uru it represents 16±7% in the DS and

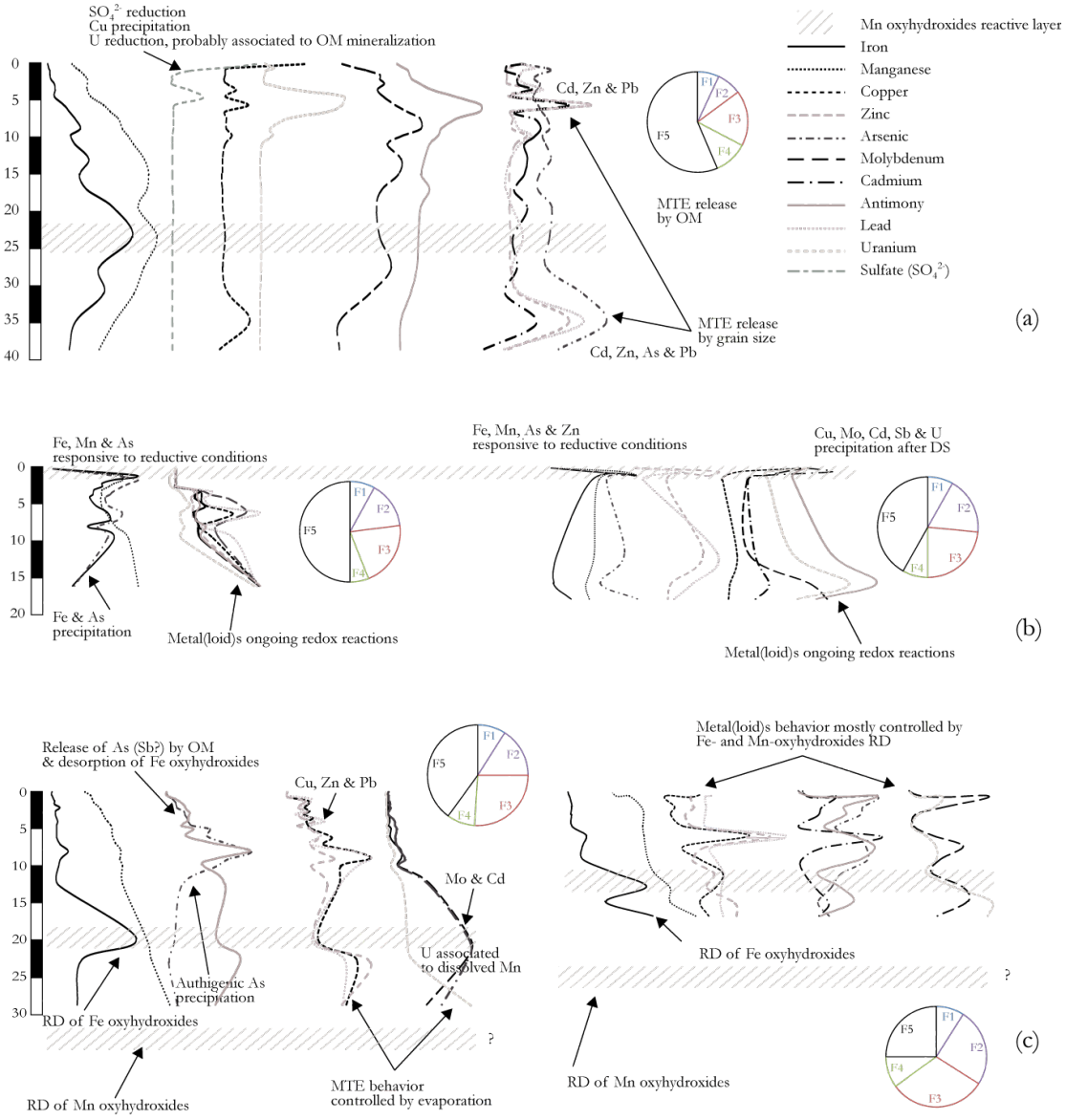

Figure 4.4.4: Schematic conceptual model of early diagenetic processes within Bolivian Altiplano lacustrine environments. (a) Cala Cala Lagoon sediments during WS; (b) northern Lake Uru Uru; (c) southern Lake Uru Uru. RD: reductive dissolution.

17±15% in the WS. This allows us to suggest that about 89±3%, 93±2% and 80±13% of the Fe oxides present in the Cala Cala Lagoon, northern and southern Lake Uru Uru sediments have a stability close to goethite and hematite as suggested by Audry *et al.* (2006b) [302] for poorly reactive sediments (Gironde Estuary). Whereas, Mn is one of the most mobile redox species achieving an average of 113±38% extractability within all sediment samples (Table 4.11). More than 100% of Mn extraction has been reported in literature [178, 184, 348] and attributed to high potential Mn mobility [184].

Among trace metal(loid)s, the most potentially mobile species in sediments from the Altiplano region are Mo (90%), Cd (82%), As (76%), U (56%) and Sb (45%), while the less mobile species are Cu (24%), Zn (24%) and Pb (34%). As shown in the previous sections, trace metal(loid) behaviour is very responsive to the WS and reductive conditions caused by an increase in precipitation, therefore changes in redox conditions during the DS and WS play a preponderant role in trace metal(loid) mobility in Lake Uru Uru.

4.4.3.1 Metal sequestration and environmental assessment perspectives

Solid state partitioning confirms some suggestions that we made to explain trace element behaviour during early diagenetic processes. Through the SSP we prove that particulated Fe is less reactive than Mn, yet dissolved elements are influenced by Fe- and Mn-oxyhydroxide reductive dissolution when the WS causes more reductive conditions and anoxia. At our reference site, Cala Cala Lagoon, we cannot demonstrate that metal(loid)s are released from Fe- and/or Mn-oxyhydroxides, however Mn exhibits the highest SSP for this element (154±31%), showing that Mn is naturally (not anthropogenically) available in the Altiplano.

Cala Cala Lagoon sediments are anoxic and are characterized by a high demand of electron acceptors for OM mineralization and at this site early diagenetic processes are not hidden by evaporation/precipitation rates as in northern Lake Uru Uru. Despite the fact that pore water exhibits the highest mean concentration for dissolved Fe, Mn, Cu, Zn, Pb and U, the solid fraction profiles, coarser grain size, SSP and dissolved metal(loid) behaviour, allow us to confirm that this site is not disturbed by anthropogenic activities, as suggested by Tapia *et al.* (2011a) [315] and that higher concentration in pore water is a consequence of the Cala Cala Lagoon location, closer to one of the most mineralized areas in the world [217, 315]. We were not able to determine if seasonal changes exert some influence on metal(loid) behaviour within this environment, yet we can confirm that anthropogenic influence is minimal.

In the case of Lake Uru Uru, we prove that metal(loid)s within sediments from the northern

Table 4.11: Global solid state partitioning of Altiplanic sediments. F1: exchangeable; F2: carbonates; F3: Fe- and Mn-oxyhydroxides; F4: sulphides and/or OM; F5=TMC-(F1+F2+F3+F4), negative values of F5 were obtained when single digestions addition exceeds TMC because of selectivity problems of the reagents used. *m:* mean; σ: standard deviation.

	Mn		*Fe*		*Cu*		*Zn*		*As*		*Mo*		*Cd*		*Sb*		*Pb*		*U*		*Global*	
	m	σ	*m*	σ	*m*	σ	*m*	σ	*m*	σ	*m*	σ	*m*	σ	*m*	σ	*m*	σ	*m*	σ	*m*	σ
F1	*9*	*7*	*0*	*0*	*1*	*1*	*2*	*1*	*1*	*1*	*16*	*11*	*42*	*16*	*3*	*3*	*0*	*0*	*5*	*5*	*7*	*4*
F2	*35*	*21*	*2*	*2*	*16*	*9*	*10*	*8*	*16*	*7*	*0*	*0*	*21*	*12*	*7*	*4*	*24*	*14*	*22*	*16*	*8*	*3*
F3	*40*	*16*	*10*	*8*	*1*	*1*	*11*	*5*	*58*	*16*	*41*	*30*	*5*	*9*	*31*	*13*	*10*	*7*	*25*	*20*	*18*	*6*
F4	*28*	*28*	*0*	*0*	*6*	*6*	*1*	*1*	*1*	*1*	*33*	*21*	*14*	*16*	*4*	*3*	*0*	*0*	*4*	*4*	*11*	*2*
F5	*-13*	*38*	*87*	*10*	*76*	*12*	*77*	*12*	*25*	*21*	*10*	*54*	*17*	*27*	*54*	*18*	*66*	*20*	*44*	*43*	*57*	*11*

area are potentially less available and mobile than in the southern area, yet both are more reactive in comparison to the Cala Cala Lagoon sediments. Sulphate reduction is hidden in the northern area during both seasons by the evaporation effect, yet an increase in precipitation during the WS implies the return of reduced conditions, responsible of releasing metal(loid)s to the pore water and possibly to the OLW driven by Fe- and Mn-oxyhydroxide reductive dissolution. Metal(loid) behaviour, in both dissolved and solid fractions is highly affected by an increase in precipitation. All these findings allow us to propose that this area is potentially harmful during the WS and very reduced conditions caused by extremely wet years (La Niña events). Yet, when this area is influenced by extreme aridity (El Niño events), it is very probable that metal(loid)s are stable as oxides. This is because most metal(loid)s is this area are associated with the reducible fraction (Fe- and Mn-oxyhydroxides) and oxidizing conditions would release mainly the oxidizable fraction (F4), which is minimal (7±2 in the DS & 8±2 in the WS). Another change that would increase metal(loid) release is an acidification of the milieu, this is because carbonates bear a significant percentage of metal(loid)s, and as determined through SSP this fraction is not destabilized under seasonal changes (DS: 15±3%; WS 18±4%). To conclude, the northern Lake Uru Uru area is more anthropogenically impacted than the Cala Cala Lagoon, which is evidenced by the fact that solid state profiles are variable, metal(loid)s are more reactive in the particulate fraction and changes in metal(loid) partitioning between the DS and WS are moderate. The decrease of Cd partitioning during the WS might be explained by the fact that this is the only highly available element that is not associated with Fe- and Mn-oxyhydroxides and therefore, its release is not influenced by an increase in precipitation.

Southern Lake Uru Uru sediments are potentially the most available of all, especially during the WS (Table 4.9). In relation to the northern Lake Uru Uru area, sulphate reduction takes place just below the WSI and evaporation does not exert a preponderant role in the dissolved metal(loid) behaviour. In this area, dissolved Sb and Mo exhibit the highest concentration during both seasons and Cd during the DS. Within the solid fraction the establishment of reduced and anoxic conditions involves significant changes in the SSP. Indeed, Cd, Sb, Pb and U change the main contribution percentage between the DS and WS. During the DS, metal(loid)s generally are associated with residual (40±16%) > Fe- and Mn-oxyhydroxides (26±7%) > carbonates (16±6%) > OM/sulphides (9±8%) ≃ exchangeable (9±8%) fractions, whereas during the WS contributions are Fe- and Mn-oxyhydroxides (31±17%) > residual (25±35%) ≃ carbonates (25±12%) > OM/sulphides (10±9%) > exchangeable (9±4%). The high variability of the solid fraction profiles, the elevated concentration of dissolved Sb and

Mo and the extreme variability of the SSP between the DS and WS, allow us to propose that the southern Lake Uru Uru area is the most anthropogenically impacted of all the studied sites. Huanuni Mine waste may be related to high concentrations of dissolved Sb and the potential availability of this element in the solid fraction, because gangue minerals probably contain Sb present in all the metallogenic belts of the Eastern Andes Cordillera [217, 315]. Nevertheless, a Mo source has not been determined in this survey and this corresponds to an important unresolved issue, because it has been determined to compete with Cu causing dietary deficiencies in Northern Scotland farm animals [349]. As in northern Lake Uru Uru, we suggest that precaution must be taken during the WS, as metal(loid)s are easily released and might reach the OLW. We stress that it is in the southern Lake Uru Uru area where most flora and fauna are observed and fishing is usually practiced. To conclude on the danger of consuming products from the southern Lake Uru Uru area, we propose detailed studies of metal(loid) behaviour within the water column, especially during the WS and La Niña events to warn the population if necessary.

4.5 Conclusions

1. Through this study we conclude that metal(loid)s within the Cala Cala Lagoon are less available and mobile than within Lake Uru Uru. High concentrations of dissolved elements are explained by the proximity to the metallogenic belts located along the Eastern Andes Cordillera, and not by anthropogenic influence.

2. Within Lake Uru Uru metal(loid)s are more available and mobile. Northern Lake Uru Uru exhibits the lowest mean concentration for dissolved metal(loid)s (except Cu in WS). Dissolved metal(loid) behaviour is highly influenced by evaporation/precipitation rates, indeed, the reduced environment reached during the WS entails the release of metal(loid)s as reductive dissolution of Fe- and Mn-oxyhydroxides takes place. Particulate metal(loid) behaviour shows moderate changes between different seasons.

3. Despite anthropogenic influence in the northern Lake Uru Uru area (highly variable solid state profiles and moderate SSP changing), the most important influences on metal(loid) behaviour are renewed water input in the OLW and WS. Reduced conditions are responsible for releasing metal(loid)s to the pore water and probably to the OLW.

4. Metal(loid)s within the southern Lake Uru Uru area are the most reactive, available and mobile. During the DS, dissolved metal(loid) behaviour is probably influenced by evaporation while no influence is present during the WS. Dissolved concentrations of pore water are nearly the same in both seasons, and the highest concentrations of dissolved Sb and Mo are found in this area during both seasons and Cd in the DS.

5. In southern Lake Uru Uru, the SSP changes fractionation markedly during the WS. Metal(loid)s are easily released to the pore water when reducing conditions are established during this season. The most unstable behaviour in the solid phase is presented by increasing Mo, U, Sb and Pb and diminishing Cd availability during the WS.

6. We suggest that the southern Lake Uru Uru area presents the highest environmental concern. This is because, besides the influence of the WS, anthropogenic influence, mainly linked to the Huanuni Mine, might be causing the highest concentrations of dissolved Sb (and Mo). We stress that it is in this area where most flora and fauna occur and fishing is usually practiced.

7. We recommend that metal(loid) behaviour in the OLW be studied in detail, especially during the WS and La Niña events.

Chapter 5

Solid state partitioning vs. historic pollution register from lacustrine sediments in the Altiplano of Bolivia

Introduction

The intermontane Altiplano, since formation, has suffered periodic glacial advances and retreats, resulting in high-amplitude fluctuations of lacustrine phases in its northern and central parts. These conditions have existed since at least the early Pleistocene [212, 221, 224, 225, 226, 211, 227]. In recent times, the Bolivian Altiplano has been affected by interannual time scale climatic fluctuations, with marked variations of precipitation, ranging from extremely dry (dry season) to very wet (wet season) austral summer conditions. These climatic fluctuations have been described in a number of studies, general agreement involving the El Niño-Southern Oscillation (ENSO) phenomenon (e.g., [350, 351, 352]).

Historic mining activities have been documented since at least 2,000 BC, by the Tiwanacu culture [353]. Mining activities were later massively developed by the Spaniards, concentrated in the Oruro, Potosí and Cochabamba Departments [353]. Currently and throughout the 20^{th} century, mining has been Bolivia's top industry, producing much of the world's Sb, Bi, Pb, Ag, Sn, W and Zn [217].

The objectives of this study are to determine the influence of mining activities, climatic conditions and local factors such as geology and solid state partitioning of metal(loid)s in relation to metal(loid) deposition in a high altitude lake system located on the Altiplano of Bolivia. This study is based on two coring campaigns; one performed during the dry season (DS) and another during the wet season (WS). Sediment samples from these cores were subjected to total and single chemical extractions, and samples of the southern part of Lake Uru Uru (DS) were dated. Geochemical results were then submitted to statistical analysis, in particular to a Principal Component Analysis (PCA) to determine the relationships among elements within different environments, seasons, total metal(loid) content (TMC) and extractable metal(loid)s. Finally a detailed PCA analysis was performed on southern Lake Uru Uru sediments, on which age dating was performed to relate geochemical behaviours to ENSO events.

The results of this study suggest that during the last century the exploitation and production of tin deposits have influenced the deposition and accumulation of Sb-Ag-Pb in sediments of the Altiplano of Oruro. In addition, results also show that ENSO events might play an important role in the formation of authigenic minerals in Lake Uru Uru sediments during long term precipitations. Regardless of associated anthropogenic and climatic processes, results also show a natural baseline signature which is largely influenced by the regional geology. Distribution of rock outcrops and associated mineral deposits determine the natural sources of metal(loid)

products and thus influence their dispersion and deposition, including both reactive and non-reactive minerals. Results of the PCA suggest that it is the non-reactive minerals that mainly influence metal(loid) deposition. In conclusion, this survey indicates that metal(loid) deposition within Lake Uru Uru is influenced mainly by: local geology (carbonates from Ordovician-Silurian-Cretaceous sedimentary rocks), Fe- and Mn-oxyhydroxides influenced by the WS, long term floods under the probable influence of ENSO events, and historic and present time mining activities. In the Cala Cala Lagoon, with little or no anthropogenic impact, processes are mainly controlled by the local geology. To support these conclusions more studies are deemed necessary.

Paper 3. Solid state partitioning of trace metals in sediments from Lake Uru Uru: a limnological system affected by historical mine-waste drainage and the ENSO phenomenon

J. Tapia[1,2]; B. Townley[1]; S. Audry[2]

[1]Departamento de Geología, Universidad de Chile, Plaza Ercilla 803, casilla 13518, correo 21, Santiago, Chile

[2]Université de Toulouse, OMP/LMTG, 14 Av. Edouard Belin, 31400 Toulouse, France

Abstract

The Bolivian Altiplano has been historically affected by interannual timescale climatic fluctuations, experiencing strong precipitation variability, ranging from extremely dry to very wet austral summer conditions, which in a number of studies have been related to the El Niño-Southern Oscillation (ENSO) phenomenon. In this same region, historic mining activities have occurred and continued throughout the 20^{th} century. Mining in the recent past has represented Bolivia's top industry, producing much of the world's Sb, Bi, Pb, Ag, Sn, W and Zn. The analyses of geochemistry of total and single selective extractions data through Principal Component Analysis (PCA), together with age dating, have allowed determination of different processes that influence deposition of Sb-Ag-Pb. In recent and historic times, the exploitation and production of Sn has had evident impacts on metal(loid) dispersion in sediments from the Altiplano of Oruro, but additionally, results have shown other processes that have also had an important impact. Among these, ENSO events have probably played an important role in the generation of authigenic minerals in lacustrine sediments. In addition, results show an underlying baseline effect related to regional geology. The distribution of different types of rock units and mineral deposits has a fundamental effect on the distribution of metal(loid)s. These include reactive and non-reactive minerals, non-reactive minerals representing the main proportion of metal(loid) phases in the Cala Cala Lagoon and to a lesser extent within Lake Uru Uru sediments. In conclusion, we propose that different sources and conditions seem to represent the main influences on metal(loid) deposition and distribution within southern Lake

Uru Uru: historic and present time mining activities (ores and gangues), local geology (carbonates from Ordovician-Silurian-Cretaceous sedimentary rocks and recent volcanic rocks), Fe- and Mn-oxyhydroxides (influenced by the WS), and long term floods (probably associated by ENSO events). In contrast, the Cala Cala Lagoon, with little or no anthropogenic activity, might be mainly influenced by the local geology. To support these results more studies are deemed necessary in the Altiplano areas affected by historic mining, such as Potosí.

Resumen

El Altiplano de Bolivia ha sido afectado históricamente por fluctuaciones climáticas a una escala de tiempo interanual, sufriendo fuerte variabilidad de precipitaciones, que varían desde condiciones estivales australes extremadamente secas a muy húmedas, las cuales en cierto número de estudios han sido adjudicadas al fenómeno de Oscilación del Sur El Niño (ENSO). Por otra parte, actividades mineras históricas, también han existido en esta área y actualmente a través del siglo 20, la minería fue la industria más importante de Bolivia, produciendo gran cantidad del Sb, Bi, Pb, Ag, Sn, W y Zn a nivel mundial.

El análisis de digestiones totales, paralelas y datación de sedimentos, utilizando el Análisis de Componentes Principales (PCA) permitieron proponer que durante el último siglo, por una parte la explotación de Sn ha influido en la deposición de Sb-Ag-Pb-Sn en sedimentos del Altiplano de Oruro, y por la otra, los eventos ENSO han jugado probablemente un rol importante en la generación de minerales autígenos en sedimentos lacustres. La geología regional influye importantemente en la deposición de metal(oid)es, donde se encontraron ambos, minerales reactivos y no-reactivos; los no-reactivos representando la mayor proporción de metal(oid)es en el Lago Uru Uru y la Laguna Cala Cala. Para concluir, se propuso que la deposición de metal(oid)es en el Lago Uru Uru ha sido influenciada principalmente por tres fuentes: geología local (rocas sedimentarias del Ordovícico-Silúrico-Cretácico, rocas volcánicas del Plioceno a actuales), formación de minerales autigénicos bajo la influencia probable de eventos ENSO, y menas y gangas de origen minerogénico; mientras, la Laguna Cala Cala podría estar principalmente asociada a la geología local. Para apoyar estos resultados, se considera necesario realizar más estudios.

Résumé

Les hauts plateaux de la Bolivie ont été affectés par des changements d'échelle de temps interannuelle caractérisés par un été austral très sec ou très humide: cette variabilité a été associée à des événements ENSO (El Niño Southern Oscillation). En outre, l'exploitation minière a existée dans ce domaine, et maintenant et à travers le $20^{ème}$ siècle, a été le secteur industriel plus important en Bolivie, en générant une énorme quantité de Sb, Bi, Pb, Ag, Sn, W et Zn à niveau global.

L'analyse des digestions totaux, parallèles et la datation des sédiments par Analyse en Composantes Principales (PCA) ont montré que au cours du siècle dernier, l'explotation et la production du Sn ont influencé le dépôt de Sb-Ag-Pb-Sn dans les sédiments des hauts plateaux de Bolivie. Des changements inter-saisonniers associés à des événements ENSO, jouent probablement un rôle important dans le dépôt de minéraux authigènes dans les sédiments lacustres. La géologie régionale influe sur le dépôt des métaux et métalloïdes. Enfin, cette étude permet de suggérer que les dépôts des métaux et métalloïdes dans les sédiments du sud du lac Uru Uru pourraient être influencés principalement par: la géologie locale (roches sédimentaires carbonatées de l'Ordovicien-Silurien-Crétacé et roches volcaniques récentes), des minéraux authigènes probablement sous l'influence du événements ENSO, et de minerais et gangues minérogénétiques. En revanche, le dépôt des métaux et métalloïdes dans les sédiments de la lagune Cala Cala est principalement influencé par la géologie locale. Pour appuyer ces résultats, il est nécessaire de poursuivre les études.

5.1 Introduction: Oruro's mining history and ENSO events

5.1.1 Mining history

The Oruro Department, located within the Altiplano of Bolivia, is among some of the most mineralized and yet unexplored areas in the world [217, 253, 315, 316]. Mining history dates back to 2000 yr BC (Tiwanaku) and has continued until present; moreover, important historic milestones in Bolivia have been directly related to the discovery and development of Bolivia's mineral resources [353].

Pre-Columbian times. The origins of mining date back to the Tiwanacu (2,000 BC-1,200 AC) and Inca (1,380-1,550 AC) civilizations [353]. During these times, the main Bolivian ores were: gold (Au), silver (Ag), copper (Cu), mercury (Hg), iron (Fe), lead (Pb) and salts (Precolumbian gold museum).

Spaniards era. In the third decade of the 16^{th} Century, the Spaniards conquered the Inca Empire, discovering gold in Cochabamba and silver in Poopó (Oruro) and Potosí [353]. The first colonial Ag mine was located in Oruro, yet Potosí became most important after the discovery of Cerro Rico (1554), Bolivia subsequently becoming the major Ag producer in the world (1553-1825) [353]. From the mid 18^{th} Century, Ag mining in Potosí started to experience difficulties as mineral concentrations decreased and problems begun with mita-labor[1]. By the end of the 18^{th} Century, Potosí declined quickly [353].

Republic and Bolivian mining. By the beginning of the Republic times, the Bolivian mining industry was in ruins [353] and it was not until the second half of the 19^{th} Century that Ag mining grew and Sn was first extracted (1860) at the Caracoles mine in La Paz [354]. Throughout the 20^{th} century, mining was Bolivia's top industry, producing much of the world's Sb, Bi, Pb, Ag, Sn, W and Zn [217]; by the beginning of the 20^{th} Century, Bolivia became an important Sn producer. Tin quickly relegated Ag to a second place in Bolivian ore exports and Bolivia was positioned as one of the major Sn producers in the world[2]. After 1930 the Sn industry was adversely affected by declining market prices [353]. Despite this, due to high demand, between 1940 and 1947 (World War II), Bolivia exported 40,000 tons of Sn per year at a price of US$0.41 per pound to the United States (US), well below international prices [353]. Starting 1952, the Bolivian Government created the Corporación Minera de Bolivia

[1] Mita was a forced labor system whereby all indigenous people between 18 and 25 years old had to work for 12 hours a day in the mines.

[2] Between 1900 and 1913 great consortia formed and controlled Bolivian mining industry until 1952 [353].

(COMIBOL, Bolivian Mining Corporation), whereby mining operations were classified as: (1) Large Mining Sector (state owned), (2) Medium-size Mining Sector, (3) Small Mining Sector. Later a fourth group appeared, (4) Mining Cooperatives. One objective of COMIBOL was to create massive employment for miners, therefore in 1956 COMIBOL's employees reached ~36,000 [355]. During the 50s COMIBOL's production decreased progressively, and annual production reduced from 26,000 tons in 1953 to 15,000 tons in 1960 [354]. Bolivia's democratic governments were interrupted by military governments between 1964 and 1980. Later, an increase in the international prices of Sn and political stability caused a slight increase in the mining sector during the 70's, reaching 30,000 tons per year. The Vinto Smelter was built in 1971 to locally treat Bolivian ore concentrates. Before the end of military administration Sn reached the highest price ever ($7.61 per pound). In October 1985 the world tin market collapsed, the new democratic government quickly reducing the state's participation in mining[3] [353]. During 1987 production was reduced to almost zero. Since then, the mining sector has recovered, starting a transformation from single-metal production to diversified mining; ores previously extracted by private miners as W, Sb, Zn and Pb started being exploited by Cooperatives [353]. As a result, in 1992 the Mining Cooperative became the main producer of Au and Sb in Bolivia [223]. Since 1993, the Medium-size Mining Sector has become the most important Au producer in Bolivia[4] [254]. Presently, Bolivia is ranked as the third largest producer of Sb in the world, as well as the fourth in Sn and Zn, and sixth in W [217].

5.1.2 Climate: large-scale climatic changes vs. interannual timescale climatic fluctuations (ENSO)

The intermontane Altiplano, since its formation, has suffered periodic glacial advances and retreats, resulting in high-amplitude fluctuations of lacustrine phases in the northern and central Altiplano [212, 221, 224, 225, 226, 227]. The various lacustrine basins, from oldest to the most recent, are known as the paleolakes *Mataro*, *Cabana*, *Ballivian*, *Escara*, *Minchin* and *Tauca* [212, 221, 224, 225, 226, 227, 228, 229, 230, 231]; these changes in lake levels are believed to be related to large-scale climatic changes [233, 235]. In addition to the latter, the Bolivian Altiplano has also been historically affected by inter-annual timescale climatic fluctuations. The Altiplano experiences strong precipitation variability, ranging from extremely dry to very wet austral summer conditions. Between 1957 and 1996, December-January-February (DJF) precipitation

[3] 75% of COMIBOL's miners were fired and efforts only concentrated in sustainable mining operations.
[4] Mainly by Kori Kollo's Mine production that in 1995 produced ~36 tons of Ag [254].

recorded at Copacabana (16.2°S, 69.1°W; 3815 m a.s.l.; Lake Titicaca shore) ranged from 203 mm in 1990/91 to 850 mm in 1983/84 [350]. In the more arid southwestern part of the Altiplano the fluctuations are even larger (20°S, 68.8°W ; 3990 m a.s.l.; Coyacagua Station, northern Chile) where the minimum DJF precipitation recorded was 11 mm in 1982/83, while in the next rainy season, 1983/84, the maximum ever (277 mm) [350]. The strong inter-annual variability of summer precipitation has been described in a number of studies which by general agreement involves the El Niño-Southern Oscillation (ENSO) phenomenon (e.g., [350, 351, 352]). ENSO is one of the most prominent sources of inter-annual variability operating in the earth's climate system [356]. ENSO is associated worldwide with extreme weather conditions such as heavy snowstorms, floods, droughts and cyclone activities, having large ecological [357], social [358] and economic impacts [359]. Studies performed in the Altiplano area concluded that El Niño periods (warm phase of ENSO) tend to be dry, while La Niña years (ENSO cold phase) are often associated with wet conditions on the Altiplano. During the last centuries an important number of these events have been registered (Table 5.1).[5]

5.2 Materials and methods

5.2.1 Study area and sampling sites

The study area (Fig. 5.2.1) is situated within the Altiplano basin of Bolivia, the specific study and sampling sites are at Lake Uru Uru (located within part of TDPS[6] endorheic system) and Cala Cala Lagoon (located within the Eastern Andes Range sedimentary rocks). More detailed information of these areas may be found in Tapia *et al.* (2011a and 2011b) [153, 315]. At these study sites, a dry season (DS, May to September) and a wet season (WS, October to March) occur, defining a dry austral winter and wet austral summer.

5.2.2 Sampling methods

In 2008 and 2009 three sites from lacustrine environments within the Altiplano of Bolivia were sampled during the DS and WS (Details in [315, 153]). Within these coring campaigns a total of five continuous sedimentary cores were extracted, centrifuged and sliced with an acid-cleansed plastic cutter [315, 153]. For every level, an additional sediment sub-sample was immediately sealed in a pre-weighed vial and frozen for porosity analysis. During these

[5] Instrumental record of ENSO variability is limited to the past 100–150 yr [360].
[6] Lake Titicaca-Desaguadero River-Lake Poopó-Coipasa Salar.

Table 5.1: El Niño and La Niña events for the period 1870–1999 following Trenberth 1997 [361].

EL NIÑO									
1876	*1877*	*1880*	*1884*	*1885*	*1887*	*1888*	*1895*	*1896*	*1899*
1900	*1902*	*1904*	*1905*	*1911*	*1913*	*1914*	*1918*	*1919*	*1923*
1925	*1929*	*1930*	*1935*	*1939*	*1940*	*1941*	*1947*	*1951*	*1952*
1953	*1957*	*1958*	*1963*	*1965*	*1968*	*1969*	*1972*	*1976*	*1977*
1979	*1982*	*1986*	*1987*	*1990*	*1991*	*1992*	*1993*	*1994*	*1997*
LA NIÑA									
1870	*1871*	*1872*	*1873*	*1874*	*1875*	*1878*	*1879*	*1882*	*1886*
1889	*1890*	*1892*	*1893*	*1894*	*1897*	*1898*	*1903*	*1906*	*1908*
1909	*1910*	*1916*	*1917*	*1920*	*1922*	*1924*	*1933*	*1938*	*1942*
1945	*1949*	*1950*	*1954*	*1955*	*1956*	*1964*	*1967*	*1970*	*1971*
1973	*1974*	*1975*	*1983*	*1984*	*1985*	*1988*	*1995*	*1998*	*1999*

campaigns a total of 91 sediment samples and 88 porosity samples were retrieved. Back in the laboratory, sediment samples were dried at 50°C to constant weight and then powdered and homogenized with an agate mortar.

5.2.3 Analytical methods

Grain size measurements were performed with a laser granulometer (2.0 Mastersizer 2000). Porosity was determined by comparison of the weights of wet and dried sediment samples.

Dry season southern Lake Uru Uru samples were dated by ^{210}Pb, ^{137}Cs and ^{241}Am[7]. These measurements were done on 3-9 g dry samples placed in cylindrical vials. Isotope counting was performed at the underground laboratory of Ferrières[8] located at an approximate depth of 80 m, beneath rock, in the French Pyrénées (south of Foix). The volume of the germanium crystal is 280 cm^3 and the diameter of the well is 15 mm. The detector is protected by a lead castle with a low activity (15 cm thickness). The detector is equipped with an auto-sampler that can contain up to 20 samples and with a system that can fill liquid nitrogen automatically from a 250 L tank into the 20 L dewar that cools the germanium crystal. Consequently, the gamma detector thus equipped is able to analyse samples automatically. This facility provides a background of 5.8 counts per minute on the 30-2700 keV energy range, which is at least 10-20 times better than laboratories located above ground. This is equivalent to 5565 counts per day per kilogram of germanium crystal [363].

Geochemical analysis of sediment samples were undertaken using clean techniques and lab-

[7] Northern Lake Uru Uru and Cala Cala Lagoon were also dated, yet northern Lake Uru Uru has suffered complete desiccation and Cala Cala Lagoon is strongly bioturbated as seen during coring campaigns, therefore these data were highly perturbed not providing accurate and precise data.

[8] Ferrières Underground Laboratory is part of the European CELLAR network (Collaboration of European Low-level Underground Laboratories; [362]).

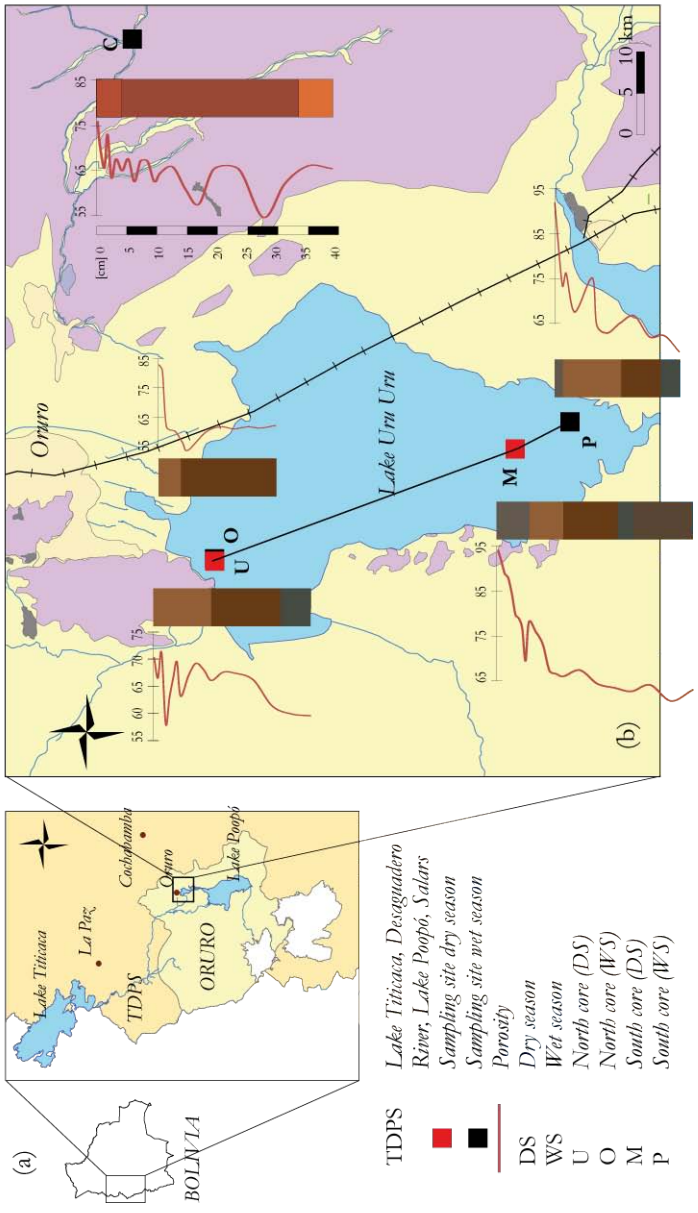

Figure 5.2.1: (a) Lake Titicaca-Desaguadero River-Lake Poopó and Salars location; (b) Lake Uru Uru and Cala Cala Lagoon location, cores and porosity.

ware following the methods described in detail in the literature [207, 210, 211]. Each batch of samples included method blanks and digestion of certified international reference materials (e.g., LKSD-1 & LKSD-3). Accuracy was within 5% of the certified values and the analytical error (relative standard deviation) was generally better than 5% for concentrations 10 times higher than detection limits. Solid state partitioning was determined using single selective extraction procedures based on the methodology of Tessier *et al.* (1979) [154] (see details in [153, 184, 207]). Reagent problems were determined for Mn, Mo and less for Cd, the most mobile elements within this system [153]. Extractability problems related to Mn have been widely determined and associated with NaOAc extraction [178, 184, 348]; exchangeable-$MgCl_2$ digestion has been found to overestimate the exchangeable fraction, particularly in the case of Cd [185, 209, 345]. Problems for Mo are probably related to exchangeable fraction overestimation, by the fact that NaOAc extraction was lower than $MgCl_2$ (see Chapter 4.4)

5.3 Results

5.3.1 Description of the sedimentary cores

Lacustrine sediments of the studied areas were classified as: Type A: superficial, dark, organic matter (OM) rich, with more than 65% water, only found within the topmost section of southern Lake Uru Uru area, Type B: dark to soft brown tones, 45 to 65% water and Type C: dark to chocolate brown, less than 45% water and poor OM (mainly roots) presence (Table 5.2)[9].

5.3.2 Metal(loid) concentration profiles

Sediment metal(loid) concentration depth profiles show different patterns. At Cala Cala some metal(loid)s show a similar behaviour in the solid fraction, for instance Mn-Fe and Cu-Zn, while others show different and isolated behaviour, for instance Pb and Cd (Fig. 5.3.1). For the Cala Cala Lagoon, only WS samples were available, therefore seasonal changes were not determined (Fig. 5.3.1). Northern and southern Lake Uru Uru area profiles are highly variable with depth (Figs. 5.3.2 and 5.3.3 respectively), yet seasonal changes in the total metallic (metalloids included) trace element (MTE) content (TMC) in the solid fraction profiles within

Table 5.2: Sedimentary cores description. MWC: mean water content; MP: mean porosity; MPOC: mean POC (Particulate Organic Carbon); MS_{tot}: mean S_{tot}; nd: not determined

Site	*Type*	*Depth* [cm]	*MWC* [%]	*MP* [%]	*Colour* (qualitative)	*Organic Matter* (observed)	*MPOC* [%]	MS_{tot} [%]	*Granulometry* [%]
U	*B*	0.0-1.5	46	69	dark brown	totora and roots	0.91	0.13	nd
	C	1.5-21	41	65	chocolate brown	not observed	1.18	0.22	nd
O	*B*	0.0-1.0	63	82	dark brown	totora and roots	0.72	0.07	silt > sand > clay
	C	1.0-18	39	62	chocolate brown	not observed	0.83	0.11	silt > sand ≥ clay
M	*A*	0.0-2.5	76	89	dark grey	myriophillum and scarce totora	4.09	1.39	nd
	B	2.5-10	51	73	dark brown	roots and some red worms	2.19	1.35	nd
	C	10-29	40	64	chocolate brown	not observed	0.82	0.61	nd
P	*A*	0.0-0.5	81	92	dark grey	myriophillum and scarce totora	6.51	1.46	nd
	B	0.5-4.8	45	68	dark brown	roots	4.92	1.43	nd
	C	4.8-17	39	63	chocolate brown	not observed	1.26	0.87	nd
C	*B*	0.0-1.6	48	71	red to ochre	scarce roots	1.71	1.78	sand ≫ silt ≥clay
	C	1.6-38	41	64	ochre to red-brown	numerous and scattered red worms	1.82	1.85	sand ≫ silt >clay

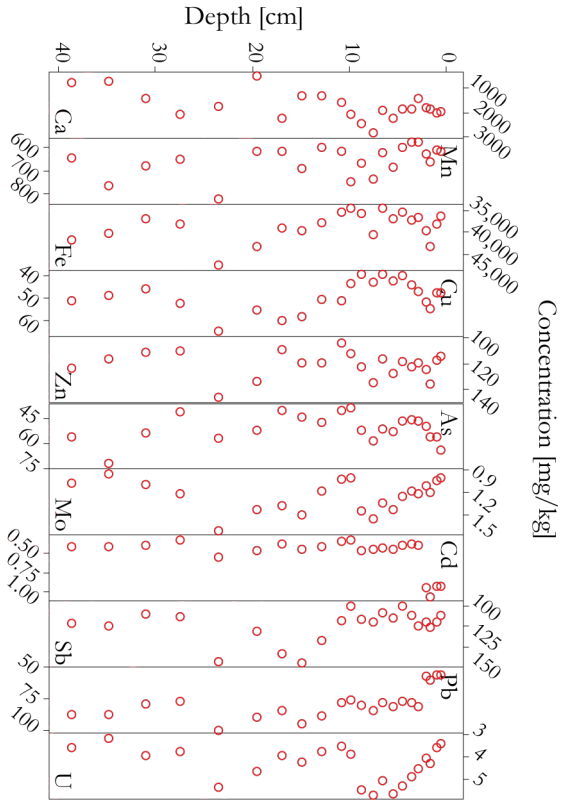

Figure 5.3.1: Sediment concentration profiles from Cala Cala Lagoon during WS.

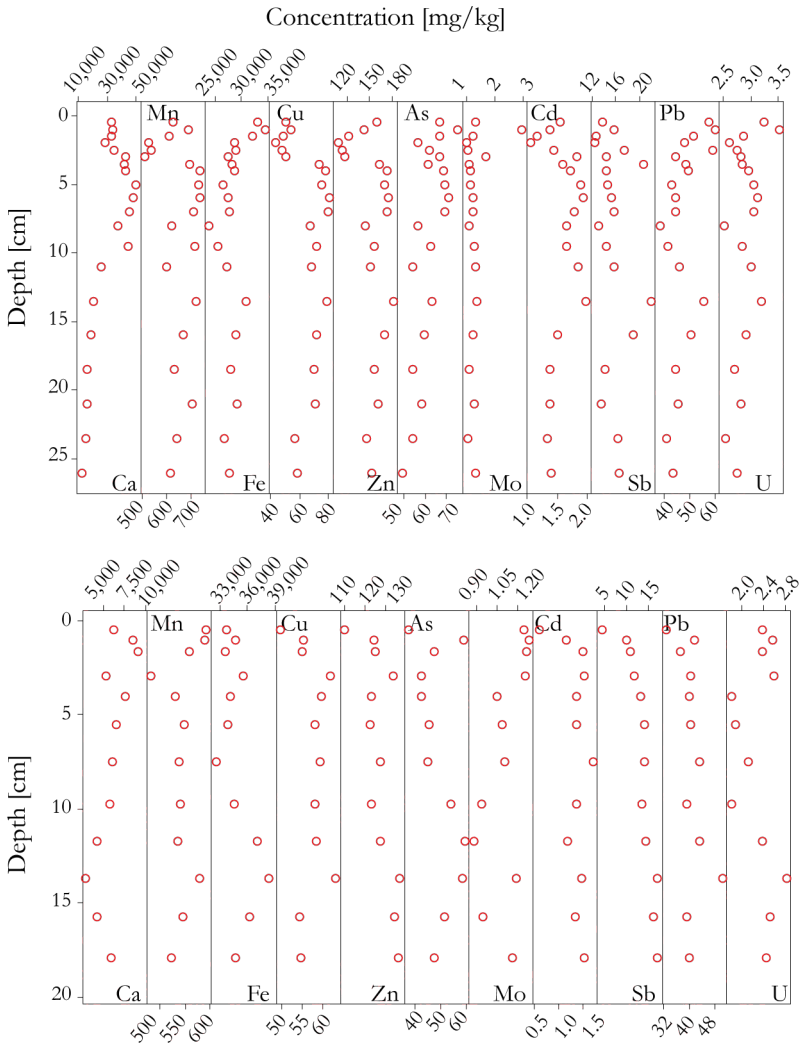

Figure 5.3.2: Sediment concentration profiles from northern Lake Uru Uru during DS (top) and DS (bottom).

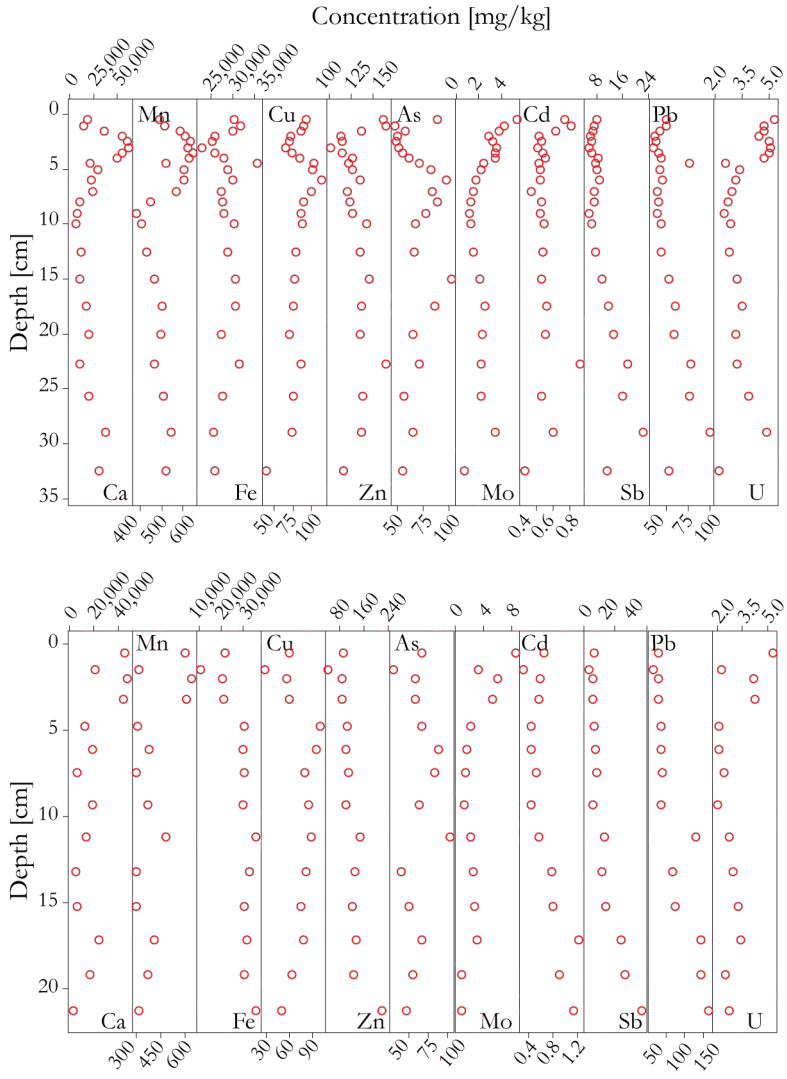

Figure 5.3.3: Sediment concentration profiles from southern Lake Uru Uru during DS (top) and WS (bottom).

each area are not so marked.

5.4 Discussions

5.4.1 ^{210}Pb, ^{137}Cs and ^{241}Am dating and sedimentation rates

South core ^{210}Pb dating exhibited a nearly constant sedimentation rate of about 0.3 mm per year, this information is close to the ^{137}Cs peak (~1956) in the central part of the profile. In the upper section there was a second ^{137}Cs peak, which was interpreted primarily to be associated with Chernobyl (1983), yet in South America the only confirmed source of ^{137}Cs is the atmospheric testing of nuclear weapons during the 1950s and 1960s (1952 to 1963) [364, 365]. Hence, in the southern hemisphere, ^{137}Cs sediment records can be used to identify sediment layers deposited in 1965 (shortly after most atmospheric testing had ceased) when ^{137}Cs deposition rates were at their peak [266, 366, 367, 368]. To confirm the ^{137}Cs peak some researchers have used the radionuclide ^{241}Am in undisturbed profiles (e.g., [369]) because evidence has shown that ^{241}Am is less mobile in lake sediments than ^{137}Cs [266] and it is more strongly particle-associated than caesium, especially under low pH conditions [267]. Although ^{241}Am activities are much lower than ^{137}Cs activities, it has been shown that the distribution of ^{241}Am in cores is a more accurate marker of maximum fallout (i.e. 1965 in the southern hemisphere) than ^{137}Cs [266]. For ^{241}Am only one peak was detected (15 cm depth), the upper ^{137}Cs peak was not present within the ^{241}Am profile, therefore, it was considered that this peak was related to maximum fallout (~1960; Fig. 5.4.1) . The determined time register spans ~120 years. In this time span two main trends were identified in relation to the TMC behaviour. The first group is probably related to Bolivian metal(loid) exploitation and mining during the past 120 years (Ag, Pb, Sb, Sn) (Fig. 5.4.2), but a second group of elements respond most likely to seasonal changes. In this group elements such as Cu and Zn have the same patterns (Fig. 5.4.2), while As and Cd show similar maximum concentration peaks, generally exhibiting an increase in these elements under long term flooding periods (Fig. 5.4.2).

5.4.2 Metal(loid) concentration profiles and solid state partitioning (SSP)

When analysing in detail concentration profiles and solid state partitioning of metal(loid)s,

[9] For Cala Cala Lagoon this classification only considered water content because sediment colour, granulometry and OM were different.

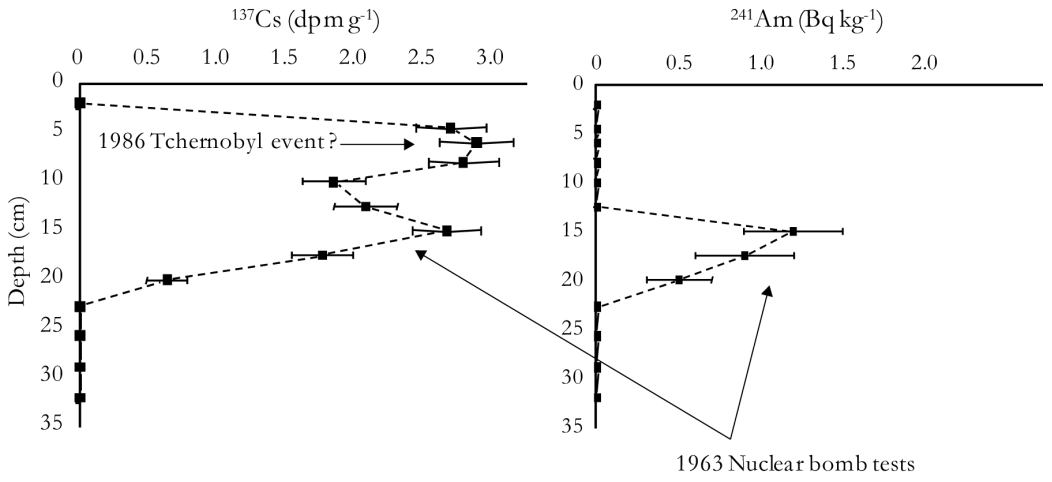

Figure 5.4.1: ^{137}Cs and ^{241} Am dating.

some interpretations from the above were confirmed. Determination coefficients (R^2) were calculated for most of the metal(loid)s and extractable fractions, globally and locally. Most of these tests showed good correlations (over 0.6) for only some TMC and extractable fractions. Related elements were then subjected to a Principal Component Analysis (PCA), with the results summarized in Table 5.3.[10]

Globally, it was determined that most of the non-reactive (i.e. residual) phases were not related by R^2 , thus they were not considered in the following analysis. Relations between total and extractable fractions from Lake Uru Uru sediments were determined to be mainly controlled by processes governing reactive phases, while mining was relegated to a second or third place. Northern Lake Uru Uru was determined to be related to reactive phases (35%) and non-reactive phases (23%), while mining provided lower contributions to this area (15%). Southern Lake Uru Uru was determined to be highly influenced by reactive phases (50%), while mining provided nearly 20% of the variance. In this area, non-reactive phases were not determined to have impacted the main responses to depositional variations. Cala Cala Lagoon was determined to be very different from Lake Uru Uru and clearly dominated by non-reactive phases, reactive elements at this site being related to OM mineralization (POC, Mo and Cu), with only minor if any mining-related impact. Data from Table 5.3 evidences the existence of two main trends within Lake Uru Uru sediments explaining the MTE-depth profile variability with time. These trends are represented by two groups, one classified as reactive metal(loid) phases that have the highest explained variance, and a second related to exploited Bolivian metal(loid)s, explaining

[10]For Cala Cala Lagoon sediments, PCA's were done with less elements because less relations (R^2) were found for this site.

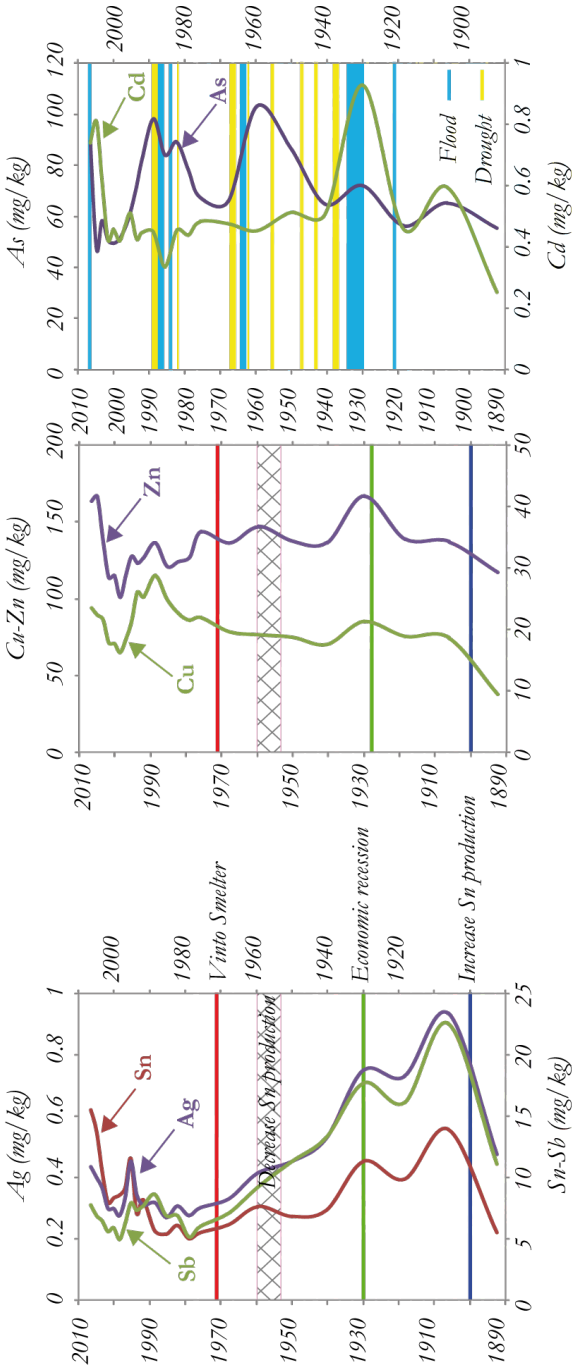

Figure 5.4.2: Modern history of southern Lake Uru Uru and its relation to mining, floods and droughts.

Table 5.3: Summary of PCA performed to selected total and extractable elements. C: component; σ: variance; σ_{cum}: cumulative variance; A: Global Lake Uru Uru; B: North Lake Uru Uru; C: South Lake Uru Uru; D: Cala Cala Lagoon. X_{res}: residual elements (not easily extractable); X_{tot}: total element concentration; X_{MgCl_2}: $MgCl_2$ leaching, exchangeable elements; X_{NaOAc}: NaOAC leaching, elements associated to carbonates; X_{asc}: ascorbate leaching, elements associated to Fe- and Mn-oxyhydroxides (reductible elements); $X_{H_2O_2}$: H_2O_2 leaching, elements associated to OM or sulphides (oxidizable elements).

	C	σ	σ_{cum}	*positive correlation*	*negative correlation*	*interpretation*
	C1	*0.49*	*0.49*	Fe_{asc}, *COP*, S_{tot}, $Cu_{H_2O_2}$, Mo_{asc}, $Mo_{H_2O_2}$, U_{asc}, $U_{H_2O_2}$, U_{NaOAc}, Mn_{NaOAc}	Fe_{res}	*reactive metal(loid) phases*
A	*C2*	*0.17*	*0.66*	*Ag*, *Sb*, $Sb_{H_2O_2}$, Sb_{NaOAc}, Sb_{asc}	S_{tot}	*mining-history related sulphides*
	C3	*0.11*	*0.77*	U_{MgCl_2}, Cu_{NaOAc}, As_{MgCl_2}	Mn_{asc}, *Ca*	*reactive carbonates*
	C4	*0.05*	*0.81*	Fe_{tot}	Cu_{asc}, As_{asc}	*non-reactive Fe- and Mn-oxyhydroxides*
	C1	*0.35*	*0.35*	*COP*, S_{tot}, $Cu_{H_2O_2}$, U_{asc}, $U_{H_2O_2}$, U_{NaOAc}, U_{MgCl_2}, $Mo_{H_2O_2}$	Fe_{res}	*reactive metal(loid) phases*
B	*C2*	*0.23*	*0.57*	Fe_{tot}, Fe_{asc}, Cu_{NaOAc}, As_{asc}, Sb_{asc}	As_{MgCl_2}	*non-reactive phases*
	C3	*0.15*	*0.72*	*Ag*, *Sb*, $Sb_{H_2O_2}$, Sb_{NaOAc}	S_{tot}	*mining-history related sulphides*
	C4	*0.09*	*0.81*	Cu_{asc}, Mo_{asc}, As_{MgCl_2}	Mn_{asc}, Mn_{NaOAc}, *Ca*	*reactive oxides and carbonates*
	C1	*0.50*	*0.50*	Mn_{NaOAc}, *COP*, $Cu_{H_2O_2}$, Mo_{asc}, U_{asc}, $U_{H_2O_2}$, U_{NaOAc}, $Mo_{H_2O_2}$, *Ca*, Mn_{asc}	Fe_{res}	*reactive metal(loid) phases*
C	*C2*	*0.21*	*0.71*	*Ag*, *Sb*, Sb_{asc}, $Sb_{H_2O_2}$, Sb_{NaOAc}	S_{tot}	*mining-history related sulphides*
	C3	*0.08*	*0.79*	Cu_{NaOAc}, U_{MgCl_2}	Mn_{asc}, *Ca*, As_{MgCl_2}	*non-reactive phases*
	C4	*0.06*	*0.89*	Fe_{tot}, Fe_{asc}, Cu_{asc}	As_{asc}	*non-reactive Fe- and Mn-oxides*
	C1	*0.29*	*0.29*	Fe_{tot}, Fe_{asc}, Mn_{NaOAc}, Sb_{NaOAc}	*Ca*	*non-reactive metal(loid) phases*
D	*C2*	*0.24*	*0.53*	Fe_{res}, *Ag*, *Sb*, $Sb_{H_2O_2}$	S_{tot}	*mining-history related sulphides*
	C3	*0.18*	*0.71*	*COP*, $Mo_{H_2O_2}$, $Cu_{H_2O_2}$		*OM mineralization*
	C4	*0.10*	*0.81*	Mn_{asc}	Mo_{asc}, Sb_{asc}	*reactive Fe- and Mn-oxyhydroxides*

from 15 to 21% of the total variance. In contrast, the Cala Cala Lagoon is mostly influenced by non-reactive phases and to a lesser degree by the mining industry.

5.4.3 Metal(loid) behaviour and relationship to mining and ENSO events

Metal(loid) behaviour and deposition changes were determined to be highly variable, and probably dominated by reactive phases. Mining exploitation has also explained metal(loid) variability in sediments (Sb-Ag±Sn mining between 1880 and 2008), yet as determined through single selective extractions, the main ores of the Altiplano occur mostly as a residual phase (over 80%, excepting Sb and Pb; Table 5.4), thus not involving important chemical reactions. Gangues such as Cd and As were determined to be highly reactive, this can be explained because ores are mainly retained while gangues are dumped in the environment in smaller sizes and with more area available to react.

A detailed PCA analysis was done on the southern Lake Uru Uru sediments (DS) including TMC and also all extractable fractions to compare sediment ages, ENSO and metal(loid) distribution. Results are summarized in Table 5.5. Main responses within southern Lake Uru Uru sediments are governed by Fe- and Mn-oxyhydroxides, carbonates and sulphides. Calcareous Ordovician to Silurian rocks are probably related to Mn and U, as determined through the Ca-Mn-C_{tot}-U association (C1, Table 5.5), whereas Fe- and Mn-oxyhydroxides are mainly influenced by the WS, as demonstrated by Tapia *et al.* (2011b) [153]. Copper, Mo and U sulphides are probably related to OM mineralization, as also interpreted by Tapia *et al.* (2011b) [153], therefore suggesting a high influence of early diagenetic processes on sediment deposition within southern Lake Uru Uru sediments.

By this analysis a new classification was determined, explaining most of the variance (C1; elements rejected by R^2 in the firsts PCA). From table 5.5, it is deduced that element behaviour can be mainly explained by diagenetic processes (C1; Table 5.5), authigenic sulphides influenced by ENSO events (C2; Table 5.5) and mining industry history (C3; Table 5.5). Through the analysis of dated southern Lake Uru Uru sediments by PCAs (Table 5.5), we propose that seasonal changes play a major role in metal(loid) distribution within sediments (as suggested by [153]), followed by authigenic mineral phases probably influenced by ENSO events and mining origin ores and gangues.

During the WS southern Lake Uru Uru sediments are highly susceptible to change solid state partitioning, showing metal(loid) release by reductive dissolution of Fe- and Mn-oxyhydroxides,

Table 5.4: Extractable and residual fractions of metal(loid) ores resources of Bolivia. F1: $MgCl_2$ (exchangeable), F2: NaOAc (carbonates); F3: asc (Fe- and Mn-oxyhydroxides; reductible); F4: H_2O_2 (OM/sulphides; oxidizable); F5: residual (F5=TMC-(F1+F2+F3+F4)). U: northern Lake Uru Uru, DS; O: northern Lake Uru Uru, WS; M: southern Lake Uru Uru, DS; P: southern Lake Uru Uru, WS; C: Cala Cala Lagoon, WS.

Site		*Cu*	*Zn*	*Ag*	*Sn*	*Sb*	*W*	*Pb*
	F1	*1*	*2*	*7*	*1*	*2*	*1*	*0*
	F2	*17*	*5*	*0*	*0*	*9*	*0*	*26*
U	*F3*	*1*	*9*	*0*	*4*	*27*	*4*	*12*
	F4	*6*	*0*	*0*	*2*	*6*	*2*	*0*
	F5	*75*	*83*	*93*	*93*	*55*	*93*	*61*
	F1	*1*	*1*	*2*	*0*	*5*	*1*	*0*
	F2	*24*	*10*	*0*	*0*	*13*	*0*	*35*
O	*F3*	*0*	*11*	*0*	*2*	*36*	*3*	*14*
	F4	*5*	*0*	*0*	*0*	*7*	*1*	*0*
	F5	*70*	*78*	*98*	*98*	*38*	*94*	*50*
	F1	*2*	*3*	*6*	*0*	*2*	*1*	*0*
	F2	*0*	*14*	*0*	*2*	*38*	*5*	*7*
M	*F3*	*5*	*0*	*0*	*0*	*2*	*0*	*0*
	F4	*18*	*18*	*0*	*0*	*7*	*0*	*16*
	F5	*73*	*63*	*94*	*97*	*51*	*93*	*77*
	F1	*0*	*1*	*1*	*0*	*5*	*1*	*0*
	F2	*24*	*9*	*0*	*0*	*10*	*0*	*47*
P	*F3*	*0*	*8*	*0*	*2*	*41*	*4*	*15*
	F4	*4*	*0*	*0*	*0*	*5*	*1*	*0*
	F5	*67*	*81*	*99*	*98*	*40*	*94*	*43*
	F1	*0*	*3*	*2*	*0*	*1*	*0*	*0*
	F2	*4*	*3*	*0*	*0*	*4*	*0*	*8*
C	*F3*	*2*	*6*	*0*	*6*	*16*	*3*	*5*
	F4	*2*	*1*	*0*	*0*	*2*	*0*	*0*
	F5	*91*	*88*	*98*	*94*	*76*	*97*	*87*

Table 5.5: Detailed analysis of southern Lake Uru Uru sediments during DS and relationships between TMC and extractable phases.

	positive correlation	*negative correlation*	*interpretation*
C1	*COP*, C_{tot}, C_{inorg}, *Ca*, *Mn*, Al_{MgCl_2}, Ca_{MgCl_2}, Ca_{NaOAc}, Mn_{asc}, Mn_{NaOAc}, Fe_{asc}, $Cu_{H_2O_2}$, Zn_{MgCl_2}, $Mo_{H_2O_2}$, Sn_{asc}, Sn_{NaOAc}, $U_{H_2O_2}$, U_{NaOAc}.	*Al*, *K*, *Ti* As_{NaOAc}, Ag_{MgCl_2} Cd_{MgCl_2}	*carbonates* *Fe- and Mn-oxyhydroxides* *sulphides*
C2	*Porosity*, *w%*, *Zn*, $Al_{H_2O_2}$, $Mn_{H_2O_2}$, Cu_{asc}, $Zn_{H_2O_2}$, $Ag_{H_2O_2}$, $Cd_{H_2O_2}$, Sn_{MgCl_2}, $Pb_{H_2O_2}$, *ENSO*	$As_{H_2O_2}$, $Sb_{H_2O_2}$, Pb_{NaOAc}, U_{MgCl_2}	*authigenic mineral phases* *influenced by ENSO events*
C3	*Mo*, *Ag*, *Cd*, *Sn*, *Sb*, *W*, *Pb*, *U*, As_{MgCl_2}, Mo_{MgCl_2}, Mo_{asc}, Ag_{MgCl_2}, Cd_{NaOAc}, Sb_{asc}, Sb_{NaOAc}, Pb_{MgCl_2}, Pb_{asc}, U_{MgCl_2}, U_{asc}, U_{NaOAc}	S_{tot}, $Ca_{H_2O_2}$, Mn_{MgCl_2}, Cu_{MgCl_2}, Cu_{NaOAc}, Zn_{NaOAc}, *ENSO*	*mining origin ores* *and gangues non-influenced* *by ENSO events*
C4	*Fe*, *Cu*, *As*, Al_{asc}, Al_{NaOAc}, Fe_{NaOAc}, As_{asc}, Cd_{asc}, Sb_{MgCl_2}	$Fe_{H_2O_2}$, Ag_{NaOAc}	*relatively resistive minerals*

important constituents of C1 besides carbonates (Table 5.5). Therefore the C1 component in the short term is dominated by seasonal changes, yet in the long term, ENSO influences sulphide and exchangeable phase behaviour (the less representative constituents of these sediments [153]). It is highly probable that long term floods are the most important condition for metal(loid) deposition within sediments, at least as observed for Cd and As (Fig. 5.4.2), two mining industry by-products, in the dated core. More studies on different lacustrine environments from the Altiplano influenced by mining activities since Colonial times are considered necessary to support these suggestions.

5.5 Conclusions

1. During the last century Sn exploitation and production has influenced deposition of Sb-Ag-Pb-Sn in sediments from the Altiplano of Oruro. Interannual seasonal changes associated with ENSO events, probably play an important role in the deposition of authigenic minerals in lacustrine sediments as seen for As and Cd after the influence of long term floods.

2. Regional geology influences metal(loid) deposition, yet within southern Lake Uru Uru sediments, the WS controls the fractionation of the solid phase, and metal(loid) deposition.

3. Finally, this study allowed to propose that metal(loid) deposition within southern Lake Uru Uru sediments might be influenced mainly by: local geology (carbonates from Ordovician-Silurian-Cretaceous sedimentary rocks), Fe- and Mn-oxyhydroxides influenced by the WS, long term floods (probably associated with ENSO events) and mining origin ores and gangues. Metal(loid) deposition within the Cala Cala Lagoon sediments is mainly influenced by the local geology.

4. We believe that more studies are necessary to understand the influence of seasonal and interannual climatic fluctuations on sediment deposition within the Altiplano of Bolivia, because this area has suffered interannual climatic fluctuations influencing the existence of immense paleolakes and recently, heavy floods and intense droughts. Additionally, we believe that more studies are necessary to understand the influence of mining on sediment deposition, because Oruro and all the Altiplano of Bolivia have suffered intense mining activities since the XVIIth century.

General Conclusions

This study contributes to a better understanding of metallic (metalloids included) trace element MTE behaviour within lacustrine sediments of the Bolivian Altiplano and allowed us to establish that MTEs in this unexplored environment are governed by different factors, such as local geology, metallogenic belts, mining and smelting activities, geomorphology, seasonal and interannual climatic changes, high altitude, etc. We noted that to better constrain MTE behaviour and understand the general geochemical context of this unique environment it is extremely necessary to perform sampling campaigns within different seasons, years and depositional areas of MTE.

The endorheic hydrological basin constituted by the Lake Titicaca-Desaguadero River-Lake Poopó-Coipasa Salar (TDPS), has suffered historical advances and retreats of glaciers generating enormous lakes in the past. Additionally, during at least the last century, the Altiplano of Bolivia has been affected by interannual variations characterized by a very dry or humid austral summer, this variability being associated with ENSO (El Niño Southern Oscillation) events. Moreover, since 2000 BC mining activities started with Tiwanacu civilization, and increased after the Spanish conquest. Currently, Bolivia is ranked as the third largest producer of Sb in the world, as well as fourth in Sn and Zn, and sixth in W.

To understand MTE behaviour within this Altiplanic environment, two coring campaigns were performed (dry-DS and wet-WS seasons), in which Lake Uru Uru (located north of Lake Poopó and drained by the Desaguadero River) and Cala Cala Lagoon (located within Eastern Andes Cordillera and drained by the Khala Khala River) were sampled. Sampling of sedimentary cores from Lake Uru Uru and Cala Cala Lagoon was conducted in April 2008 and February 2009. During these coring campaigns, the northern and southern areas of Lake Uru Uru, affected by historic mining industry, were sampled during the DS and WS. Additionally, for comparison purposes, the Cala Cala Lagoon, a non mining-impacted area, was sampled during the WS. Coring campaigns resulted in a total of five sediment cores, which implied 222 pore water and 91 sediment samples. Pore water samples were analysed for trace elements

(ICP-MS) and major elements (Cl^- , SO_4^{2-} ; HPLC) and nutrients (NO_3^- , NH_4^+ ; HPLC). Sediment samples were subjected to total and single selective extractions, the resulting supernatant MTE content was measured by ICP-MS and ICP-OES. Additionally, sediments were dated (^{210} Pb, ^{137} Cs and ^{241} Am) and mineralogically characterized by XRD, SEM and microprobe. Our sediment measurements were complemented with the Oruro Pilot Project (PPO) data base and geographical information system (GIS) to obtain the geochemical distribution of MTE. All results were statistically studied and correlated. The main conclusions derived from this survey are explained below.

First, we generated a geochemical background and present-time baseline of sediments from the Altiplano of Bolivia. We concluded that on the Bolivian highlands of the Oruro Department the natural geochemical background of As and Sb is significantly enhanced in comparison to the upper continental crust (UCC) composition, world background levels, industrial sites and historical mining sites, therefore, we suggest that environmental legislation should be generated according to the characteristic geochemical signature of Bolivian highlands, especially for these elements. This part of the study also demonstrated that the use of enrichment factors (EFs) based on the UCC average concentration cannot exhibit the natural geochemical characteristics of this area, as demonstrated by the use of a local EF_{CCLAC} based on the average composition of Eastern Andes Cordillera lacustrine sediments. Then we conclude that the use of the UCC for normalizing and calculating EFs, is not appropriated for determining contaminant enrichment and, on the contrary, we support the use of local EFs. We also determined that a strong multiplicity of metal(loid) sources exists that makes it difficult to discriminate between natural and anthropogenic input into this endorheic drainage basin, yet despite the multiplicity of MTE sources it was proposed that the anthropogenic impact on superficial soils is mainly related to the spreading of contaminants from the Vinto Smelter, while Lake Uru Uru was suggested to be influenced by mining activities, particularly the past and present drainage waste of the San José and Huanuni Mines.

To estimate potential mobilization and bioavailability of metal(loid)s within the Lake Uru Uru and Cala Cala Lagoon lacustrine basins, solid state partitioning (SSP) was determined through single extractions. These results plus the MTE content (TMC), major and trace elements and nutrients within pore water, diffusive fluxes and mineral determination through XRD, SEM and microprobe, helped to elucidate early diagenetic processes within these systems. The Cala Cala Lagoon sediments are anoxic and characterized by a high demand of electron acceptors for organic matter (OM) mineralization and at this site early diagenetic processes

are not hidden by evaporation/precipitation rates as in northern Lake Uru Uru. Despite the fact that pore water exhibits the highest mean concentration for dissolved Fe, Mn, Cu, Zn, Pb and U, solid fraction profiles, coarser grain size, SSP and dissolved MTE behaviour, allowed us to confirm that this site is not disturbed by anthropogenic activities and that a higher concentration in pore water is a consequence of the Cala Cala Lagoon location, closer to one of the most mineralized areas in the world. We were not able to determine if seasonal changes exert some influence on metal(loid) behaviour within this environment.

In the case of Lake Uru Uru, we proved that MTE within sediments from the northern area are less potentially available and mobile than in the southern area, yet both are more reactive in comparison to Cala Cala Lagoon sediments. Sulphate reduction is hidden in the northern area during both seasons by an evaporation effect, yet an increase in precipitation during the WS entails the return of reductive conditions responsible of releasing MTE to the pore water and possibly to the overlying water (OLW) driven by Fe- and Mn-oxyhydroxide reductive dissolution. Metal(loid) behaviour, in both dissolved and solid fractions is highly affected by an increase of precipitation. All these findings allowed us to propose that this area is potentially harmful during the WS and very reduced conditions caused by extremely rainy years (La Niña events), yet when this area is influenced by extreme aridity (El Niño events) it is very probable that MTE are stable as oxides. This is because most MTE in this area are associated with the reducible fraction (Fe- and Mn-oxyhydroxides) and oxidative conditions would release mainly the oxidizable fraction (F4), that is minimal (7±2 in DS & 8±2 in WS). Another change that would increase MTE release is an acidification of the milieu, this is because carbonates bear a significant percentage of metal(loid)s, and as determined through SSP this fraction is not destabilized under seasonal changes (DS: 15±3%; WS 18±4%). To conclude, the northern Lake Uru Uru area is more anthropogenically impacted than the Cala Cala Lagoon, as evidenced by the fact that MTEs are more reactive in the solid fraction and changes in MTEs partitioning between the DS and WS are moderate. The decrease of Cd partitioning during the WS might be explained by the fact that this is the only highly available element that is not associated with Fe- and Mn-oxyhydroxides and therefore, its release is not influenced by an increase in precipitation.

Southern Lake Uru Uru sediments are potentially the most available of all, especially during the WS. In relation to the northern Lake Uru Uru area, sulphate reduction takes place just below the WSI and evaporation does not play a significant role in dissolved MTE behaviour. In this area dissolved Sb and Mo exhibit the highest concentration during both

seasons and Cd during the DS. Within the solid fraction the establishment of reduced and anoxic conditions implies important changes in SSP, indeed, Cd, Sb, Pb and U change the main contribution percentage between the DS and WS. During the DS, MTEs are globally associated with residual (40±16%) > Fe- and Mn-oxyhydroxides (26±7%) > carbonates (16±6%) > OM/sulphides (9±8%) ≃ exchangeable (9±8%) fractions, whereas during the WS global contributions are Fe- and Mn-oxyhydroxides (31±17%) > residual (25±35%) ≃ carbonates (25±12%) > OM/sulphides (10±9%) > exchangeable (9±4%). The high variability of solid fraction profiles, the elevated concentration of dissolved Sb and Mo and the extreme variability of the SSP between the DS and WS, allow us to propose that the southern Lake Uru Uru area is the most anthropogenically impacted of all the studied sites. Huanuni Mine wastes may be related to high concentrations of dissolved Sb and the potential availability of this element in the solid fraction, because Sb is contained in most gangue minerals present in the metallogenic belts of the Eastern Andes Cordillera. Nevertheless, the Mo source has not been determined through this survey and this corresponds to an important unresolved issue, because Mo represents a competition for Cu and as demonstrated by other studies this causes dietary deficiencies in farm animals. As in northern Lake Uru Uru, we suggest that precaution must be taken during the WS, as MTEs are easily released and might reach the OLW. We stress that it is in the southern Lake Uru Uru area where most flora and fauna are observed and fishing is usually practiced. To conclude on the danger of consuming products from the southern Lake Uru Uru area, we propose detailed studies of MTE behaviour within the water column, especially during the WS and La Niña events to warn the population if necessary.

The last part of this study was related to mining history and climate influence on MTE deposition in lacustrine sediments of this area. This was achieved through southern Lake Uru Uru sediment dating and principal component analysis (PCA) performed with data of TMC, SSP, dated sediments and historic data of ENSO events in the Altiplano of Bolivia. The conclusions of this study were that during the last century, Sn exploitation has influenced deposition of Sb-Ag-Pb-Sn in sediments of the Altiplano of Oruro. Interannual seasonal changes associated with ENSO events, probably play an important role in the deposition of authigenic minerals in lacustrine sediments as seen for As and Cd after the influence of long term floods. Regional geology influences MTE deposition, yet within southern Lake Uru Uru sediments, the WS determines fractionation of solid phases, and MTE deposition. Finally, this study allowed us to propose that MTE deposition within southern Lake Uru Uru sediments might be influenced mainly by: local geology (carbonates from Ordovician-Silurian-Cretaceous sedimentary rocks

and recent volcanic rocks), Fe- and Mn-oxyhydroxides influenced by the WS, long term floods (probably associated with ENSO events) and mining origin ores and gangues. Metal(loid) deposition within Cala Cala Lagoon sediments is mainly influenced by the local geology. We believe that more studies are necessary to understand the influence of mining and seasonal and interannual climatic fluctuations on sediment deposition in this area, because Oruro and all the Altiplano of Bolivia have suffered intense mining activities since the XVIIth century and interannual climatic fluctuations have controlled the existence of immense paleolakes and recently, heavy floods and intense droughts in this area.

Conclusiones Generales

Este estudio contribuye a una mejor comprensión del comportamiento de los elementos traza metálicos (MTE; metaloides incluídos) en sedimentos lacustres del Altiplano de Bolivia y nos ha permitido establecer que los MTE en este entorno inexplorado se rigen por diferentes factores, tales como: la geología local, los cinturones metalogénicos, las actividades mineras y fundiciones, la geomorfología, los cambios climáticos estacionales e interanuales, la altitud, etc. A través de este estudio, notamos que para restringir mejor el comportamiento de los MTE y entender el contexto geoquímico general de este entorno único es extremadamente necesario realizar campañas de muestreo en las diferentes estaciones, años y áreas de deposición de los MTE.

La cuenca hidrológica endorreica constituida por el lago Titicaca-río Desaguadero-lago Poopó-salar de Coipasa (TDPS), ha sufrido avances y retrocesos históricos de glaciares generando enormes lagos en el pasado. Además, al menos durante el último siglo, el altiplano de Bolivia se ha visto afectado por variaciones de escala de tiempo interanual caracterizadas por un verano austral muy seco o húmedo, esta variabilidad asociada a los eventos ENSO (El Niño Southern Oscillation). Por otra parte, desde el año 2000 BC comenzó la actividad minera con la civilización Tiwanaku, la que se incrementó después de la conquista de los Españoles. Actualmente, Bolivia es considerado como el tercer mayor productor de Sb en el mundo, así como el cuarto en Sn y Zn, y sexto en W.

Para entender el comportamiento de los MTE en este entorno altiplánico, se realizaron dos campañas de extracción de testigos sedimentarios (estación seca-DS y estación de lluvias-WS), en las que el lago Uru Uru (situado al norte del lago Poopó y drenado por el río Desaguadero) y la laguna Cala Cala (localizada en la Cordillera de los Andes Oriental y drenada por el río Khala Khala) se muestrearon. Las campañas de muestreo en el lago Uru Uru y la laguna Cala Cala se llevaron a cabo en abril del 2008 y febrero del 2009. Durante estas campañas, las zonas norte y sur del lago Uru Uru, afectadas por minería histórica, fueron muestreadas durante la DS y la WS y con fines de comparación, la laguna Cala Cala, una zona no afectada por la minería, fue muestreada durante la WS. Ambas campañas resultaron en un total de cinco

testigos de sedimento, que dieron un total de 222 muestras de agua intersticial y 91 muestras de sedimento. Las muestras de agua intersticial fueron analizadas por elementos traza (ICP-MS), elementos mayores (Cl^- , $SO_4{}^{2-}$; HPLC) y nutrientes ($NO_3{}^-$ y $NH_4{}^+$; HPLC). Las muestras de sedimento fueron sometidas a digestion total y digestiones secuenciales paralelas, el contenido de los MTE en el sobrenadante se determinó a través de ICP-MS y ICP-OES. Además, los sedimentos fueron datados (^{210} Pb, ^{137} Cs y ^{241} Am) y caracterizados mineralógicamente por DRX, SEM y microsonda. Nuestras mediciones en los sedimentos fueron complementadas con la base de datos del Proyecto Piloto Oruro (PPO) y por sistemas de información geográfico (GIS) para obtener la distribución geoquímica de los MTE. Todos los resultados fueron estudiados estadísticamente y correlacionados. Los principales resultados conducidos por este estudio se muestran en los párrafos siguientes.

En primer lugar, hemos generado un background y una línea de base geoquímica para los sedimentos del altiplano de Bolivia. A través de estos resultados llegamos a la conclusión que en el altiplano boliviano del Departamento de Oruro, el background geoquímico natural de As y Sb es significativamente mayor en comparación con la composición de la corteza continental superior (UCC), niveles background mundiales, centros industrializados y sitios mineros históricos, por lo tanto, sugerimos que la legislación ambiental debe ser generada de acuerdo con el fondo geoquímico característico del altiplano de Bolivia, especialmente para estos elementos. Esta parte del estudio también demostró que el uso de factores de enriquecimiento (EFs) basados en la concentración media de la UCC no pueden exhibir las características geoquímicas naturales de esta zona, como lo demuestra el uso de un EF_{CCLAC} local basado en la composición media de los sedimentos lacustres de la Cordillera de los Andes Oriental. Por lo tanto llegamos a la conclusión que el uso de la UCC para la normalización y el cálculo de los EFs, no es apropiada para determinar enriquecimiento de contaminantes y, por el contrario, apoyamos el uso de la EFs locales. También determinamos que existe una gran multiplicidad de fuentes de MTE las que dificultan distinguir los aportes naturales y antropogénicos de MTE en esta cuenca endorreica, sin embargo, y a pesar de la multiplicidad de fuentes de MTE se propuso que el impacto antropogénico en los suelos superficiales se relaciona principalmente con la difusión de contaminantes desde la fundición de Vinto, mientras que el lago Uru Uru es afectado por las actividades mineras, en particular los residuos pasados y presentes de las minas San José y Huanuni.

Para estimar el potencial de movilización y biodisponibilidad de los MTE en los sistemas lacustres del lago Uru Uru y la laguna Cala Cala, se determinó el particionamiento en estado

sólido (SSP) mediante extracciones paralelas. Estos resultados más el contenido total de MTE (TMC), los elementos traza, mayores y nutrientes en el agua intersticial, flujos difusivos y determinación de minerales a través de DRX, SEM y microsonda, ayudaron a esclarecer los procesos diagenéticos tempranos en estas cuencas. Los sedimentos de la laguna Cala Cala son anóxicos y se caracterizan por una alta demanda de receptores de electrones para la mineralización de la materia orgánica (OM) y en este sitio los procesos de diagénesis temprana no están ocultos por las tasas de evaporación/precipitación como en el norte del lago Uru Uru. A pesar que el agua intersticial presenta la mayor concentración media de Fe, Mn, Zn, Pb y U disuelto, los perfiles de la fracción sólida, el tamaño de grano más grueso, el SSP y el comportamiento de los MTE disueltos, nos permitieron confirmar que este sitio no es perturbado por las actividades antropogénicas y que la mayor concentración en el agua intersticial es una consecuencia de la localización de la laguna Cala Cala, cerca de una de las zonas más mineralizadas del mundo. No hemos podido determinar si los cambios estacionales ejercen cierta influencia en el comportamiento de los MTE en este entorno.

En el caso del lago Uru Uru, hemos demostrado que los MTE en los sedimentos de la zona norte son potencialmente menos disponibles y móviles que en la zona sur, sin embargo, ambos son más reactivos en comparación con sedimentos de la laguna Cala Cala. Durante las dos temporadas, la reducción de sulfato no se observa en la zona norte debido al efecto de la evaporación, sin embargo, el aumento de las precipitaciones durante la WS implica la restitución de las condiciones reductoras, responsables de la liberación de MTE en el agua intersticial y, posiblemente, en la columna de agua sobreyacente (OLW) conducido por la disolución reductiva de oxihidróxidos de Fe y Mn. El comportamiento de los MTE, tanto, en la fracción disuelta como sólida está fuertemente afectado por el aumento de las precipitaciones. Todos estos resultados nos permitieron proponer que esta área es potencialmente nociva durante la WS y condiciones muy reductivas producidas en años extremadamente lluviosos (La Niña). Sin embargo, cuando esta zona está afectada por extrema aridez (El Niño) es muy probable que los MTE se encuentren estables en forma oxidada. Esto es porque la mayor contribución de MTE en esta área está asociada a la fracción reducible (oxihidróxidos de Fe y Mn) y bajo condiciones oxidantes se liberaría principalmente la fracción oxidable (F4), que es mínima (7±2% en DS y 8±2 % en WS). Otro cambio que podría incrementar la liberación de MTE es una acidificación del medio, esto es debido a que los carbonatos se asocian significativamente a los MTE, y según determinaciones de SSP esta fracción no se desestabiliza por cambios estacionales (DS: 15±3%, WS: 18±4%). Para concluir, la zona norte del lago Uru Uru presenta más impacto

antropogénico que la laguna Cala Cala, esto se evidencia por el hecho que los MTE son más reactivos en la fracción particulada y por los cambios moderados en SSP entre la DS y WS. La disminución de la contribución global de Cd durante la WS podría explicarse por el hecho que este es el único elemento potencial y altamente disponible que no está asociado a oxihidróxidos de Fe y Mn y por lo tanto, su liberación no está asociada al aumento de las precipitaciones.

Los sedimentos del sector sur del lago Uru Uru son potencialmente los más disponibles de todos, especialmente durante la WS. A diferencia de la zona norte del lago Uru Uru, la reducción de sulfatos se lleva a cabo justo bajo la WSI y la evaporación no ejerce un papel preponderante en el comportamiento de los MTE disueltos. En esta área Sb y Mo disuelto presentan la mayor concentración durante las dos temporadas y Cd en DS. En la fracción sólida el establecimiento de condiciones reductoras y anóxicas implica cambios importantes en el SSP, de hecho, las contribuciones de Cd, Sb, Pb y U, cambian entre la DS y WS. En la DS, globalmente los MTE están asociados a la fracción residual (40±16%) > oxihidróxidos de Fe y Mn (26±7%) > carbonatos (16±6%) > OM/sulfuros (9±8%) ≃ fracción intercambiable (9±8%), mientras que las contribuciones globales en la WS son oxihidróxidos de Fe y Mn (31±17%) > residual (25±35%)≃ carbonatos (25±12%) > OM/sulfuros (10±9%) > intercambiables (9±4%). La alta variabilidad de los perfiles de la fracción sólida, la elevada concentración de Sb y Mo disuelto y la extrema variabilidad del SSP entre la DS y WS, nos permiten proponer que la zona sur del lago Uru Uru es la que presenta mayor impacto antropogénico de todos los sitios estudiados. Los desechos de la mina de Huanuni pueden estar relacionados con las altas concentraciones de Sb disuelto y la potencial disponibilidad de este elemento en la fracción sólida, debido a que este elemento se encuentra en la mayoría de los minerales de ganga presentes en los cinturones metalogénicos de la Cordillera de los Andes Oriental. Sin embargo, la fuente de Mo disuelto no se ha determinado a través de este estudio, lo que corresponde a un tema no resuelto importante, ya que Mo representa una competencia para Cu y como se ha demostrado en otros estudios esto podría causar deficiencias en la dieta de los animales de granja. Al igual que en el norte del lago Uru Uru, se sugiere precaución durante la WS, debido a que los MTE se liberan con facilidad y podrían alcanzar la OLW. Hacemos hincapié en que es la zona sur del lago Uru Uru, donde la mayoría de la flora y la fauna se observa y generalmente se practica la pesca. Para concluir, en relación a la peligrosidad de los productos de consumo obtenidos en la zona sur del lago Uru Uru, se proponen estudios detallados del comportamiento de los MTE en la columna de agua, especialmente durante la WS y los episodios de La Niña, en caso de advertir a la población si fuese necesario.

La última parte de este estudio estuvo relacionada con la historia de la minería y la influencia del clima sobre la deposición de MTE en sedimentos lacustres de la zona de estudio. Esto se logró a través sedimentos datados del sur del lago Uru Uru y análisis de componentes principales (PCA) realizados con datos de TMC, SSP, sedimentos datados y datos históricos de eventos ENSO en el altiplano de Bolivia. Las conclusiones de este estudio implican que durante el siglo pasado, la explotación y la producción de Sn han influido en la deposición de Sb-Ag-Pb-Sn en los sedimentos del altiplano de Oruro. Cambios estacionales interanuales asociados a los eventos ENSO, probablemente desempeñan un papel importante en la deposición de minerales autigénicos en los sedimentos lacustres como se observa para As y Cd después de períodos de inundación de largo plazo. La geología regional influye en la deposición de MTE, sin embargo, en los sedimentos del sur del lago Uru Uru, la WS influye importantemente en el SSP y la deposición de MTE. Por último, este estudio permitió proponer que la deposición MTE en los sedimentos del sur del lago Uru Uru podría estar influenciada principalmente por: la geología local (carbonatos en rocas sedimentarias del Ordovícico-Silúrico-Cretácico y rocas volcánicas recientes), oxihidróxidos de Fe y Mn influenciados por la WS e inundaciones de largo plazo (probablemente asociadas a eventos ENSO) y menas y gangas minerogenéticas. En cambio, la deposición de MTE en los sedimentos de la laguna Cala Cala está principalmente influenciada por la geología local. Creemos que se necesitan más estudios para comprender la influencia de la minería y las fluctuaciones climáticas estacionales e interanuales en la deposición de sedimentos en esta área, debido a que Oruro y todo el altiplano de Bolivia han sufrido actividades mineras intensas desde el siglo XVII y las fluctuaciones climáticas interanuales han controlado la existencia de enormes paleolagos y, recientemente, profusas inundaciones y largas sequías en este sector.

Conclusions Générales

Cette étude contribue à une meilleure compréhension du comportement des éléments traces métalliques (MTE; métalloïdes inclus) dans les sédiments lacustres de l'Altiplano de Bolivie et nous a permis d'établir que les MTE dans cet environnement inexploré sont régis par différents facteurs, tels que: la géologie, les ceintures métallogéniques, les activités minières et de fonderie, la géomorphologie, les changements climatiques saisonniers et interannuels, l'altitude, etc. Grâce à cette étude, nous avons constaté que pour mieux contraindre le comportement des MTE et comprendre le contexte géochimique général de cet environnement unique, des campagnes d'échantillonnage au cours des différentes saisons, années et dans les zones de dépôt des MTE sont extrêmement nécessaires.

Le bassin hydrologique endoréique composé par le Lac Titicaca- la Rivière Desaguadero-le Lac Poopó-le Salar de Coipasa (TDPS) a souffert des avancées et des retraits historiques des glaciers en créant d'immenses lacs dans le passé. En outre, au moins au cours du siècle dernier, les hauts plateaux de la Bolivie ont été affectés par des changements d'échelle de temps interannuelle caractérisés par un été austral très sec ou très humide: cette variabilité a été associée à des événements ENSO (El Niño Southern Oscillation). En outre, depuis 2000 av. J.C. l'exploitation minière a commencé avec la civilisation Tiwanaku. Cette exploitation a augmenté après la conquête espagnole. Actuellement, la Bolivie est considérée comme le troisième plus grand producteur de Sb dans le monde, le quatrième de Sn et Zn, et le sixième de W.

Pour comprendre le comportement des MTE dans cet environnement montagneux, deux campagnes d'échantillonnage de carottes sédimentaires (l'une en saison sèche-DS et l'autre en saison des pluies-WS) on été réalisées, dans le lac Uru Uru (situé au nord du lac Poopó et drainé par la Rivière Desaguadero) et la lagune Cala Cala (située dans la Cordillère des Andes Orientale et drainée par la Rivière Khala Khala). Ces campagnes d'échantillonnage ont eu lieu en avril 2008 et février 2009. Au cours de ces campagnes, le nord et le sud du lac Uru Uru, touchés par l'exploitation minière historique, ont été échantillonnés au cours

de la DS et la WS, et à titre de comparaison, la lagune Cala Cala, une région non touchée par l'exploitation minière, a été échantillonnée au cours de la WS. Les deux campagnes ont abouti à un total de cinq carottes de sédiments qui ont donné un total de 222 échantillons d'eau interstitielle et 91 échantillons de sédiments. Les échantillons d'eau interstitielle ont été analysés pour les éléments traces (ICP-MS), les éléments majeurs (Cl^- , $SO_4{}^{2-}$, HPLC) et les nutriments ($NO_3{}^-$ et $NH_4{}^+$, HPLC). Les échantillons de sédiments ont été soumis à digestion totale et digestions parallèles séquentielles. Les contenus des MTE dans le surnageant ont été déterminés par ICP-MS et ICP-OES. En outre, les sédiments ont été datés (^{210} Pb, ^{137} Cs et ^{241} Am) et minéralogiquement caractérisés par DRX, MEB et microsonde. Nos mesures dans les sédiments ont été complétées par la base des données du Projet Pilote Oruro (PPO) et les systèmes d'information géographique (GIS) pour obtenir la distribution géochimique des MTE. Tous les résultats ont été étudiés statistiquement et corrélés. Les principaux résultats menés par cette étude sont présentés dans les paragraphes suivants.

Tout d'abord, nous avons généré un bruit du fond et une ligne de fond géochimique pour les sédiments de l'Altiplano bolivien. Grâce à ces résultats, nous concluons que dans l'Altiplano bolivien du département d'Oruro, le fond géochimique naturel de As et Sb est significativement plus élevé par rapport à la composition de la croûte continentale supérieure (UCC), les niveaux de fond mondial, les centres industriels, les sites miniers historiques, et par conséquent, laissent penser que la législation environnementale doit être générée en fonction des caractéristiques de fond géochimique de l'Altiplano bolivien, en particulier de ces éléments. Cette partie de l'étude a également montré que l'utilisation de facteurs d'enrichissement (EF) basée sur la concentration moyenne de l'UCC ne peut pas afficher les caractéristiques géochimiques naturelles de cette région, comme en témoigne l'utilisation d'un EF_{CCLAC} local basé sur la composition moyenne des sédiments lacustres des Andes Orientales. Donc, nous concluons que l'utilisation de l'UCC pour la normalisation et le calcul des EFs n'est pas appropriée pour déterminer l'enrichissement de polluants et, au contraire, nous soutenons l'utilisation des EFs locaux. Nous avons également déterminé qu'il existe une multiplicité de sources des MTE et il est difficile de distinguer les apports naturels et anthropiques des MTE dans ce bassin endoréique. Cependant, malgré la multiplicité des sources des MTE, l'impact humain sur la surface du sol est lié principalement à la diffusion des polluants provenant de la Fonderie de Vinto, tandis que le lac Uru Uru est affecté par les activités minières, notamment les résidus du passé et actuels des Mines San José et Huanuni.

Pour estimer le potentiel de mobilisation et la biodisponibilité des MTE dans les systèmes

lacustres du lac Uru Uru et la lagune Cala Cala, nous avons déterminé la partition à l'état solide (SSP) par des extractions parallèles. Ces résultats, plus le contenu total des MTE (TMC), les éléments traces, les éléments majeurs et les nutriments dans l'eau interstitielle, les flux diffusifs et la détermination des minéraux par DRX, MEB et microsonde électronique, ont permis de clarifier les processus diagénétiques précoces dans ces systèmes. Les sédiments de la lagune Cala Cala sont anoxiques et sont caractérisés par une forte demande pour les accepteurs d'électrons pour la minéralisation de la matière organique (OM) et sur ce site les processus diagénétiques précoces ne sont pas masqués par le taux d'évaporation/précipitation, comme dans le nord du lac Uru Uru. Bien que l'eau interstitielle ait la plus forte concentration moyenne de Fe, Mn, Cu, Zn, Pb et U dissous, les profils de la fraction solide, la taille de grain la plus grosse, le SSP et le comportement des MTE dissous, nous sommes en mesure de confirmer que ce site n'est pas perturbé par les activités anthropiques et que la plus forte concentration dans l'eau interstitielle est une conséquence de l'emplacement de la lagune Cala Cala, près de l'un des domaines les plus minéralisés du monde. Nous n'avons pas pu déterminer si des changements saisonniers exercent une certaine influence sur le comportement des MTE dans cet environnement.

Dans le cas du lac Uru Uru, nous avons démontré que les MTE dans les sédiments du nord sont disponibles et potentiellement moins mobiles que dans le sud, bie que les deux sont plus réactifs par rapport aux sédiments de la Lagune Cala Cala. Au cours des deux saisons, la réduction du sulfate n'a pas été observée dans le nord en raison de l'effet de l'évaporation. Cependant, une augmentation des précipitations au cours du WS implique la restauration des conditions réductrices responsables de la libération des MTE dans l'eau interstitielle et, éventuellement, dans la colonne d'eau (OLW) entraînée par la dissolution réductrice des oxyhydroxydes de Fe et Mn. Le comportement des MTE, à la fois dans la fraction dissoute et solide, est fortement affecté par l'augmentation des précipitations. Tous ces résultats nous ont permis de proposer que cette région est potentiellement dangereuse pendant la WS et des conditions très réductrices produites dans les années humides (La Niña). Toutefois, lorsque cette région est touchée par une extrême aridité (El Niño), il est très probable que les MTE soient stables sous forme oxydée. C'est parce que la contribution principale des MTE dans ce domaine est associée à la fraction réductible (oxyhydroxydes de Fe et Mn) et que sous des conditions oxydantes la fraction oxydable (F4) serait libérée principalement, qui est minime (7±2% DS et 8±2% WS). Un autre changement qui pourrait augmenter la libération des MTE est une acidification du milieu. Ceci s'explique parce que les carbonates ont un pourcentage important des MTE, et comme ont montré des déterminations du SSP, cette fraction n'est pas déstabilisée par les changements

saisonniers (DS: 15±3%; WS: 18±4%). En conclusion, la zone au nord du lac Uru Uru a plus d'impact anthropique que la lagune Cala Cala, ce qui se traduit par le fait que les MTE sont plus réactifs dans la fraction particulaire et par des changements modérés du SSP entre la DS et WS. La diminution de la contribution globale de Cd au cours de la WS pourrait être expliquée par le fait que c'est le seul élément potentiel et hautement disponible qui n'est pas associé aux oxyhydroxydes du Fe et Mn et, par conséquent, leur libération n'est pas associée à une augmentation des précipitations.

Les sédiments du secteur sud du lac Uru Uru sont potentiellement les plus disponibles, en particulier au cours de la WS. Contrairement à la partie nord du Lac Uru Uru, la réduction du sulfate se déroule juste en dessous du l'interphase eau-sédiment (WSI) et l'évaporation n'exerce pas un rôle dans le comportement des MTE dissous. Dans ce domaine, Sb et Mo dissous ont la plus forte concentration au cours des deux saisons et Cd dans la DS. Dans la fraction solide, l'établissement des conditions réductrices et anoxiques implique des changements importants dans la SSP: en fait, la contribution du Cd, Sb, Pb et U change entre la DS et WS. Dans la DS, les MTE sont généralement associés à la fraction résiduelle (40±16%) > oxyhydroxydes de Fe et Mn (26±7%) > carbonates (16±6%) > OM/sulfures (9±8%) ≃ fraction échangeable (9±8%), tandis que l'ensemble des contributions dans la WS sont des oxyhydroxydes de Fe et Mn (31±17%) > fraction résiduelle (25±35%) ≃ carbonates (25±12%) > OM/sulfures (10±9%) > fraction échangeable (9±4%). La grande variabilité des profils de la fraction solide, la forte concentration de Mo et Sb dissous et l'extrême variabilité du SSP entre DS et WS, suggèrent que la zone sud du lac Uru Uru est celle qui a le plus d'impact anthropique entre tous les sites étudiées. Les déchets de la Mine de Huanuni peuvent être liés à des fortes concentrations de Sb dissous et la disponibilité éventuelle de cet élément dans la fraction solide, car Sb est présent dans la majorité des minéraux de gangue dans les ceintures métallogéniques de la Cordillère des Andes Orientale. Toutefois, la source du Mo dissous n'a pas été déterminée dans cette étude, ce qui correspond à une question importante non résolue, puisque Mo est une compétition pour le Cu, comme cela a été montré dans d'autres études, ce qui cause des déficiences dans l'alimentation des animaux de ferme. Comme dans le nord du lac Uru Uru, nous appelons à la prudence lors de la WS, parce que les MTE sont facilement libérés et pourraient atteindre l'OLW. Nous soulignons que la zone sud du lac Uru Uru est la zone où la plupart de la flore et de la faune est observé et où la pêche se fait habituellement. En conclusion, concernant le danger des produits de consommation obtenus dans la région sud du lac Uru Uru, nous proposons des études détaillées sur le comportement des MTE dans la colonne d'eau, en particulier au cours

de la WS et La Niña pour avertir la population si nécessaire.

La dernière partie de cette étude est liée à l'histoire minière et l'influence du climat sur les dépôts des MTE dans les sédiments lacustres de la zone d'étude. Ceci a été réalisé par des sédiments datés du sud du lac Uru Uru et des analyses en composantes principales (ACP) réalisées sur les données des TMC, SSP, des sédiments datés et des données historiques des événements ENSO sur les hauts plateaux de Bolivie. Les résultats de cette étude ont montré qu'au cours du siècle dernièr, l'exploitation et la production du Sn ont influencé le dépôt de Sb-Ag-Pb-Sn dans les sédiments des hauts plateaux d'Oruro. Des changements inter-saisonniers associés à des événements ENSO, jouent probablement un rôle important dans le dépôt de minéraux authigènes dans les sédiments, comme cela a été observé pour l'As et Cd après des périodes d'inondations à long terme. La géologie régionale influe sur le dépôt des MTE. Cependant, les sédiments du sud du lac Uru Uru, sont influencés par la WS, surtout le SSP et le dépôt des MTE. Enfin, cette étude permet de suggérer que les dépôts des MTE dans les sédiments du sud du lac Uru Uru pourraient être influencés principalement par: la géologie locale (roches sédimentaires carbonatées de l'Ordovicien-Silurien-Crétacé et roches volcaniques récentes), et des oxyhydroxydes de Fe et Mn influencée par des inondations à long terme (probablement associées à des événements ENSO) et les minerais et gangues minérogénétiques. En revanche, le dépôt des MTE dans les sédiments de la lagune Cala Cala est principalement influencé par la géologie locale. Nous pensons que des études supplémentaires sont nécessaires pour comprendre l'influence de l'exploitation minière et les fluctuations climatiques saisonnières et interannuelles sur les dépôts des sédiments dans ce domaine en raison que l'Altiplano de Bolivie a subi des activités minières intenses depuis le XVII^{eme} siècle et des fluctuations interannuelles du climat ont contrôlé l'existence d'énormes paléolacs et, récemment, les inondations abondantes et les sécheresses prolongées dans ce secteur.

Bibliography

[1] ALBANESE, S., DE VIVO, B., LIMA, A. & CICCHELLA, D. 2007. Geochemical background and baseline values of toxic elements in stream sediments of Campania region (Italy). *Journal of Geochemical Exploration*, **93**, 21–34.

[2] MARTÍNEZ, J., LLAMAS, J., DE MIGUEL, E., REY, J. & HIDALGO, M.C. 2007. Determination of the geochemical background in a metal mining site: example of the mining district of Linares (South Spain). *Journal of Geochemical Exploration*, **94**, 10-29.

[3] GALÁN, E., FERNÁNDEZ-CALIANI, J.C., GONZÁLEZ, I., APARICIO, I., ROMERO, A. 2008. Influence of geological setting on geochemical baselines of trace elements in soils. Application to soils of South-West Spain. *Journal of Geochemical Exploration*, **98**, 89-106.

[4] REIMANN, C. & GARRETT, R. 2005. Geochemical background-concept and reality. *Science of the Total Environment*, **350**, 12-27.

[5] HAWKES, H. E. & WEBB, J. S. 1962. Geochemistry in Mineral Exploration. New York: Harper.

[6] GARRETT, RG. 1991. *The management, analysis and display of exploration geochemical data*. Exploration geochemistry workshop. Ottawa: Geological Survey of Canada; 1991. Open File 2390.

[7] DARNLEY. A.G., BJIRKLUND, A., BOLVIKEN, B., GUSTAVAON, N., KOVAL, P., PLANT, J.A., STEENFELT, A., TAUCHID, M., XIE, X., GARRETT, R.G. & HALL, G.E.M. 1995. *A global geochemical database for environmental and resource management*. UNESCO, Paris.

[8] SALMINEN, R. & TARVAINEN, T. 1997. The problem of defining geochemical baselines. A case study of selected elements and geological materials in Finland. *Journal of Geochemical Exploration*, **60**, 91-98.

[9] SALMINEN, R. & GREGORAUSKIENE, V. 2000. Considerations regarding the definition of a geochemical baseline of elements in the surficial materials in areas differing in basic geology. *Applied Geochemistry*, **15**, 647-653.

[10] TARVAINEN, T. & KALLIO, E. 2002. Baselines of certain bioavailable and total heavy metal concentrations in Finland. *Applied Geochemistry*, **17**, 975–980.

[11] GARRETT, RG. 2003 *Geochemistry in Geological Surveys into the 21st Century*. Norwegian Geological Survey Report 2003.078, 2003.

[12] GOLDBERG, E.D. editor. 1972. *Baseline studies of pollutants in the marine environment and research recommendations*. The International Decade of Ocean Exploration (IDOE) Baseline Conference, 24-26 May 1972, New York.

[13] ZOLLER, W.H., GLADNEY, E.S., DUCE, R.A. 1974. Atmorpheric concentrations and sources of trace metals at the South Pole. *Science*, **183**, 199-201.

[14] DUCE, R.A., HOFFMANN, G.L., ZOLLER, W.H. 1975. Atmospheric trace metals at remote northern and southern hemisphere sites: pollution or natural? *Science*, **187**, 59-61.

[15] AUDRY, S., SCHÄFER, J., BLANC, G. & JOUANNEAU, J.M. 2004. Fifty-year sedimentary record of heavy metal pollution (Cd, Zn, Cu, Pb) in the Lot River reservoirs (France). *Environmental Pollution*, **132**, 413-426.

[16] SALVARREDY-ARANGUREN, M., PROBST, A., ROULET, M. & ISAURE, M. P. 2008 Contamination of surface waters by mining wastes in the Milluni Valley (Cordillera Real, Bolivia): Mineralogical and hydrological influences. *Applied Geochemistry*, **23**, 1299–1324.

[17] PUCKETT, K.J. & FINEGAN, E.J. 1980. An analysis of the element content of lichens from the Northwest Territories, Canada. *Canadian Journal of Botany*, **58**, 2073-2089.

[18] DONGARRA, G., OTTONELLO, D., SABATINO, G., TRISCARI, M. 1995. Use of lichens in detecting environmental risk and in geochemical prospecting. *Environmental Geology*, **26**, 139-146.

[19] CHABAS, A. & LEFÈVRE, R.A. 2000. Chemistry and microscopy of atmospheric particulates at Delos (Cyclades–Greece). *Atmospheric Environment*, **34**, 225-238.

[20] REIMANN, C. & DE CARITAT, P. 2000. Intrinsic flaws of element enrichment factors (EFs) in environmental geochemistry. *Environmental Science & Technology*, **34**, 5084-5091.

[21] REIMANN, C. & DE CARITAT, P. 2005. Distinguishing between natural and anthropogenic sources for elements in the environment: regional geochemical surveys versus enrichment factors. *Science of the Total Environment*, **337**, 91-107.

[22] JANSSEN, CR., DE SCHAMPHELAERE, K., HEIJERICK, D., MUYSSEN, B., LOCK, K., BOSSUYT, B., VANGHELUWE, M., VAN SPRANG, P. 2000. Uncertainties in the environmental risk assessment of metals. *Human and Ecological Risk Assessment*, **6**, 1003-1018.

[23] ALLEN, HE., EDITOR. 2002. *Bioavailability of Metals in Terrestrial Ecosystems: Importance of Partitioning for Bioavailability to Invertebrates*, Microbes, and Plants. Pensecola, FL, USA: SETAC.

[24] DAS, D., CHATTERJEE, A., MANDAL, BK., SAMANTA, G., CHAKRABORTI, D. 1995. Arsenic in groundwater in six districts of West Bengal, India: the biggest arsenic calamity in the world: Part 2. Arsenic concentration in drinking water, hair, nails, urine, skin scale and liver tissue (biopsy) of the affected people. *Analyst*, **120**, 917 – 24.

[25] SMITH, AH., LINGAS, EO., RAHMAN, M. 2000. Contamination of drinking-water by arsenic in Bangladesh: a public health emergency. *Bulletin of World Health Organisation*, **78**, 1093–1103.

[26] TAN JIANAN, EDITOR. 1989. *The Atlas of Endemic Diseases and their Environments in the People's Republic of China*. Beijing, China: Science Press.

[27] COMBS Jr GF., WELCH, RM., DUXBURY, JM., UPHOFF, NT., NESHEIM, MC., EDITORS. 1996. *Food-based Approaches to Preventing Micronutrient Malnutrition: An International Research Agenda.* Cornell, New York: CIIFAD, Cornell University.

[28] RILEY, JP. & CHESTER, R. 1971. *Introduction to Marine Chemistry.* Academic Press, New York, 465 pp.

[29] MARTIN, JM. & WHITFIELD, M. 1983. *The significance of the river input of chemical elements to the ocean. In Trace metals in sea water.* Wong, CS., Boyle, E., Bruland, KW., Burton, JD. and Goldberg, ED. (eds). New York: Plenum; pp. 265-296.

[30] FERGUSSON, JE. 1990. *Heavy elements in the environment. In The heavy elements: Chemistry, Environmental Impact and Health Effects.* Pergamon Press, pp. 143-166.

[31] GARRELS, RM. & MACKENZIE, FT. 1971. *Evolution of sedimentary rocks.* Norton, W.W. (Ed), New York, 397 pp.

[32] PIDWIRNY, M. 2006. *The Hydrologic Cycle.* Fundamentals of Physical Geography, 2nd Edition. Date Viewed. Pidwirny, M. 2006

[33] DREVER, JI. 1988. *The geochemistry of natural waters.* Prentice Hall, 388 pp.

[34] RICHERSON, J., WIDMER, C., KITTEL, T. 1977. The limnology of Lake Titicaca (Peru-Bolivia), a large, high altitude, tropical lake. *Institute of Ecology Publication*, **14**.

[35] BELL, R.E., STUDINGER, M., TIKKU, A.A., CLARKE, G.K.C. GUTNER, M.M., MEERTENS, C. 2002. Origin and fate of Lake Vostok water frozen to the base of the East Antarctic ice sheet, *Nature*, **417**, 307-310, doi:10.1038/416307a.

[36] WHITE, A.F. & BLUM, A.E., 1995. Effects of climate on chemical weathering in watersheds. *Geochimica et Cosmochimica Acta*, **59**, 1729-1747.

[37] ZHANG, J. 1995. Geochemistry of Trace Metals from Chinese River/Estuary Systems: An Overview. Estuarine, *Coastal and Shelf Science*, **41**, 631-658.

[38] SHAFER, MM., OVERDIER, JT., PHILLIPS, H., WEBB, D., SULLIVAN, JR., ARMSTRONG, DE. 1999. Trace metals levels and partitioning in Wisconsin Rivers. *Water, Air and Soil Pollution*, **110**, 273-311.

[39] POULTON, SW. & RAISWELL, R. 2000. Solid phase associations, oceanic fluxes and the anthropogenic perturbation of transition metals in world river particulates. *Marine Chemistry*, **72**, 17-31.

[40] BRICKER, OP. & JONES, BF. 1995. *Main factors affecting the composition of natural waters.* In Trace Elements in Natural Waters. Salbu, B. and Steinnes, E. (eds); CRC Press, pp. 1-20.

[41] MARTIN, JM. & MEYBECK, M. 1979. Elemental mass-balance of material carried by major world rivers. *Marine Chemistry*, **7**, 173-206.

[42] TUREKIAN, KK. 1977. The fate of metals in the oceans. *Geochimica et Cosmochimica Acta*, **41**, 1139-1144.

[43] HOLLAND, HD. 1978. *The chemistry of the Atmosphere and Oceans.* Wiley, New York.

[44] BLUTH, GJS. & KUMP, LR. 1994. Lithologic and climatologic control of river chemistry. *Geochimica et Cosmochimica Acta*, **58**, 2341-2359.

[45] GOLDISH, SS. 1938. A study of rock weathering. *Journal of Geology*, **46**, 17-58.

[46] STALLARD, RF. 1988. *Weathering and erosion in the humid tropics.* In Physical and Chemical Weathering in Geochemical Cycles. Lerman, A. and Meybeck, M. (eds), Kluwer, pp. 225-246.

[47] CANFIELD, DE. 1997. The geochemistry of river particulates from the continental USA: Major elements. *Geochimica et Cosmochimica Acta*, **61**, 3349-3365.

[48] GALLOWAY, JN., THORNTON, JD., NORTON, SA., VOLCHOK, HL., McLEAN, RAN. 1982. Trace metals in atmospheric deposition: a review and assessment. *Atmospheric Environment*, **16**, 1677-1700.

[49] NRIAGU, JO. 1989. A global assessment of natural sources of atmospheric trace metals. *Nature*, **338**, 47-49.

[50] PACYNA, JM. 1986. Atmospheric trace elements from natural and anthropogenic sources. *Advances in Environmental Science and Technology*, **17**, 33-52.

[51] PATTERSON, CC. & SETTLE, DM. 1987. Review of data on eolian fluxes of industrial and natural lead to the lands and seas in remote regions on a global scale. *Marine Chemistry*, **22**, 163–177.

[52] TALBOT, RW., ANDREAE, MO., ANDREAE, TW., HARRISS, RC. 1988. Regional aerosol chemistry of the Amazon Basin during the dry season. *Journal of Geophysical Research*, 93, 1499-1508.

[53] JENNE, EA. 1995. Metal adsorption onto and desorption from sediments, 2. Artifact effects. *Marine & Freshwater Research*, **46**, 1-18.

[54] PETERSEN, W., WALLMAN, K., LI, P., SCHROEDER, F., KNAUTH, HO. 1995. Exchange of trace elements at the sediment-water interface during early diagenetic processes. *Marine & Freshwater Research,* **46**, 19-26.

[55] MORFORD, JL. & EMERSON, S. 1999. The geochemistry of redox sensitive trace metals in sediments. *Geochimica et Cosmochimica Acta*, **63**, 1735-1752.

[56] ANSCHUTZ, P., SUNDBY, B., LEFRANÇOIS, I., LUTHER, GW., MUCCI, A. 2000. Interactions between metal oxides and nitrogen and iodine in bioturbated marine sediments. *Geochimica et Cosmochimica Acta*, **64**, 2751-2763.

[57] WARREN, LA. & HAACK, EA. 2001. Biogeochemical controls on metal behaviour in freshwater environments. *Earth-Science Reviews*, **54**, 261-320.

[58] NELSON, YM., LION, LW., GHIORSE, WC., SHULER, ML. 1999a. Production of biogenic Mn oxydes by Leptothrix discophora S-1 in a chemically defined growth medium and evaluation of their Pb adsorption characteristics. *Applied and Environmental Microbiology*, **65**, 175-180.

[59] STUCKI, JR., KOMADEL, P., WILKINSON, HT. 1987. Microbial reduction of structural Iron(III) in smectites. *Soil Science Society of American Journal*, **51**, 1663-1665.

[60] ARNOLD, RG., DICHRISTINA, TJ., HOFFMAN, MR. 1988. Reductive dissolution of Fe(III) oxides by Pseudomonas sp. 200. *Biotechnology and Bioengineering,* **32**, 1081-1096.

[61] LOVLEY, DR. 1991. Dissimilatory Fe(III) and Mn(IV) reduction. *Microbiological Reviews*, **55**, 259-289.

[62] PARMAR, N., WARREN, LA., RODEN, EE., FERRIS, FG. 2000. Solid phase capture of strontium by the iron reducing bacteria Shewanella alga strain BrY. *Chemical Geology*, **169**, 281-288.

[63] PHILLIPS, EJ., LOVLEY, DR., RODEN, EE. 1993. Composition of non-microbially reducible Fe(III) in aquatic sediments. *Applied Environmental Microbiology*, **59**, 2727-2729.

[64] REICHARDT, W. 1998. *Ecotoxicity of certain heavy metals affecting bacteria-mediated biogeochemical pathways in sediments.* In Sediments and Toxic Substances. Calmano, W. and Förstner, U. (eds); pp. 159-178.

[65] CHESTER, R. 1990. *Marine Geochemistry.* Unwin Hyman, London. 698 pp.

[66] SKOUSEN, JG., SEXSTONE, A., ZIEMKIEWICKZ, PF. 2000. *Acid mine drainage control and treatment.* Eds. Barnhisel, RI., Darmody, RG., Daniels, WL. Reclamation of drastically disturbed lands. p 131-168 SKOUSE, J., HILTON, T., FAULKNER, B. Overview of Acid Mine Drainage Treatment with Chemicals. West Virginia University, Extension Service. Skousen et al.

[67] AXTMANN, EV. & LUOMA, SN. 1991. Large scale distribution of metal contamination in fine-grained sediments of the Clarl Fork river, Montana, USA. *Applied Geochemistry*, **6**, 75-88.

[68] SALOMONS, W. 1995. Environmental impact of metals derived from mining activities: Processes, predictions, prevention. *Journal of Geochemical Exploration*, **52**, 5-23.

[69] TOWN, RM. & FILELLA, M. 2002. Implications of natural organic matter binding heterogeneity on understanding lead(II) complexation in aquatic systems. *Science of the Total Environment*, **300**, 143–154.

[70] KIMBALL, BA., CALLENDER, E., AXTMANN, EV. 1995. Effects of colloids on metal transport in a river receiving acid mine drainage, upper Arkansas River, Colorado, U.S.A. *Applied Geochemistry*, **10**, 285-306.

[71] SANTSCHI, PH., LENHART, JJ., HONEYMAN, BD. 1997. Heterogeneous processes affecting trace contaminant distribution in estuaries: the role of natural organic matter. *Marine Chemistry*, **58**, 99-125.

[72] MOREL, FMM. & GSCHWEND, PM. 1987. *The role of colloids in the partitioning of solutes in natural waters.* In Aquatic Surface Chemistry. Stumm., W. (ed.), Wiley, New York.

[73] SCHULTNESS, CP. & HUANG, CP. 1991. *Journal of Soil Science Society of America*, **55**, 34–42.

[74] TIPPING, E. 1981. Adsorption by goethite (α-FeOOH) of humic substances from three different lakes. *Chemical Geology*, **33**, 81-89.

[75] HETLAND, S., MARTINSEN, I., RADZUK, B., THOMASSEN, Y. 1991. Species analysis of inorganic compounds in workroom air by atomic spectroscopy. *Analytical Sciences*, **7**, 1029-1032.

[76] TEMPLETON, DM., ARIESE, F., CORNELIS, R., DANIELSSON, LG., MUNTAU, H., VAN LEEUWEN, HP. 2000. IUPAC guidelines for terms related to chemical speciation and fractionation of trace elements. *Pure Applied Chemistry*, **72**, 72-143.

[77] BERNHARD, M., BRINCKMAN, FE., SADLER, PS. (EDS). 1986. *The importance of chemical "speciation" in environmental processes* (Springer-Verlag, Berlin). Dahlem-Konferenzen, Life Sciences Research Report 33, 763p.

[78] GÓMEZ-ARIZA, JL., MORALES, E., GIRÁLDEZ, I., SÁNCHEZ-RODAZ, D. 2001. *Sample treatment and Storage in Speciation Analysis.* In Trace Element Speciation for Environment, Food and Health. Ebdon, L., Pitts, L., Cornelis, R., Crews, H., Donard, O.F.X. and Quevauviller, Ph. (eds). Royal Society of chemistry, Cambridge, 51-80.

[79] SALOMONS, W. & FÖRSTNER, U. 1984. *Metals in the hydrocycle* (Springer-Verlag, Berlin Heidelberg New York Tokyo).

[80] FILLELA, M., TOWN, R., BUFFLE, J. 1995. *Speciation in fresh waters.* In Chemical Speciation in the environment. Ure, A.M. and Davidson, C.M. (eds); Blackie Academic and Professional, 169-200.

[81] JENNE, EA. 1968. *Controls on Mn, Fe, Co, Ni, Cu, and Zn concentrations in soils and water: the significant role of hydrous Mn and Fe oxides.* In Trace Inorganics in water. Baker, R.A. (ed), ACS Publication 73, Washington, 337-387.

[82] HONEYMAN, BD. & SANTSCHI, PH. 1988. Metals in aquatic systems. *Environmental Science & Technology*, **22**, 862-871.

[83] WARREN, LA. & ZIMMERMAN, AP. 1994. The importance of surface area in metal sorption by oxides and organic matter in a heterogeneous natural sediment. *Applied Geochimistry*, **9**, 245-254.

[84] TESSIER, A. 1993. *Sorption of trace elements on natural particles in oxic environments.* In Environmental Particles, 2, 425-453. BUFFLE, J.R. & VAN LEEUWEN, H.P. (eds), Lewis Publishers.

[85] BUFFLE, J. & VAN LEEUWEN, HP. 1992. *Environmental particles I.* – Environmental Analytical and Physical Chemistry Series, Lewis Publishers, 554 pp.

[86] PULS, RW., POWELL, RM., CLARK, D., ELDRED, CJ. 1991. Effect of pH, solid/solution ratio, ionic strength, and organic acids on Pb and Cd sorption to Kaolinite. *Water, Air and Soil Pollution*, **57-58**, 423-430.

[87] AHMANN, D., KRUMHOLTZ, LR., HERMOND, HF., LOVLEY, DR., MOREL, FMM. 1997. Microbial mobilization from sediments of the Aberjona watershed. *Environmental Science & Technology*, **31**, 2923-2930.

[88] BROWN, DA., SHERIFF, BL., SAWICKI, JA., SPARLING, R. 1999a. Precipitation of iron minerals by a natural microbial consortium. *Geochimica et Cosmochimica Acta*, **63**, 2163-2169.

[89] BROWN, GE., HENRICH, VE., CASEY, WH., CLARK, DL., EGGLESTON, C., FELMY, A., GOODMAN, DW., GRATZEL, M., MACIEL, G., McARTHY, MI., NEALSON, KH., SVERJENSKY, DA., TONEY, MF., ZACHARA, JM. 1999b. Metal oxide surfaces and their interactions with aqueous solution and microbial organisms. *Chemical Reviews*, **99**, 77-174.

[90] RICHARD, FC. & BOURG, CM. 1991. Aqueous geochemistry of chromium: a review. *Water Research*, **25**, 807-816.

[91] BARUTHIO, F. 1992. Toxic effects of chromium and its compounds. *Biological Trace Element Research*, **32**, 145-153.

[92] POHL, C. & HENNINGS, U. 1999. The effect of redox processes on the partitioning of Cd, Pb, Cu and Mn between dissolved and particulate phases in the Baltic Sea. *Marine Chemistry*, **65**, 41-53.

[93] NOLTING, RF., HELDER, W., DE BAAR, HGW., GERINGA, LJA. 1999. Contrasting behavior of trace metals in the Scheldt estuary in 1978 compared to recant years. *Journal of Sea Research*, **42**, 275-290.

[94] DZOMBACK, D., ASCE, AM., MOREL, FMM. 1987. Adsorption of inorganic pollutants in aquatic systems. *The Journal of Hydraulic Engineering*, **113**, 430-475.

[95] WARREN, LA. & ZIMMERMAN, AP. 1994. The importance of surface area in metal sorption by oxides and organic matter in a heterogeneous natural sediment. *Applied Geochimistry*, **9**, 245-254.

[96] COSTON, JA., FULLER, CC., DAVIS, JA. 1995. Pb^{2+} and Zn^{2+} adsorption by a natural aluminium- and iron-bearing surface coating on a aquifer sand. *Geochimica et Cosmochimica Acta*, **59**, 3535-3547.

[97] BUCKLEY, A. 1989. An electron microprobe investigation of the chemistry of ferromanganese coatings on freshwater sediments. *Geochimica et Cosmochimica Acta*, **53**, 115-124.

[98] TESSIER, A., FORTIN, D., BELZILE, N., DeVITRE, RR., LEPPARD, GG. 1996. Metal sorption to diagenetic iron and manganese oxyhydroxides and associated organic matter: narrowing the gap between field and laboratory measurements. *Geochimica et Cosmochimica Acta*, **60**, 387-404.

[99] MARTÍNEZ, CE. McBRIDE, MB. 1998. Solubility of Cd^{2+}, Cu^{2+}, Pb^{2+} and Zn^{2+} in aged coprecipitates with amorphous iron hydroxydes. *Environmental Science & Technology*, **32**, 743-748.

[100] WEBSTER, JG., SWEDLUND, PJ., WEBSTER, KS. 1998. Trace metal adsorption onto an acid mine drainage iron(III) oxyhydroxysulfate. *Environmental Science & Technology*, 32, 1361-1368.

[101] STUMM, W. & MORGAN, JJ. 1996. *Aquatic chemistry.* 3rd ed. John Wiley and sons, Inc., New York; 1022 pp.

[102] SCHWERTMAN, U. CORNELL, RM. 1991. *Iron Oxides in the Laboratory: Preparation and Characterization.* VCH.

[103] DAVIDSON, W. & DE VITRE, R. 1993. *Iron particles in freshwater.* In Environmental Particles. Buffle, J. and van Leeuwen, H.P. (eds); Lewis Publishers, 1,315-355.

[104] FORD, RG., BERTSCH, PM., FARLEY, KJ. 1997. Changes in transition and heavy metal partitioning during hydrous iron oxide aging. *Environmental Science & Technology*, **31**, 2028-2033.

[105] LABERTY, C. & NAVROTSKY, A. 1998. Energetics of stable and metastable low-temperature iron oxides and oxyhydroxides. *Geochimica et Cosmochimica Acta*, **62**, 2905-2913.

[106] MANDERNACK, KW., POST, J., TEBO, BM. 1995. Manganese mineral formation by bacterial spores of a marine Bacillus strain SG-1: evidence for the direct oxydation of Mn(II) to Mn(IV). *Geochimica et Cosmochimica Acta*, **59**, 4393-4408.

[107] HEM, JD. & LIND, CJ. 1983. Noneequilibrium models for predicting forms of precipitated manganese oxides. *Geochimica et Cosmochimica Acta*, **47**, 2037-2046.

[108] BALISTRIERI, LS. & MURRAY, JW. 1982. The surface chemistry of δ-MnO_2 in major ion seawater. *Geochimica et Cosmochimica Acta*, **46**, 1041-1052.

[109] FULLER, CC. & HARVEY, JW. 2000. Reactive uptake of trace metals in the hyporheic zone of a mining-contaminated stream, Pinal Creek, Arizona. *Environmental Science & Technology*, **34**, 1150-1155.

[110] BENDELL-YANG, LI. & HARVEY, HH. 1992. The relative importance of manganese and iron oxides and organic matter in the sorption of trace metals by surficial lake sediments. *Geochimica et Cosmochimica Acta*, 56, 1175-1186.

[111] EMERSON, D. 2000. *Microbial oxidation of Fe(II) and Mn(II) at circumneutral pH.* In Environmental Microbe-Metal Interactions. Lovley, D.R. (ed); ASM Press, Washington, pp. 31-52.

[112] BUFFLE, J., ALTMANN, RS., FILELLA, M., TESSIER, A. 1990. Complexation by natural heterogeneous compounds: site occupation, distribution functions a normalized description of metal complexation. *Geochimica et Cosmochimica Acta*, **54**, 1535-1553.

[113] BUFFLE, J., WILKINSON, KJ., STOLL, S., FILELLA, M., ZHANG, J. 1998. A generalized description of aquatic colloidal interactions: the three-colloidal component approach. *Environmental Science & Technology*, **32**, 2887-2899.

[114] CABANISS, SE., ZHOU, SE., MAURICE, PA., CHIN, Y., AIKEN, GR. 2000. A log-normal distribution model for the molecular weight of aquatic fulvic acids. *Environmental Science & Technology*, **34**, 1103-1109.

[115] PERDUE, EM. 1989. *Effects of humic substances on metal speciation.* In Aquatic Humic Substances. Influence on Fate and Treatment of Pollutants. Suffer, I.H. and MacCarthy, P. (eds). American Chemical Society, pp. 281-295.

[116] GREEN, SA., MOREL, FMM., BLOUGH, NV. 1992. Investigation for the electrostatic properties of humic substances by fluorescence quenching. *Environmental Science & Technology*, **26**, 294-302.

[117] DAVIES-COLLEY, RJ., NELSON, PO., WILLIAMSON, KJ. 1984. Copper and cadmium uptake by estuarine sedimentary phases. *Environmental Science & Technology*, **18**, 491-499.

[118] ZACHARA, JM., RESCH, CT., SMITH, SC. 1994. Influence of humic substances on Co^{2+} sorption by a subsurface mineral separate and its mineralogic components. *Geochimica et Cosmochimica Acta,* Acta, **58**, 533-566.

[119] NELSON, YM., LION, LW., SHULER, ML., GHIORSE, WC. 1999b. Lead binding to metal oxide and organic phases of natural aquatic biofilms. *Limnology and Oceanography*, **44**, 1715-1729.

[120] VERMEER, AWP., McCULLOCH, JK., VAN RIEMSDIJK, WH., KOOPAL, LK. 1999. Metal ion adsorption to complexes of humic acid and metal oxides: deviations from additivity rule. *Environmental Science & Technology*, **33**, 3892-3897.

[121] DÜCKER, A., LEDIN, A., KARLSSON, S., ALLARD, B. 1995. Adsorption of zinc on colloidal (Hydr)oxides of Si, Al and Fe in the presence of a fulvic acid. *Applied Geochimistry*, **10**, 197-205.

[122] LENHART, JJ. & HONEYMAN, BD. 1999. Reactions at the solid/solution interface-Uranium(VI) sorption to hematite in the presence of humic acid. *Geochimica et Cosmochimica Acta*, **63**, 2891-2901.

[123] FRIMMEL, FH. & HUBER, L. 1996. Influence of humic substances on the aquatic adsorption of heavy metals on defined mineral phases. *Environment International*, **22**, 507-517.

[124] ZUYI, T., TAIWEI, C., JINZHOU, D., XIONGXIN, D., YINGJIE, G. 2000. Effect of fulvic acids on sorption of U(VI), Zn, Yb, I and Se(IV) onto oxides of aluminium, iron and silicon. *Applied Geochemistry*, **15**, 133-139.

[125] LOFTS, S. & TIPPING, E. 1998. An assemblage model for cation binding by natural particulate matter. *Geochimica et Cosmochimica Acta*, **62**, 2609-2625.

[126] FLEMMING, CA., FERRIS, FG., BEVERIDGE, TJ., BAILEY, GW. 1990. Remobilization of toxic heavy metals adsorbed to bacterial wall-clay composites. *Applied Environmental Microbiology*, **56**, 3191-3203.

[127] NELSON, YM., LO, W., LION, LW., SHULER, ML., GHIORSE, WC. 1995. Lead distribution in a simulated aquatic environment: effects of bacterial biofilms and iron oxide. *Water Research*, **29**, 1934-1944.

[128] SMALL, TD., WARREN, LA., RODEN, EE., FERRIS, FG. 1999. Sorption of strontium by bacteria, Fe(III) oxide and bacteria-Fe(III) oxide composites. *Environmental Science & Technology*, **33**, 4465-4470.

[129] DAUGHNEY, CJ. & FEIN, JB. 1998. Sorption of 2,4,6-trichlorophenol by Bacillus subtilis. *Environmental Science & Technology*, **32**, 749-752.

[130] FEIN, JB. & DELEA, D. 1999. Experimental study of the effects of EDTA on Cd adsorption by Bacillus subtilis: a test of the chemical equilibrium approach. *Chemical Geology*, **161**, 375-383.

[131] PEDERSEN, TF., VOGEL, JS., SOUTHON, JR. 1986. Copper and Manganese in hemipelagic sediments at 21°N, East Pacific Rise: Diagenetic contrasts. *Geochimica et Cosmochimica Acta*, **50**, 2019-2031.

[132] FINNEY, BP., LYLE, MW., HEATH, GR. 1988. Sedimentation at MANOP site H (Eastern Equatorial Pacific) over the past 400,000 years: Climatically induced redox effect on transition metal cycling. *Paleoceanography*, **3**, 169-189.

[133] SHAW, TJ., GIESKES, JM., JAHNKE, RA. 1990. Early diagenesis in differing depositional environments: The response of transition metals in pore water. *Geochimica et Cosmochimica Acta*, **54**, 1233-1246.

[134] FROELICH, PN., KLINKHAMMER, GP., BENDER, ML., LUEDTKE, NA., HEATH, GR., CULLEN, D., DAUPHIN, P., HAMMOND, D., HARTMAN, B., MAYNARD, V. 1979. Early oxidation of organic matter in pelagic sediments of the Eastern Equatorial Atlantic: suboxic diagenesis. *Geochimica et Cosmochimica Acta*, **43**, 1075-1090.

[135] DE LANGE, GJ. 1986. Early diagenetic reaction in interbeded pelagic and turbiditic sediments in the Nares Abyssal Plain (Western North Atlantic): consequences for the composition of sediment and interstitial water. *Geochimica et Cosmochimica Acta*, **50**, 2543-2561.

[136] BERNER, RA. 1980. *Early Diagenesis: A theoritical Approach.* Princeton Univ. Press.

[137] REDFIELD, AC., KETCHUM, BH., RICHARDS, FA. 1963. *The influence of organisms on the composition of sea-water.* In The Sea, 2. Hill, M.N. (ed); Wiley Interscience, New York; pp. 26-77.

[138] FURRER, G. & WEHRLI, B. 1996. Microbial reactions, chemical speciation, and multicomponent diffusion in pore waters of a eutrophic lake. *Geochimica et Cosmochimica Acta*, **60**, 2333-2346.

[139] DE VITRE, R., BELZILE, R., TESSIER, A. 1991. Speciation and adsorption of arsenic on diagenetic iron oxyhydroxides. *Limnology and Oceanography*, **36**, 1480-1485.

[140] MUCCI, A., BOUDREAU, B., GUIGNARD, C. 2003. Diagenetic mobility of trace elements in sediments covered by a flash flood deposit: Mn, Fe and As. *Applied Geochemistry*, **18**, 1011-1026.

[141] CANFIELD, D., THAMDRUP, B., HANSEN, J.W. 1993. The anaerobic degradation of organic matter in Danish coastal sediments: Fe reduction, Mn reduction, and sulfate reduction. *Geochimica et Cosmochimica Acta*, **57**, 3867-3883.

[142] URE, AM., QUEVAUVILLER, P., MUNTAU, H., GRIEPINK, B. 1993. Speciation of heavy metals in soils and sediments. An account of the improvement and harmonization of extraction techniques undertaken under the auspices of the BCR of the commission of the European Communities. *International Journal of Environmental Analytical Chemistry*, **51**, 135-151.

[143] QUEVAUVILLER, P. 2002. Operationally-defined extraction procedures for soil and sediment analysis. Part 3: New CRMs for trace-element extractable contents. *Trends in Analytical Chemistry*, **21**, 774-784.

[144] FÖRSTNER, U. & WITTMANN, GTW. 1981. *Metal pollution in the aquatic environment* (Springer-Verlag, Berlin Heidelberg New York Tokyo).

[145] PICKERING, WF. 1986. Metal ion speciation; soils and sediments (a review). *Ore Geology Reviews*, **1**, 83-146.

[146] TESSIER, A. & CAMPBELL, PGC. 1987. Partitionning of trace metals in sediments: relationships with bioavailibility. *Hydrobiologia*, **149**, 43-52.

[147] BATLEY, GE. (ED) 1989. *Trace element spéciation: Analytical methods and problems* (CRC Press, Boca Raton, Florida).

[148] SALOMONS, W. & FÖRSTNER, U. 1980. Trace Metal Analysis on Polluted Sediments. Part II: Evaluation of Environmental Impact. *Environmental Technology Letters*, **1**, 506-517.

[149] FÖRSTNER, U. 1993. Metal speciation–General concepts and applications. *International Journal of Environmental Analytical Chemistry*, **51**, 5-23.

[150] TRAMONTANO, JM. & BOHLEN, WF. 1984. The nutrient and trace metal geochemistry of a dredge plume. *Estuarine, Coastal and Shelf Science*, **18**, 385-401.

[151] BENOIT, G., OKTAY-MARSHALL, SD., CANTU, A., HOOD, EM., COLEMAN, CH., CORAPCIOGLU, MO., SANTSCHI, PH. 1994. Partitioning of Cu, Pb, Ag, Zn, Fe, Al, and Mn between filter-retained particles, colloids, and solution in six Texas estuaries. *Marine Chemistry*, **45**, 307-336.

[152] FLEGAL, AR. & SANUDO-WILHELMY, SA. 1993. Comparable levels of trace metals contamination in two semi-enclosed embayments: San Diego Bay and South San Francisco Bay. *Environmental Science & Technology*, **27**, 1934-1936.

[153] TAPIA, J., AUDRY, S., TOWNLEY, B. 2011b. *Early diagenesis and availability of trace metals (Cu, Zn, Mo, Cd, Pb and U) and metalloids (As, Sb) in mining and smelting impacted and non-impacted lacustrine environments of the Bolivian Altiplano*. Chapter 4.

[154] TESSIER, A., CAMPBELL, PGC., BISSON, M. 1979. Sequential extraction procedure for the speciation of particulate trace metals. *Analytical Chemistry*, **51**, 844-851.

[155] CUNDY, AB. & CROUDACE, IW. 1995. Physical and chemical associations of radionuclides and trace metals in estuarine sediments: an example from Poole Harbour, Southern England. *Journal of Environmental Radioactivity*, **29**, 191-211.

[156] OUDDANE, B., BOUGHRIET, A., FISCHER, JC., WARTEL, M. 1997. Speciation of dissolved and particulate manganese in the Seine River estuary. *Marine Chemistry*, **58**, 189-201.

[157] CHESTER, R. & HUGES, MJ. 1967. A chemical technique for the separation of ferro-manganese minerals, carbonate minerals and adsorbed trace elements from pelagic sediments. *Chemical Geology*, **2**, 249-262.

[158] GIBBS, RJ. 1977. Transport phases of transition metals in the Amazon and Yukon rivers. *Geological Society of America Bulletin* , **88**, 829-843.

[159] SANTSCHI, PH., ADLER, D., O'HARA, P., LI, YH., DOERING, P. 1987. Relative mobility of radioactive trace elements across the sediment-water interface in the MERL model ecosystems of the Narragansett Bay. *Journal of Marine Research*, **45**, 1007-1048.

[160] GUPTA, SK. & ATEN, C. 1993. Comparison and evaluation of extraction media and their suitability in a simple model to predict the biological relevance of heavy metal concentrations in contaminated soils. *International Journal of Environmental Analytical Chemistry*, **51**, 25-46.

[161] SZEFER, P., GLASBY, GP., PEMPKOWIAK, J., KALISZAN, R. 1995. Extraction studies of heavy metal pollutants in surficial sediments from the Southern Baltic Sea off Poland. *Chemical Geology*, **120**, 111-126.

[162] BOROVEC, Z. 1995. Evaluation of the concentrations of trace elements in stream sediments by factor and cluster analysis and the sequential extraction procedures. *Science of the Total Environment*, **177**, 237-250.

[163] QUEVAUVILLER, P., URE, A., MUNTAU, H., GRIEPINK, B. 1993a. Improvement of analytical measurements within the BCR-program-Single and sequential extraction procedures applied to soil land sediments analysis. *International Journal of Environmental Analytical Chemistry*, 51, 129-134.

[164] QUEVAUVILLER, P., URE, A., MUNTAU, H., GRIEPINK, B. 1993b. Conclusions of the workshop-Single and sequential extractions in sediments and soils. *International Journal of Environmental Analytical Chemistry*, **51**, 231-235.

[165] QUEVAUVILLER, P. 1998. Operationally-defined extraction procedures for soil and sediment analysis. Part 1. Standardization. *Trends in Analytical Chemistry*, **17**, 289-298.

[166] RAPIN, F., TESSIER, A., CAMPBELL, PGC., CARIGNAN, R. 1986. Potential artifacts in the determination of metal partitioning in sediments by a sequential extraction procedure. *Environmental Science & Technology*, **20**, 836-840.

[167] KERSTEN, M. & FÖRSTNER, U. 1986. Chemical fractionation of heavy metals in anoxic estuarine and coastal sediments. *Water Science and Technology*, **18**, 121-130.

[168] RAURET, G., RUBIO, R., LÓPEZ-SÁNCHEZ, JF., CASASSAS, E. 1989a. Specific procedure for metal solid speciation in heavily polluted river sediments. *International Journal of Environmental Analytical Chemistry*, **35**, 89-100.

[169] RAURET, G., RUBIO, R., LÓPEZ-SANCHEZ, JF. 1989b. Optimization of Tessier procedure for metal solid speciation in river sediments. *International Journal of Environmental Analytical Chemistry*, **36**, 69-83.

[170] DAVIDSON, CM., THOMAS, RP., McVEY, SE., PERALA, R., LITTLEJOHN, D., URE, AM. 1994. Evaluation of a sequential extraction procedure for the speciation of heavy metals in sediments. *Analytica Chimica Acta*, **291**, 277-286.

[171] QUEVAUVILLER, P., RAURET, G., MUNTAU, H., URE, AM., RUBIO, R., LÓPEZ-SÁNCHEZ, JF., FIEDLER, HD., GRIEPINK, B. 1994. Evaluation of a sequential extraction procedure for the determination of extractable trace metal contents in sediments. *Fresenius' Journal of Analytical Chemistry*, **349**, 808-814.

[172] WHALLEY, C. & GRANT, A. 1994. Assessment of the phase selectivity of the European Community Bureau of Reference (BCR). Sequential extraction procedure for metals in sediment. *Analytica Chimica Acta*, **291**, 287-295.

[173] URE, AM. 1996. Single extraction schemes for soil analysis and related applications. *Science of the Total Environment*, **178**, 3-10.

[174] MARIN, B., VALLADON, M., POLVE, M., MONACO, A. 1997. Reproductibility testing of a sequential extraction scheme for the determination of trace metals speciation in a marine reference sediment by ICP-MS. *Analytica Chimica Acta*, **342**, 91-112.

[175] MESTER, Z., CREMISINI, C., GHIARA, E., MORABITO, R. 1998. Comparison of two sequential extraction procedures for metal fractionation in sediment samples. *Analytica Chimica Acta*, **359**, 133-142.

[176] MOSSOP, KF. & DAVIDSON, CM. 2002. Comparison of original and modified BCR sequential extraction procedures for the fractionation of copper, iron, lead; manganese and zinc in soils and sediments. *Analytica Chimica Acta*, **478**, 111-118.

[177] NIREL, P., THOMAS, AJ., MARTIN, JM. 1986. *A critical evaluation of sequential extraction techniques.* In Speciation of Fission and Activation Products in the environment. Bulman, R.A. et Cooper, J.R. (eds). Elsevier, 19-26.

[178] MARTIN, JM., NIREL, P., THOMAS, AJ. 1987. Sequential extraction techniques: promises and problems. *Marine Chemistry*, **22**, 313-341.

[179] BOURG, ACM. 1987. Trace metal adsorption modeling and particle-water interactions in estuarine environments. *Continental Shelf Research*, **7**, 1319-1332.

[180] TESSIER, A. & CAMPBELL, PGC. 1988. *Partitioning of trace metals in sediment.* In Metals Speciation: Theory, Analysis and Application. Kramer, J.R. et Allen, H.E. (eds) ; Lewis Publishers, Inc., 183-453.

[181] VAN BENSCHOTEN, JE., MATSUMOTO, MR., YOUNG, WH. 1997. Evaluation and analysis of soil washing for seven lead-contaminated soils. *Journal of Environmental Engineering*, **123**, 217-224.

[182] BERMOND, AP. & YOUSFI, I. 1997. Etude de la validité de comparaisons fondées sur l'application de procédures d'extractions séquentielles appliquées à des échantillons de terre. *Environmental Technology*, **18**, 219-224.

[183] HARRINGTON, JM., LAFORCE, MJ., REMBER, WC., FENDORF, SE., ROSENZWEIG, RF. R.F., 1998. Phase associations and mobilization of iron and trace elements in Coeur d'Alene Lake, Idaho. *Environmental Science & Technology*, **32**, 650-656.

[184] AUDRY, S., BLANC, G., SCHÄFER, J. 2006a. Solid state partitioning of trace metals in suspended particulate matter from a river system affected by smelting-waste drainage. *Science of the Total Environment,* **363**, 216 – 236.

[185] GLEYZES, C., TELLIER, S., ASTRUC, M. 2002. Fractionation of trace elements in contaminated soils and sediments: a review of sequential extraction procedures. *Trends in Analytical Chemistry*, **21**, 451-467.

[186] KHEBOIAN, C. & BAUER, F. 1987. Accuracy of selective extraction procedures for metal speciation in model aquatic sediments. *Analytical Chemistry*, **59**, 1417-1423.

[187] CHLOPECKA, A., BACON, JR., WILSON, MJ., KAY, J. 1996. Forms of cadmium, lead, and zinc in contaminated soils from Southwest Poland. *Journal of Environmental Quality*, **25**, 69-79.

[188] ARUNACHALAM, J., EMONS, H., KRASNODEBSKA, B., MOHL, C. 1996. Sequential extraction studies on homogenized forest soil samples. *Science of the Total Environment*, **181**, 147-159.

[189] RAKSASATAYA, M., LANGDON, AG., KIM, ND. 1996. Assessment of the extent of lead redistribution during sequential extraction by two different methods. *Analytica Chimica Acta*, **332**, 1-14.

[190] TESSIER, A., CAMPBELL, PGC. 1991. Comments on " Pitfalls of sequential extractions" by Nirel, M.V. and Morel, F.M.M. Wat. Res., 24: 1055-1056 (1990). *Water Research*, **25**, 115-117.

[191] BELZILE, P., LECONTE, P., TESSIER, A. 1989. Testing readsorption of trace elements during partial chemical extractions of bottom sediments. *Environmental Science & Technology*, **23**, 1015-1020.

[192] CHAO, TT. 1984. Use of partial dissolution techniques in geochimical-exploration. *Journal of Geochemical Exploration*, **20**, 101-135.

[193] STERCKEMAN, T., GOMEZ, A., CIESIELSKY, H. 1996. Soil and waste analysis for environmental risk assessment in France. *Science of the Total Environment*, **173**, 63-69.

[194] HOUBA, VGJ., LEXMOND, ThM., NOVOZAMBSKY, I. 1996. State of the art and future developments in soil analysis for bioavailability. *Science of the Total Environment*, **173**, 21-28.

[195] ATEN, CF. & GUPTA, SK. 1996. On heavy metal in soils ; rationalization of extractions by dilute salt solutions, comparison of the extracted concentrations with uptake by ryegrass and lettuce, and the possible influence of pyrophosphate on plant uptake. *Science of the Total Environment*, **173**, 45-53.

[196] TACK, FMG. & VERLOO, MG. 1996. Impact of single reagent extraction using NH4OAc-EDTA on the solid phase distribution of metals in a contaminated dredged sediment. *Science of the Total Environment*, **178**, 29-36.

[197] KENNEDY, VH., SANCHEZ, AL., OUGHTON, DH., ROWLAND, AP. 1997. Use of single and sequential chemical extractants to assess radionuclide and heavy metal availability from soils for root uptake. *Analyst*, **122**, 89-100.

[198] MEIMA, JA. & COMANS, RNJ. 1998. Application of surface complexation/precipitation modeling to contaminant to contaminant leaching from weathered solid waste incinerator bottom ash. *Environmental Science & Technology*, **32**, 688-693.

[199] ULLRICH, SM., RAMSEY, MH., HELIOS-RYBICKA, E. 1999. Total and exchangeable concentrations of heavy metals in soils near Bytom, an area of Pb/Zn mining and smelting in upper Silesia, Poland. *Applied Geochemistry*, **14**, 187-196.

[200] FARRAH, H. & PICKERING, WF. 1993. Factors influencing the potential mobility and bioavailability of metals in dried lake sediments. *Chemical Speciation and Bioavailability*, **5**, 81–96.

[201] ROSEMBERG, E. & ARIESE, F. 2001. *Quality control in speciation analysis.* In Trace element speciation for environment, food and health. Ebdon, L., Pitts, L., Cornelis, R., Crews, H., Donard, O.F.X. and Quevauviller, Ph. (eds), The Royal Society of Chemistry, Cambridge, UK.

[202] TACK, FMG., VOSSIUS, HAH., VERLOO, MG. 1996. A comparison between sediment metal fractions, obtained from sequential extraction and estimated from single samples. *International Journal of Environmental Analytical Chemistry,* **63**, 61-66.

[203] RAURET, G. 1998. Extraction procedures for the determination of heavy metals in contaminated soil and sediment. *Talanta*, **46**, 449-455.

[204] SHUMAN, LM. 1983. Separating soil-iron- and manganese- oxide fractions for microelement analysis. *Soil Science Society of America Journal*, **47**, 656-660.

[205] ANSCHUTZ, P., ZHONG, S., SUNDBY, B., MUCCI, A., GOBEIL, C. 1998. Burial efficiency of phosphorus and the geochemistry of iron in continental margin sediments. *Limnology and oceanography*, **43**, 53-64.

[206] KOTSKA, JE. & LUTHER III, GW. 1994. Partitioning and speciation of solid phase iron in saltmarsh sediments. *Geochemica et Cosmochimica Acta,* **58**, 1701–1710.

[207] AUDRY S. 2003. *Bilan géochimique du transport des éléments traces métalliques dans le système fluvial anthropisé Lot-Garonne-Gironde.* PhD Thesis, Université Bordeaux 1, Bordeaux.

[208] TERASHIMA, S. & TANIGUSHI, M. 1998. Mineralogical associations of arsenic and antimony in thirty five geochemical reference materials by sequential extraction with hydride generation and atomic absorption spectrometry. *Geostand Newslett*, **22**, 103-112.

[209] GOMMY, C. 1997. *Optimisation d'un schéma de spéciation des métaux Pb, Zn, Cd et Cu: Application à des sols pollués du Nord de la France.* Thèse, Université De Technologie de Compiègne, France.

[210] SCHÄFER, J. & BLANC, G. 2002. Relationship between ore deposits in river catchments and geochemistry of suspended particulate matter from six rivers in southwest France. *Science of the Total Environment*, **298**, 103-118.

[211] SCHÄFER, J., BLANC, G., LAPAQUELLERIE, Y., MAILLET, N., MANEUX, E., ETCHEBER, H. 2002. Ten-year observation of the Gironde tributary fluvial system: fluxes of suspended matter, particulate organic carbon and cadmium. *Marine Chemistry*, **79**, 229-242.

[212] LAVENU, A. 1992. Formation and geological evolution. In: C. Dejoux & A. litis (eds.), Lake Titicaca. A synthesis of Limnological Knowledge,Kluwer Academic Publishers. *Monogr. Biol.*, **68**, 3-15.

[213] CUNNINGHAM, C., McNAMEE, J., PINTO, J. & ERICKSEN, G. 1991. A model of volcanic dome-hosted precious metal deposits in Bolivia. *Economic Geology*, **86**, 415-421.

[214] SERTECGEOMIN. 2000. *Estudios Temáticos Integrados de los Recursos Naturales Renovables y No Renovables de Bolivia, Departamento de Oruro, Escala 1:500,000.* Publicación SGM Serie II-MTB-DEP-18, 1 mapa.

[215] GEOBOL 1992a. *Carta Geológica de Bolivia, Hoja Oruro, 6140. Escala 1:100.000.* Publicación SGB Serie I-CGB-11, 1 mapa.

[216] GEOBOL 1992b. *Carta Geológica de Bolivia, Hoja Machacamarca, 6139. Escala 1:100.000.* Publicación SGB Serie I-CGB-12, 1 mapa.

[217] ARCE-BURGOA, O. & GOLDFARB, R. 2009. *Metallogeny of Bolivia.* Society of Economic Geologists Newsletter, 79 pp, http://www.osvaldoarce.com/Metallogeny.html.

[218] AHLFELD, F. 1967. Metallogenic Epochs and Provinces of Bolivia. *Mineralium Deposita*, **2**, 291-311.

[219] WALLIANOS, A., DIETRICH, A., LEHMANN, B., MOSBAH, M. & TRAXELL, K. 1999. Trace elements analyses of melt inclusions as probes for the evolution of Bolivian tin porphyry deposits. *Nuclear Instruments and Methods in Physics Research B*, **158**, 621-627.

[220] SERTECGEOMIN. 2004. *Mapa de Depósitos Metálicos, Departamento de Oruro, Escala 1:750.000.* Publicación SGM Serie II-MTB-DEP-1D, 62 pp, 1 mapa.

[221] FORNARI, M., RISACHER, F., FERAUD, G. 2001. Dating of paleolakes in the central Altiplano of Bolivia. *Palaeogeography, Palaeoclimatology, Palaeoecology,* **172**, 269-282.

[222] USGS & GEOBOL (U.S. Geological Survey & Servicio Geólogico de Bolivia). 1992. *Geology and Mineral Resources of the Altiplano and Cordillera Occidental, Bolivia.* USGS Bulletin, 1975, 365 pp.

[223] REDWOOD, S. 1993. *The Metallogeny of the Bolivian Andes: Vancouver, British Columbia.* University of British Columbia. Mineral Deposit Research Unit, 15, 59 pp.

[224] AHLFELD, F. 1972. *Geología de Bolivia.* Editorial "Los Amigos del Libro", La Paz, 190 pp.

[225] SERVANT, M. & FONTES. J. 1978. Les lacs quaternaires des hauts plateaux des Andes boliviennes Premières interprétations paléoclimatiques. *Cahiers ORSTOM, Série Géologie*, **10**, 9-23.

[226] SERVANT, M., FOURNIER, M., ARGOLLO, J., SERVANT-VILDARY, S., SYLVESTRE, F., WIRRMANN, D., YBERT, JP. 1995. La derniere transition glaciaire/interglaciaire des Andes tropicales du sud (Bolivie) d'apres l'etude des variations des niveaux lacustres et des fluctuations glaciaires. *C. R. Acad. Sci. Paris,* **320**, 729-736.

[227] MOURGUIART, P., ARGOLLO, J., CORREGE, T., MARTIN, L., MONTENEGRO, ME., SIFEDDINE, A., WIRRMANN, D 1997. Changements limnologiques et climatologiques dans le bassin du lac Titicaca (Bolivie), depuis 30,000 ans. *C.R. Acad. Sci. Paris,* **325**, 139-146.

[228] SERVANT, M. 1977. Le cadre stratigraphique du Plio-Quaternaire de l'Altiplano des Andes tropicales en Bolivie. Bulletin AFEQ. Recherches françaises sur le Quaternaire, *lNQUA*, **1**, 323-327.

[229] LAVENU, A., FORNARI, M., SEBRIER, M. 1984. Existence de deux nouveaux episodes lacustres quaternaires dans l'Altiplano Peróu-Bolivien. *Cahiers ORSTOM, ser. Geol.,* **14**, 103-114.

[230] WIRRMANN, D. 1988. *Paleohidrologia del lago Titicaca durante el Holoceno.* Memorias del Congreso iberoamericano y del Caribe.

[231] WIRRMANN, D. & MOURGUIART, P. 1995. Late quaternary spatio-temporal limnological variations in the Altiplano of Bolivia and Peru. *Quaternary Research*, **43**, 344-354.

[232] SYLVESTRE, F., SERVANT, M., SERVANT-VILDARY, S., CAUSSE, C., FOURNIER, M., YBERT, JP. 1999. Lake-level chronology on the southern Bolivian Altiplano (18-23 S) during late-glacial time and the early Holocene. *Quaternary Research*, **51**, 54-66.

[233] BAKER, PA., SELTZER, GO., FRITZ, SC., DUNBAR, RB., GROVE, MJ., CROSS, SL., TAPIA, P., ROWE, HD., BRODA, JP. 2001. The history of South American tropical precipitation for the past 25,000 years. *Science,* **291**, 640–643.

[234] BOWMAN, I. 1909. The physiography of the Central Andes. *American Journal of Sciences*, **4**, 373-402.

[235] SYLVESTRE, F. 1997. *La derniere transition glaciaire/interglaciaire (18,000±8,000 ^{14}C ans bp) des Andes tropicales du sud (Bolivie) d'apres l'etude des diatomees.* These Doct. Museum National d'Histoire Naturelle, Paris, pp. 317

[236] WIRRMANN, D. & OLIVEIRA-ALMEIDA, LF. 1987. Low Holocene level (7,700-3,650 years ago) of Lake Titicaca (Bolivia). *Palaeogeography, Palaeoclimatology, Palaeoecology*, **59**, 315-323.

[237] WIRRMANN, D., MOURGUIART, P., OLIVEIRA-ALMEIDA, LF. 1988. *Holocene sedimentology and ostracodes repartition in Lake Titicaca. Paleohydrological interpretations.* In: Quaternary of South America and Antartic Peninsula, 6 (Rabbasa J. Ed.), pp. 89-127 (Balkema, Rotterdam).

[238] WIRRMANN, D., YBERT, JP., MOURGUIART, P. 1992. *A 20,000 years paleohydrological record from Lake Titicaca.* In: Dejoux, C., Iltis, A. (Eds.). Lake Titicaca, A Synthesis of Limnological Knowledge. Kluwer Academic Publisher, Dodrecht, pp. 40-48.

[239] RISACHER, F. & FRITZ, B. 1991. Quaternary geochemical evolution of the salars of Uyuni and Coipasa, central Altiplano, Bolivia. *Chemical Geology*, **90**, 211-231.

[240] LAZZARO, X. 1981. Biomasses, peuplements phytoplanctoniques et production primaire du lac Titicaca. *Hydrobiol. trop.*, **14**, 349-380.

[241] MOURGUIART, P. 2000. Historical changes in the environment of Lake Titicaca: Evidence from ostracod Ecology and evolution. *Advances in ecological research*, **31**, 497-520.

[242] BAUCOM, P.C., AND RIGSBY, C.A., 1996, *Quaternary fluvial sedimentology of the Rio Desaguadero Bolivia: Terrace development and implications for lake-level fluctuations (abstract):* Geological Society of America, Abstracts with Programs, 28, 304–305.

[243] BAUCOM, P.C., AND RIGSBY, C.A., 1997, *Terrace development along the Rio Desaguadero, Bolivia: Indications of Holocene climatic changes and water-level fluctuations of Lake Titicaca (abstract)*: Geological Society of America, Abstracts with Programs, 29, 219.

[244] BAUCOM, P. & RIGSBY, C. 1999. Climate and Lake-Level History of the Northern Altiplano, Bolivia, as Recorded in Holocene Sediments of the Rio Desaguadero. *Journal of Sedimentary Research*, **69**, 597-611.

[245] UNEP 1996. *Diagnóstico Ambiental del Sistema TDSP.* División de Aguas Continentales de las Naciones Unidas para el Medio Ambiente.

[246] PPO 1993-1996. *Proyecto Piloto Oruro.* Ministerio de Desarrollo Sostenible y Medio Ambiente Secretaría Nacional de Minería, Swedish Geological AB.

[247] PPO-9606 1996. *Proyecto Piloto Oruro: Hydrology of the PPO Area.* Ministerio de Desarrollo Sostenible y Medio Ambiente Secretaría Nacional de Minería, Swedish Geological AB.

[248] HASTENRATH, S. & KUTZBACH, J. 1985. Late Pleistocene climate and water budget of the South American Altiplano. *Quaternary Research*, **24**, 249-256.

[249] ROUCHY, JM., SERVANT, M., FOURNIER, M., CAUSSE, C. 1996. Extensive carbonate algal bioherms in upper Pleistocene saline lakes of the central Altiplano of Bolivia. *Sedimentology,* **43**, 973-993.

[250] PPO-9701 1997. *Proyecto Piloto Oruro: Final Report: Findings, recommendations and the environmental management plan.* Ministerio de Desarrollo Sostenible y Medio Ambiente Secretaría Nacional de Minería, Swedish Geological AB.

[251] ROCHE, MA., BOURGES, J., CORTÉS, J., MATTOS, R. 1992. Climatology and hydrology of the Lake Titicaca basin. In: Lake Titicaca, A synthesis of Limnological Knowledge, Kluwer Academic Publishers. *Monogr. Biol.*, **68**, 63-88.

[252] PPO-9612 1996. *Proyecto Piloto Oruro: Impacto de la Minería y el Procesamiento de Minerales en Cursos de Aguas y Lagos.* Ministerio de Desarrollo Sostenible y Medio Ambiente Secretaría Nacional de Minería, Swedish Geological AB.

[253] GARCÍA, M.E. 2006. *Transport of Arsenic and Heavy Metals to lake Poopó – Bolivia – Natural Leakage and anthropogenic effects.* PhD Thesis Lund University, Sweeden.

[254] PPO-9604. 1996. *Proyecto Piloto Oruro: Evaluación de Recursos Minerales y su Utilización.* Ministerio de Desarrollo Sostenible y Medio Ambiente Secretaría Nacional de Minería, Swedish Geological AB.

[255] PPO-9505. 1995. *Proyecto Piloto Oruro: Contenido de metales en los sedimentos del lago, en Totoras y Myriophyllum del Lago Uru Uru.* Ministerio de Desarrollo Sostenible y Medio Ambiente Secretaría Nacional de Minería, Swedish Geological AB.

[256] LILJA, A. & LINDE, G. 2006. *Occurrence and Distribution of Heavy Metals in three rivers on the Bolivian high plateau. A minor field study conducted in Bolivia.* MSc Thesis, University of Lund, Sweeden.

[257] GARCÍA, M.E., BUNDSCHUH, J., PERSSON, K., BENGTSSON, L., BERNDTSSON, R., RAMOS, O. & QUINTANILLA, J. 2005a. Heavy Metals in aquatic plants and their relationship to concentrations in surface water, groundwater and sediments – A case study of Poopó. *Revista Boliviana de Química*, **22**, 1.

[258] VAN DAMME, P. A., HAMEL, C., AYALA, A. & BERVOETS, L. 2008. Macroinvertebrate community response to acid mine drainage in rivers of the High Andes (Bolivia). *Environmental Pollution*, **156**, 1061-1068.

[259] MERCADO, M., GARCÍA, M. E. & QUINTANILLA, J. 2009. Evaluación de los niveles de contaminación por plomo y arsénico en muestras de suelos y productos agrícolas procedentes de la región cercana al Complejo Metalúrgico de Vinto. *Revista Boliviana de Química*, **26**, 101-110.

[260] PPO 1993-1996. *Proyecto Piloto Oruro.* Ministerio de Desarrollo Sostenible y Medio Ambiente Secretaría Nacional de Minería, Swedish Geological AB.

[261] WEDEPOHL, K. H. 1995. The composition of the continental crust. *Geochemica et Cosmochemica Acta*, **59**, 1217-1232.

[262] JCPDS-ICDD .1997. *The International Centre for Diffraction Data.*

[263] BARTHELMY, D., 2005. X-Ray Spacing.

[264] CHOMEL, P. 1990. *Le Microscope Electronique à Balayage, instrument et fonctions.* Club MEB toulouse, Toulouse.

[265] APPLEBY, PG. & OLDFIELD, F. 1983. The assessment of ^{210}Pb data from sites with varying sediment accumulation rates. *Hydrobiologia,* **103**, 29-35.

[266] APPLEBY, PG., RICHARDSON, N., NOLAN, PJ. 1991. ^{241}Am dating of lake sediments. *Hydrobiologia* **214**, 35–42

[267] OLDFIELD, F., RICHARDSON, N., APPLEBY, PG. 1995 Radiometric dating (^{210}Pb, ^{137}Cs, ^{241}Am) of recentombrotrophic peat accumulation and evidence for changes in mass balance. *The Holocene*, **5**, 141–148.

[268] VALLADON, M. 2005. Geostandards and Geoanalytical Research Bibliographic Review 2005. *Geostandards and Geoanalytical Research*, **30**, 273–305.

[269] YEGHICHEYAN, D., CARIGAN, J., VALLADON, M., BOUHNIK LE COZ, M., LE CORNEC, F., CASTREC-ROUELLE, M., ROBERT, M., AQUILINA, L., AUBRY, E., CHURLAUD, C., DIA, A., DEBERDT, S., DUPRÉ, B., FREYDIER, R., GRUAU, G., HÉNIN, O., DE KERSABIEC, AM., MACÉ, J., MARIN, L., MORIN, N., PETITJEAN, P., SERRAT, E. 2001. A compilation of silicon and thirty one trace elements measured in the Natural River Water Reference material SLRS-4 (NRC-CNRC). *Geostandards Newsletter*, **25**, 465-474.

[270] LYNCH, J. 1999. Additional Provisional Elemental values for LKSD-1, LKSD-2, LKSD-3, LKSD-4, STSD-1, STSD-2, STSD-3 and STSD-4. *Geostandards Newsletter*, **23**, 251-260.

[271] REIMANN, C., FILZMOSER, P. & GARRETT, R. G. 2005. Background and threshold: critical comparison of methods of determination. *Science of the Total Environment*, **346**, 1-16.

[272] REDWOOD, S. D. & RICE, C. M. 1997. Petrogenesis of Miocene basic shoshonitic lavas in the Bolivian Andes and implications for hydrothermal gold, silver and tin deposits. *Journal of South American Earth Sciences*, **10**, 203-221.

[273] PPO-9503 1995. *Proyecto Piloto Oruro: Interim Report March 1994-May 1995.* Ministerio de Desarrollo Sostenible y Medio Ambiente Secretaría Nacional de Minería, Swedish Geological AB.

[274] PPO-9607 1996. *Proyecto Piloto Oruro: Aspectos Ambientales de los Metales y Metaloides en el Sistema Hidrológico del Desaguadero.* Ministerio de Desarrollo Sostenible y Medio Ambiente Secretaría Nacional de Minería, Swedish Geological AB.

[275] PPO-9608 1996. *Proyecto Piloto Oruro: Studies of the Terrestrial flora and metal contamination of soils and plants in the PPO area.* Ministerio de Desarrollo Sostenible y Medio Ambiente Secretaría Nacional de Minería, Swedish Geological AB.

[276] STEINMANN, P. & SHOTYK, W. 1997. Geochemistry, mineralogy, and geochemical mass balance on major elements in two peat bog profiles (Jura Mountains, Switzerland. *Chemical Geology*, **138**, 25-53.

[277] REIMANN, C. & FILZMOSER, P. 2000. Normal and Lognormal data distributions in geochemistry: death of a myth. Consequences for the statistical treatment of geochemical and environmental data. *Environmental Geology*, **39**, 1001-1014.

[278] BONARDI, G., D'ARGENIO, D. & PERRONE, V. 1998. *Carta geologica dell'Appennino meridionale.* Memoria della Societa Geologica Italiana 41.

[279] FONTBOTÉ, J.M. 1982. *Mapa geológico y memoria explicativa de la hoja 70 (Linares), escala 1:200.000.* Instituto Geológico y Minero de España, Madrid.

[280] HOROWITZ, A. J., ELRICK, K. A. & COOK, R. B. 1993. Effect of mining and related activities on the sediments trace element geochemistry of Lake Coeur d'Alene, Idaho, USA. Part I: surface sediments. *Hydrological Processes*, **7**, 403-423.

[281] HOROWITZ, A. J., ELRICK, K. A., ROBBINS, J. A. & COOK, R. B. 1995. A summary of the effects of mining and related activities on sediment trace element geochemistry of Coeur d'Alene Lake, Idaho, USA. Part II: subsurface sediments. *Hydrological Processes*, **9**, 35-54.

[282] GROSBOIS, C. A., HOROWITZ, H., SMITH, J. & ELRICK, K. 2002. The effect of mining and related activities on the sediment trace element geochemistry of the Spokane River Basin, Washington, USA. *Geochemistry: Exploration, Environment, Analysis*, **2**, 131-142.

[283] REECE, D., FELKEY., J. & WAI, C. 1978. Heavy metal pollution in the sediments of the Coeur d'Alene River, Idaho. *Environmental Geology*, **2**, 289-293.

[284] INOANNOU, C. 1979. *Distribution, transport and reclamation of abandoned mine tailings along the channel of the South Fork, Coeur d'Alene River and tributaries, Idaho.* MSc Thesis, University of Idaho, Moscow, Idaho.

[285] HOROWITZ, A. J. 1991. *A primer on sediment-trace element chemistry.* Chelsea. Lewis Publ. Inc.

[286] PERSAUD, D., JAAGUMAGI, R. & HAYTON, A. 1993. *Guidelines for the protection and management of aquatic sediment quality in Ontario.* Ontario Ministry of the Environment and Energy, Queen's Printer for Ontario, Canada.

[287] GOIX, S., POLVÉ, M., POINT, D., OLIVA, P., GARDON, J., MAZUREK, H., DUPREY, J. L., CAZIOT, C. & FREYDIER, R. 2009. *Trace metals atmospheric survey in the mining region of the Bolivian Altiplano.* Environment, Pollution & Human Health, William Smith Meeting September 2009, London, UK.

[288] BGR (Brundesanstalt für Geowissenschaften und Rohstoffe) & Geobol (Servicio Geológico de Bolivia). 1994. Prospección y exploración de metales preciosos en el Departamento de Potosí, Bolivia. Informe Final (Tomo I-III), 510 pp and Especial Boletín del Servicio Geológico de Bolivia 5, 204 pp.

[289] GOBEIL, C., MACDONALD, R., SUNDBY, B. 1997. Diagenetic separation of cadmium and manganese in suboxic continental margin sediments. *Geochimica et Cosmochimica Acta*, **61**, 4647-4654.

[290] ALLER 1990. Bioturbation and manganese cycling in hemipelagic sediments. *Philosophical Transactions of the Royal Society of London*, **331**, 51-68.

[291] ALLER 1994. The sedimentary Mn cycle in Long Island Sound: Its role as intermediate oxidant and the influence of bioturbation, O_2 and C_{org} flux on diagenetic reaction balances. *Journal of Marine Research*, **52**, 259-295.

[292] ALLEN, JR., RAE, JE., ZANIN, PE. 1990. Metal speciation (Cu, Zn and Pb) and organic matter in an oxic salt marsh, Seven Estuary, Southwest Britain. *Marine Pollution Bull*etin, **21**, 574–580.

[293] CALVERT, S.E. & PEDERSEN, T.F. 1993. Geochemistry of recent and anoxic marine sediments: Implication for the geological records. *Marine Geol*ogy, **113**, 67–88.

[294] LASLETT, R. & BALLS, P. 1995. The behavior of dissolved Mn, Ni and Zn in the Forth, an industrialized, partially mixed estuary. *Marine Chemistry*, **48**, 311-328.

[295] ROSENTHAL, Y., LAM, P., BOYLE, E., THOMSON, J. 1995. Authigenic cadmium enrichments in suboxic sediments: Precipitation and postdepositional mobility. *Barthand Planetary Science Letters*, **132**, 99-111.

[296] KRAEPIEL, A., CHIFFOLEAU, J., MARTIN, J., MOREL, F. 1997. Geochemistry of trace metals in the Gironde estuary. *Geochimica et Cosmochimica Acta*, **61**, 1421-1436.

[297] SLOMP, C., MALSCHAERT, J., LOHSE, L., VAN RAAPHORST, W. Iron and manganese cycling in different sedimentary environments on the North Sea continental margin. *Continental Shelf Research*, **17**, 1083-1117.

[298] TANG, D., WARNKEN, K., SANTSCHI, P. 2002. Distribution and partitioning of trace metals (Cd, Cu, Ni, Pb, Zn) in Galveston Bay waters. *Marine Chemistry*, **78**, 29-45.

[299] WHITELEY, J. & PEARCE, N. 2003. Metal distribution during diagenesis in the contaminated sediments of Dulas Bay, Anglesey, N. Wales, UK. *Applied Geochemistry*, **18**, 901–913.

[300] SUNDBY, B., MARTINEZ, P., GOBEIL, C. 2004. Comparative geochemistry of cadmium, rhenium, uranium, and molybdenum in continental margin sediments. *Geochemica et Cosmochimica Acta*, **68**, 2485–2493.

[301] MORFORD, J. EMERSON, S., BRECKEL, E, KIM, S. 2005. Diagenesis of oxyanions (V, U, Re, and Mo) in pore waters and sediments from a continental margin. *Geochemica et Cosmochimica Acta*, **69**, 5021–5032.

[302] AUDRY, S., BLANC, G., SCHÄFER, J., CHAILLOU, G., ROBERT, S. 2006b. Early diagenesis of trace metals (Cd, Cu, Co, Ni, U, Mo and V) in the freshwater reaches of a macrotidal estuary. *Geochemica et Cosmochimica Acta*, **70**, 2264-2286.

[303] SOTO-JIMENEZ, M. & PAEZ-OSUNA, F. 2008. Diagenetic processes on metals in hypersaline mudflat sediments from a subtropical saltmarsh (SE Gulf of California): Postdepositional mobility and geochemical fractions. *Applied Geochemistry*, **23**, 1202–1217.

[304] POSTMA, D. & JAKOBSEN, R. 1996. Redox zonation: Equilibrium constraints on the Fe(III)/SO_4^{2-} reduction interface. *Geochemica et Cosmochimica Acta,* **60**, 3169–3175.

[305] HYACINTHE, C., ANSCHUTZ, P., CARBONEL, P., JOUANNEAU, J., JORISSEN, -F. 2001. Early diagenetic processes in the muddy sediments of the Bay of Biscay. *Marine Geol*ogy, **177**,111-128.

[306] VAN CAPPELLEN, P., VIOLLIER, E., ROYCHOUDHURY, A. 1998. Biogeochemical cycles of manganese and iron at the oxic - anoxic transition of a stratified marine Basin (Orca Basin, Gulf of Mexico). *Environmental Science & Technology*, **32**, 2931-2939.

[307] TROMP, T., VAN CAPPELLEN, P., KEY, R. 1995. A global model for the early diagenesis of organic carbon and organic phosphorus in marine sediments. *Geochimica et Cosmochimica Acta*, **59**, 1259-1284.

[308] WANG, Y. & VAN CAPPELLEN, P. 1996. A multicomponent reactive transport model of early diagenesis: Application to redox cycling in coastal marine sediments. *Geochimica et Cosmochimica Acta*, **60**, 2993-3014.

[309] CANAVAN, R., VAN CAPPELLEN, P., ZWOLSMAN, J., VAN DEN BERG, G., SLOMP, C. 2007. Geochemistry of trace metals in a fresh water sediment: Field results and diagenetic modelling. *Science of the Total Environment*, **381**, 263–279.

[310] GRANINA, L., MÜLLER, B., WEHRLI, B. 2004. Origin and dynamics of Fe and Mn sedimentary layers in Lake Baikal. *Chemical Geology,* **205**, 55-72.

[311] LESVEN, L., GAO, Y., BILLON, G., LEERMAKERS, M., OUDDANE, B., FISCHER, J., BAEYENS, W. Early diagenetic processes aspects controlling the mobility of dissolved trace metals in three riverine sediment columns. *Science of the Total Environment*, **407**, 447-459.

[312] HUERTA-DÍAZ, M., TESSIER, A., CARIGNAN, R. 1998. Geochemistry of trace metals associated with reduced sulfur in freshwater sediments. *Applied Geochemistry*, **13**, 213–233.

[313] PEDERSEN, T. 1985. Early diagenesis of copper and molybdenum in mine tailings and natural sediments in Rupert and Holberg inlets, British Columbia. *Canadian Journal of Earth Sciences*, **22**, 1474-1484.

[314] AUDRY, S., GROSBOIS, C., BRIL, H., SCHÄFER, J., KIERCZACK, J., BLANC, G. 2010. Post-depositional redistribution of trace metals in reservoir sediments of a mining/smelting-impacted watershed (the Lot River, SW France). *Applied Geochemistry*, **25**, 778-794.

[315] TAPIA, J., AUDRY, S., TOWNLEY, B., DUPREY, JL. 2011a. Geochemical background, baseline and origin of contaminants from sediments in the mining-impacted Altiplano and Eastern Cordillera of Oruro, Bolivia. *Geochemistry: Environment, Exploration, Analysis (GEEA)*, online.

[316] TAPIA, J., AUDRY, S., TOWNLEY, B. 2010. Impact of historical mining activities on soils and lacustrine sediments in Oruro, Bolivian Altiplano. Goldschmidt conference 2010, June 13-18, Knoxville, Tennessee, USA.

[317] ALBORÉS, AF., CID, BP., GOMEZ, EF., LOPEZ, EF. 2000. Comparison between sequential extraction procedures and single extractions for metal partitioning in sewage sludge samples. *Analyst,* **125**, 1353– 1357.

[318] MA, Y. & UREN, NC. 1995. Application of a new fractionation scheme for heavy metals in soils. *Communications in Soil Science and Plant Analysis,* **26**, 3291–3303.

[319] BOUDREAU, B. 1996. The diffusive tortuosity of fine-grained unlithified sediments. *Geochemica et Cosmochimica Acta,* **60**, 3139-3142.

[320] WIDERLUND, A. & INGRI, J. 1995. Early diagenesis of arsenic in sediments of the Kalix River estuary, northern Sweden. *Marine Geol*ogy, **125**, 185-196.

[321] LI, Y. & GREGORY, S. 1974. Diffusion of ions in sea water and in deep-sea sediments. *Geochimica et Cosmochimica Acta*, **38**, 708-714.

[322] HULTH, S., ALLER, R., GILBERT, F. 1999. Coupled anoxic nitrification/manganese reduction in marine sediments. *Geochimica et Cosmochimica Acta*, **63**, 49-66.

[323] CANAVAN, R., SLOMP, C., JOURABCHI, P., VAN CAPPELLEN, P., LAVERMAN, A., VAN DEN BERG, G. 2006. Organic matter mineralization in sediment of a coastal freshwater lake and response to salinitization. *Geochimica et Cosmochimica Acta*, **70**, 2836-2855.

[324] LOVLEY, D. & PHILLIPS, E. 1986. Organic matter mineralization with reduction of ferric iron in anaerobic sediments. *Applied and Environmental Microbiology*, **51**, 683-689.

[325] MÜLLER, J., RUPPERT, H., MURAMATSU, Y., SCHNEIDER, J. 1999, Reservoir sediments - a witness of mining and industrial development (Malter Reservoir, eastern Erzgebirge, Germany). *Environmental Geology*, **39**, 1341-1351.

[326] DILL, H.G. 1988. Evolution of Sb mineralization in modern fold belts: a comparison of the Sb mineralization in the Central Andes (Bolivia) and the Western Carpathians (Slovakia). *Mineralium Deposita*, **33**, 359-378.

[327] NISSENBAUM, A., STILLER, M., NISHRI, A. 1990. Nutrients in pore waters from the Dead Sea sediments. *Hydrobiologia*, **197**, 83-89.

[328] GEHLER, E. 1984. *Comportamiento de Schoenoplectus totora (totora) frente al hierro y plata*. Tesis de Licenciatura en Química, UMSA, La Paz, Bolivia, 46 pp.

[329] GEHLER, E. 1984b. Comportamiento de Schoenoplectus totora (totora) frente al hierro y plata en soluciones acuosas. *Revista Boliviana de Química*, **5**, 21-31.

[330] KLINKHAMMER, G.P. & PALMER, M.R. 1991. Uranium in the oceans: where it goes and why. *Geochimica et Cosmochimica Acta*, **55**, 1799-1806.

[331] LANGMUIR, D. 1978. Uranium solution-mineral equilibria at low temperatures with applications to sedimentary ore deposits. *Geochimica et Cosmochimica Acta*, **42**, 547-569.

[332] COCHRAN, K., CAREY, A., SHOLKOVITZ, E., SURPRENANT, L. 1986. The geochemistry of uranium and thorium in coastal marine sediments and sediment pore waters. *Geochimica et Cosmochimica Acta*, **50**, 663-680.

[333] LOVLEY, D. & PHILIPS, J.P. 1992. Reduction of Uranium by Desulfovibrio desulfuricans. *Applied and Environmental Microbiology*, **58**, 850-856.

[334] MAGALHÃES, C. 2002. Arsenic. An environmental problem limited by solubility. *Pure Applied Chemistry*, **74**, 1843-1850.

[335] BELZILE, N. & TESSIER, A. 1990. Interactions between arsenic and iron oxyhydroxides in lacustrine sediments. *Geochimica et Cosmochimica Acta*, **54**, 103-109.

[336] SMEDLEY, P. & KINNIBURGH, D. 2002. A review of the source, behavior and distribution of arsenic in natural waters. *Applied Geochemistry*, **17**, 517-568.

[337] SEYLER, P. & MARTIN, J. 1989. Biogeochemical processes affecting arsenic species distribution in a permanently stratified lake. *Environmental Science & Technology*, **23**, 1258-1263.

[338] MASSCHELEYN, P., DELAUNE, R., PATRICK, W. 1991. Effect of redox potential and pH on arsenic speciation and solubility in a contaminated soil. *Environmental Science & Technology*, **25**, 1414-1419.

[339] ZOBRIST, J., DOWDLE, P., DAVIS, J., OREMLAND, R. 2000. Mobilization of arsenite by dissimilatory reduction of adsorbed arsenates. *Environmental Science & Technology*, **34**, 4747-4753.

[340] BELZILE, N. 1988. The fate of arsenic in sediments of the Laurentian Trough. *Geochimica et Cosmochimica Acta*, **52**, 2293-2302.

[341] COUTURE, R., SHAFEI, B., VAN CAPPELLEN, P., TESSIER, A., GOBEIL, C. 2010. Non-steady state modeling of arsenic diagenesis in lake sediments. *Environmental Science & Technology*, **44**, 197-203.

[342] CHEN, Y., DENG, T., FILELLA, M., BELZILE, N. 2003. Distribution and early diagenesis of antimony in sediments and pore waters of freshwater lakes. *Environmental Science & Technology*, **37**, 1163-1168.

[343] HELZ, G., VALERIO, M., CAPPS, N. 2002. Antimony speciation in alkaline sulfide solutions: role of zerovalent sulfur. *Environmental Science & Technology*, **36**, 943-948.

[344] FILELLA, M., BELZILE, N., CHEN, Y. 2002. Antimony in the environment: a review focused on natural waters: II. Relevant solution chemistry. *Earth Science Rev*iew, **59**, 265-285.

[345] KRISHNAMURTI, GSR., HUANG, PM., VAN REES, KCJ., KOZAK, LM., ROSTAD, LM. 1995. Speciation of particulate-bound Cadmium of soils and its bioavailability. *Analyst*, **120**, 659-665.

[346] SWARZENSKI, P.W., McKEE, B.A., SKEI, J.M., TODD, J.F. 1999. Uranium biogeochemistry across the redox transition zone of a permanently stratified fjord: Framvaren, Norway. *Marine Chemistry*, **67**, 181-198.

[347] ELBAZ-POULICHET, F., SEIDEL, J.L., JÉZÉQUEL, D., METZGER, E., PRÉVOT, F., SIMONUCCI, C., SARAZIN, G., VIOLLIER, E., ETCHEBER, H., JOUANNEAU, J.M., WEBER, O., RADAKOVITCH, O. 2005. Sedimentary record of redox-sensitive elements (U, Mn, Mo) in a transitory anoxic basin (the Thau lagoon, France). *Marine Chemistry*, **95**, 271-281.

[348] SLAVECK, J., WORLD, J., PICKERING, WF. 1982. Extraction of metal ions associated with humic acids. *Talanta,* **29**, 743–750.

[349] BERROW, ML. & URE AM. 1986. Trace element distribution and mobilization in Scottish soils with particular reference to cobalt, copper and molybdenum. *Environmental Geochemistry and Health*, **8**, 19-24.

[350] GARREAUD, R., VUILLE, M., CLEMENT, A. 2003. The climate of the Altiplano: observed current conditions and mechanisms of past changes. *Palaeogeography, Palaeoclimatology, Palaeoecology*, **194**, 5-22.

[351] RONCHAIL, J. 1995. *Variabilidad interanual de las precipitaciones en Bolivia*, Bulletin de l'Institut Français des Etudes Andines, **24**, 369-378. Ronchail 1995.

[352] GARREAUD, R., ACEITUNO, P. 2001.Interannual Rainfall Variability over the South American Altiplano. *Journal of Climate*, **14**, 2779–2789. Garreaud & Aceituno 2001.

[353] GARCÍA, ME., PERSSON, KM., BENGTSSON, L., BERNDTSSON, R. 2005b. History of mining in the Lake Poopó Region and Environmental Consequences, *Vatten*, **61**, 243-248. In GARCÍA, M.E. 2006. *Transport of Arsenic and Heavy Metals to lake Poopó–Bolivia–Natural Leakage and anthropogenic effects.* PhD Thesis Lund University, Sweden.García et al. 2005

[354] CAPRILES-VILLAZÓN, O. 1977. *Historia de la mineria boliviana*, pp 268.

[355] TROËNG, B. & RIERA-KILIBARDA, C. 1996. *Mapas temáticos de recursos minerales de Bolivia, Boletin del Servicio Geológico de Bolivia*, 12, 9, La Paz. In [253].

[356] TRENBERTH, KE. & CARON, JM. 2000. The Southern Oscillation revisited: Sea level pressures, surface temperatures and precipitation. *Journal of Climate,* **13**, 4358–4365.

[357] HOLMGREN, M., SCHEFFER, M., EZCURRA, E., GUTIÉRREZ, JR., MOHREN, GMJ. 2001. El Niño effects on the dynamics of terrestrial ecosystems. *Trends in Ecology & Evolution*, **16**, 89–94.

[358] BOUMA, MJ., KOVATS, RS., GOUBERT, SA., COX, JSH., HAINES, A. 1997. Global assessment of El Niño's disaster burden. *Lancet*, **350**, 1435–1438.

[359] CHEN, C., McCARL, B., ADAMS, R. 2001. Economic implications of potential ENSO frequency and strength shifts. *Climatic Change*, **49**, 147–159.

[360] CHRISTIE, D., LARA, A., BARICHIVICH, J., VILLALBA, R., MORALES, M., CUQ, E. 2009. El Niño-Southern Oscillation signal in the world's highest-elevation tree-ring chronologies from the Altiplano, Central Andes. *Palaeogeography, Palaeoclimatology, Palaeoecology*, **281**, 309–319.

[361] TRENBERTH, KE. 1997. The definition of El Niño. *Bulletin of the American Meteorological Society*, **78**, 2771–2777. Trenberth 1997.

[362] LAUBENSTEIN, M., HULT, M., GASPARRO, J., ARNOLD, D., NEUMAIER, S., HEUSSER, G., KOHLER, M., POVINEC, P., REYSS, JL., SCHWAIGER, M., THEODORSSON, P. 2004. Underground measurements of radioactivity. *Applied Radiation and Isotopes*, **61**, 167–172.

[363] VAN BEEK, P., SOUHAUT, M., REYSS, JL. 2010. Measuring the radium quartet (^{228}Ra, ^{226}Ra, ^{224}Ra, ^{223}Ra) in seawater samples using gamma spectrometry. *Journal of Environmental Radioactivity*, **101**, 521–529.

[364] SCHULLER, P., LOBVENGREEN, CH., HANDL, J. 1993. ^{137}Cs Concentration in Soil, Prairie Plants, and Milk from Sites in Southern Chile. *Health Physics*, **64**, 157-161.

[365] SCHULLER, P., VOIGT, G., HANDL, A., ELLIES, A., OLIVA, L. 2002. Global weapons' fallout 137Cs in soils and transfer to vegetation in south–central Chile. *Journal of Environmental Radioactivity*, **62**, 181-193

[366] PENNINGTON, W., CAMBRAY, RE., FISHER, EMR. 1973. Observations on lake sediments using fallout ^{137}Cs as a tracer. *Nature*, **242**, 324–6.

[367] CAMBRAY, RS., PLAYFORD, K, LEWIS, GNJ., CARPENTER, RC. 1989. *Radioactive fallout in air and rain: results to the end of 1987 AERE-R 13226.* London: HMSO.

[368] UNSCEAR 2000. *Sources and effects of ionizing radiation.* UNSCEAR 2000 report to the General Assembly, with scientific annexes. Sources. New York, United Nations; 654 pp.

[369] ARNAUD, F., MAGAND, O., CHAPRON, E., BERTRAND, S., BÖES, X., CHARLET, F., MÉLIÈRES, MA. 2006. Radionuclide dating (^{210}Pb, ^{137}Cs, ^{241}Am) of recent lake sediments in a highly active geodynamic setting (Lakes Puyehue and Icalma—Chilean Lake District). *Science of the Total Environment*, **366**, 837–850.

Appendix A

Nomenclature

Nomenclature

AL	Altiplano
AMD	Acid mine drainage; drenaje ácido de mina; drainage minier acide
BCR	Community Bureau of Reference; Oficina Comunitaria de Referencia; Bureau Communautaire de Référence
BEC	Backscattered electron composition; composición de electrones retrodispersados; composition d'électrons rétrodiffusés
BES	Backscattered electron shadow; sombra de electrones retrodispersados; ombre d'électrons rétrodiffusés
BW	Bottom water; agua de fondo; eau de fond
CCLAC	Cala Cala Lagoon average composition; composición promedio de la laguna Cala Cala; composition moyen du lagoon Cala Cala
DJF	December, January, February; Diciembre, Enero, Febrero; Decembre, Janvier, Fevrier
DL	Detection limit; límite de detección; limite de détection
DOM	Dissolved organic matter; materia orgánica disuelta; matière organique dissoute
DS	Dry season; temporada seca; saison sèche
EC	Eastern Cordillera; Cordillera Oriental; Cordillère orientale
ECOLAB	Laboratoire d'Écologie Fonctionnelle
EDS	Energy dispersion spectrometer; espectrómetro de dispersión de energía; spectrometre à dispersion d'energie
EF	Enrichment factor; factor de enriquecimiento; facteur d'enrichissement
ENSO	El Niño Southern Oscillation; Oscilación del Sur El Niño; Oscillation Australe El Niño
F1	Exchangeable fraction; fracción intercambiable; fraction échangeable
F2	Carbonates; carbonatos; carbonates
F3	Reducible (Fe- and Mn oxyhydroxides); reducible (oxihidróxidos de Fe- y-Mn); réductible (oxyhydroxydes de Fe- et- Mn)
F4	Oxidizable (OM and sulfides); oxidable (OM y sulfuros); oxydables (OM et sulfures)
F5	Residual; residual; résiduelle

GIS	Geographical information system; sistema de información geográfica; système d'information géographique
HPLC	High performance liquid chromatography; cromatografía líquida de alta resolución; chromatographie liquide de haute resolution
ICP-MS	Inductively coupled plasma mass spectrometry; espectrómetro de masa con fuente de plasma de acoplamiento inductivo; spectromètre de masse par torche à plasma
ICP-OES	Inductively coupled plasma optical emission spectroscopy; espectrómetro de emisión óptica con fuente de plasma de acoplamiento inductivo; spectromètre d'émission optique par torche à plasma
INE	National Statistics Institute; Instituto Nacional de Estadística; Institut National de Statistique
ITCZ	Inter-tropical convergence zone; Zona de convergencia inter-tropical; zone de convergence Intertropicale
IUPAC	International Union of Pure and Applied Chemistry; Unión Internacional de Química Pura y Aplicada; Union Internationale de Chimie Pure et Appliquée
LEGOS	Laboratoire d'Etude en Géophysique et Océanographie Spatiales
LMTG	Laboratoire des Mécanismes et Transferts en Géologie
MAC	Maximum admissible concentration; concentración admisible máxima; concentration maximale admissible
MAD	Median absolute deviation; desviación absoluta de la mediana; déviation absolue du médiane
MTE	Metallic (metalloids included) trace elements; elementos traza metálicos (metaloides incluídos); éléments traces métalliques (métalloïdes compris)
NOM	Natural organic matter; materia orgánica natural; matière organique naturelle
OLW	Overlying water column; columna de agua sobreyacente; colonne d'eau sus-jacent
OM	Organic matter; materia orgánica; matière organique
OMP	Observatoire Midy-Pyrinees
PIC	Particulate inorganic carbon; carbono inorgánico particulado; carbone inorganique particulaire
PIC	Particulate inorganic carbon; carbono inorgánico particulado; carbone inorganique particulaire
POC	Particulate organic carbon; carbono orgánico particulado; carbone organique particulaire
POM	Particulate organic matter; materia orgánica particulada; matière organique particulaire
PPO	Oruro Pilot Project; Proyecto piloto Oruro; Projet pilote Oruro
RSD	Relative standard deviation; desviación estandar relativa; écart type relatif

SEI	Secondary electron image; imagen de electrones secundarios; image d'électrons secondaires
SEM	Scanning electron microscopy; microscopía electrónica de barrido; microscope electronque à balage
SENAMHI	Meteorology and Hydrology National Service; Servicio Nacional de Hidrología y Meteorología; Service National de Météorologie et Hydrologie
SERTECGEOMIN	Bolivian Geological and Mining Service; Servicio Geológico y Minero de Bolivia; Service Géologique et Minière de Bolivie
SGAB	Swedish Geological AB; AB Geológica Sueca; AB Géologique Suédoise
SIDA	Swedish International Development Authority; Autoridad de Desarrollo Internacional Sueca; Autorité de Développement International Suédoise
TDPS	Lake Titicaca-Desaguadero River-Lake Poopó-Salars; Lago Titicaca-Río Desaguadero-Lago Poopó-Salares; Lac Titicaca-Rivière Desaguadero-Lac Poopó-Salars
TMC	Total metal content (metalloids included); contenido metálico total (metaloides incluídos); teneur totale en métaux (métalloïdes compris)
UCC	Upper continental crust; corteza continental superior; croûte continentale supérieure
USEPA	United States Environmental Protection Agency; Agencia de Protección Ambiental de los Estados Unidos; Agence de Protection de l'Environnement des États-Unis
WC	Western Cordillera; Cordillera Occidental; Cordillère occidentale
WHO	World Health Organization; Organización Mundial de la Salud; Organisation Mondiale de la Santé
WMO	World Meteorological Organization; Organización Mundial de Meteorología; Organisation Météorologique Mondiale
WS	Wet season; temporada de lluvias; saison des pluies
WSI	Water-sediment interface; interfase agua-sedimento; eau-sédiment interface
XRD	X-Ray diffraction; difracción de rayos-X; diffraction des rayons-X

Appendix B

Samples

Samples

1 porosity; 2 POC (%); PIC (%); C_{tot} (%); S_{tot} (%); 3 total digestion; 4 $MgCl_2$ single extraction; 5 NaOAc single extraction; 6 Asc single extraction; 7 H_2O_2 single extraction; 8 dissolved major anions; 9 dissolved major cations; 10 dissolved trace elements

	Site	*UTM*	*UTM*	*depth*	*sediment*							*porewater*		
		N	*E*	*[cm]*	*1*	*2*	*3*	*4*	*5*	*6*	*7*	*8*	*9*	*10*
1	*UBW*	*8.005.541*	*696.753*	*0.0*	×	×	×	×	×	×	×	✓	✓	✓
2	*U1*	*8.005.541*	*696.753*	*0.5*	✓	✓	✓	✓	✓	✓	✓	✓	✓	×
3	*U2*	*8.005.541*	*696.753*	*1.0*	✓	✓	✓	✓	✓	✓	✓	✓	✓	✓
4	*U3*	*8.005.541*	*696.753*	*1.5*	✓	✓	✓	✓	✓	✓	✓	✓	✓	✓
5	*U4*	*8.005.541*	*696.753*	*2.0*	✓	✓	✓	✓	✓	✓	✓	✓	✓	✓
6	*U5*	*8.005.541*	*696.753*	*2.5*	✓	✓	✓	✓	✓	✓	✓	✓	✓	✓
7	*U6*	*8.005.541*	*696.753*	*3.0*	✓	✓	✓	✓	✓	✓	✓	✓	✓	✓
8	*U7*	*8.005.541*	*696.753*	*3.5*	✓	✓	✓	✓	✓	✓	✓	✓	✓	✓
9	*U8*	*8.005.541*	*696.753*	*4.0*	✓	✓	✓	✓	✓	✓	✓	✓	✓	✓
10	*U9*	*8.005.541*	*696.753*	*5.0*	✓	✓	✓	✓	✓	✓	✓	✓	✓	✓
11	*U10*	*8.005.541*	*696.753*	*6.0*	✓	✓	✓	✓	✓	✓	✓	✓	✓	✓
12	*U11*	*8.005.541*	*696.753*	*7.0*	✓	✓	✓	✓	✓	✓	✓	✓	✓	✓
13	*U12*	*8.005.541*	*696.753*	*8.0*	✓	✓	✓	✓	✓	✓	✓	✓	✓	✓
14	*U13*	*8.005.541*	*696.753*	*9.5*	✓	✓	✓	✓	✓	✓	✓	✓	✓	✓
15	*U14*	*8.005.541*	*696.753*	*11.0*	✓	✓	✓	✓	✓	✓	✓	✓	✓	✓
16	*U15*	*8.005.541*	*696.753*	*13.5*	✓	✓	✓	✓	✓	✓	✓	✓	✓	✓
17	*U16*	*8.005.541*	*696.753*	*16.0*	✓	✓	✓	✓	✓	✓	✓	✓	✓	✓
18	*U17*	*8.005.541*	*696.753*	*18.5*	✓	✓	✓	✓	✓	✓	✓	×	×	×
19	*U18*	*8.005.541*	*696.753*	*21.0*	✓	✓	✓	✓	✓	✓	✓	×	×	×
20	*U19*	*8.005.541*	*696.753*	*23.5*	×	✓	✓	✓	✓	✓	✓	×	×	×
21	*U20*	*8.005.541*	*696.753*	*26.0*	×	✓	✓	✓	✓	✓	✓	×	×	×
22	*OBW*	*8.005.542*	*696.710*	*0.0*	×	×	×	×	×	×	×	✓	✓	✓
23	*O1*	*8.005.542*	*696.710*	*0.5*	✓	✓	✓	✓	✓	✓	✓	✓	✓	✓
24	*O2*	*8.005.542*	*696.710*	*1.0*	✓	✓	✓	✓	✓	✓	✓	✓	✓	✓
25	*O3*	*8.005.542*	*696.710*	*1.6*	✓	✓	✓	✓	✓	✓	✓	✓	✓	✓
26	*O4*	*8.005.542*	*696.710*	*2.9*	✓	✓	✓	✓	✓	✓	✓	✓	✓	×
27	*O5*	*8.005.542*	*696.710*	*4.0*	✓	✓	✓	✓	✓	✓	✓	✓	✓	×
28	*O6*	*8.005.542*	*696.710*	*5.5*	✓	✓	✓	✓	✓	✓	✓	✓	✓	×
29	*O7*	*8.005.542*	*696.710*	*7.5*	✓	✓	✓	✓	✓	✓	✓	✓	✓	×
30	*O8*	*8.005.542*	*696.710*	*9.7*	✓	✓	✓	✓	✓	✓	✓	✓	✓	×
31	*O9*	*8.005.542*	*696.710*	*11.7*	✓	✓	✓	✓	✓	✓	✓	×	×	✓
32	*O10*	*8.005.542*	*696.710*	*13.7*	✓	✓	✓	✓	✓	✓	✓	×	×	✓
33	*O11*	*8.005.542*	*696.710*	*15.7*	✓	✓	✓	✓	✓	✓	✓	×	×	✓
34	*O12*	*8.005.542*	*696.710*	*17.9*	✓	✓	✓	✓	✓	✓	✓	×	×	✓
35	*MBW*	*7.993.357*	*701.175*	*0.0*	×	×	×	×	×	×	×	✓	✓	✓
36	*M1*	*7.993.357*	*701.175*	*0.5*	✓	✓	✓	✓	✓	✓	✓	✓	✓	✓
37	*M2*	*7.993.357*	*701.175*	*1.0*	✓	✓	✓	✓	✓	✓	✓	✓	✓	✓
38	*M3*	*7.993.357*	*701.175*	*1.5*	✓	✓	✓	✓	✓	✓	✓	✓	✓	✓
39	*M4*	*7.993.357*	*701.175*	*2.0*	✓	✓	✓	✓	✓	✓	✓	✓	✓	✓
40	*M5*	*7.993.357*	*701.175*	*2.5*	✓	✓	✓	✓	✓	✓	✓	✓	✓	✓
41	*M6*	*7.993.357*	*701.175*	*3.0*	✓	✓	✓	✓	✓	✓	✓	✓	✓	✓
42	*M7*	*7.993.357*	*701.175*	*3.5*	✓	✓	✓	✓	✓	✓	✓	✓	✓	✓
43	*M8*	*7.993.357*	*701.175*	*4.0*	✓	✓	✓	✓	✓	✓	✓	✓	✓	✓
44	*M9*	*7.993.357*	*701.175*	*4.5*	✓	✓	✓	✓	✓	✓	✓	✓	✓	✓
45	*M10*	*7.993.357*	*701.175*	*5.0*	✓	✓	✓	✓	✓	✓	✓	✓	✓	✓
46	*M11*	*7.993.357*	*701.175*	*6.0*	✓	✓	✓	✓	✓	✓	✓	✓	✓	✓
47	*M12*	*7.993.357*	*701.175*	*7.0*	✓	✓	✓	✓	✓	✓	✓	✓	✓	✓
48	*M13*	*7.993.357*	*701.175*	*8.0*	✓	✓	✓	✓	✓	✓	✓	✓	✓	✓

	Site	UTM N	UTM E	depth [cm]	sediment 1	2	3	4	5	6	7	porewater 8	9	10
49	M14	7.993.357	701.175	9.0	✓	✓	✓	✓	✓	✓	✓	✓	✓	✓
50	M15	7.993.357	701.175	10.0	✓	✓	✓	✓	✓	✓	✓	✓	×	×
51	M16	7.993.357	701.175	12.5	✓	✓	✓	✓	✓	✓	✓	✓	✓	✓
52	M17	7.993.357	701.175	15.0	✓	✓	✓	✓	✓	✓	✓	✓	✓	×
53	M18	7.993.357	701.175	17.5	✓	✓	✓	✓	✓	✓	✓	✓	✓	×
54	M19	7.993.357	701.175	20.0	✓	✓	✓	✓	✓	✓	✓	×	×	✓
55	M20	7.993.357	701.175	22.7	✓	✓	✓	✓	✓	✓	✓	×	×	✓
56	M21	7.993.357	701.175	25.7	✓	✓	✓	✓	✓	✓	✓	×	×	×
57	M22	7.993.357	701.175	28.9	✓	✓	✓	✓	✓	✓	×	×	×	✓
58	M23	7.993.357	701.175	32.5	×	✓	✓	✓	✓	✓	✓	×	×	×
59	PBW	7.991.158	701.620	0.0	×	×	×	×	×	×	×	✓	✓	✓
60	P1	7.991.158	701.620	0.5	✓	✓	✓	✓	✓	✓	✓	✓	✓	✓
61	P2	7.991.158	701.620	1.5	✓	✓	✓	✓	✓	✓	✓	×	×	×
62	P3	7.991.158	701.620	2.0	✓	✓	✓	✓	✓	✓	✓	✓	✓	✓
63	P4	7.991.158	701.620	3.2	✓	✓	✓	✓	✓	✓	✓	✓	✓	✓
64	P5	7.991.158	701.620	4.8	✓	✓	✓	✓	✓	✓	✓	✓	✓	✓
65	P6	7.991.158	701.620	6.1	✓	✓	✓	✓	✓	✓	✓	✓	✓	✓
66	P7	7.991.158	701.620	7.5	✓	✓	✓	✓	✓	✓	✓	✓	✓	✓
67	P8	7.991.158	701.620	9.3	✓	✓	✓	✓	✓	✓	✓	✓	✓	✓
68	P9	7.991.158	701.620	11.2	✓	✓	✓	✓	✓	✓	✓	✓	✓	✓
69	P10	7.991.158	701.620	13.2	✓	✓	✓	✓	✓	✓	✓	✓	✓	✓
70	P11	7.991.158	701.620	15.2	✓	✓	✓	✓	✓	✓	✓	×	×	✓
71	P12	7.991.158	701.620	17.2	✓	✓	✓	✓	✓	✓	✓	×	×	✓
72	P13	7.991.158	701.620	19.2	×	✓	✓	✓	✓	✓	✓	×	×	×
73	P14	7.991.158	701.620	21.3	×	✓	✓	✓	✓	✓	✓	×	×	×
74	CBW	8.008.417	716.738	0.0	×	×	×	×	×	×	×	✓	✓	✓
75	C1	8.008.417	716.738	0.5	✓	✓	✓	✓	✓	✓	✓	✓	✓	✓
76	C2	8.008.417	716.738	0.9	✓	✓	✓	✓	✓	✓	✓	✓	✓	✓
77	C3	8.008.417	716.738	1.6	✓	✓	✓	✓	✓	✓	✓	✓	✓	✓
78	C4	8.008.417	716.738	2.1	✓	✓	✓	✓	✓	✓	✓	✓	✓	✓
79	C5	8.008.417	716.738	2.8	✓	✓	✓	✓	✓	✓	✓	✓	✓	✓
80	C6	8.008.417	716.738	3.5	✓	✓	✓	✓	✓	✓	✓	✓	✓	✓
81	C7	8.008.417	716.738	4.5	✓	✓	✓	✓	✓	✓	✓	✓	✓	✓
82	C8	8.008.417	716.738	5.5	✓	✓	✓	✓	✓	✓	✓	✓	✓	✓
83	C9	8.008.417	716.738	6.5	✓	✓	✓	✓	✓	✓	✓	✓	✓	✓
84	C10	8.008.417	716.738	7.5	✓	✓	✓	✓	✓	✓	✓	✓	✓	✓
85	C11	8.008.417	716.738	8.7	✓	✓	✓	✓	✓	✓	✓	✓	✓	✓
86	C12	8.008.417	716.738	9.8	✓	✓	✓	✓	✓	✓	✓	✓	✓	✓
87	C13	8.008.417	716.738	10.8	✓	✓	✓	✓	✓	✓	✓	✓	✓	✓
88	C14	8.008.417	716.738	12.8	✓	✓	✓	✓	✓	✓	✓	✓	✓	✓
89	C15	8.008.417	716.738	14.9	✓	✓	✓	✓	✓	✓	✓	✓	✓	✓
90	C16	8.008.417	716.738	17.0	✓	✓	✓	✓	✓	✓	✓	✓	✓	✓
91	C17	8.008.417	716.738	19.5	✓	✓	✓	✓	✓	✓	✓	✓	✓	✓
92	C18	8.008.417	716.738	23.5	✓	✓	✓	✓	✓	✓	✓	✓	✓	✓
93	C19	8.008.417	716.738	27.5	✓	✓	✓	✓	✓	✓	✓	✓	✓	✓
94	C20	8.008.417	716.738	31.0	✓	✓	✓	✓	✓	✓	✓	✓	✓	✓
95	C21	8.008.417	716.738	34.8	✓	✓	✓	✓	✓	✓	✓	✓	✓	✓
96	C22	8.008.417	716.738	38.7	✓	✓	✓	✓	✓	✓	✓	✓	✓	✓

Appendix C

Oruro Pilot Project Data Base

Sample		Coordinates			As	Cd	Cu	Pb	Sb	Zn
Type	name	N UTM	E UTM	depth [cm]			[$\mu g \cdot g^{-1}$]			
Superficial soil	1001	8012600	705800	0	190	2	17	414	733	175
Superficial soil	1002	8013200	707300	0	170	3	66	871	808	346
Superficial soil	1003	8012800	708400	0	230	3	11	308	783	143
Superficial soil	1004	8011900	709800	0	230	2	25	533	820	197
Superficial soil	1005	8011000	710800	0	270	4	29	273	918	125
Superficial soil	1006	8010200	707200	0	280	4	73	313	770	174
Superficial soil	1007	8009400	708100	0	230	3	26	296	709	170
Superficial soil	1008	8010500	706100	0	210	3	60	293	795	146
Superficial soil	1009	8011600	706500	0	220	4	27	744	828	273
Superficial soil	1010	8011200	710700	0	463	6	535	3307	752	471
Superficial soil	1011	8012100	709200	0	328	17	79	298	104	223
Superficial soil	1012	8012800	710700	0	386	9	58	65	103	122
Superficial soil	1013	8012900	712000	0	447	5	75	31	100	142
Superficial soil	1014	8034300	662700	0	454	6	97	32	178	122
Superficial soil	1015	8022400	676500	0	331	5	57	31	63	143
Superficial soil	1016	7955200	728700	0	291	8	58	64	102	218
Superficial soil	1017	7948500	718800	0	293	4	57	32	64	168
Superficial soil	1018	7989200	717100	0	311	6	77	96	65	241
Superficial soil	1019	7903000	734200	0	228	4	197	321	9	123
Superficial soil	1020	7894200	734200	0	242	3	56	62	12	140
Superficial soil	1021	7882400	735200	0	270	4	37	62	15	117
Superficial soil	1022	7925500	725200	0	321	4	57	63	21	166
Superficial soil	1023	8014500	707800	0	327	6	73	61	46	137
Superficial soil	1024	8012800	707100	0	227	4	58	97	18	97
Superficial soil	1025	8018300	707500	0	316	4	59	65	21	123
Superficial soil	1026	8025800	709200	0	294	4	58	65	23	122
Superficial soil	1027	8009500	715800	0	289	8	99	1222	143	1214
Superficial soil	1028	8007800	719000	0	231	4	57	94	25	142
Superficial soil	1029	8008400	707500	0	234	4	47	121	59	132
Superficial soil	1030	8006500	708400	0	304	13	53	161	65	185
Superficial soil	1031	8004800	710000	0	176	5	44	83	59	98
Superficial soil	1032	7998900	710500	0	452	14	65	104	32	190
Superficial soil	1033	7977000	712800	0	278	1	53	58	59	131
Superficial soil	1034	7974500	712800	0	150	1	50	71	43	198
Superficial soil	1035	7966500	715800	0	149	19	8	179	99	497
Superficial soil	1036	7992400	711800	0	166	15	62	126	66	178
Superficial soil	1037	7989000	718800	0	281	17	47	124	89	199
Superficial soil	1038	7985800	717900	0	240	18	65	76	71	244
Superficial soil	1039	7963700	721800	0	315	10	40	259	62	154
Superficial soil	1040	7960500	722800	0	310	14	43	29	63	124
Superficial soil	1041	7946400	723700	0	185	12	36	22	55	145
Superficial soil	1042	7943500	718800	0	160	9	35	24	57	90
Superficial soil	1043	7955000	715100	0	192	21	36	53	64	79
Superficial soil	1044	8008800	713900	0	212	22	60	201	79	80
Superficial soil	1045	8007500	714200	0	256	15	37	99	68	153
Superficial soil	1046	8006500	714100	0	181	15	25	26	66	28
Superficial soil	1047	8029200	710200	0	206	1	19	65	79	129
Superficial soil	1048	8035200	709800	0	367	3	39	48	53	118
Superficial soil	1049	8042000	707300	0	339	1	20	39	39	99
Superficial soil	1050	8048000	707800	0	249	2	29	44	26	127
Superficial soil	1051	8048000	700000	0	160	1	21	40	40	90
Superficial soil	1052	8052000	687000	0	256	1	38	48	26	130
Superficial soil	1053	8058000	678000	0	277	2	39	48	27	127

Sample		Coordinates			As	Cd	Cu	Pb	Sb	Zn
Type	name	N UTM	E UTM	depth [cm]			[$\mu g \cdot g^{-1}$]			
Superficial soil	1054	8040000	693000	0	373	1	39	37	39	128
Superficial soil	1055	7977900	679800	0	238	2	20	44	25	129
Superficial soil	1056	7977500	689700	0	375	1	78	49	66	129
Superficial soil	1057	7975800	691800	0	385	2	139	48	26	150
Superficial soil	1058	7984000	693800	0	379	2	40	47	39	199
Superficial soil	1059	8020700	698800	0	165	4	45	210	1047	124
Superficial soil	1060	8020000	699600	0	240	4	43	225	1173	68
Superficial soil	1061	8019300	700300	0	230	1	35	194	933	25
Superficial soil	1062	8018700	701000	0	223	4	43	223	1099	60
Superficial soil	1063	8018100	701800	0	264	3	47	222	1155	55
Superficial soil	1064	8017500	702500	0	240	4	50	259	943	58
Superficial soil	1065	8017000	703200	0	213	3	66	178	801	56
Superficial soil	1066	8016800	703500	0	133	3	24	171	644	46
Superficial soil	1067	8016600	703500	0	135	2	20	129	597	39
Superficial soil	1068	8016800	703600	0	156	3	55	528	944	274
Superficial soil	1069	8016600	703700	0	229	2	26	144	713	32
Superficial soil	1070	8012000	705500	0	193	3	50	454	877	134
Superficial soil	1071	8012500	704700	0	187	2	60	244	910	40
Superficial soil	1072	8013100	703900	0	155	4	66	1298	982	95
Superficial soil	1073	8013600	703100	0	174	3	46	321	873	146
Superficial soil	1074	8014200	702300	0	265	2	32	186	851	107
Superficial soil	1075	8014700	701400	0	146	9	25	158	745	75
Semi superficial soil	V1	8011200	710700	0-5	32	3.4	339	1930	495	223
Semi superficial soil	V2	8012100	709200	0-5	40	2.9	24	245	38	113
Semi superficial soil	V3	8012800	710700	0-5	31	3.0	19	214	24	71
Semi superficial soil	V4	8012900	712000	0-5	36	2.8	68	41	10	68
Semi superficial soil	IR1	8034300	662700	0-5	19	3.2	39	49	84	92
Semi superficial soil	Silluta 1	8022400	676500	0-5	14	3.1	38	33	89	61
Semi superficial soil	B1	7955200	728700	0-5	29	3.0	28	75	96	136
Semi superficial soil	Pazña 1	7948500	718800	0-5	21	2.3	14	34	33	97
Semi superficial soil	H2	7989200	717100	0-5	30	3.1	25	82	15	221
Semi superficial soil	C1	7903000	734200	0-5	23	1.9	11	24	21	76
Semi superficial soil	C2	7894200	734200	0-5	30	3.0	17	33	58	77
Semi superficial soil	C3	7882400	735200	0-5	28	2.8	21	33	103	67
Semi superficial soil	C4	7925500	725200	0-5	25	2.0	18	32	43	64
Semi superficial soil	V5	8014500	707800	0-5	27	3.1	66	323	55	86
Semi superficial soil	V6	8012800	707100	0-5	28	2.7	23	120	12	75
Semi superficial soil	V7	8018300	707500	0-5	28	2.8	26	49	21	75
Semi superficial soil	V8	8025800	709200	0-5	34	3.0	35	25	10	73
Semi superficial soil	V9	8009500	715800	0-5	36	3.7	65	36	99	717
Semi superficial soil	V10	8007800	719000	0-5	33	2.8	14	50	16	72
Semi superficial soil	V11	8008400	707500	0-5	37	2.7	23	55	30	76
Semi superficial soil	V12	8006500	708400	0-5	34	3.1	30	99	30	96
Semi superficial soil	V13	8004800	710000	0-5	41	3.2	19	51	26	59
Semi superficial soil	V14	7998900	710500	0-5	53	3.5	28	59	88	96
Semi superficial soil	V15	7977000	712800	0-5	39	3.3	21	57	58	108
Semi superficial soil	V16	7974500	712800	0-5	29	3.2	21	55	83	154
Semi superficial soil	V17	7966500	715800	0-5	22	5.5	35	156	151	705
Semi superficial soil	V18	7992400	711800	0-5	50	3.5	49	90	133	187
Semi superficial soil	V19	7989000	718800	0-5	49	3.4	30	170	83	178
Semi superficial soil	V20	7985800	717900	0-5	27	3.2	35	41	52	142
Semi superficial soil	V21	7963700	721800	0-5	29	2.9	14	29	30	69
Semi superficial soil	V22	7960500	722800	0-5	30	3.2	17	33	28	92

Sample		Coordinates			As	Cd	Cu	Pb	Sb	Zn
Type	name	N UTM	E UTM	depth [cm]			[µg·g^{-1}]			
Semi superficial soil	V23	7946400	723700	0-5	34	3.0	12	25	30	55
Semi superficial soil	V24	7943500	718800	0-5	34	2.1	10	27	94	60
Semi superficial soil	V25	7955000	715100	0-5	63	2.9	13	21	29	53
Semi superficial soil	V26	8008800	713900	0-5	40	3.7	27	183	92	111
Semi superficial soil	V27	8007500	714200	0-5	49	3.5	21	51	81	115
Semi superficial soil	V28	8006500	714100	0-5	28	2.9	21	33	52	78
Semi superficial soil	P1	8029200	710200	0-5	35	2.8	28	65	77	61
Semi superficial soil	P2	8035200	709800	0-5	34	2.7	32	33	65	70
Semi superficial soil	P3	8042000	707300	0-5	32	2.3	21	33	57	59
Semi superficial soil	P4	8048000	708000	0-5	30	3.0	32	50	75	75
Semi superficial soil	P5	8048000	700000	0-5	30	3.8	28	33	89	67
Semi superficial soil	P6	8052000	687000	0-5	35	3.7	25	201	90	88
Semi superficial soil	P7	8058000	678000	0-5	29	3.1	27	254	60	99
Semi superficial soil	P8	8040000	693000	0-5	29	2.8	45	305	247	109
Semi superficial soil	T1	7977900	679800	0-5	34	3.2	26	59	63	66
Semi superficial soil	T2	7977500	689700	0-5	48	3.0	36	55	69	86
Semi superficial soil	T3	7975800	691800	0-5	38	3.1	61	57	71	74
Semi superficial soil	T4	7984000	693800	0-5	35	3.3	24	61	56	69
Semi superficial soil	S1	8020700	698800	0-5	35	0.4	16	32	270	104
Semi superficial soil	S2	8020000	699600	0-5	38	0.4	28	200	60	512
Semi superficial soil	S3	8019300	700300	0-5	33	<0.2	31	58	200	144
Semi superficial soil	S4	8018700	701000	0-5	28	<0.2	13	12	30	46
Semi superficial soil	S5	8018100	701800	0-5	34	<0.2	20	26	20	77
Semi superficial soil	S6	8017500	702500	0-5	55	<0.2	124	36	<20	116
Semi superficial soil	S7	8017000	703200	0-5	51	<0.2	4	8	30	32
Semi superficial soil	Hj1	8016800	703500	0-5	38	<0.2	12	12	<20	56
Semi superficial soil	Hj2	8016600	703500	0-5	30	<0.2	12	12	<20	59
Semi superficial soil	A1	8012000	705500	0-5	32	<0.2	10	8	<20	38
Semi superficial soil	A2	8012500	704700	0-5	33	0.4	22	54	<20	124
Semi superficial soil	A3	8013100	703900	0-5	40	0.2	17	16	30	54
Semi superficial soil	A4	8013600	703100	0-5	30	<0.2	15	16	10	78
Semi superficial soil	A5	8014200	702300	0-5	34	<0.2	43	16	10	83
Semi superficial soil	A6	8014700	701400	0-5	29	<0.2	26	16	<20	69
Semi superficial soil	V16/0	7974500	712800	0-5	29	<0.2	21	16	<20	60
Semi superficial soil	V17/0	7966500	715800	0-5	46	<0.2	52	36	<20	204
Semi superficial soil	V20/0	7985800	717900	0-5	52	nd	nd	nd	nd	nd
Semi superficial soil	V25/0	7955000	715100	0-5	20	nd	nd	nd	nd	nd
Semi superficial soil	T1/0	7977900	679800	0-5	17	nd	nd	nd	nd	nd
Semi superficial soil	T3/0	7975800	691800	0-5	29	nd	nd	nd	nd	nd
Semi superficial soil	C1/0	7903000	734200	0-5	9	nd	nd	nd	nd	nd
Semi superficial soil	C2/0	7894200	734200	0-5	42	nd	nd	nd	nd	nd
Semi superficial soil	C3/0	7882400	735200	0-5	33	nd	nd	nd	nd	nd
Semi superficial soil	C4/0	7925500	725200	0-5	18	nd	nd	nd	nd	nd
Semi superficial soil	H2/0	7989200	717100	0-5	15	nd	nd	nd	nd	nd
Semi superficial soil	Silluta 1/0	8022400	676500	0-5	17	nd	nd	nd	nd	nd
Semi superficial soil	Pazña 1/0	7948500	718800	0-5	30	nd	nd	nd	nd	nd
Semi superficial soil	P2/0	8035200	709800	0-5	15	nd	nd	nd	nd	nd
Semi superficial soil	P3/0	8042000	707300	0-5	15	nd	nd	nd	nd	nd
Semi superficial soil	P4/0	8048000	708000	0-5	33	nd	nd	nd	nd	nd
Semi superficial soil	B1/0	7955200	728700	0-5	88	nd	nd	nd	nd	nd
Deep soil	V1	8011200	710700	20-25	19	3.6	524	2793	694	277
Deep soil	V2	8012100	709200	20-25	22	2.8	17	203	27	101
Deep soil	V3	8012800	710700	20-25	18	3.0	16	265	10	69

Sample		Coordinates			As	Cd	Cu	Pb	Sb	Zn
Type	name	N UTM	E UTM	depth [cm]			[$\mu g \cdot g^{-1}$]			
Deep soil	V4	8012900	712000	20-25	18	3.1	72	36	9	76
Deep soil	IR1	8034300	662700	20-25	17	3.1	38	33	89	80
Deep soil	Silluta 1	8022400	676500	20-25	12	2.3	18	19	29	67
Deep soil	B1	7955200	728700	20-25	19	2.8	25	50	27	112
Deep soil	Pazña 1	7948500	718800	20-25	18	2.7	12	25	40	56
Deep soil	H2	7989200	717100	20-25	21	3.3	29	49	13	105
Deep soil	C1	7903000	734200	20-25	14	2.0	12	23	33	46
Deep soil	C2	7894200	734200	20-25	22	2.5	11	24	53	74
Deep soil	C3	7882400	735200	20-25	24	2.9	18	32	49	65
Deep soil	C4	7925500	725200	20-25	18	1.9	17	34	57	55
Deep soil	V5	8014500	707800	20-25	20	2.9	61	66	45	103
Deep soil	V6	8012800	707100	20-25	20	3.1	34	190	40	104
Deep soil	V7	8018300	707500	20-25	20	3.1	28	34	15	74
Deep soil	V8	8025800	709200	20-25	21	2.8	33	33	18	75
Deep soil	V9	8009500	715800	20-25	18	2.8	28	66	13	71
Deep soil	V10	8007800	719000	20-25	21	2.6	14	49	43	69
Deep soil	V11	8008400	707500	20-25	22	3.3	28	49	22	70
Deep soil	V12	8006500	708400	20-25	20	3.2	30	99	24	89
Deep soil	V13	8004800	710000	20-25	22	3.2	19	40	68	53
Deep soil	V14	7998900	710500	20-25	24	3.6	28	59	87	104
Deep soil	V15	7977000	712800	20-25	24	3.2	23	38	96	102
Deep soil	V16	7974500	712800	20-25	19	3.3	23	40	79	79
Deep soil	V17	7966500	715800	20-25	19	5.2	37	169	129	625
Deep soil	V18	7992400	711800	20-25	21	3.7	33	81	119	143
Deep soil	V19	7989000	718800	20-25	23	3.9	32	177	51	273
Deep soil	V20	7985800	717900	20-25	18	2.9	27	30	98	137
Deep soil	V21	7963700	721800	20-25	18	2.7	20	27	85	63
Deep soil	V22	7960500	722800	20-25	20	3.5	23	33	107	94
Deep soil	V23	7946400	723700	20-25	22	3.0	16	24	57	56
Deep soil	V24	7943500	718800	20-25	22	2.1	10	20	20	46
Deep soil	V25	7955000	715100	20-25	24	3.4	14	27	71	64
Deep soil	V26	8008800	713900	20-25	19	3.9	33	179	87	100
Deep soil	V27	8007500	714200	20-25	19	3.4	23	45	75	128
Deep soil	V28	8006500	714100	20-25	18	2.3	19	32	18	77
Deep soil	P1	8029200	710200	20-25	15	2.3	31	65	90	61
Deep soil	P2	8035200	709800	20-25	17	2.9	28	33	56	65
Deep soil	P3	8042000	707300	20-25	16	2.3	35	32	60	78
Deep soil	P4	8048000	708000	20-25	17	3.3	43	49	76	91
Deep soil	P5	8048000	700000	20-25	23	4.1	35	32	76	82
Deep soil	P6	8052000	687000	20-25	18	3.6	26	247	40	92
Deep soil	P7	8058000	678000	20-25	21	3.4	27	243	65	95
Deep soil	P8	8040000	693000	20-25	19	3.2	43	259	236	91
Deep soil	T1	7977900	679800	20-25	19	3.1	24	57	41	63
Deep soil	T2	7977500	689700	20-25	22	2.4	31	50	40	100
Deep soil	T3	7975800	691800	20-25	18	2.3	35	56	73	56
Deep soil	T4	7984000	693800	20-25	26	3.6	21	58	31	73
Deep soil	S1	8020700	698800	20-25	23	nd	nd	nd	nd	nd
Deep soil	S2	8020000	699600	20-25	23	nd	nd	nd	nd	nd
Deep soil	S3	8019300	700300	20-25	16	nd	nd	nd	nd	nd
Deep soil	S4	8018700	701000	20-25	21	nd	nd	nd	nd	nd
Deep soil	S5	8018100	701800	20-25	24	nd	nd	nd	nd	nd
Deep soil	S6	8017500	702500	20-25	26	nd	nd	nd	nd	nd
Deep soil	S7	8017000	703200	20-25	27	nd	nd	nd	nd	nd

Sample		Coordinates			As	Cd	Cu	Pb	Sb	Zn
Type	name	N UTM	E UTM	depth [cm]			[$\mu g \cdot g^{-1}$]			
Deep soil	Hj1	8016800	703500	20-25	21	nd	nd	nd	nd	nd
Deep soil	Hj2	8016600	703500	20-25	19	nd	nd	nd	nd	nd
Deep soil	A1	8012000	705500	20-25	24	nd	nd	nd	nd	nd
Deep soil	A2	8012500	704700	20-25	24	nd	nd	nd	nd	nd
Deep soil	A3	8013100	703900	20-25	21	nd	nd	nd	nd	nd
Deep soil	A4	8013600	703100	20-25	21	nd	nd	nd	nd	nd
Deep soil	A5	8014200	702300	20-25	19	nd	nd	nd	nd	nd
Deep soil	A6	8014700	701400	20-25	18	nd	nd	nd	nd	nd
Lacustrine sediments	A	8015600	693800	0	65	1.4	54	35	0.2	165
Lacustrine sediments	B	8005700	695900	0	36	0.5	80	35	0.1	124
Lacustrine sediments	C	7987000	702000	0	66	0.6	55	63	0.3	157
Lacustrine sediments	D	7985000	703000	0	15	0.3	44	41	0.2	58
Lacustrine sediments	1	7992800	703800	0	32	0.8	30	55	0.7	118
Lacustrine sediments	2	8004400	702500	0	79	1.9	75	75	0.6	182
Lacustrine sediments	3	8004500	702700	0	130	3.3	164	166	0.4	522
Lacustrine sediments	4	8002800	703600	0	53	1.0	50	119	0.5	130
Lacustrine sediments	5	7999100	705100	0	158	0.6	26	96	34.1	105
Lacustrine sediments	6	7999200	705300	0	35	0.5	29	68	1.0	95
Lacustrine sediments	7	7999600	706000	0	25	0.2	22	70	0.8	83
Lacustrine sediments	8	7997400	706100	0	38	0.4	22	44	0.4	102
Lacustrine sediments	9	7997500	705300	0	59	0.2	25	60	0.6	104
Lacustrine sediments	10	8002100	708400	0	28	0.1	13	31	1.1	53
Lacustrine sediments	11	8002300	707400	0	35	0.2	24	109	1.8	94
Lacustrine sediments	12	8003700	708600	0	30	0.1	12	38	4.6	42
Lacustrine sediments	13	7985900	702500	0	314	2.4	133	1980	7.6	388
Lacustrine sediments	14	7989300	702700	0	25	0.4	13	81	2.0	114
Lacustrine sediments	15	8002700	705800	0	20	0.3	22	78	0.9	87
Lacustrine sediments	16	8002700	705800	0	27	0.1	16	18	0.1	68
Lacustrine sediments	17	8002700	705800	0	59	0.4	17	13	0.2	61
Lacustrine sediments	18	8002700	705800	0	36	0.0	10	9	0.2	38
Lacustrine sediments	19	7995400	703900	0	27	0.2	16	28	0.2	72
Lacustrine sediments	20	7991600	703300	0	101	0.8	28	105	0.8	193
Lacustrine sediments	21	7984400	704600	0	390	3.0	167	292	2.8	605
Lacustrine sediments	22	7984400	704600	0	215	0.3	50	255	4.2	102
Lacustrine sediments	23	7984400	704600	0	431	0.3	81	527	2.4	150
Lacustrine sediments	24	7991000	700000	0	33	0.4	71	27	0.1	90
Lacustrine sediments	25	7992000	698900	0	52	0.5	115	43	0.1	128
Lacustrine sediments	26	8000600	698400	0	35	0.4	101	41	0.1	124
Lacustrine sediments	27	7999400	698600	0	32	0.4	95	40	0.0	126
Lacustrine sediments	28	8002600	694000	0	39	0.4	84	40	0.1	120
Lacustrine sediments	29	7993500	698400	0	32	0.4	118	44	0.0	123
Lacustrine sediments	30	7995100	698500	0	62	0.5	105	28	0.1	119
Lacustrine sediments	31	7997300	698200	0	58	0.4	100	30	0.0	129
Lacustrine sediments	32	8001300	697100	0	82	0.4	83	26	0.1	106
Lacustrine sediments	33	8010400	693800	0	138	1.4	53	70	0.4	127
Lacustrine sediments	34	8008100	693600	0	62	1.0	74	44	0.1	146
Lacustrine sediments	35	7952200	724200	0	663	9.3	378	1190	5.4	2710
Lacustrine sediments	36	8056300	677000	0	34	0.2	20	21	0.1	67
Lacustrine sediments	37	8055500	678800	0	58	0.2	14	17	0.1	55
Lacustrine sediments	38	7969000	706600	0	319	86.4	405	265	1.1	6510
Lacustrine sediments	39	7977000	706200	0	440	8.7	190	459	2.8	1800

Appendix D

Sediments

D.1 Water content, porosity, POC, PIC, C_{tot} and S_{tot}

	Site	depth [cm]	water content [%]	porosity [%]	POC [%]	PIC [%]	C_{tot} [%]	S_{tot} [%]
1	U1	0.5	47	70	0.88	0.63	1.52	0.12
2	U2	1.0	43	66	0.97	0.59	1.57	0.13
3	U3	1.5	48	71	0.86	0.71	1.57	0.13
4	U4	2.0	34	58	0.95	0.71	1.65	0.15
5	U5	2.5	39	63	1.12	0.95	2.07	0.21
6	U6	3.0	43	66	1.48	1.42	2.90	0.36
7	U7	3.5	46	70	1.41	0.88	2.29	0.27
8	U8	4.0	39	63	1.40	0.95	2.35	0.32
9	U9	5.0	43	67	1.55	1.15	2.70	0.34
10	U10	6.0	46	69	1.57	1.15	2.72	0.38
11	U11	7.0	45	68	1.39	1.11	2.50	0.32
12	U12	8.0	42	66	1.46	0.95	2.41	0.23
13	U13	9.5	44	68	nd	nd	2.51	0.29
14	U14	11.0	44	67	1.19	0.64	1.83	0.19
15	U15	13.5	42	66	0.89	0.48	1.37	0.13
16	U16	16.0	37	61	0.97	0.45	1.42	0.09
17	U17	18.5	36	60	0.96	0.14	1.10	0.07
18	U18	21.0	36	60	0.82	0.34	1.16	0.11
19	U19	23.5	nd	nd	0.98	0.19	1.17	0.13
20	U20	26.0	nd	nd	0.74	0.25	0.99	0.18
21	O1	0.5	64	83	0.72	0.36	1.08	0.07
22	O2	1.0	61	81	0.88	0.32	1.20	0.15
23	O3	1.6	38	62	0.91	0.28	1.19	0.19
24	O4	2.9	37	60	0.81	0.26	1.07	0.13
25	O5	4.0	33	56	0.90	0.24	1.14	0.10
26	O6	5.5	53	75	0.74	0.43	1.17	0.11
27	O7	7.5	36	60	0.87	0.32	1.19	0.11
28	O8	9.7	38	62	0.79	0.27	1.06	0.08
29	O9	11.7	37	61	0.74	0.20	0.94	0.07
30	O10	13.7	38	62	0.89	0.08	0.97	0.09
31	O11	15.7	38	61	0.76	0.25	1.01	0.09
32	O12	17.9	38	62	0.85	0.31	1.16	0.11
33	M1	0.5	86	94	6.04	0.01	6.05	1.31
34	M2	1.0	80	92	3.12	0.07	3.19	1.09
35	M3	1.5	75	89	3.50	0.90	4.40	1.60
36	M4	2.0	73	88	3.58	1.98	5.55	1.54
37	M5	2.5	67	84	4.23	2.25	6.49	1.40
38	M6	3.0	60	80	4.91	2.36	7.27	1.30
39	M7	3.5	59	79	4.48	1.98	6.46	1.37
40	M8	4.0	56	77	3.58	1.53	5.11	1.37
41	M9	4.5	46	69	2.23	0.95	3.18	1.42
42	M10	5.0	57	78	1.94	0.74	2.69	1.56
43	M11	6.0	55	76	1.12	0.59	1.70	1.50
44	M12	7.0	51	73	0.99	0.78	1.77	1.62
45	M13	8.0	44	67	1.05	0.03	1.08	1.57
46	M14	9.0	43	67	0.78	0.00	0.77	1.03
47	M15	10.0	42	66	0.76	0.00	0.70	0.76
48	M16	12.5	44	67	0.70	0.12	0.82	0.77
49	M17	15.0	41	64	0.84	0.11	0.95	1.02
50	M18	17.5	40	63	0.98	0.37	1.35	1.04

	Site	depth [cm]	water content [%]	porosity [%]	POC [%]	PIC [%]	C_{tot} [%]	S_{tot} [%]
51	M19	20.0	39	63	0.87	0.43	1.29	0.76
52	M20	22.7	40	64	0.82	0.00	0.78	0.64
53	M21	25.7	37	61	0.82	0.47	1.29	0.30
54	M22	28.9	39	63	1.04	0.83	1.87	0.28
55	M23	32.5	nd	nd	0.49	0.64	1.14	0.08
56	P1	0.5	81	92	6.51	2.14	8.66	8.66
57	P2	1.5	51	73	6.35	2.33	8.68	8.68
58	P3	2.0	55	76	6.01	2.54	8.55	8.55
59	P4	3.2	44	67	5.65	2.54	8.19	8.19
60	P5	4.8	31	54	1.67	0.43	2.09	2.09
61	P6	6.1	41	65	1.15	0.92	2.08	2.08
62	P7	7.5	39	63	1.27	0.94	2.21	2.21
63	P8	9.3	41	65	1.25	0.32	1.57	1.57
64	P9	11.2	43	67	1.27	0.81	2.08	2.08
65	P10	13.2	38	62	0.91	0.18	1.09	1.09
66	P11	15.2	38	62	0.90	0.45	1.35	1.35
67	P12	17.2	35	59	1.50	1.03	2.53	2.53
68	P13	19.2	nd	nd	1.82	0.69	2.50	0.29
69	P14	21.3	nd	nd	1.30	0.14	1.44	0.14
70	C1	0.5	54	76	1.92	0.00	1.89	0.06
71	C2	0.9	48	71	1.57	0.09	1.66	0.05
72	C3	1.6	42	65	1.65	0.12	1.78	0.05
73	C4	2.1	51	73	1.56	0.06	1.61	0.05
74	C5	2.8	39	63	1.68	0.00	1.68	0.05
75	C6	3.5	44	68	1.55	0.06	1.61	0.05
76	C7	4.5	41	65	1.96	0.04	2.00	0.06
77	C8	5.5	44	68	2.29	0.04	2.33	0.06
78	C9	6.5	39	63	2.21	0.06	2.28	0.06
79	C10	7.5	44	67	1.87	0.01	1.88	0.05
80	C11	8.7	43	67	2.30	0.06	2.36	0.06
81	C12	9.8	39	63	1.49	0.00	1.47	0.04
82	C13	10.8	41	64	1.45	0.06	1.50	0.03
83	C14	12.8	42	66	1.61	0.06	1.67	0.04
84	C15	14.9	37	61	1.78	0.00	1.74	0.04
85	C16	17.0	34	58	1.64	0.08	1.73	0.03
86	C17	19.5	42	65	1.98	0.00	1.98	0.06
87	C18	23.5	41	65	2.22	0.00	2.20	0.06
88	C19	27.5	31	55	1.48	0.02	1.50	0.03
89	C20	31.0	38	62	2.11	0.05	2.16	0.06
90	C21	34.8	42	66	1.64	0.13	1.77	0.07
91	C22	38.7	42	65	1.77	0.00	1.73	0.08

D.2 $MgCl_2$ single selective extraction

	Site	depth [cm]	Mn	Fe	Cu	Zn	As	Mo	Cd	Sb	Pb	U
							[$\mu g \cdot g^{-1}$]					
1	U1	0.5	17	0.0	0.6	3.4	1.1	0.3	0.4	0.7	0.1	0.0
2	U2	1.0	18	0.0	0.6	5.2	1.0	0.2	0.4	0.4	0.1	0.1
3	U3	1.5	15	0.8	0.5	4.4	1.0	0.1	0.4	0.3	0.1	0.0
4	U4	2.0	16	0.0	0.7	3.3	1.0	0.1	0.5	0.2	0.1	0.0
5	U5	2.5	17	0.9	0.6	3.1	0.9	0.1	0.6	0.3	0.1	0.1
6	U6	3.0	16	0.0	1.0	7.5	0.6	0.1	0.8	0.2	0.1	0.1
7	U7	3.5	13	0.1	0.8	3.1	0.8	0.1	0.7	0.2	0.1	0.1
8	U8	4.0	13	0.9	0.8	3.0	1.0	0.1	0.9	0.2	0.1	0.1
9	U9	5.0	20	0.5	0.8	3.0	0.7	0.2	1.0	0.3	0.1	0.2
10	U10	6.0	19	1.1	0.8	3.1	0.8	0.1	1.0	0.3	0.1	0.2
11	U11	7.0	24	0.0	0.8	3.1	0.9	0.4	1.1	0.9	0.1	0.2
12	U12	8.0	24	0.0	0.9	3.7	1.1	0.3	1.1	0.5	0.1	0.1
13	U13	9.5	22	0.0	0.9	3.3	1.2	0.3	1.1	0.4	0.0	0.2
14	U14	11.0	25	0.0	1.3	3.0	1.7	0.2	1.1	0.3	0.1	0.1
15	U15	13.5	47	0.0	1.1	3.6	1.4	0.2	1.1	0.3	0.1	0.1
16	U16	16.0	49	0.0	0.7	3.3	1.4	0.2	1.0	0.3	0.1	0.1
17	U17	18.5	24	0.4	0.9	3.9	1.5	0.1	0.9	0.2	0.1	0.1
18	U18	21.0	36	0.0	0.7	2.8	1.2	0.1	0.9	0.2	0.0	0.1
19	U19	23.5	28	0.0	0.5	3.1	0.9	0.1	1.0	0.3	0.1	0.1
20	U20	26.0	29	0.5	0.5	2.9	0.5	0.1	1.1	0.2	0.0	0.1
21	O1	0.5	18	0.0	0.6	1.6	0.8	0.3	0.3	0.7	0.1	0.1
22	O2	1.0	18	0.0	0.4	2.1	0.4	0.3	0.5	0.6	0.1	0.1
23	O3	1.6	31	0.0	0.3	1.7	0.3	0.3	0.7	0.6	0.0	0.2
24	O4	2.9	33	0.0	0.3	1.8	0.3	0.3	0.5	0.7	0.1	0.1
25	O5	4.0	15	0.0	0.3	1.5	0.5	0.1	0.7	0.7	0.1	0.1
26	O6	5.5	20	0.0	0.3	2.0	0.5	0.2	0.5	0.7	0.1	0.1
27	O7	7.5	23	0.0	0.3	1.9	0.5	0.2	0.7	0.7	0.1	0.1
28	O8	9.7	12	0.0	0.4	1.8	0.5	0.1	0.7	0.6	0.1	0.1
29	O9	11.7	8	0.0	0.2	3.8	0.6	0.0	0.7	0.6	0.0	0.0
30	O10	13.7	22	0.0	0.4	2.3	0.4	0.2	0.7	0.8	0.1	0.1
31	O11	15.7	20	0.0	0.3	2.2	0.4	0.1	0.6	0.7	0.1	0.1
32	O12	17.9	27	0.0	0.2	1.8	0.3	0.2	0.5	0.9	0.1	0.2
33	M1	0.5	40	0.0	0.9	3.1	0.4	0.7	0.3	0.7	0.1	0.1
34	M2	1.0	66	0.0	1.2	3.2	0.1	0.6	0.4	0.3	0.0	0.0
35	M3	1.5	35	0.0	1.3	2.9	0.2	0.6	0.2	0.2	0.1	0.2
36	M4	2.0	42	0.0	1.1	2.6	0.2	0.5	0.1	0.2	0.0	0.3
37	M5	2.5	50	0.0	1.3	2.7	0.2	0.6	0.1	0.2	0.0	0.4
38	M6	3.0	81	0.0	1.3	3.1	0.2	0.8	0.1	0.2	0.1	0.4
39	M7	3.5	82	0.0	1.4	3.5	0.2	0.6	0.1	0.2	0.0	0.3
40	M8	4.0	92	0.0	1.5	2.8	0.2	0.6	0.2	0.1	0.1	0.2
41	M9	4.5	75	0.0	1.7	2.8	0.2	0.4	0.2	0.1	0.0	0.2
42	M10	5.0	79	0.0	2.2	2.9	0.2	0.4	0.2	0.1	0.0	0.2
43	M11	6.0	77	0.0	1.8	2.9	0.2	0.3	0.2	0.1	0.0	0.1
44	M12	7.0	80	0.0	1.6	2.7	0.4	0.5	0.2	0.7	0.0	0.2
45	M13	8.0	76	0.0	1.5	1.7	0.3	0.4	0.3	0.4	0.0	0.1
46	M14	9.0	59	0.0	1.4	3.1	0.3	0.2	0.3	0.2	0.1	0.0
47	M15	10.0	53	0.0	1.0	1.6	0.2	0.2	0.3	0.2	0.0	0.0
48	M16	12.5	45	0.0	1.0	1.5	0.3	0.2	0.2	0.1	0.0	0.1
49	M17	15.0	50	0.0	1.4	2.0	0.4	0.4	0.3	0.2	0.0	0.1

	Site	depth [cm]	Mn	Fe	Cu	Zn	As	Mo	Cd	Sb	Pb	U
							[$\mu g \cdot g^{-1}$]					
50	M18	17.5	56	0.0	1.8	1.6	0.3	0.4	0.3	0.2	0.0	0.1
51	M19	20.0	49	0.0	1.3	1.7	0.3	0.4	0.2	0.2	0.0	0.2
52	M20	22.7	47	0.0	1.0	1.9	0.3	0.3	0.5	0.1	0.0	0.0
53	M21	25.7	28	0.0	0.9	1.7	0.5	0.5	0.3	0.2	0.0	0.4
54	M22	28.9	25	1.5	0.9	2.3	0.9	1.0	0.3	0.3	0.1	0.7
55	M23	32.5	15	1.6	0.1	1.6	2.3	0.2	0.1	0.1	0.1	0.0
56	P1	0.5	24	0.0	0.1	1.4	0.2	1.1	0.1	0.7	0.0	0.8
57	P2	1.5	64	0.0	0.1	1.2	0.1	1.3	0.1	0.4	0.0	0.7
58	P3	2.0	64	0.0	0.3	2.0	0.1	0.8	0.1	0.3	0.0	0.6
59	P4	3.2	108	0.0	0.2	1.3	0.1	0.8	0.1	0.2	0.0	0.6
60	P5	4.8	51	0.0	0.6	2.0	0.1	0.7	0.1	0.3	0.0	0.3
61	P6	6.1	59	0.0	0.9	1.2	0.1	0.6	0.1	0.4	0.0	0.4
62	P7	7.5	62	0.0	0.7	1.2	0.1	0.5	0.1	0.4	0.0	0.3
63	P8	9.3	43	0.0	0.5	2.5	0.2	0.6	0.1	0.5	0.0	0.2
64	P9	11.2	63	0.0	0.4	1.3	0.1	0.5	0.3	0.5	0.0	0.3
65	P10	13.2	59	0.0	0.3	1.1	0.1	0.8	0.2	0.5	0.0	0.2
66	P11	15.2	66	0.0	0.2	1.2	0.1	1.0	0.2	0.7	0.0	0.5
67	P12	17.2	32	0.4	0.4	2.8	0.3	0.9	0.3	1.1	0.1	0.8
68	P13	19.2	18	0.6	0.2	1.1	0.5	0.1	0.2	1.4	0.3	0.4
69	P14	21.3	14	2.6	0.1	2.0	0.4	0.0	0.2	1.5	0.4	0.0
70	C1	0.5	98	0.0	0.1	2.1	0.2	0.2	0.2	0.7	0.1	0.0
71	C2	0.9	112	0.0	0.0	2.0	0.1	0.1	0.1	0.4	0.1	0.0
72	C3	1.6	113	0.0	0.0	2.4	0.1	0.1	0.2	0.2	0.2	0.0
73	C4	2.1	109	0.0	0.1	2.4	0.1	0.0	0.2	0.2	0.2	0.0
74	C5	2.8	60	0.0	0.0	3.2	0.1	0.0	0.2	0.1	0.2	0.0
75	C6	3.5	53	0.0	0.0	2.4	0.1	0.0	0.2	0.1	0.2	0.0
76	C7	4.5	38	0.0	0.0	3.4	0.0	0.0	0.2	0.1	0.1	0.0
77	C8	5.5	82	0.0	0.0	5.0	0.1	0.0	0.2	0.1	0.2	0.0
78	C9	6.5	40	0.0	0.0	3.2	0.1	0.0	0.2	0.1	0.1	0.0
79	C10	7.5	47	0.0	0.0	3.4	0.1	0.0	0.2	0.1	0.1	0.0
80	C11	8.7	48	1.8	0.0	3.9	0.0	0.0	0.2	0.1	0.2	0.0
81	C12	9.8	46	0.0	0.1	3.2	0.1	0.3	0.2	0.6	0.2	0.0
82	C13	10.8	34	0.0	0.0	2.5	0.1	0.1	0.2	0.4	0.2	0.0
83	C14	12.8	147	0.0	0.0	3.9	0.1	0.1	0.2	0.3	0.3	0.0
84	C15	14.9	52	0.0	0.0	2.2	0.0	0.1	0.1	0.2	0.2	0.0
85	C16	17.0	30	0.0	0.2	3.2	0.1	0.1	0.1	0.2	0.1	0.0
86	C17	19.5	168	0.0	0.0	3.8	0.1	0.0	0.2	0.2	0.3	0.0
87	C18	23.5	271	0.0	0.0	3.3	0.1	0.0	0.2	0.2	0.3	0.0
88	C19	27.5	19	0.9	0.1	1.5	0.1	0.0	0.1	0.1	0.1	0.0
89	C20	31.0	30	3.5	0.0	6.6	0.1	0.1	0.2	0.1	0.1	0.0
90	C21	34.8	126	3.6	0.1	1.9	0.2	0.1	0.1	0.2	0.0	0.0
91	C22	38.7	241	4.1	0.2	3.7	0.1	0.0	0.2	0.1	0.3	0.0

D.3 NaOAc Single selective extraction

	Site	depth [cm]	Mn	Fe	Cu	Zn	As	Mo	Cd	Sb	Pb	U
							[$\mu g \cdot g^{-1}$]					
1	U1	0.5	211	210	8	4	11	nd	0.3	0.4	11	0.2
2	U2	1.0	211	298	9	3	12	nd	0.3	0.8	11	0.2
3	U3	1.5	204	288	9	3	12	nd	0.3	0.8	11	0.2
4	U4	2.0	214	252	8	5	11	nd	0.3	1.0	12	0.2
5	U5	2.5	237	295	10	8	13	nd	0.4	1.3	12	0.3
6	U6	3.0	247	370	12	6	13	nd	0.5	1.5	12	0.4
7	U7	3.5	203	236	12	8	12	nd	0.5	1.4	12	0.4
8	U8	4.0	210	228	12	8	13	nd	0.4	1.7	13	0.4
9	U9	5.0	269	444	13	12	13	nd	0.5	2.0	12	0.6
10	U10	6.0	241	397	14	12	14	nd	0.5	1.8	12	0.5
11	U11	7.0	238	379	14	10	14	nd	0.3	1.2	13	0.5
12	U12	8.0	237	336	14	10	15	nd	0.5	1.5	13	0.5
13	U13	9.5	244	244	13	9	15	nd	0.4	1.6	12	0.5
14	U14	11.0	183	116	12	6	15	nd	0.5	1.6	14	0.5
15	U15	13.5	173	102	11	6	13	nd	0.4	1.8	14	0.4
16	U16	16.0	180	120	11	6	12	nd	0.2	1.6	14	0.4
17	U17	18.5	162	89	12	5	12	nd	0.3	1.4	12	0.4
18	U18	21.0	177	98	11	6	12	nd	0.2	1.2	11	0.3
19	U19	23.5	187	147	9	8	9	nd	0.3	1.7	11	0.4
20	U20	26.0	153	155	9	9	7	nd	0.2	1.6	11	0.5
21	O1	0.5	182	376	10	3	9	nd	0.1	0.0	7	0.2
22	O2	1.0	200	801	12	9	14	nd	0.2	0.6	10	0.2
23	O3	1.6	246	1209	16	15	12	nd	0.5	1.4	14	0.3
24	O4	2.9	212	919	15	14	11	nd	0.5	1.4	16	0.3
25	O5	4.0	176	699	15	11	11	nd	0.3	1.7	15	0.2
26	O6	5.5	201	795	15	12	12	nd	0.4	1.9	16	0.2
27	O7	7.5	233	790	16	15	14	nd	0.6	2.0	16	0.3
28	O8	9.7	196	799	14	13	14	nd	0.3	1.9	14	0.2
29	O9	11.7	165	627	14	7	13	nd	0.2	1.5	12	0.2
30	O10	13.7	252	959	14	13	11	nd	0.3	2.2	14	0.4
31	O11	15.7	238	807	12	12	11	nd	0.4	2.1	13	0.3
32	O12	17.9	310	952	13	17	11	nd	0.5	2.3	16	0.4
33	M1	0.5	124	440	8	11	7	nd	0.2	0.0	6	1.4
34	M2	1.0	87	363	10	6	3	nd	0.1	0.0	4	1.2
35	M3	1.5	221	686	13	9	3	nd	0.2	0.4	5	1.5
36	M4	2.0	334	574	11	8	5	nd	0.2	0.4	5	1.7
37	M5	2.5	380	582	10	8	5	nd	0.1	0.4	5	1.9
38	M6	3.0	428	523	8	8	6	nd	0.2	0.4	5	2.1
39	M7	3.5	382	614	10	7	5	nd	0.1	0.5	5	1.7
40	M8	4.0	316	662	13	7	5	nd	0.2	0.5	5	1.5
41	M9	4.5	238	620	18	5	5	nd	0.1	0.5	6	0.9
42	M10	5.0	220	770	22	6	5	nd	0.1	0.6	6	0.8
43	M11	6.0	210	581	27	5	6	nd	0.1	0.6	7	0.6
44	M12	7.0	243	581	29	4	8	nd	0.1	0.1	8	0.7
45	M13	8.0	91	548	23	5	10	nd	0.0	0.3	9	0.5
46	M14	9.0	58	347	21	3	10	nd	0.1	0.2	7	0.4
47	M15	10.0	49	343	20	5	9	nd	0.0	0.3	9	0.3
48	M16	12.5	83	331	16	4	8	nd	0.1	0.5	8	0.4
49	M17	15.0	77	390	14	4	10	nd	0.0	0.6	10	0.5
50	M18	17.5	162	555	16	6	8	nd	0.1	0.9	11	0.7

	Site	depth [cm]	Mn	Fe	Cu	Zn	As	Mo	Cd	Sb	Pb	U
							[$\mu g \cdot g^{-1}$]					
51	M19	20.0	179	636	18	8	7	nd	0.1	1.2	13	0.8
52	M20	22.7	57	303	14	5	8	nd	0.1	1.1	12	0.6
53	M21	25.7	151	576	18	6	10	nd	0.1	1.7	28	1.3
54	M22	28.9	215	400	16	5	13	nd	0.2	2.3	41	2.0
55	M23	32.5	111	48	3	0	14	nd	0.0	0.6	18	0.2
56	P1	0.5	423	1064	9	15	6	nd	0.2	0.2	9	3.2
57	P2	1.5	546	1208	9	17	7	nd	0.2	0.3	10	2.7
58	P3	2.0	545	1057	10	15	7	nd	0.2	0.4	9	2.5
59	P4	3.2	494	1271	11	15	7	nd	0.2	0.4	10	2.4
60	P5	4.8	148	2475	32	9	10	nd	0.2	0.5	16	0.8
61	P6	6.1	206	1468	33	9	12	nd	0.1	0.7	16	0.7
62	P7	7.5	200	1467	29	9	14	nd	0.1	0.7	17	0.5
63	P8	9.3	95	1650	23	7	17	nd	0.2	0.7	19	0.5
64	P9	11.2	177	1533	21	12	11	nd	0.2	1.1	26	0.7
65	P10	13.2	97	2053	25	13	7	nd	0.2	1.2	28	0.5
66	P11	15.2	185	2014	21	16	12	nd	0.3	1.6	40	0.9
67	P12	17.2	243	1217	18	31	15	nd	0.4	2.6	77	1.4
68	P13	19.2	182	604	12	7	15	nd	0.2	2.9	87	0.7
69	P14	21.3	69	339	5	8	10	nd	0.1	3.1	66	0.3
70	C1	0.5	179	1379	2.4	5.2	10	nd	0.0	0.2	11	0.7
71	C2	0.9	149	1257	2.6	4.9	7	nd	0.1	0.5	11	0.7
72	C3	1.6	132	1145	2.2	4.6	5	nd	0.1	0.6	10	0.8
73	C4	2.1	133	1094	2.4	4.3	5	nd	0.1	0.7	10	0.8
74	C5	2.8	110	950	1.9	3.2	4	nd	0.0	0.6	8	0.9
75	C6	3.5	109	989	1.5	4.4	4	nd	0.0	0.5	7	1.1
76	C7	4.5	101	948	1.1	3.4	4	nd	0.0	0.4	6	1.3
77	C8	5.5	133	1139	1.3	3.6	5	nd	0.0	0.5	7	1.4
78	C9	6.5	113	1036	1.2	4.5	4	nd	0.0	0.5	5	1.3
79	C10	7.5	112	1127	1.2	3.8	5	nd	0.0	0.5	6	1.1
80	C11	8.7	120	1211	1.3	4.2	5	nd	0.0	0.6	6	1.3
81	C12	9.8	124	867	1.8	2.3	4	nd	0.0	0.0	8	1.0
82	C13	10.8	116	790	3.4	1.9	4	nd	0.0	0.3	9	0.6
83	C14	12.8	140	1076	3.0	2.8	4	nd	0.0	0.6	12	0.6
84	C15	14.9	125	826	3.1	1.6	4	nd	0.0	0.6	10	0.4
85	C16	17.0	104	623	3.7	0.1	3	nd	0.0	0.6	8	0.3
86	C17	19.5	121	1158	1.9	3.2	4	nd	0.0	0.6	9	0.9
87	C18	23.5	127	1290	2.5	3.9	5	nd	0.0	0.6	11	0.8
88	C19	27.5	124	940	2.8	2.1	4	nd	0.0	0.6	8	0.5
89	C20	31.0	181	1504	2.2	0.0	9	nd	0.0	0.7	9	0.8
90	C21	34.8	317	2135	3.3	5.3	11	nd	0.1	1.0	15	0.4
91	C22	38.7	143	1653	2.7	3.6	6	nd	0.0	0.7	14	0.6

D.4 Ascorbate single selective extraction

	Site	depth [cm]	Mn	Fe	Cu	Zn	As	Mo	Cd	Sb	Pb	U
							[$\mu g \cdot g^{-1}$]					
1	U1	0.5	339	964	0.3	11	24	0.4	0.1	2.8	5.1	0.2
2	U2	1.0	374	1238	0.3	10	28	0.2	0.0	2.7	6.0	0.2
3	U3	1.5	321	1242	0.2	10	28	0.1	0.0	2.5	5.8	0.1
4	U4	2.0	315	1146	0.2	10	25	0.1	0.0	2.6	5.7	0.1
5	U5	2.5	298	1286	0.4	13	27	0.1	0.0	3.1	5.9	0.3
6	U6	3.0	329	1679	0.4	18	32	0.2	0.0	3.7	5.7	0.5
7	U7	3.5	316	1585	0.4	15	32	0.2	0.0	3.8	5.5	0.4
8	U8	4.0	322	1602	0.5	14	36	0.3	0.0	4.3	6.8	0.5
9	U9	5.0	297	2037	0.7	19	39	0.4	0.0	5.0	6.3	0.6
10	U10	6.0	240	1961	0.6	18	40	0.4	0.0	4.8	5.6	0.6
11	U11	7.0	302	1794	0.5	18	38	0.6	0.0	5.1	5.2	0.6
12	U12	8.0	338	1754	0.6	17	40	0.5	0.0	5.2	6.8	0.6
13	U13	9.5	307	1617	0.6	17	40	0.5	0.0	4.7	6.5	0.6
14	U14	11.0	272	1120	2.8	13	39	0.6	0.5	4.5	6.5	0.6
15	U15	13.5	281	1225	3.7	14	38	0.4	0.6	5.1	7.4	0.4
16	U16	16.0	331	1416	1.9	15	41	0.3	0.6	5.0	7.8	0.4
17	U17	18.5	335	1047	0.3	13	35	0.2	0.0	4.0	3.3	0.4
18	U18	21.0	304	1246	0.5	12	37	0.3	0.4	3.5	5.4	0.3
19	U19	23.5	336	1560	0.1	16	35	0.2	0.0	5.6	5.4	0.4
20	U20	26.0	281	1709	0.1	18	30	0.5	0.0	5.3	2.9	0.5
21	O1	0.5	0	929	0.5	6	22	0.2	0.1	1.2	3.2	0.2
22	O2	1.0	344	1967	0.1	12	43	0.4	0.0	2.8	3.7	0.3
23	O3	1.6	306	2454	0.1	15	37	0.5	0.1	4.1	6.1	0.4
24	O4	2.9	251	1869	0.2	12	26	0.4	0.0	3.8	4.8	0.4
25	O5	4.0	275	1625	0.2	20	30	0.2	0.0	4.8	5.8	0.2
26	O6	5.5	278	1760	0.1	13	31	0.3	0.0	5.4	6.4	0.3
27	O7	7.5	280	1667	0.1	15	30	0.3	0.1	5.0	5.6	0.3
28	O8	9.7	348	2040	0.2	15	45	0.2	0.0	5.2	6.7	0.2
29	O9	11.7	341	1947	1.7	13	48	0.0	0.4	4.9	7.3	0.1
30	O10	13.7	345	2396	0.1	15	46	0.2	0.0	6.0	4.6	0.3
31	O11	15.7	349	2019	0.1	14	34	0.1	0.0	6.0	5.6	0.4
32	O12	17.9	348	2219	0.0	17	31	0.3	0.0	8.2	6.4	0.5
33	M1	0.5	122	5443	1.1	18	59	2.8	0.1	3.0	10.4	1.8
34	M2	1.0	111	5994	1.7	18	31	2.8	0.0	2.4	5.6	1.4
35	M3	1.5	168	7300	0.7	16	34	2.8	0.0	2.9	3.0	1.8
36	M4	2.0	214	6794	0.7	15	35	2.3	0.0	2.8	2.9	2.1
37	M5	2.5	240	7127	0.7	13	33	2.3	0.0	2.5	3.1	2.3
38	M6	3.0	256	6504	0.7	12	34	2.8	0.0	2.1	3.0	2.5
39	M7	3.5	233	6587	0.7	13	38	2.5	0.0	2.5	2.9	2.1
40	M8	4.0	197	6160	0.5	13	38	2.5	0.0	2.6	1.9	1.8
41	M9	4.5	129	5309	0.6	12	39	1.7	0.0	2.8	1.6	1.1
42	M10	5.0	185	5367	0.4	12	43	1.7	0.0	3.1	1.1	0.9
43	M11	6.0	118	4178	0.3	11	43	1.3	0.0	3.1	1.0	0.6
44	M12	7.0	170	3528	0.3	10	46	1.3	0.0	3.5	0.9	0.8
45	M13	8.0	126	3201	0.3	10	57	0.9	0.0	3.0	0.8	0.6
46	M14	9.0	92	2723	0.2	9	50	0.6	0.0	1.9	0.9	0.3
47	M15	10.0	47	2457	0.1	9	43	0.5	0.0	1.9	0.9	0.3
48	M16	12.5	112	3058	0.2	9	41	0.8	0.0	2.5	1.9	0.4
49	M17	15.0	101	3173	0.3	10	55	1.2	0.0	2.7	1.7	0.6
50	M18	17.5	147	4482	0.3	13	56	2.0	0.0	4.4	2.8	0.8

	Site	depth [cm]	Mn	Fe	Cu	Zn	As	Mo	Cd	Sb	Pb	U
							[$\mu g \cdot g^{-1}$]					
51	M19	20.0	140	4519	0.3	14	47	1.7	0.0	5.8	4.8	0.9
52	M20	22.7	100	3641	0.4	15	47	1.4	0.0	6.4	6.0	0.6
53	M21	25.7	143	2599	0.2	10	40	1.3	0.0	5.3	6.0	1.6
54	M22	28.9	185	2224	0.2	10	42	2.4	0.0	7.3	10.0	2.5
55	M23	32.5	138	576	0.0	2	28	0.0	0.0	1.3	5.7	0.2
56	P1	0.5	0	5866	1.7	20	44	7.3	0.0	3.1	5.2	4.2
57	P2	1.5	184	6121	0.8	15	44	5.6	0.0	2.7	7.3	3.3
58	P3	2.0	205	5775	0.9	14	41	5.2	0.0	2.3	6.5	3.0
59	P4	3.2	182	6160	0.9	15	40	4.3	0.0	2.1	3.7	2.8
60	P5	4.8	78	3864	0.3	8	27	1.7	0.0	2.4	2.9	0.8
61	P6	6.1	86	2979	0.1	9	39	1.2	0.0	3.0	2.8	0.8
62	P7	7.5	94	2902	0.2	9	44	0.9	0.0	2.5	3.8	0.7
63	P8	9.3	71	2816	0.1	8	46	0.9	0.0	3.0	2.7	0.6
64	P9	11.2	102	3673	0.1	12	46	1.4	0.0	4.2	7.5	0.8
65	P10	13.2	79	3604	0.0	9	23	1.5	0.0	4.4	8.3	0.6
66	P11	15.2	112	3377	0.1	11	34	1.9	0.0	6.3	11.5	1.1
67	P12	17.2	134	2492	0.1	15	41	1.8	0.0	8.3	29.6	1.8
68	P13	19.2	111	1866	0.3	9	39	0.3	0.0	9.0	32.2	1.0
69	P14	21.3	43	1226	nd	13	21	0.0	0.0	8.8	26.0	0.2
70	C1	0.5	26	4059	0.5	11	48	0.3	0.0	3.2	8.7	1.0
71	C2	0.9	365	2893	0.2	7	28	0.2	0.0	2.1	6.2	0.7
72	C3	1.6	322	2815	0.2	7	22	0.2	0.0	1.9	5.9	0.9
73	C4	2.1	347	2894	0.3	7	21	0.1	0.0	1.9	5.8	0.9
74	C5	2.8	336	2847	0.8	7	20	0.1	0.1	1.9	5.9	1.0
75	C6	3.5	371	3053	0.6	12	22	0.2	0.0	1.9	5.7	1.6
76	C7	4.5	324	2663	2.0	8	19	0.2	0.1	1.4	4.3	1.5
77	C8	5.5	340	3116	0.5	8	22	0.2	0.0	1.6	4.3	1.5
78	C9	6.5	345	2953	1.8	9	22	0.3	0.1	1.6	4.5	1.4
79	C10	7.5	279	2636	0.7	8	20	0.2	0.0	1.4	4.1	1.3
80	C11	8.7	290	2980	1.2	10	21	0.2	0.1	1.6	4.9	1.5
81	C12	9.8	318	2217	1.7	7	15	0.3	0.1	1.9	5.2	1.1
82	C13	10.8	303	2275	2.5	5	16	0.2	0.1	2.0	6.1	0.6
83	C14	12.8	486	3062	0.8	7	19	0.2	0.1	2.3	7.3	0.6
84	C15	14.9	266	2130	1.8	4	13	0.1	0.1	2.0	6.3	0.4
85	C16	17.0	145	1596	1.5	4	10	0.1	0.1	1.6	4.5	0.3
86	C17	19.5	311	4469	2.4	10	24	0.3	0.1	2.2	7.4	1.2
87	C18	23.5	312	3767	0.6	7	19	0.2	0.0	2.0	6.4	0.8
88	C19	27.5	232	2337	2.4	5	14	0.1	0.0	1.7	5.2	0.4
89	C20	31.0	356	3944	2.0	9	28	0.2	0.1	2.1	6.9	0.8
90	C21	34.8	499	5141	0.1	6	42	0.1	0.0	2.4	7.7	0.4
91	C22	38.7	294	4730	0.1	6	26	0.1	0.0	2.3	7.2	0.6

D.5 H_2O_2 single selective extraction

	Site	depth [cm]	Mn	Fe	Cu	Zn	As	Mo	Cd	Sb	Pb	U
							[$\mu g \cdot g^{-1}$]					
1	U1	0.5	65	0.0	3.0	0.1	1.4	0.1	0.1	0.5	0.0	0.0
2	U2	1.0	101	0.0	3.8	0.1	1.5	0.2	0.1	0.6	0.0	0.0
3	U3	1.5	55	0.0	3.0	0.0	1.2	0.1	0.1	0.5	0.0	0.0
4	U4	2.0	73	0.0	3.1	0.1	1.4	0.1	0.1	0.6	0.0	0.0
5	U5	2.5	64	0.0	3.8	0.1	1.3	0.2	0.1	0.7	0.0	0.1
6	U6	3.0	47	0.0	4.2	0.1	1.0	0.3	0.1	0.8	0.0	0.1
7	U7	3.5	56	0.0	3.6	0.1	1.1	0.3	0.1	0.7	0.0	0.1
8	U8	4.0	62	0.0	3.8	0.2	1.1	0.3	0.1	0.8	0.0	0.1
9	U9	5.0	71	0.0	5.4	0.1	1.2	0.5	0.2	0.9	0.0	0.1
10	U10	6.0	52	0.0	4.4	0.1	1.1	0.5	0.1	0.8	0.0	0.1
11	U11	7.0	53	0.0	4.2	0.1	1.2	0.5	0.1	0.9	0.0	0.1
12	U12	8.0	50	0.0	4.1	0.1	1.4	0.4	0.1	0.9	0.0	0.1
13	U13	9.5	70	0.0	5.5	0.1	1.7	0.6	0.1	1.0	0.0	0.1
14	U14	11.0	90	0.0	4.3	0.1	2.4	0.7	0.3	1.1	0.0	0.1
15	U15	13.5	98	0.0	3.4	0.1	2.2	0.5	0.3	1.3	0.0	0.1
16	U16	16.0	102	0.0	3.5	0.1	2.1	0.4	0.2	1.2	0.0	0.1
17	U17	18.5	94	0.0	3.1	0.1	2.4	0.3	0.2	1.0	0.0	0.0
18	U18	21.0	86	0.0	3.1	0.1	2.4	0.4	0.2	0.9	0.0	0.0
19	U19	23.5	94	0.0	2.8	0.2	1.7	0.3	0.2	1.2	0.0	0.0
20	U20	26.0	72	0.0	2.1	0.1	1.0	0.4	0.2	0.9	0.0	0.1
21	O1	0.5	161	0.0	2.6	0.1	1.5	0.2	0.1	0.2	0.0	0.0
22	O2	1.0	65	0.0	3.0	0.1	1.1	0.5	0.1	0.5	0.0	0.0
23	O3	1.6	48	0.0	3.1	0.2	0.6	0.7	0.1	0.6	0.0	0.1
24	O4	2.9	44	0.0	2.8	0.1	0.7	0.6	0.1	0.8	0.0	0.0
25	O5	4.0	72	0.0	3.4	0.2	0.8	0.4	0.2	0.9	0.0	0.0
26	O6	5.5	84	0.0	3.2	0.2	0.9	0.6	0.2	1.1	0.0	0.0
27	O7	7.5	83	0.0	3.7	0.3	1.0	0.6	0.3	1.1	0.0	0.0
28	O8	9.7	87	0.0	2.7	0.2	0.9	0.4	0.2	1.0	0.0	0.0
29	O9	11.7	91	0.0	2.7	0.1	1.1	0.1	0.1	1.1	0.0	0.0
30	O10	13.7	92	0.0	2.7	0.2	0.7	0.6	0.2	1.1	0.0	0.0
31	O11	15.7	82	0.0	2.3	0.2	0.7	0.3	0.2	1.4	0.0	0.0
32	O12	17.9	66	0.0	2.8	0.1	0.6	0.6	0.1	1.2	0.0	0.1
33	M1	0.5	261	1.9	6.3	10.6	6.3	0.1	0.3	0.1	0.1	0.5
34	M2	1.0	311	9.5	5.5	7.3	4.4	0.0	0.4	0.1	0.0	0.3
35	M3	1.5	228	0.1	3.7	4.5	2.1	0.0	0.3	0.1	0.0	0.2
36	M4	2.0	32	0.0	0.5	7.7	0.1	0.4	0.0	0.2	0.0	0.2
37	M5	2.5	63	0.3	0.6	9.7	0.2	0.5	0.0	0.2	0.0	0.5
38	M6	3.0	68	0.3	0.8	10.3	0.2	0.7	0.0	0.2	0.0	0.6
39	M7	3.5	52	0.2	0.6	10.0	0.1	0.6	0.0	0.2	0.0	0.3
40	M8	4.0	40	0.0	0.5	8.2	0.3	0.5	0.0	0.2	0.0	0.4
41	M9	4.5	14	0.0	0.4	5.7	0.1	0.3	0.0	0.2	0.0	0.3
42	M10	5.0	12	0.0	0.3	4.6	0.1	0.3	0.0	0.1	0.0	0.2
43	M11	6.0	8	0.0	0.2	2.6	0.1	0.2	0.0	0.1	0.0	0.1
44	M12	7.0	10	0.0	0.4	5.2	0.2	0.3	0.0	0.1	0.0	0.2
45	M13	8.0	7	0.0	0.2	2.7	0.1	0.2	0.0	0.1	0.0	0.1
46	M14	9.0	176	8.1	4.0	5.5	2.9	0.0	0.4	0.0	0.0	0.2
47	M15	10.0	152	7.0	3.6	4.7	1.8	0.0	0.3	0.1	0.1	0.1
48	M16	12.5	100	0.0	1.0	1.6	0.4	0.0	0.1	0.1	0.0	0.0
49	M17	15.0	174	0.9	4.0	3.0	1.6	0.0	0.3	0.1	0.1	0.0
50	M18	17.5	5	0.0	0.1	1.5	0.1	0.3	0.0	0.2	0.0	0.1

	Site	depth [cm]	Mn	Fe	Cu	Zn	As	Mo	Cd	Sb	Pb	U
							[$\mu g \cdot g^{-1}$]					
51	M19	20.0	6	0.0	0.2	1.9	0.1	0.4	0.0	0.4	0.0	0.2
52	M20	22.7	83	0.0	1.1	1.5	0.5	0.1	0.3	0.2	0.0	0.1
53	M21	25.7	7	0.0	0.1	2.5	0.1	0.9	0.0	0.7	0.0	0.3
54	M22	28.9	0	0.0	0.0	0.0	0.0	0.0	0.0	0.0	0.0	0.0
55	M23	32.5	8	0.0	0.0	0.8	0.0	3.4	0.0	0.6	0.0	0.0
56	P1	0.5	57	0.5	13.2	0.3	0.8	4.4	0.0	0.4	0.0	0.5
57	P2	1.5	77	0.8	14.4	0.3	0.8	3.7	0.0	0.4	0.0	0.5
58	P3	2.0	92	0.8	14.1	0.3	0.7	2.9	0.0	0.4	0.0	0.7
59	P4	3.2	101	0.7	12.9	0.3	0.7	2.2	0.0	0.3	0.0	0.7
60	P5	4.8	16	0.0	3.4	0.2	0.1	0.8	0.0	0.1	0.0	0.1
61	P6	6.1	5	0.0	2.3	0.1	0.2	0.7	0.0	0.1	0.0	0.1
62	P7	7.5	4	0.0	2.2	0.1	0.2	0.6	0.0	0.1	0.0	0.1
63	P8	9.3	256	0.7	4.4	2.8	0.0	0.8	0.4	0.0	0.1	0.1
64	P9	11.2	5	0.0	2.4	0.2	0.2	0.9	0.0	0.2	0.0	0.1
65	P10	13.2	4	0.0	1.6	0.3	0.1	1.4	0.0	0.3	0.0	0.1
66	P11	15.2	5	0.0	2.6	0.1	0.3	2.1	0.0	0.6	0.0	0.2
67	P12	17.2	10	0.0	4.1	0.3	0.7	2.4	0.0	1.2	0.0	0.4
68	P13	19.2	13	0.0	3.6	0.2	0.8	0.6	0.0	1.7	0.1	0.2
69	P14	21.3	18	0.0	0.4	0.2	0.4	0.2	0.1	1.9	0.2	0.0
70	C1	0.5	450	0.0	0.6	0.6	0.1	0.2	0.1	0.3	0.0	0.0
71	C2	0.9	507	0.3	0.7	0.7	0.1	0.2	0.1	0.2	0.0	0.1
72	C3	1.6	464	0.0	1.1	0.8	0.1	0.1	0.1	0.2	0.0	0.1
73	C4	2.1	456	0.0	0.9	0.6	0.0	0.1	0.1	0.2	0.0	0.1
74	C5	2.8	427	0.0	0.9	0.6	0.1	0.1	0.1	0.2	0.0	0.1
75	C6	3.5	408	0.0	0.8	0.7	0.0	0.1	0.1	0.2	0.0	0.1
76	C7	4.5	469	0.0	0.9	1.0	0.0	0.2	0.1	0.2	0.0	0.2
77	C8	5.5	544	1.4	2.0	1.9	0.0	0.2	0.1	0.2	0.0	0.3
78	C9	6.5	559	1.3	1.6	1.8	0.0	0.2	0.1	0.2	0.0	0.3
79	C10	7.5	442	0.2	1.0	1.0	0.1	0.2	0.1	0.2	0.0	0.2
80	C11	8.7	454	0.6	1.3	1.4	0.1	0.2	0.1	0.2	0.0	0.3
81	C12	9.8	453	0.0	0.7	0.6	0.1	0.2	0.1	0.2	0.0	0.1
82	C13	10.8	443	0.0	1.0	0.5	0.1	0.1	0.1	0.3	0.0	0.1
83	C14	12.8	486	0.0	1.1	0.7	0.1	0.1	0.1	0.3	0.0	0.1
84	C15	14.9	406	0.0	1.2	0.8	0.1	0.1	0.1	0.3	0.0	0.1
85	C16	17.0	276	0.0	1.2	0.5	0.1	0.1	0.0	0.4	0.0	0.0
86	C17	19.5	496	0.1	1.4	1.0	0.0	0.1	0.1	0.2	0.0	0.1
87	C18	23.5	490	0.1	1.5	1.1	0.0	0.2	0.1	0.3	0.0	0.1
88	C19	27.5	358	0.0	0.9	0.4	0.1	0.1	0.0	0.2	0.0	0.0
89	C20	31.0	512	0.1	1.5	1.0	0.1	0.1	0.0	0.2	0.0	0.1
90	C21	34.8	712	0.1	0.8	0.8	0.1	0.1	0.1	0.2	0.0	0.0
91	C22	38.7	531	0.8	1.0	1.0	0.0	0.2	0.1	0.1	0.0	0.1

D.6 Total digestion

	Site	depth [cm]	Mn	Fe	Cu	Zn	As	Mo	Cd	Sb	Pb	U
							[$\mu g \cdot g^{-1}$]					
1	U1	0.5	629	33.311	50	160	67	1.3	1.6	14	57	3.2
2	U2	1.0	692	34.769	54	142	76	3.0	1.4	16	60	3.5
3	U3	1.5	612	32.184	48	122	67	1.2	1.2	13	51	2.9
4	U4	2.0	526	28.744	43	107	57	0.9	1.1	12	48	2.6
5	U5	2.5	537	29.045	47	113	62	1.0	1.4	17	59	2.7
6	U6	3.0	508	27.586	50	117	67	1.7	1.8	14	44	2.8
7	U7	3.5	699	28.242	74	164	61	1.0	1.6	21	48	2.8
8	U8	4.0	744	28.776	78	174	69	1.1	1.7	14	49	2.9
9	U9	5.0	736	26.672	76	170	70	1.1	1.9	15	43	3.0
10	U10	6.0	741	27.524	81	175	71	1.2	1.9	15	44	3.1
11	U11	7.0	716	27.923	80	174	70	1.2	1.8	16	44	3.1
12	U12	8.0	623	23.854	67	144	56	1.1	1.7	13	38	2.5
13	U13	9.5	721	25.571	72	157	62	1.3	1.7	14	41	2.8
14	U14	11.0	602	27.432	68	151	54	1.3	1.9	16	46	3.0
15	U15	13.5	725	31.142	79	183	63	1.3	2.0	22	56	3.2
16	U16	16.0	670	29.076	71	171	60	1.2	1.5	19	50	2.9
17	U17	18.5	635	28.029	70	157	54	1.0	1.4	14	44	2.7
18	U18	21.0	712	29.340	71	161	58	1.3	1.4	14	45	2.8
19	U19	23.5	643	26.892	56	147	54	1.0	1.3	16	41	2.5
20	U20	26.0	615	27.881	58	153	49	1.3	1.4	17	43	2.7
21	O1	0.5	591	33.588	49	109	37	1.2	0.6	4	33	2.4
22	O2	1.0	588	34.571	55	124	59	1.3	1.2	10	41	2.5
23	O3	1.6	558	33.431	55	125	47	1.3	1.5	11	37	2.4
24	O4	2.9	481	35.552	62	134	42	1.2	1.5	12	40	2.6
25	O5	4.0	532	34.107	60	123	42	1.0	1.4	13	40	1.8
26	O6	5.5	549	33.760	58	123	45	1.1	1.4	14	40	1.9
27	O7	7.5	538	32.378	59	128	45	1.1	1.7	14	43	2.1
28	O8	9.7	540	34.483	58	123	54	0.9	1.4	14	39	1.8
29	O9	11.7	537	37.055	58	128	60	0.9	1.2	15	43	2.4
30	O10	13.7	580	38.440	63	138	59	1.2	1.5	17	50	2.8
31	O11	15.7	546	36.160	54	135	51	0.9	1.3	16	39	2.5
32	O12	17.9	523	34.591	55	137	48	1.2	1.5	17	40	2.4
33	M1	0.5	491	30.317	94	163	90	5.4	0.7	8	48	5.3
34	M2	1.0	518	31.735	89	166	47	4.3	0.8	7	49	4.7
35	M3	1.5	586	30.014	87	138	58	3.8	0.6	6	42	4.7
36	M4	2.0	611	25.943	71	114	51	2.9	0.4	6	35	4.4
37	M5	2.5	633	25.255	71	115	49	3.2	0.5	6	36	5.0
38	M6	3.0	622	22.778	65	101	51	3.6	0.4	5	33	5.0
39	M7	3.5	650	25.905	74	116	56	3.4	0.5	6	40	5.0
40	M8	4.0	628	28.008	85	128	62	3.4	0.5	8	43	4.7
41	M9	4.5	519	35.767	104	123	72	2.4	0.4	7	76	2.5
42	M10	5.0	609	28.952	101	127	82	2.2	0.4	8	42	3.3
43	M11	6.0	605	30.125	115	136	98	1.7	0.4	9	44	3.1
44	M12	7.0	571	27.334	100	121	84	1.4	0.3	7	39	2.9
45	M13	8.0	449	27.735	90	124	89	1.2	0.5	7	39	2.6
46	M14	9.0	381	28.067	86	127	78	1.1	0.4	5	38	2.4
47	M15	10.0	406	30.260	88	144	67	1.2	0.5	6	43	2.8
48	M16	12.5	434	28.825	78	137	66	1.5	0.5	7	43	2.7
49	M17	15.0	470	30.672	77	147	103	2.0	0.5	9	51	3.1
50	M18	17.5	501	30.540	75	137	86	2.5	0.5	11	59	3.4

	Site	depth [cm]	Mn	Fe	Cu	Zn	As	Mo	Cd	Sb	Pb	U
							[$\mu g \cdot g^{-1}$]					
51	M19	20.0	495	27.254	71	136	65	2.2	0.5	13	58	3.1
52	M20	22.7	470	31.497	85	167	72	2.2	0.9	18	77	3.1
53	M21	25.7	508	27.771	75	139	56	2.1	0.5	16	76	3.8
54	M22	28.9	544	25.670	75	137	65	3.5	0.6	23	100	4.9
55	M23	32.5	522	25.815	38	117	55	0.6	0.3	11	52	2.1
56	P1	0.5	605	22.019	61	94	66	8.6	0.7	6	28	5.4
57	P2	1.5	319	10.176	28	43	30	3.2	0.3	3	13	2.2
58	P3	2.0	647	20.990	57	88	58	6.0	0.6	5	27	4.1
59	P4	3.2	615	21.064	61	87	59	5.2	0.6	5	27	4.2
60	P5	4.8	311	31.127	103	106	68	2.1	0.4	6	35	2.0
61	P6	6.1	380	30.641	97	102	88	1.6	0.4	7	34	2.0
62	P7	7.5	300	30.949	83	111	83	1.3	0.5	8	38	2.4
63	P8	9.3	375	30.363	87	100	63	1.2	0.4	6	33	1.9
64	P9	11.2	486	36.702	91	147	104	2.1	0.6	13	128	2.7
65	P10	13.2	298	33.593	83	132	41	2.5	0.8	11	65	2.9
66	P11	15.2	302	31.064	76	125	51	2.7	0.8	14	73	3.2
67	P12	17.2	416	31.946	80	138	68	3.0	1.3	24	139	3.4
68	P13	19.2	375	30.780	66	129	56	0.8	0.9	27	141	2.4
69	P14	21.3	321	36.494	52	222	48	0.8	1.2	38	163	2.6
70	C1	0.5	614	36.434	48	114	64	1.0	0.9	11	62	3.4
71	C2	0.9	609	38.170	48	118	56	1.0	0.9	12	61	3.5
72	C3	1.6	661	43.462	55	137	56	1.2	1.1	13	69	4.3
73	C4	2.1	626	39.874	52	125	50	1.1	0.9	12	63	4.0
74	C5	2.8	572	36.805	47	119	46	1.2	0.4	12	113	4.5
75	C6	3.5	577	37.247	45	123	45	1.2	0.4	11	106	4.9
76	C7	4.5	597	35.533	40	119	46	1.2	0.4	10	103	5.3
77	C8	5.5	685	37.143	43	128	53	1.4	0.4	11	113	5.7
78	C9	6.5	624	34.510	39	117	51	1.3	0.4	11	106	5.1
79	C10	7.5	742	40.716	43	135	58	1.5	0.4	12	118	5.7
80	C11	8.7	671	35.910	40	123	52	1.4	0.4	11	110	5.5
81	C12	9.8	753	34.434	44	113	38	1.0	0.3	10	102	3.8
82	C13	10.8	618	35.616	52	104	40	1.0	0.3	12	105	3.5
83	C14	12.8	598	38.043	51	120	47	1.2	0.4	14	127	3.7
84	C15	14.9	694	39.727	59	119	44	1.5	0.4	17	140	4.2
85	C16	17.0	615	39.122	60	110	39	1.4	0.4	16	119	3.9
86	C17	19.5	619	43.470	56	135	52	1.4	0.4	13	129	4.7
87	C18	23.5	833	47.840	66	147	57	1.7	0.5	17	149	5.4
88	C19	27.5	652	38.122	53	110	40	1.2	0.3	11	104	3.7
89	C20	31.0	682	37.087	46	112	53	1.1	0.4	11	108	3.9
90	C21	34.8	774	40.482	49	117	72	0.9	0.4	12	126	3.1
91	C22	38.7	646	41.816	52	124	56	1.1	0.4	12	125	3.6

Appendix E

Pore water

E.1 Dissolved major elements content

	sample	depth [cm]	SO_4^{2-} [mM]	Cl^- [mM]	NO_3^- [µM]	NH_4^+ [mM]
1	UBW	0.0	2.46	8.11	0.22	dl
2	U1	0.5	3.18	10.26	nd	dl
3	U2	1.0	4.04	13.56	nd	dl
4	U3	1.5	3.73	13.48	0.27	dl
5	U4	2.0	3.28	12.08	0.56	dl
6	U5	2.5	3.71	14.65	0.21	dl
7	U6	3.0	4.36	21.89	nd	dl
8	U7	3.5	3.83	16.02	0.30	dl
9	U8	4.0	4.60	22.93	nd	dl
10	U9	5.0	3.40	19.20	nd	dl
11	U10	6.0	5.36	24.97	0.68	dl
12	U11	7.0	5.63	22.31	0.20	dl
13	U12	8.0	6.42	32.93	0.22	dl
14	U13	9.5	6.34	23.86	0.54	dl
15	U14	11.0	10.85	48.14	2.19	dl
16	U15	13.5	10.85	48.14	2.19	dl
17	U16	16.0	10.85	48.14	2.19	dl
18	U17	18.5	nd	nd	nd	dl
19	U18	21.0	nd	nd	nd	dl
20	U19	23.5	nd	nd	nd	dl
21	U20	26.0	nd	nd	nd	dl
22	OBW	0.0	2.65	12.32	0.82	dl
23	O1	0.5	2.90	13.72	0.96	dl
24	O2	1.0	3.06	15.20	1.62	dl
25	O3	1.6	3.11	15.88	1.15	dl
26	O4	2.9	3.02	16.25	7.60	dl
27	O5	4.0	2.97	16.76	3.08	dl
28	O6	5.5	2.43	10.46	1.05	dl
29	O7	7.5	3.06	16.67	3.59	dl
30	O8	9.7	3.27	17.06	3.81	dl
31	O9	11.7	nd	nd	nd	nd
32	O10	13.7	nd	nd	nd	nd
33	O11	15.7	nd	nd	nd	nd
34	O12	17.9	nd	nd	nd	nd
35	MBW	0.0	2.24	10.48	0.10	dl
36	M1	0.5	1.24	13.08	0.39	0.27
37	M2	1.0	1.33	14.94	0.53	0.34
38	M3	1.5	1.55	15.71	0.96	0.37
39	M4	2.0	1.88	18.17	1.10	0.38
40	M5	2.5	2.20	20.82	1.06	0.38
41	M6	3.0	2.83	21.19	1.21	0.43
42	M7	3.5	3.73	25.05	0.92	0.53
43	M8	4.0	5.02	28.15	1.32	dl
44	M9	4.5	5.35	30.91	2.12	0.64
45	M10	5.0	6.25	31.86	1.46	0.65
46	M11	6.0	7.47	37.48	1.29	0.70
47	M12	7.0	8.55	36.49	1.47	0.68
48	M13	8.0	10.77	48.57	3.68	dl
49	M14	9.0	12.89	55.76	3.25	0.78
50	M15	10.0	nd	nd	nd	nd

	sample	depth [cm]	SO_4^{2-} [mM]	Cl^- [mM]	NO_3^- [µM]	NH_4^+ [mM]
51	M16	12.5	16.46	68.67	8.28	dl
52	M17	15.0	20.88	78.70	5.06	dl
53	M18	17.5	22.72	78.94	1.49	dl
54	M19	20.0	nd	nd	nd	nd
55	M20	22.7	nd	nd	nd	nd
56	M21	25.7	nd	nd	nd	nd
57	M22	28.9	nd	nd	nd	nd
58	M23	32.5	nd	nd	nd	nd
59	PWB	0.0	8.42	38.64	0.21	dl
60	P1	0.5	4.95	27.98	0.88	0.45
61	P2	1.5	nd	nd	nd	nd
62	P3	2.0	6.52	45.75	3.44	0.43
63	P4	3.2	6.34	44.53	5.16	0.43
64	P5	4.8	6.06	45.98	0.86	dl
65	P6	6.1	5.85	47.38	1.81	dl
66	P7	7.5	5.81	51.34	1.28	dl
67	P8	9.3	6.83	55.75	1.52	dl
68	P9	11.2	7.28	55.21	2.07	dl
69	P10	13.2	9.05	67.92	1.59	dl
70	P11	15.2	nd	nd	nd	nd
71	P12	17.2	nd	nd	nd	nd
72	P13	19.2	nd	nd	nd	nd
73	P14	21.3	nd	nd	nd	nd
74	CBW	0.0	0.33	0.59	1.13	0.19
75	C1	0.5	0.22	0.55	1.84	0.28
76	C2	0.9	0.06	0.51	2.98	0.30
77	C3	1.6	0.00	0.44	1.44	0.32
78	C4	2.1	0.00	0.40	4.38	0.33
79	C5	2.8	0.00	0.40	2.01	0.36
80	C6	3.5	0.06	0.38	1.83	0.16
81	C7	4.5	0.12	0.31	1.02	0.16
82	C8	5.5	0.01	0.30	2.29	0.19
83	C9	6.5	0.01	0.27	2.88	0.27
84	C10	7.5	0.01	0.21	2.47	0.26
85	C11	8.7	0.00	0.23	1.91	0.48
86	C12	9.8	0.00	0.22	5.19	0.40
87	C13	10.8	0.00	0.20	3.81	nd
88	C14	12.8	0.00	0.20	2.01	0.85
89	C15	14.9	0.00	0.21	4.20	0.97
90	C16	17.0	0.00	0.23	3.01	0.85
91	C17	19.5	0.00	0.22	3.89	0.88
92	C18	23.5	0.00	0.30	4.24	1.27
93	C19	27.5	0.00	0.38	1.69	0.95
94	C20	31.0	0.00	0.55	1.89	1.45
95	C21	34.8	0.00	0.84	2.86	1.03
96	C22	38.7	0.00	0.82	5.61	0.97

E.2 Dissolved trace elements content

	sample	depth [cm]	Mn [µM]	Fe [µM]	Cu [nM]	Zn [nM]	As [µM]	Mo [nM]	Cd [nM]	Sb [nM]	Pb [nM]	U [nM]
1	UBW	0.0	2	dl	dl	dl	1	dl	dl	dl	dl	4
2	U1	0.5	nd	nd	nd	nd	nd	nd	nd	nd	nd	nd
3	U2	1.0	281	346	dl	dl	10	dl	dl	dl	dl	dl
4	U3	1.5	281	247	dl	dl	12	dl	dl	dl	dl	dl
5	U4	2.0	245	202	dl	dl	10	dl	dl	dl	dl	dl
6	U5	2.5	223	206	dl	dl	10	dl	dl	dl	dl	dl
7	U6	3.0	199	168	6	36	8	15	0.07	9	0.9	6
8	U7	3.5	198	163	6	40	8	12	0.10	9	0.8	8
9	U8	4.0	194	152	6	34	7	12	0.15	9	0.7	9
10	U9	5.0	198	177	7	39	8	18	0.19	10	0.8	13
11	U10	6.0	217	227	14	37	10	10	0.20	9	2.1	7
12	U11	7.0	239	236	11	40	9	13	0.14	9	1.3	7
13	U12	8.0	260	143	6	64	7	14	0.11	13	0.6	10
14	U13	9.5	306	254	9	63	8	16	0.13	10	1.4	8
15	U14	11.0	346	81	21	183	4	54	0.25	37	2.0	56
16	U15	13.5	346	81	21	183	4	54	0.25	37	2.0	56
17	U16	16.0	346	81	21	183	4	54	0.25	37	2.0	56
18	U17	18.5	nd	nd	nd	nd	nd	nd	nd	nd	nd	nd
19	U18	21.0	nd	nd	nd	nd	nd	nd	nd	nd	nd	nd
20	U19	23.5	nd	nd	nd	nd	nd	nd	nd	nd	nd	nd
21	U20	26.0	nd	nd	nd	nd	nd	nd	nd	nd	nd	nd
22	OBW	0.0	4	1	79	22	2	63	0.21	25	0.6	11
23	O1	0.5	163	57	21	56	6	47	0.27	13	2.1	1
24	O2	1.0	201	134	8	53	9	30	0.10	8	1.1	1
25	O3	1.6	114	64	5	35	7	15	0.06	9	0.9	2
26	O4	2.9	nd	nd	nd	nd	nd	nd	nd	nd	nd	nd
27	O5	4.0	nd	nd	nd	nd	nd	nd	nd	nd	nd	nd
28	O6	5.5	nd	nd	nd	nd	nd	nd	nd	nd	nd	nd
29	O7	7.5	nd	nd	nd	nd	nd	nd	nd	nd	nd	nd
30	O8	9.7	nd	nd	nd	nd	nd	nd	nd	nd	nd	nd
31	O9	11.7	103	10	18	50	9	16	0.08	56	3.2	8
32	O10	13.7	nd	nd	nd	nd	nd	nd	nd	nd	nd	nd
33	O11	15.7	85	5	13	37	7	66	0.11	112	2.4	22
34	O12	17.9	94	33	10	36	10	81	0.07	38	1.8	8
35	MBW	0.0	2	dl	dl	dl	1	dl	dl	dl	dl	0
36	M1	0.5	6	dl	dl	dl	1	dl	dl	dl	dl	1
37	M2	1.0	8	1	3	53	2	7	0.05	65	0.7	5
38	M3	1.5	9	1	3	44	3	7	0.05	102	0.7	5
39	M4	2.0	12	2	3	35	4	5	0.06	121	0.4	4
40	M5	2.5	14	1	3	59	6	12	0.01	133	0.5	4
41	M6	3.0	16	1	2	37	6	14	0.01	154	0.3	7
42	M7	3.5	18	1	4	47	7	35	0.12	143	0.9	11
43	M8	4.0	20	1	3	80	7	35	0.20	138	1.1	13
44	M9	4.5	23	1	3	32	8	25	0.20	102	0.7	6
45	M10	5.0	24	1	4	67	13	70	0.24	175	0.7	10
46	M11	6.0	24	1	6	92	13	56	0.23	131	1.0	8
47	M12	7.0	27	2	5	70	20	126	0.25	309	0.7	17
48	M13	8.0	31	3	10	98	26	281	0.40	530	2.0	43
49	M14	9.0	30	2	12	135	19	282	0.48	354	2.5	33
50	M15	10.0	33	2	8	71	15	204	0.31	232	2.1	27

	sample	depth [cm]	Mn [μM]	Fe [μM]	Cu [nM]	Zn [nM]	As [μM]	Mo [nM]	Cd [nM]	Sb [nM]	Pb [nM]	U [nM]
51	M16	12.5	33	1	7	118	5	865	1.19	377	1.6	88
52	M17	15.0	nd	nd	nd	nd	nd	nd	nd	nd	nd	nd
53	M18	17.5	nd	nd	nd	nd	nd	nd	nd	nd	nd	nd
54	M19	20.0	53	17	4	82	3	1706	2.28	323	0.7	109
55	M20	22.7	56	6	10	240	1	1599	2.17	474	1.7	134
56	M21	25.7	nd	nd	nd	nd	nd	nd	nd	nd	nd	nd
57	M22	28.9	71	5	8	149	4	794	1.39	309	1.6	427
58	M23	32.5	nd	nd	nd	nd	nd	nd	nd	nd	nd	nd
59	PWB	0.0	4	2	8	54	2	49	0.06	59	1.5	10
60	P1	0.5	12	2	1	41	13	366	0.21	532	0.5	36
61	P2	1.5	nd	nd	nd	nd	nd	nd	nd	nd	nd	nd
62	P3	2.0	17	3	3	43	11	195	0.15	331	0.6	31
63	P4	3.2	18	3	2	36	11	72	0.13	343	0.4	17
64	P5	4.8	18	3	4	44	7	65	0.05	208	0.6	11
65	P6	6.1	18	9	15	102	10	142	0.44	381	9.1	23
66	P7	7.5	19	7	4	52	12	264	0.15	518	1.1	32
67	P8	9.3	20	8	7	43	12	170	0.05	434	1.6	33
68	P9	11.2	23	20	11	59	8	135	0.06	169	2.4	23
69	P10	13.2	31	34	10	54	6	261	0.12	307	2.1	47
70	P11	15.2	31	17	7	75	4	283	0.18	385	2.0	78
71	P12	17.2	45	36	8	76	6	159	0.12	191	2.4	75
72	P13	19.2	nd	nd	nd	nd	nd	nd	nd	nd	nd	nd
73	P14	21.3	nd	nd	nd	nd	nd	nd	nd	nd	nd	nd
74	CBW	0.0	89	9	125	251	1	40	0.22	23	2.6	26
75	C1	0.5	149	47	11	22	9	89	0.15	35	4.3	73
76	C2	0.9	191	88	9	21	10	122	0.14	40	2.8	33
77	C3	1.6	253	101	9	33	6	165	0.21	44	2.4	27
78	C4	2.1	297	120	8	28	5	165	0.20	47	2.2	23
79	C5	2.8	302	238	11	33	7	180	0.21	60	2.9	30
80	C6	3.5	298	256	25	421	5	158	0.27	80	5.4	178
81	C7	4.5	350	233	10	71	4	177	0.17	119	1.2	432
82	C8	5.5	529	559	42	1309	6	219	0.47	162	11.8	423
83	C9	6.5	620	720	9	84	7	255	0.19	161	1.5	357
84	C10	7.5	731	899	11	127	9	302	0.30	124	1.7	153
85	C11	8.7	783	1106	11	100	10	306	0.33	96	2.2	57
86	C12	9.8	858	781	20	329	7	246	0.29	90	3.9	70
87	C13	10.8	946	915	9	169	8	191	0.24	76	2.4	14
88	C14	12.8	1091	1375	6	79	10	238	0.26	68	1.1	6
89	C15	14.9	1145	1079	4	64	6	229	0.24	63	0.5	6
90	C16	17.0	1121	1321	5	76	6	172	0.19	76	0.5	10
91	C17	19.5	1006	2177	6	71	10	154	0.26	61	1.3	10
92	C18	23.5	1267	2822	9	90	10	164	0.18	58	2.8	7
93	C19	27.5	1082	1721	5	87	9	204	0.20	55	1.3	9
94	C20	31.0	937	1880	12	202	20	133	0.14	45	2.4	6
95	C21	34.8	671	948	45	981	28	29	0.30	28	11.0	2
96	C22	38.7	453	753	1	42	12	27	0.00	27	0.2	4